AN INVESTIGATION INTO COMBINED AMORPHOUS FORM OF SUFADOXINE, PYRIMETHAMINE AND AZITHROMYCIN

GEOFFREY OKELLO (B. PHARM)

A full thesis submitted in the partial fulfilment of the requirements for the degree of *Master in pharmaceutical science*

Faculty of Natural Science, School of Pharmacy,

Discipline of Pharmaceutics

University of the Western Cape, Bellville, South Africa.

Supervisor: Prof. Marique Aucamp

November 2021

Appendix Preface/ Declaration (plagiarism declaration)

DECLARATION

I **Geoffrey Okello**, declare that

(i)   The research reported in this thesis, except where otherwise indicated, is my original work.

(ii)   This thesis has not been submitted for any degree or examination at any other University.

(iii)   This thesis does not contain other persons' data, pictures, graphs or other information, unless specifically acknowledged as being sourced from other persons.

(iv)   This thesis does not contain other persons' writing, unless specifically acknowledged as being sourced from other researchers. Where other written sources have been quoted, then:

a) their words have been re-written but the general information attributed to them has been referenced;

b) where their exact words have been used, their writing has been placed inside quotation marks, and referenced.

(v)   Where I have reproduced a publication of which I am author, co-author or editor, I have

indicated in detail which part of the publication was actually written by myself alone and have fully referenced such publications. This thesis does not contain text, graphics or tables copied and pasted from the Internet, unless specifically acknowledged, and the source being detailed in the thesis and in the References sections.

Signed:_____   Date: 11th/Nov/2021

Dedication

I dedicate this work to my nuclear family, if there is anything I should treasure the most, it's your kind supports, to my mother whose motivation continues to propel my feet above the sky. Her message that stood the test of time; "*Your current circumstance should not limit your original values and potential to achieve anything in life*" and lastly to my entire family and friends.

Oral presentation

1. Okello G, Aucamp M. An investigation into combined amorphous forms(s) of sulfadoxine, pyrimethamine and azithromycin. Virtually presented at the 6th University of the Western Cape School of Pharmacy Postgraduate Research Symposium, School of Pharmacy, University of the Western Cape, Cape Town (22nd September 2021).

Abstract

An investigation into combined amorphous form of sulfadoxine, pyrimethamine and azithromycin.

Background:

Malaria remains one of the top mortality causes in the sub-Saharan African region, especially among pregnant women and infants. Despite several measures being implemented within the affected areas such as the use of treated mosquito nets, sulfadoxine and pyrimethamine (SUL-PYR) as an intermittent preventive treatment (IPTp-SP) is still considered the standard prophylactic regimen for pregnant women. Recently, the WHO increased the regimen of IPTp-SP from three to four doses on a monthly interval, this recommendation poses a potential risk of toxicity and resistance to the drugs. An improvement towards this challenge is under clinical trial and consists of the inclusion of azithromycin (AZI), a macrolide antibiotic, to the current IPTp-SP treatment regimen. This will not only aid in the prophylaxis of malaria in pregnant women but will also assist in other pregnancy related infections. All three these drugs exhibit poor aqueous solubility; requiring high concentrations for oral administration to achieve therapeutic plasma concentrations. This in itself is a risk to patients and when considering the addition of another dosage form to the IPTp-SP regimen the issue of reduced adherence due to the high "pill burden" may potentially contribute to antiprotozoal and antimicrobial resistance.

Aim:

It is a proven fact that amorphous solid-state forms of drugs exhibit superior aqueous solubility over their respective crystalline forms. The current study undertook investigation of combining SUL, PYR and AZI into a ternary amorphous solid-state form as potential solution to the poor solubility of the three drugs which could potentially also have a positive effect on dose reduction and reduced pill-burden.

Methods:

A physical mixture consisting of SUL, PYR and AZI in the ratio of 1 : 0.05 : 1 w/w/w termed SPA-C was prepared as a control preparation. Quench cooling of the melt and solvent evaporation techniques were investigated as solid-state form preparation techniques in an effort to convert SPA-C to an amorphous solid-state form. The physicochemical properties of the individual drugs, SPA-C as well as the resulting solid-state form preparations were

analysed utilising hot-stage microscopy (HSM), thermogravimetric analysis (TGA), differential scanning calorimetry (DSC), Fourier-transform infrared spectroscopy (FTIR), powder X-ray diffraction (PXRD), vapour sorption analysis, equilibrium solubility and dissolution rate testing. To aid in the equilibrium solubility and dissolution rate testing, a novel HPLC method capable of simultaneously detecting and quantifying all three compounds was developed and validated.

Results:

Thermal, spectroscopic and XRPD analyses confirmed that a ternary amorphous solid-state system consisting of SUL, PYR and AZI was successfully prepared using the quench cooling of the melt method. The physico-chemical characterisation of this amorphous solid-state form was compared to that of pure crystalline SUL, PYR and AZI as well as to SPA-C. Amorphous solid-state forms are known to be metastable forms thus providing higher solubility concentrations and increased dissolution rates but with the drawback of decreased physical stability. Solubility and dissolution data obtained for the prepared ternary amorphous solid-state form elucidated solubility increases of 1681.9, 37.4 and 711.8% respectively for SUL, PYR and AZI and increases of over 100% in terms of dissolution rates for each of the three drugs in distilled water, as opposed to the individual crystalline counterparts. In this study improved stability of the ternary amorphous form was proven in comparison with that of the reported neat amorphous forms of SUL and AZI.

Conclusion:

These findings concluded the possibility to prepare a novel ternary amorphous system which exhibits superior physical stability and improved aqueous solubility and dissolution rate, showing that the possibility to prepare ternary amorphous systems using only active pharmaceutical ingredients is possible.

Keywords

Malaria, sulfadoxine, pyrimethamine, azithromycin, quench cooling, equilibrium solubility, dissolution rate.

Acknowledgements

With respect and due honour, I would like to extend my appreciation to:

- Prof. Marique Aucamp: You opened me the door of an opportunity, the day you accepted my research proposal and since then, you never ceased guiding and supporting me through the entire study, I will forever remain indebted to your unending kindness, professional mentorship, and supervision, thank you.

- Prof. Samsodien, thanks for your support throughout this study, your training and guidance left a permanent mark of knowledge.

- Dr Ebrahim: Thank you, your motivation is felt and has driven me steps ahead.

- To the pharmaceutics research team: Marise, Candidah, Alicia, Dr. Nadine, Venissa, Sandrine, Bola, Yves, DR. Jean, Nnamdi, Alicia – You were all amazing, you brough wealth of knowledge and freely shared with me.

- To Mr. Kippie: Thank you for your kind sharing of knowledge on the analytical equipment that facilitated the success of my work.

- To my family and friends- Your continuous supports yielded a lasting fruit, a journey we will all be amazed when we reflect upon. May God richly bless you and be reassured, this achievement belongs to you.

- Thank you to the pharmaceutics lecturers entirely for shaping me to a better person through research development. I never thought at first in my early stages of undergrad that I would be part of this department, your encouragement in various forms paved the way.

- To UWC school of pharmacy, thanks for all the support and provision of the training environment.

- And lastly to the University of the Western Cape for availing resources that catalysed the tension of work and challenges and smoothened the rough path this research project traversed.

List of Abbreviations

API: Active pharmaceutical ingredient

AZI: Azithromycin

CDC: Center of disease control

DMF: Dimethyl formamide

DMSO: Dimethyl sulfoxide

DSC: Differential scanning calorimetry

FDA: Food and Drug Authority

FTIR: Fourier Transform infrared

GMM: Genetically modified male mosquito

HPLC: High performance liquid chromatography

ICH: International Conference of Harmonisation

IPTp-SP: Intermittent preventive treatment Sulfadoxine pyrimethamine

LOD: Limit of detection

LOQ: Limit of quantification

ML: Millilitre

PXDR: Powder X-Ray refraction

PYR: Pyrimethamine

RH: Relative humidity

RP-HPLC: Reverse phase high performance chromatography

RSD: Relative standard deviation

SD: Standard deviation

SPA-A   Sulfadoxine Pyrimethamine Azithromycin- Amorphous

SPA-C: Sulfadoxine Pyrimethamine Azithromycin- physical mixture
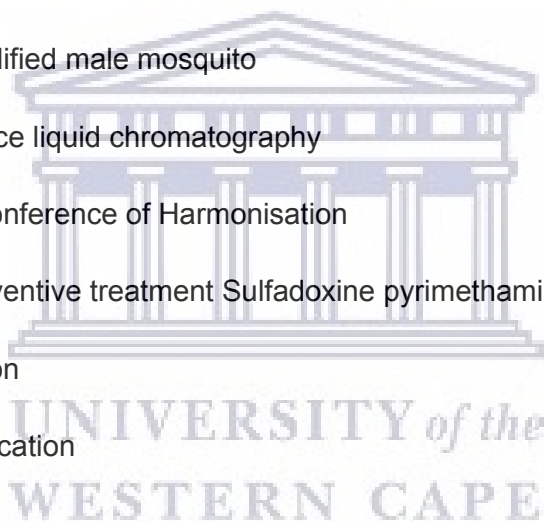
SUL: Sulfadoxine

TGA: Thermogravimetric analysis

USP: United State Pharmacopeia

UV: Ultra-violet

V/V: Volume/volume

W/W: Weight/weight

WHO: World Health Organization

UNIVERSITY *of the*
WESTERN CAPE

List of tables   **page**

Table 7.16: Effect of storage conditions on the retention time of the three analytes………164

List of Equations

Table of contents

Chapter 1: An introduction to the investigation into combined amorphous form(s) of sulfadoxine, pyrimethamine and azithromycin……………………………………………..1

Chapter 2: An overview of malaria infection and its global impact………...…….……....6

Chapter 3: Solid-state chemistry of drugs...**16**

CHAPTER 1

An introduction to the investigation into combined amorphous form(s) of sulfadoxine, pyrimethamine and azithromycin

1.1 Introduction

The development of new drugs faces numerous challenges that compromise their final approval and formulation into pharmaceutical dosage forms for real-life application. The biggest challenge is related to poor water solubility. As described in Lipinski's rule of 5, compounds with a logP above 5, possessing over 5 hydrogen bond donor species, more than 10 hydrogen bond recipient species and molecular weight of over 500 daltons show high lipophilic properties and poor hydrophilicity tendencies, limiting their use as pharmaceutical drugs intended for oral administration (Halberstadt, 2017). To address this problem, medicinal compounds have to be manipulated either during the drug development stage or during dosage form formulation (Van den Mooter, 2012; Ozaki *et al.*, 2013; Singh *et al.*, 2017; Schittny *et al.*, 2018; Shi, Moinuddin and Cai, 2019; Wang *et al.*, 2019). Depending on the route of administration, many dosage form formulation strategies are available specifically aimed at improving the physico-chemical property of drug solubility. A pre-formulation strategy also aimed at improving drug solubility is that of manipulating the specific solid-state form in which a drug exists and many efforts are made to incorporate solid-state forms into dosage forms that possess multi-fold higher aqueous solubility (Huang *et al.*, 2017; Maher *et al.*, 2016). Amorphous drugs have been proven to improve aqueous solubility as opposed to the crystalline forms of the same drug (Huang *et al.*, 2017). The most common cause of illness in Sub-Saharan Africa still remains malaria infection (World Health Organization (WHO), 2021). People at higher risk are pregnant mothers, children and immunocompromised persons such as the elderly and those with comorbid chronic conditions (Marealle *et al.*, 2018; Sabin *et al.*, 2018). To keep pregnant women safe the WHO recommends an intermittent preventative treatment with sulfadoxine-pyrimethamine (IPTp-SP) approach. The IPTp-SP is typically given to pregnant women from the second trimester to term. The WHO recommends up to four doses of sulfadoxine-pyrimethamine (SP) given one month apart (World Health Organization (WHO), 2018). Due to an unmet need in the management and prophylaxis of malaria in pregnant women, the attempt to improve the existing regimen of IPTp-SP by adding azithromycin (AZI) as a third drug is currently investigated as a clinical trial (Luntamo *et al.*, 2012; Wilson *et al.*, 2015; Unger *et al.*, 2015)

All three mentioned drugs present with poor bioavailability due to their inherently poor aqueous solubility. The potential of addressing the solubility and bioavailability problems through

altering the solid-state forms of the three drugs is considered a promising and potentially cost-effective strategy, not only attempting to solve the challenge of malaria prophylaxis in pregnant women but also addressing the drug dosing strength and frequency. Thereby, directly impacting positively on toxicity issues and minimising or delaying the development of resistance of the plasmodium parasites to the drugs, improve compliance and ultimately the treatment experience.

The current study focused on the amorphous forms of sulfadoxine (SUL), pyrimethamine (PYR) and azithromycin (AZI) and the combination of these amorphous forms as a ternary amorphous system, all in an effort to enhance their aqueous solubility performance. This thesis is subdivided into eight chapters with Chapter 2 providing an overview of malaria pathophysiology, the populations and sub-sections of populations that are at risk, the impact to social economic development both to the affected individual and governments in the endemic zones, current preventative measures that are provided, and finally focus is placed on pharmacological management of this life-threatening disease.

Chapter 3 elaborates on the physico-chemical properties of drugs and how different solid-state forms of any given drug influences the physico-chemical properties which inevitably will influence the pharmacological action in terms of potentially improving drug permeability and bioavailability due to improved aqueous solubility. This, of course, is highly dependent on the specific Biopharmaceutical Classification System (BCS) class to which a particular drug belongs to, which is also discussed in-depth in Chapter 3.

In chapter 4, the specific physico-chemical properties of SUL, PYR and AZI are discussed that may impede or enhance their inherent aqueous solubility characteristics, mode of action, and pharmacokinetic. Chapter 5 deals with the materials and methodology employed in this study. Solid-state form preparation methods and analytical techniques used to characterise and evaluate these solid-state forms are discussed.

Chapter 6 describes the data obtained firstly during the preliminary physico-chemical characterisation of the single compounds linking that to the physico-chemical properties of a physical mixture of the three crystalline drugs (SPA-C). Subsequently, the preparation of amorphous solid-state form combinations of the three drugs and finally the physico-chemical characterisation of these combinations are discussed.

An imperative aspect of any pharmaceutical preformulation and formulation study is the availability of a suitable analytical technique which will allow the determination of drug concentration, either immediately after the preparation of the solid-state forms or during equilibrium solubility testing and dissolution rate studies. During a literature search it became

apparent that no HPLC method for the simultaneous detection and quantification of SUL, PYR and AZI exists. One would argue that methods for the single compounds exist, therefore why not utilise those methods? However, as these three compounds were combined, it became imperative to analyse them together especially to investigate the influence that the three compounds have on one another. Chapter 7 therefore discusses the method development and validation of a high-performance liquid chromatographic (HPLC) method developed to simultaneously detect and quantify SUL, PYR and AZI. Chapter 8 provides an in-depth conclusion as well as future recommendations that eluded from this study.

1.2 Conclusion

This chapter provided a general structure of this thesis, highlighting the important aspects in the preceding chapters, hypothesis, aim and objectives of the study. It's thus paramount to link each section to have a comprehensive understanding and conclusion.

1.3 References

Halberstadt (2017) '乳鼠心肌提取 HHS Public Access', *Physiology & behavior*, 176(5), pp. 139–148. doi: 10.1016/j.addr.2016.05.007.BDDCS.

Huang, Y., Zhang, Q., Wang, J.-R., Lin, K.-L. & Mei, X. Amino acids as co-amorphous excipients for tackling the poor aqueous solubility of valsartan. Pharm. Dev. Technol. 22, 69–76 (2017).

Luntamo, M., Rantala, A., Meshnick, S., Cheung, Y., Kulmala, T., Maleta, K. and Ashorn, P., 2012. The Effect of Monthly Sulfadoxine-Pyrimethamine, Alone or with Azithromycin, on PCR-Diagnosed Malaria at Delivery: A Randomized Controlled Trial. *PLoS ONE*, 7(7), p.e41123.

Maher, E. M., Ali, A. M. A., Salem, H. F. & Abdelrahman, A. A. In vitro/in vivo evaluation of an optimized fast dissolving oral film containing olanzapine co-amorphous dispersion with selected carboxylic acids. Drug Deliv. 23, 3088–3100 (2016).

Marealle, A.I., Mbwambo, D.P., Mikomangwa, W.P., Kilonzi, M., Mlyuka, H.J. and Mutagonda, R.F. (2018). A decade since sulfonamide-based anti-malarial medicines were limited for intermittent preventive treatment of malaria among pregnant women in Tanzania. *Malaria Journal*, 17(1).

Ozaki, S., Kushida, I., Yamashita, T., Hasebe, T., Shirai, O. and Kano, K., 2013. Inhibition of Crystal Nucleation and Growth by Water-Soluble Polymers and its Impact on the Supersaturation Profiles of Amorphous Drugs. *Journal of Pharmaceutical Sciences*, 102(7), pp.2273-2281.

Schittny, A., Ogawa, H., Huwyler, J. and Puchkov, M., 2018. A combined mathematical model linking the formation of amorphous solid dispersions with hot-melt-extrusion process parameters. European Journal of Pharmaceutics and Biopharmaceutics, 132, pp.127-145.

Shi, Q., Moinuddin, S. M. and Cai, T. (2019) 'Advances in co-amorphous drug delivery systems', *Acta Pharmaceutica Sinica B*. Elsevier B.V., 9(1), pp. 19–35. doi: 10.1016/j.apsb.2018.08.002.

Singh, G., Kaur, L., Gupta, G.D. and Sharma, S. (2017). Enhancement of the Solubility of Poorly Water Soluble Drugs through Solid Dispersion: A Comprehensive Review. *Indian Journal of Pharmaceutical Sciences*, 79(5).

Unger, H., Ome-Kaius, M., Wangnapi, R., Umbers, A., Hanieh, S., Suen, C., Robinson, L., Rosanas-Urgell, A., Wapling, J., Lufele, E., Kongs, C., Samol, P., Sui, D., Singirok, D., Bardaji, A., Schofield, L., Menendez, C., Betuela, I., Siba, P., Mueller, I. and Rogerson, S., 2015. Sulphadoxine-pyrimethamine plus azithromycin for the prevention of low birthweight in Papua New Guinea: a randomised controlled trial. *BMC Medicine*, 13(1).

Van Den Mooter, G. (2012) 'The use of amorphous solid dispersions : A formulation strategy to overcome poor solubility and dissolution rate', *Drug Discovery Today: Technologies*. 9(2), pp. e79–e85. doi: 10.1016/j.ddtec.2011.10.002.

Wang, Z., Sun, M., Liu, T., Gao, Z., Ye, Q., Tan, X., Hou, Y., Sun, J., Wang, D. and He, Z. (2019). Co-amorphous solid dispersion systems of lacidipine-spironolactone with improved dissolution rate and enhanced physical stability. *Asian Journal of Pharmaceutical Sciences*, 14(1), pp.95–103.

Wilson, D., Goodman, C., Sleebs, B., Weiss, G., de Jong, N., Angrisano, F., Langer, C., Baum, J., Crabb, B., Gilson, P., McFadden, G. and Beeson, J., 2015. Macrolides rapidly inhibit red blood cell invasion by the human malaria parasite, Plasmodium falciparum. *BMC Biology*, 13(1). an. 2019, pp. 95–103, 10.1016/j.ajps.2018.11.001. Accessed 26 Oct. 2021.

Who.int. 2021. Fact sheet about Malaria. [online] Available at: <https://www.who.int/news-room/fact-sheets/detail/malaria> [Accessed 26 October 2021].

World Health Organization (2018). *Implementing malaria in pregnancy programs in the context of World Health Organization recommendations on antenatal care for a positive pregnancy experience*. [online] apps.who.int. Available at: https://apps.who.int/iris/handle/10665/259954 [Accessed 26 Feb. 2021].

CHAPTER 2

An overview of malaria infection and its global impact

2.1 Introduction

Malaria is one of the oldest tropical protozoal diseases affecting mankind and stretches way back in human existence where environmental conditions favour the vector (mosquito) life cycle. It presents as the top healthcare burden in sub-Saharan Africa with direct and substantial physiological and economic implications (Doumbe-Belisse *et al*., 2018). Although it is such an old and well-known disease, millions of people are still being affected by it annually. Despite mentionable progress made there are still significant gaps in terms of treatment success. This chapter will focus on the spread of this disease, its impact on sufferers thereof as well as proposed treatment regimens.

2.2 Classification and aetiology

Malaria is caused by Plasmodium parasites' (*Falciparum, vivax, ovale* and *malariae*) spread through an infected female anopheles mosquito. During the feeding process, the mosquito that is the first host, injects the uninucleate sporozoites residing in the salivary glands, into the bloodstream of the human body (second host) (Doumbe-Belisse *et al*., 2018). The parasite's lifecycle includes vector (mosquito) and human, once the parasite invades the human body it will first accumulate in the liver maturing into *schizonts* which would rapture, causing the release of new parasites called *merozoites.* The cycle continues with new attacks onto uninvaded red blood cells (RBC) where they destroy haemoglobin, interfere with the shape and ease of flow of RBC, leading to sticking on the wall of blood vessels, this mechanism facilitates parasitic shielding from the host's immune system. The RBC (erythrocytic) phase is the one responsible for infection symptoms manifested in the human host, and may take   weeks before signs and symptoms of malaria infection manifests (Sulaiman & Jamaludin, 2013). **Figure 2.1** below, shows the schematic summary of a comprehensive malaria parasite life cycle and transmission mechanism between mosquito and human.
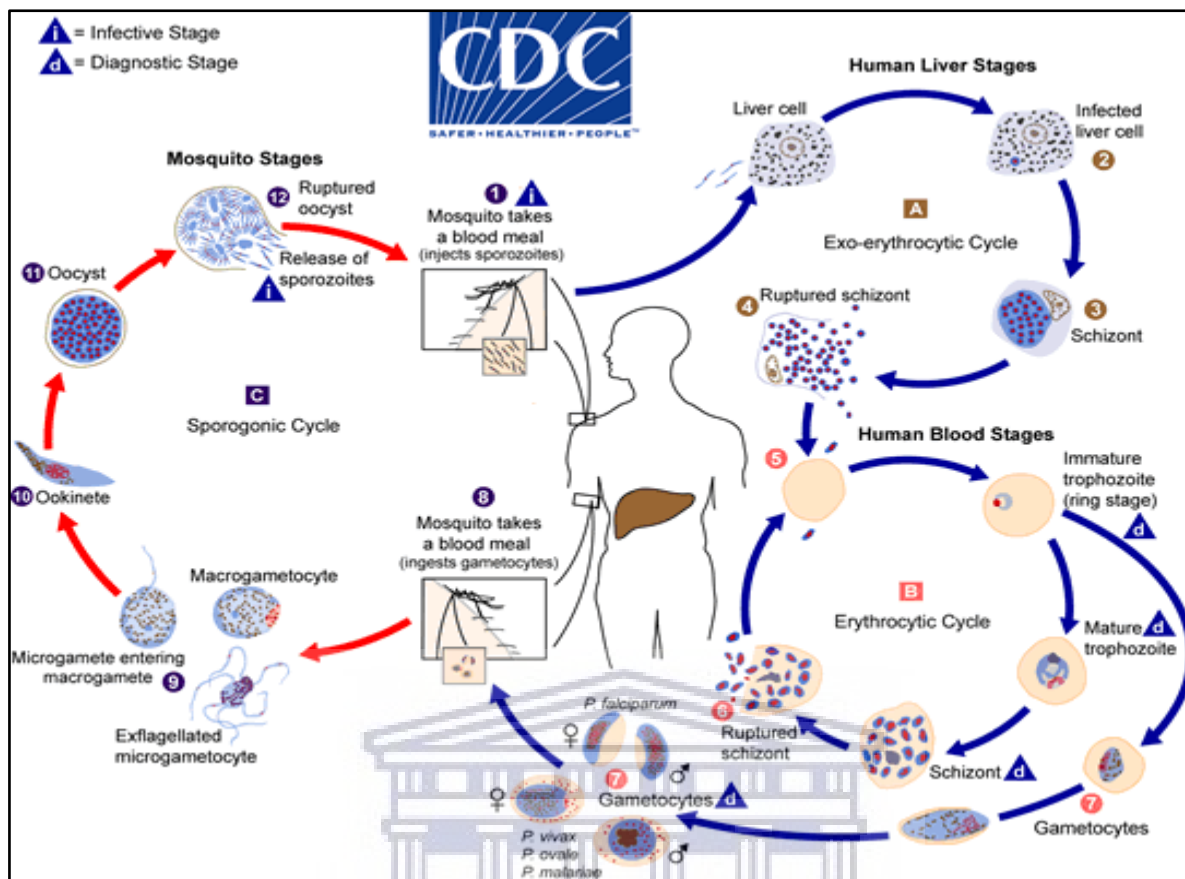
Figure 2.1: Malaria parasite' life cycle (Adapted from CDC - Malaria - About Malaria - Biology, 2020).

The disease is clinically classified into (a) uncomplicated and (b) severe malaria based on several factors such as host immune response, parasite species, rate of erythrocytic asexual multiplication, number of parasites transmitted, prior use of prophylaxis, to name but just a few. Uncomplicated malaria is always associated with minor clinical manifestations, people infected show a whole range of sign and symptoms which include fever, chills, vomiting, general body malaise with lesser discomfort or effect to the general physiological system, and they may recover without medication or with the use of first line antimalarial drugs to combat the parasites. Complicated or severe malaria on the other hand is commonly due to *P. falciparum* species involving the central nervous (cerebral malaria), renal, pulmonary and hematopoietic systems with associated, severe anaemia leading to full blown clinical features. This type of malaria may lead to hospitalisation, leave permanent tissue damage and can be fatal if no immediate management and intervention is attempted (Crutcher & Hoffman, 1996; Halberstadt, 2017; WHO., 2020a).

2.3 Malaria and its global health impact

Malaria affects over 80 countries globally with registered continuous transmission. An estimated 228 million cases and 405,000 deaths were reported worldwide in 2018, of these cases an estimated 85% was in the African region. The World Health Organisation's (WHO) 2019 report on malaria indicates a decline in incidence and death rate when comparing the 2018 and 2017 statistics. Although the above trends show positive indications towards achieving malaria eradication, India and 19 African countries were still reported to have significantly large numbers of infections. This report shows that there is still high demand for individual governments and a need for a global effort in an attempt to eradicate the epidemic (WHO, 2018). Unfortunately, the predominant population and communities affected are those within the low socio-economic bracket, where preventive measures such as use of treated mosquito nets, mosquito repellents, and control of bushes around homes, which encourages breeding and ease of spread of parasites among individuals as the vector invades, are challenging.
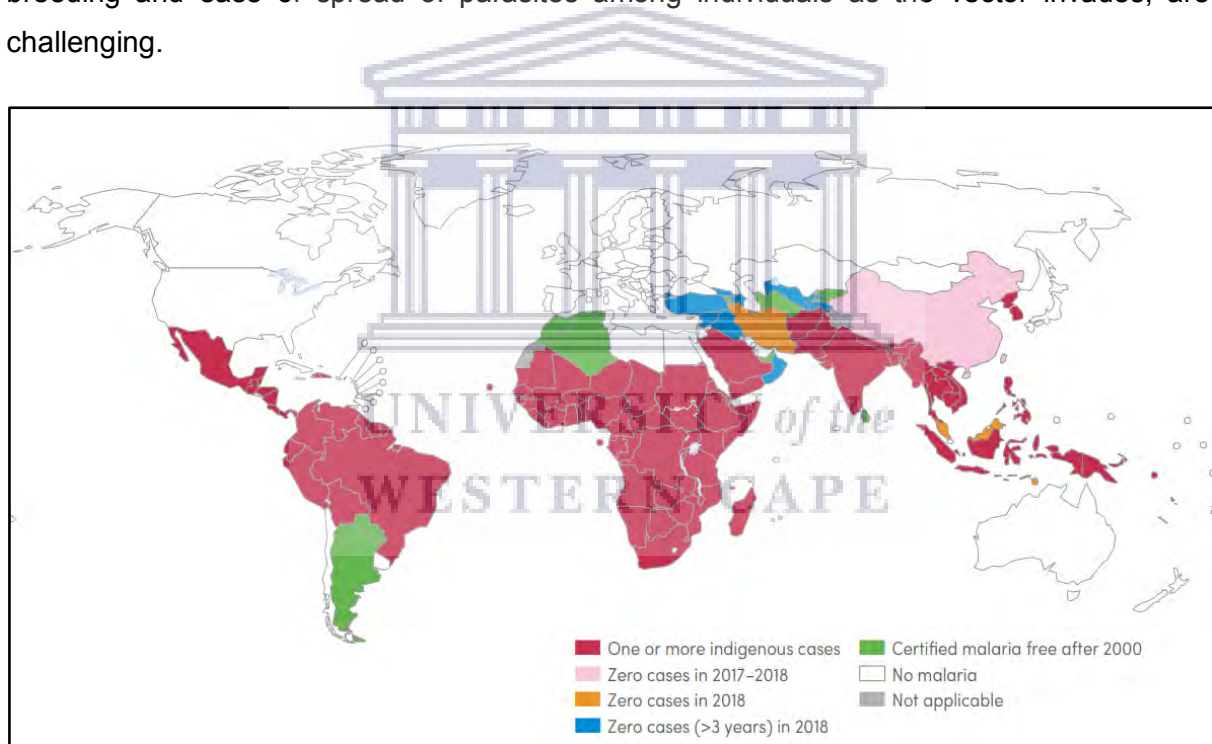
Figure 2.2: World map indicating countries with indigenous malaria cases in 2000 and their status by 2018 (WHO, 2019).

2.4 Malaria in pregnant women and children

Patients at higher risk are pregnant mothers, children and immunocompromised persons such as the elderly and those with comorbid chronic conditions such as diabetes (Marealle et al., 2018; Sabin *et al*., 2018).

In 2018, the WHO provided a statistical approximation of 10,000 cases of malaria-associated deaths during pregnancy globally, and 11% of all neonatal deaths in Africa could be attributed to malaria infection (WHO, 2018). This, despite the multi-sectoral collaborations aimed at preventing and treating malaria in children and pregnant mothers. Malaria also presents several complications to infants which include: low birth weight (LBW), preterm parturition, intrauterine growth retardation and megaloblastic anaemia (Chico *et al*., 2008). According to the WHO, over 11 million pregnant mothers in sub-Saharan Africa were exposed to malaria infection in 2018 and whose babies (872,000 (16%)), later in 2019 presented with LBW as a complication of inappropriate malaria management during antenatal care (ANC) (WHO, 2018), A combination of these physiological health effects has a huge financial impact, with an estimated $12 billion expenditure for governments and global organisations involved in fighting the malaria epidemic in high transmission regions. This expenditure accounts for resources that provides vector controls, intermittent preventive therapy (IPTs), rapid diagnostic tests (RDTs), artemisinin-based combination therapy ACT, severe and complicated malaria therapies, training staff and community health workers, strengthening health infrastructure, monitoring and evaluation, epidemic prevention and response (CDC, 2020).

2.5 Management of malaria

Management of malaria includes both preventative and curative measures by use of chemotherapies. The global approach is always to firstly implement prevention and the use of medication rather as a last resort due to the obvious cost implication and associated resistance of the first line drugs. The use of insecticide-treated bed nets, clearing bushes, mosquito repellents, and taking chemoprophylaxis before entering a malaria zone have been intensively advocated and implemented in several countries to combat the transmission (Musiime *et al*., 2019; Salvador, 2020). Treatments include, among others, the use of antimalarials from first line drugs such as artemisinin-based combination therapy (ACT) for treating uncomplicated malaria, higher level drugs such as quinine are commonly used in hospitalised cases presenting with severe (complicated) malaria.

In pregnancy however, the approach to lower the effect was initiated in 1998 in Kenya through administration of sulfadoxine and pyrimethamine (SP) as an intermittent preventative treatment (IPTp-SP) given to pregnant women from the second trimester to term. During that time a total of 2 doses were considered adequate but over time the doses were increased to three and most recently the WHO recommends up to four doses of SP given one month apart (WHO, 2018). This fourth dose of SP is intended to minimise the drop in plasma concentration approaching term and curbing parasitic resistance to the drugs. At times additional drugs such as dihydroartemisinin-piperaquine may be employed alongside SP based on individual case data (Hoglund *et al*., 2017). Despite the implementation of IPTp-SP in some of the sub-Saharan African countries, the adverse effect of malaria continues to rampage the at risk community as parasites develop resistance to these cost-effective drugs. Although a complete resistance mechanism is not well established, point mutation in the dihydrofolate reductase (DHFR) gene that converts serine amino acid to asparagine at codon 108 of the DHFR domain has been reported. The effect of this mutation results in alteration of the DHFR enzyme structure leading to a reduction in the binding affinity for drugs such as SP SP (Alker *et al*., 2004; Haldar *et al*., 2018). On the other hand, drug toxicity also imposes more health issues to patients. SP shows long half-lives of 200 and 100 hours respectively, and increased dose frequency as recommended by WHO in the above information would have pharmacokinetic implications (Liu *et al*., 2012).

Furthermore, the effects of malaria in pregnancy such as low birth weight (LBW), stillbirth, intrauterine growth retardation (IUGR) and premature birth are being found to be exacerbated by treatable sexually transmitted diseases/infections (STDs/STIs) such as chlamydia trachomatis, syphilis, gonorrhoea, bacterial vaginosis and trichomonas vaginalis (Chico *et al*., 2017). To curb down these adverse effects during antenatal care (ANC), parturition and postpartum in both the mother and expected baby, a study done in Papua New Guinea in 2015, involving the addition of azithromycin, a long acting macrolide that binds to the 70S ribosomal subunit of the bacteria and *P. Falciparum* (Chico & Chandramohan, 2011) in intermittent preventive treatment (IPTp-SP) attracted much attention by the WHO. The addition of azithromycin in the IPTp also may reduce parasitic resistance to SP when used alone (Unger *et al*., 2019). Azithromycin (AZI) is commonly recommended for treatment of respiratory infections (bacterial pathogens), urinary tract infections, STDs and in combination with other antimalarial drugs for less severe malaria management. It has a long half-life as opposed to the first-generation macrolides (erythromycin) resulting in fewer doses prescribed, such as a two day dose of 1 gram each per day.

2.6 Control of malaria

The global trend is to get rid of malaria once and for all, control is different from "elimination" which is a regional scope and "eradication" is global. Control aims at reduction of disease burdens to endemic populations. Multiple approaches have been studied and being applied. The WHO grants countries that register no indigenous infection cases for three consecutive years certification for a malaria free country; 38 countries were declared malaria free and the list is still growing as governments and organisations in support of eliminating malaria continue the battle against this deadly vector borne disease (Salvador, 2020). The first approach is vector management to disrupt transmission cycle, either by killing the vector (mosquitoes) using insecticides or ensuring that the breeding environment is unsuitable especially near human living areas (bush clearing), draining stagnant water bodies, among others. And the protection of susceptible individuals; methods like sleeping under insecticide treated bed-net (Long lasting insecticides nets- LLIT), vector repellents used both indoor and outdoor, have been intensively applied (Musiime *et al*., 2019; Salvador, 2020; Wilson *et al*., 2020). A second approach involves case management, use of chemoprophylaxis, early diagnosis, and treatment with antimalarial drugs. Attempts on vaccines have not yet yielded any success due to the complexity of the parasites and human immune system against the parasites. All these mentioned approaches have reduced burdens and death tremendously over the years in malaria endemic areas. However, there have been drawbacks as vectors adapt to environmental changes, develop resistance to insecticides and parasites, continue drug resistance patterns and spread across boundaries, as such; malaria control becomes complex requiring multiple approaches to achieve the goal (WHO, 2020c).

Recent studies on new measures to combat mosquito vector has emerged on biological control, researchers are working around the clock developing predators to prey on various species at different metamorphosis stages, the larvae and pupae can be eaten up by insects, fish, adult vector destroyed by plants, new species of mosquito such as *Wolbachia,* irradiated mosquitoes replacing the *Anopheles* species and dangerous species suppression by genetically modified male mosquitoes (GMM) (Benelli *et al*., 2016). The WHO takes a position on this novel strategy as over 750 million GMM gets ready to be released in 2021 in Florida (United States of America), the strain of male mosquito is an altered form of *Aedes aegypti* and upon mating with the wild female, their offspring won't survive to maturity stage, limiting the chance of infection and spreading of the parasites across susceptible individuals, this follows the previous similar GM in other parts of the world, Brazil and the Cayman Islands that were reported to have no potential harm (WHO, 2020c). Although this approach of control may sound more environmentally friendly, it will require much more resources to circulate GMM to over 80 endemic countries globally. All the measures mentioned above have their limitations

and different regions may have implementation based on resource availability, political will, sustainability, and malaria local transmission relapse is most likely possible in the long run of such approach, thus far, it seems scientifically unrealistic to say a malaria free world is at hand, this therefore means that the use of drugs as chemoprophylaxis, therapeutic agents will be necessary to reduce burdens and death associated to malaria. The continuation of care during pregnancy and children less than 5 years remains essential as the key target groups due to their compromised immunity and under development, respectively. Adoption to WHO treatment guidelines and implementation of sustainable control measures will be our place to go for a while before we can eradicate malaria from the global perspective.

2.7 Conclusion

This chapter affirms that a world without malaria is far from realisation and hence this study problem statement holds value for an unpredicted age ahead of us. Appropriate choices and use of antimalarial drugs will save more lives as the struggle continues to curb and eradicate this life-threatening disease.
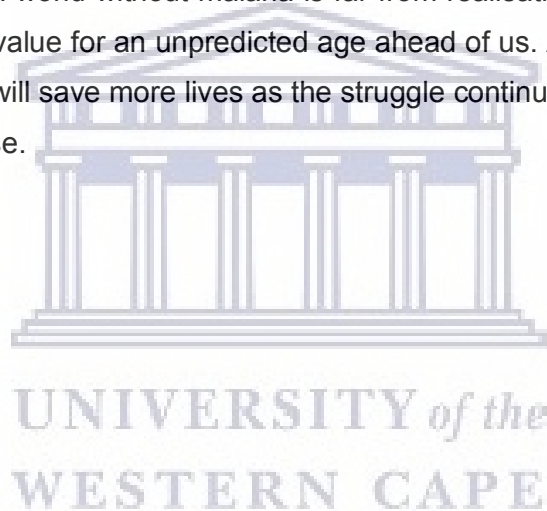
References

Alker, A. P., Mwapasa, V., & Meshnick, S. R. (2004). Rapid real-time PCR genotyping of mutations associated with sulfadoxine-pyrimethamine resistance in Plasmodium falciparum. Antimicrobial Agents and Chemotherapy, 48(8), 2924–2929. https://doi.org/10.1128/AAC.48.8.2924-2929.2004.

Benelli, G., Jeffries, C. L., & Walker, T. (2016). Biological control of mosquito vectors: Past, present, and future. Insects, 7(4), 1–18. https://doi.org/10.3390/insects7040052.

CDC (2021). *CDC - Malaria - Malaria Worldwide - Impact of Malaria*. [online] CDC. Available at: https://www.cdc.gov/malaria/malaria_worldwide/impact.html [Accessed 26 Feb. 2021].

CDC (2019). *CDC - Malaria - About Malaria - Biology*. [online] www.cdc.gov. Available at: https://www.cdc.gov/malaria/about/biology/index.html#:~:text=The%20malaria%20parasite%20life%20cycle [Accessed 26 Feb. 2021].

Chico, R. M., & Chandramohan, D. (2011). Intermittent preventive treatment of malaria in pregnancy: At the crossroads of public health policy. Tropical Medicine and International Health, 16(7), 774–785. https://doi.org/10.1111/j.1365-3156.2011.02765.x.

Chico, R. M., Chaponda, E. B., Ariti, C., & Chandramohan, D. (2017). Sulfadoxine-pyrimethamine exhibits dose-response protection against adverse birth outcomes related to malaria and sexually transmitted and reproductive tract infections. Clinical Infectious Diseases, 64(8), 1043–1051. https://doi.org/10.1093/cid/cix026.

Chico, R. M., Pittrof, R., Greenwood, B., & Chandramohan, D. (2008). Azithromycin-chloroquine and the intermittent preventive treatment of malaria in pregnancy. Malaria Journal, 7(January). https://doi.org/10.1186/1475-2875-7-255.

Crutcher, J., & Hoffman, S. (1996). Chapter 83: Malaria. Medical Microbiology 4th Edition, 3, 1–26.

Doumbe-Belisse, P., Ngadjeu, C. S., Sonhafouo-Chiana, N., Talipouo, A., Djamouko-Djonkam, L., Kopya, E., Bamou, R., Toto, J. C., Mounchili, S., Tabue, R., Awono-Ambene, P., Wondji, C. S., Njiokou, F., & Antonio-Nkondjio, C. (2018). High malaria transmission sustained by Anopheles gambiae s.L. occurring both indoors and outdoors in the city of Yaoundé, Cameroon [version 1; referees: 2 approved]. Wellcome Open Research, 3(0), 1–14. https://doi.org/10.12688/wellcomeopenres.14963.1.

Halberstadt. (2017). 乳鼠心肌提取 HHS Public Access. Physiology & Behavior, 176(5), 139–

148. https://doi.org/10.1016/j.addr.2016.05.007.BDDCS.

Haldar, K., Bhattacharjee, S., & Safeukui, I. (2018). Drug resistance in Plasmodium. Nature Reviews Microbiology, 16(3), 156–170. https://doi.org/10.1038/nrmicro.2017.161.

Hoglund, R. M., Workman, L., Edstein, M. D., Thanh, N. X., Quang, N. N., Zongo, I., Ouedraogo, J. B., Borrmann, S., Mwai, L., Nsanzabana, C., Price, R. N., Dahal, P., Sambol, N. C., Parikh, S., Nosten, F., Ashley, E. A., Phyo, A. P., Lwin, K. M., McGready, R., … Tarning, J. (2017). Population Pharmacokinetic Properties of Piperaquine in Falciparum Malaria: An Individual Participant Data Meta-Analysis. PLoS Medicine, 14(1), 1–23. https://doi.org/10.1371/journal.pmed.1002212.

Liu, Y. M., Zhang, K. E., Liu, Y., Zhang, H. C., Song, Y. X., Pu, H. H., Lu, C., Liu, G. Y., Jia, J. Y., Zheng, Q. S., Zhu, J. M., & Yu, C. (2012). Pharmacokinetic Properties and Bioequivalence of Two Sulfadoxine/Pyrimethamine Fixed-Dose Combination Tablets: A Parallel-Design Study in Healthy Chinese Male Volunteers. Clinical Therapeutics, 34(11), 2212–2220. https://doi.org/10.1016/j.clinthera.2012.10.001.

Marealle, A. I., Mbwambo, D. P., Mikomangwa, W. P., Kilonzi, M., Mlyuka, H. J., & Mutagonda, R. F. (2018). A decade since sulfonamide-based anti-malarial medicines were limited for intermittent preventive treatment of malaria among pregnant women in Tanzania. Malaria Journal, 17(1), 1–7. https://doi.org/10.1186/s12936-018-2565-1.

Musiime, A. K., Smith, D. L., Kilama, M., Rek, J., Arinaitwe, E., Nankabirwa, J. I., Kamya, M. R., Conrad, M. D., Dorsey, G., Akol, A. M., Staedke, S. G., Lindsay, S. W., & Egonyu, J. P. (2019). Impact of vector control interventions on malaria transmission intensity, outdoor vector biting rates and Anopheles mosquito species composition in Tororo, Uganda. Malaria Journal, 18(1), 1–9. https://doi.org/10.1186/s12936-019-3076-4.

Sabin, L., Hecht, E. M. S., Brooks, M. I., Singh, M. P., Yeboah-Antwi, K., Rizal, A., Wylie, B. J., Bondzie, P. A., Banos, M., Tuchman, J., Singh, N., & Hamer, D. H. (2018). Prevention and treatment of malaria in pregnancy: What do pregnant women and health care workers in East India know and do about it? Malaria Journal, 17(1), 1–13. https://doi.org/10.1186/s12936-018-2339-9.

Salvador, E. (2020). Becoming malaria free by China is hosting the 3rd. ed -2020 global. January 2018, 1–5.

Sulaiman, S. A., & Jamaludin, S. E. (2013). A Study on the Use of Orifice Plates as Steam Traps. 201(4), 593–598. https://doi.org/10.1007/s00430-012-0272-z.Malaria.

Unger, H. W., Hansa, A. P., Buffet, C., Hasang, W., Teo, A., Randall, L., Ome-Kaius, M., Karl, S., Anuan, A. A., Beeson, J. G., Mueller, I., Stock, S. J., & Rogerson, S. J. (2019). Sulphadoxine-pyrimethamine plus azithromycin may improve birth outcomes through impacts on inflammation and placental angiogenesis independent of malarial infection. Scientific Reports, 9(1), 1–12. https://doi.org/10.1038/s41598-019-38821-2.

WHO (2020a). *WORLD MALARIA REPORT 2020*. [online] Available at: https://reliefweb.int/sites/reliefweb.int/files/resources/WMR-2020-v5-double-embargoed.pdf [Accessed 25 Jan. 2021].

WHO (2020b). *WHO takes a position on genetically modified mosquitoes*. [online] www.who.int. Available at: https://www.who.int/news/item/14-10-2020-who-takes-a-position-on-genetically-modified-mosquitoes. [Accessed 25 Jan. 2021].

WHO (2018). *This year's World malaria report at a glance*. [online] www.who.int. Available at: https://www.who.int/news/item/19-11-2018-this-year-s-world-malaria-report-at-a-glance [Accessed 26 Jan. 2021].

WHO (2019). *World malaria report 2019*. [online] www.who.int. Available at: https://www.who.int/publications/i/item/9789241565721 [Accessed 26 Feb. 2021].

Wilson, A. L., Courtenay, O., Kelly-Hope, L. A., Scott, T. W., Takken, W., Torr, S. J., & Lindsay, S. W. (2020). The importance of vector control for the control and elimination of vector-borne diseases. In PLoS Neglected Tropical Diseases (Vol. 14, Issue 1). https://doi.org/10.1371/journal.pntd.0007831.

World Health Organization (2018). *Implementing malaria in pregnancy programs in the context of World Health Organization recommendations on antenatal care for a positive pregnancy experience*. [online] apps.who.int. Available at: https://apps.who.int/iris/handle/10665/259954 [Accessed 26 Feb. 2021].

CHAPTER 3

Solid-state chemistry of drugs

3.1 Introduction

Limited solubility of over 40% of drugs in biological fluids have always posed immense challenges to the pharmaceutical industry. A large percentage of drugs are developed for oral administration due to the advantages this route holds over other administration routes. Despite being the most acceptable route of administration, poor aqueous solubility of drugs makes using the oral administration route challenging, especially in instances where effective drug treatment is critical (Homayun *et al*., 2019). This chapter will focus on the physico-chemical properties of drugs, the typical solid-state form modifications that may be used as strategies to improve aqueous solubility of any given drug and how these preformulation aspects link to drug absorption and bioavailability.

3.2 Physico-chemical properties of drugs

As already mentioned, most drug compounds have inherent poor aqueous solubility and diversified tissue permeation properties that hinder their application for therapeutic functions (Vogel et al., 2013). This led to the development of a drug grouping system by Amidon *et al*, (1995), Biopharmaceutics Classification System (BCS)) (Amidon et al., 1995); based on the solubility and permeability properties of a drug. It categorises drugs into one of four classes, as summarised in (**Table 3.1).** BCS, class I drugs have high solubility and high permeability.. These characteristics facilitate the rapid dissolution of the drugs belonging to this class into the gastro-intestinal fluids and compared to the other BCS classes these drugs are preferred in solid dosage formulation. BCS II drugs possess low solubility characteristics with high permeability properties; drugs belonging to this class may require some level of manipulation during pre-formulation to increase the poor solubility of the drug to attain a reasonable amount of drug in the gastro-intestinal tract (GIT) which could potentially increase the drug concentration reaching the systemic circulation. BCS III drugs are exactly opposite to those belonging to the BCS II class, exhibiting good solubility and poor permeability. This class too may be modified to improve absorption and bioavailability, typically by formulating these drugs together with molecules that exhibit permeation enhancing attributes. BCS IV drugs are the most complicated drugs to deal with, these drugs exhibit both poor solubility and permeability characteristics (Benet, 2013; Prashantha Kumar *et al*., 2010), only about 6% of drugs in the BCS IV class reach the market, due to the core challenges not only with regards to the dosage

formulation process but also linked to inherent molecular attributes which renders these drugs poorly soluble and permeable across biological membranes. About 70% of available marketed dosage forms are solid preparations, either in the form of tablets, capsules or powders and hence solubility in gastro-intestinal fluids to aid cellular permeation are essential. These two factors play a key role in determining dose strength of a particular drug.

Table 3.1: Summary of BCS drug classes (Jagtap *et al*., 2018)

Class	Solubility	Permeability
Class I	High	High
Class II	Low	High
Class III	High	Low
Class IV	Low	Low

3.3 Solubility

This refers to the capacity of the solute to dissolve in a solvent. With regards to drugs, the amount of drug that gets dissolved in aqueous media is of essence to pharmaceutical companies (Byrn *et al.*, 2017). Solubility and dissolution are completely different though they may have similar outcomes in practice. Solubility is basically the maximum amount of the solute that a pure solvent can hold homogeneously, any excess added may result in solvent saturation, a state where no more solute gets dissolved. It does not indicate the time duration the process takes, but the final endpoint. The understanding of how fast or slow a solute mixes with a solvent to form a solution is where the term dissolution rate is applied. Some drugs may have poor solubility with fast dissolution rate or good solubility with slow dissolution rate and vice versa (Dhobale & Dhembre, 2018; Jagtap et al., 2018; Savjani et al., 2012). It can be expressed in general terms as being soluble, slightly soluble, and insoluble or termed precisely by unit as follow:, milligram/millilitre (ml/mL), gram/litre (g/L), percentage gram (g%), ultimately showing the amount of solute solubilized in a solvent at equilibrium. Solubility is affected by several factors such as:

- **Particle size**: smaller particles have greater interaction with solvent, decreasing particle size of an insoluble solid material would not necessarily mean improving its

solubility property. This comparison applies for same or similar compounds with intrinsic solubility capacity.

- **Temperature**: increasing the energy of the system facilitates the molecular movement and reduces the time for equilibrium to be attained. It depends greatly on whether a particular solubility system is endothermic, requiring addition of energy in the system or exothermic, emitting energy off the system to complete its process.
- **Polarity:** The like-dissolves-like principle rules here, polar solute is solubilised by polar solvent, non-polar solute is dissolved in non-polar solvent.
- **Thermodynamics of the solute and solvent:** this relates to the system's available energy measured at constant temperature and pressure, and was represented mathematically by Gibbs as:

$$\Delta G = \Delta H - T\Delta S \qquad \text{(Equation 3.1)}$$

Where ΔG is the change in Gibbs free energy, ΔH, denotes the change in enthalpy, T signifies temperature and ΔS, the change in entropy. Generally, a negative ΔG is considered thermodynamically favourable although this alone does not imply a solute will definitely be soluble in a given solvent, other factors play a role too (Byrn et al., 2017).

- **Molecular size and weight:** Large molecules are difficult to dissolve as solvent takes a longer time to surround and penetrate into the intramolecular space and solubilise it (Jagtap et al., 2018).

3.4 Dissociation constant (pKa)

The acid-base dissociation constant, pKa, is one of the essential parameters in determining biological interactions with drugs, physiological systems have wide range of pH and the rate at which a drug diffuses across membranes is directly affected by its ionic states, there is direct correlation between the pKa of the drug and the lipophilicity, pharmacokinetic properties; solubility, absorption, metabolism, distribution, and elimination (ADME) of the compound. Most pharmaceutical medicinal compounds and marketed drugs are weak acids and bases meaning they are affected by pH of the environment for their ionisation. Weak acids dissociate in higher pH whilst weak bases ionise in low pH conditions (Bertone, 2020; Manallack, 2011). A drug with poor aqueous solubility can be manipulated during formulation by enhancing its ionisation through application of the salt form of such drug, an approach that will be discussed further along in this chapter (Gupta et al., 2018).

As discussed, physico-chemical properties of drugs have a significant impact on not only the processability of a drug but also the ultimate behaviour of the drug post administration to the patient.

3.5 Solid-state forms of drugs

Numerous strategies have been applied by the pharmaceutical industry to solve the poor aqueous solubility exhibited by a significant number of drugs. These are associated with physico-chemical characteristics of such drugs, polymorphism, solvate, amorphous, co-crystals, co-amorphous.

3.5.1 Polymorphism

The term polymorphism comes from a Greek word; *poly* meaning many, *morph* meaning form. This is the ability of a solid material to exist into two or more crystal forms, due to the differences in molecular arrangement, each of the polymorphic forms may consist of a complete different set of physico-chemical properties, such as melting point, hardness, structural arrangement, solubility, dissolution rate, physical and chemical stability and so forth. These characteristic differences would therefore influence the choice of the form to be used during processing and design of the dosage formulation (Chistyakov & Sergeev, 2020). Of the various forms, one is always stable at all conditions possible, often than not, the more unstable (metastable) form is more soluble as opposed to the stable form (Lakshmi Prasanthi *et al.*, 2016). Which therefore poses a question, could there be ways to use the unstable form, if possible, what conditions are required to maximise its potential for improved solubility and how can those conditions be kept constant throughout the drug's shelf life? Studies have shown that over 59% of molecules have some form of polymorphism in nature, and they can convert from one form to the other, especially the meta-stable form(s). It is therefore critical to evaluate pharmaceutical preparation and understand conditions influencing each crystal alteration to avoid the negative impact it may result in such as solubility, bioavailability and toxicity (Censi & Di Martino, 2015; Raza, 2014; Saifee *et al.*, 2009).

3.5.2 Solvates

When a specific solid-state form of a drug undergoes recrystallisation, it may trap solvent molecules within the molecular structure, this results in a packed crystal structure with solvent molecules inside it, this is called solvates or hydrates when water is entrapped. Any crystals without solvate (water) entrapment are called anhydrates. This may happen during production processes where formulation applications require solvent addition such as spray dry, solvent

evaporation, lyophilisation, wet granulation, film coating or may be affected by environmental factors during. Solvates may play diversified roles in crystallisation, stability; when solvates are involved in hydrogen bonding in the particles packing, it improves on crystal structural stability and desolvation may lead to crystal collapse and when recrystallised, a new form of crystal lattice is formed (Alexander Taylor Florence, 2011). These solvates have poor solubility behaviour due to the aforementioned phenomena. The second type of solvates occur without affecting the crystal lattice, once removed from the system, no further recrystallisation occurs, this may also be termed as a *pseudopolymorphic* solvate. Contrary to the previous type, solubility of the final product may not be altered as solvent does not form part of the crystal lattice, simply occupies the void space within the structure. Drugs may have different amounts of solvate and hence they may be classified as mono-, di-, tri- (hydrates) in the case of water, for example; azithromycin dihydrate and atorvastatin calcium trihydrate (Alexander Taylor Florence, 2011; Chadha *et al*., 2012; Ranjan *et al*., 2020). Thorough investigation and understanding of the drug interaction with solvent is crucial in the pharmaceutical industry, to guide the choice of whether to use an anhydrous or hydrate form of a compound. These different forms have implications in solubility, absorption, efficacy and bioavailability properties (Gupta *et al*., 2018).

3.5.3 Co-crystal

There is similarity between co-crystals and solvates; both contain two different molecules in the solid structure, the difference lies in the matter state of compounds involved. The former involves a liquid and solid packing pattern while co-crystal is a solid-to-solid crystalline lattice packing in the final solid structure. The process is facilitated by the intermolecular force through hydrogen bonding and its possible between functional groups such as carboxylic acid– amide, carboxylic acid–aromatic nitrogen, and alcohol–pyridine; interaction results into a slightly weaker bonding compared to ionic and covalent bonds and this has pharmaceutical benefits, (Thayyil *et al*., 2020) although ionic and Van der Waals forces, lipophilic-lipophilic interactions and pi-pi interactions have shown impact in co-crystallisation. The alteration of structural packing has been shown to change physico-chemical properties such as melting point, dissolution rate, and solubility, to mention a few, **Figure 3.1** shows a possible packing pattern of co-crystals. A study conducted on co-crystals of the anti-tuberculosis drug, isoniazid, yielded multiple options of solid drugs providing different properties; co-crystal, eutectic and hydrated mixture ionization complexes were formed and all had improved solubility (Cherukuvada et al., 2016). Drugs do not naturally exist as co-crystals; the process requires certain formulation techniques to attain a final stable solid form of interest. The techniques that have been proven include among others; (i) solvent evaporation method,

where two drugs or API and co-former are dissolved in an organic solvent and allowed to recrystallise while solvent is removed, (ii) mechanical methods, grinding either with solvent aided or without solvent, (iii) Spray drying method, (iv) crystallisation from the melt (hot melt extrusion) (Patole Tanvee & Deshpande Ashwini, 2014).
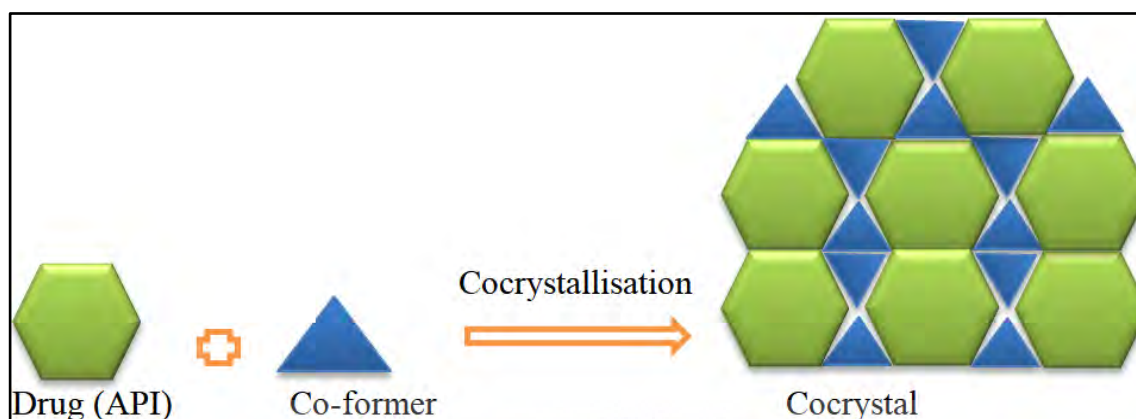
Figure 3.1: An illustrative example of packing pattern of co-crystal (Patole Tanvee & Deshpande Ashwini, 2014).

3.5.4 Salt solid forms

Modification of solid drugs by salt formation has been known and applied in drug development and manufacturing processes for years. Over 50% of the United States (U.S) Food and Drug Agency (FDA) approved drugs have salt modifications, this mechanism alters the physical structure of the drug and can completely differ from its acid conjugate, the alteration provides benefits by increase ionisation properties at physiological pH ranges. Furthermore, physico-chemical properties such as crystal habit, hygroscopicity, solubility, dissolution rate, stability, and impurity profiles of a compound can be influenced by salt formation and ultimately bioavailability of such drugs can be affected (Gupta *et al*., 2018; Paulekuhn *et al*., 2007). It is important to note that adding salt as an ionisation enhancer does not always improve solubility. An appropriate choice of the compound and chemical entity has to be considered during the process, being the only chemical modification applied in pharmaceutical industry to improve drug poor aqueous solubility both at development stage and formulation, critical understanding of the pKa of the drug, pH of intended site of absorption and the strength of counterion involved in the chemical interaction are valid aspects to be analysed beforehand. Crystallinity and precipitation of the salt compound in physiological conditions are dependent upon the proton exchange capability and are the propelling reasons for types of acceptable salt entities in the pharmaceutical industry. Most available pharmaceutical salts contain hydrochloride and sodium as bases and acid API entities respectively (Brittain, 2009; Hubs, 2020). Additionally,

salt formation may be an option to stabilise an API from degradative activities, the presence of an ionic bond in a structure could lead to a more stable crystalline structural lattice as opposed to the individual salt free compound. A study done on atorvastatin indicated that atorvastatin calcium or sodium resists lactone formation that occurs in an acid environment due to a chemical degradation process (Hubs, 2020).

3.5.5 Amorphous and co-amorphous solid-state forms

The process of forming amorphous drugs may lead to various classes of solid-state forms. An amorphous compound is a solid-state form signified by a disorganised molecular structure with the lattice showing short orderly arrangement of molecules as compared to the crystalline, highly organised molecular arrangement. When two compounds are prepared and allowed to interact and form an amorphous solid dispersion, the resultant structure is termed co-amorphous (Descamps, 2016). With increasing poor aqueous drug solubility, pharmaceutical sciences search for alternative solid dosage formulation. The challenge in terms of drug bioavailability can be addressed through selecting its amorphous form in the preparation of the oral dose. Co-amorphous forms of drug molecules have been extensively studied as a measure to enhance drug solubility properties (Chavan et al., 2016a). The formation of co-amorphous forms is associated with molecular structural functional groups such as hydrogen bond donors and acceptors that provide available intermolecular interactions between the different APIs. This phenomenon leads to a disorganized state of molecular arrangement within the overall structure as opposed to their individual crystalline structure and it is advantageous in that the internal system provides enough energy that ultimately enhances solubility (Newman et al., 2018). The resultant solid product may be classified further on the basis of physical state and solid phase as:

- **Eutectic mixture**, it is a mixture of two or more solid components without necessarily having chemical interactions to form a new solid entity but, based on certain ratios may inhibit the crystallisation process of the individual amorphous compound in the mixture leading to a solid-state system possessing a lower melting point than either of the components (Stott et al., 1998). This can occur between drugs (drug-drug), drugs and excipients or excipients (excipient-excipient), and has a vast scope in pharmaceutical applications. Factors responsible for eutectic mixture formation are: (a) compatibility, since the components must be miscible in liquid form and highly immiscible in solid state, (b) intimate contact between components is necessary for contact induced melting point depression, and (c) functional groups, the presence of chemical groups that is capable of forming physical bonds such has intermolecular hydrogen bonding are essential for eutectic mixture formation (Bi *et al*., 2003).

- **Glass suspension,** this system consists of components that may have amorphous carriers and the drug in the form of either molecular dispersion or an amorphous precipitate into the carrier, and can possibly recrystallise or form phases during a favourable condition in time (Janssens & Van den Mooter, 2009). It can also occur through the conversion of glass solution to a glass suspension. Studies have shown that drug may remain in the amorphous form, and exhibits an increase in dissolution behaviour as compared to its crystalline counterpart, however, it has a high affinity for recrystallisation facilitated by the different in transition temperatures (Tg), often than not, the Tg of the drug or drug-rich phase is lower than the Tg of the polymer carrier or polymer-rich phase (Singh *et al.*, 2017) The phenomenon results in limited benefit in oral dosage formulation.

- **Glass solution** is generally a homogenous system consisting of glassy components, resulting from a solute being dissolved in a solvent that is in a glassy state or by other methods such as hot melt. A sudden quenching of the melt may lead to a glass of either a pure chemical or their mixtures in a vitreous (glassy) state. Furthermore, there is significant difference in the chemical bonds of a glass solution in both strength and length, and as such; no exact temperature breaks these bonds simultaneously, hence the system does not exhibit a sharp melting point. Studies have shown that compounds such as sugars, glucose, sucrose, and ethanol, 3-methylhexane can form glasses readily upon rapid cooling of the liquid state. In addition, the higher dissolution rates have been associated with the glass solution formed by combining aqueous insoluble API with water-soluble polymer/ carrier following fast dissolution of the carrier compound upon exposure to aqueous medium. This dissolution rate is expected to be higher in comparison to that of the solid solution formulation (Craig *et al.*, 1999; Singh *et al.*, 2017).

This solid dispersion form is also termed as glass structure and may exist as a single phase of the API or APIs where co-formulation is involved (Karagianni *et al.*, 2018).
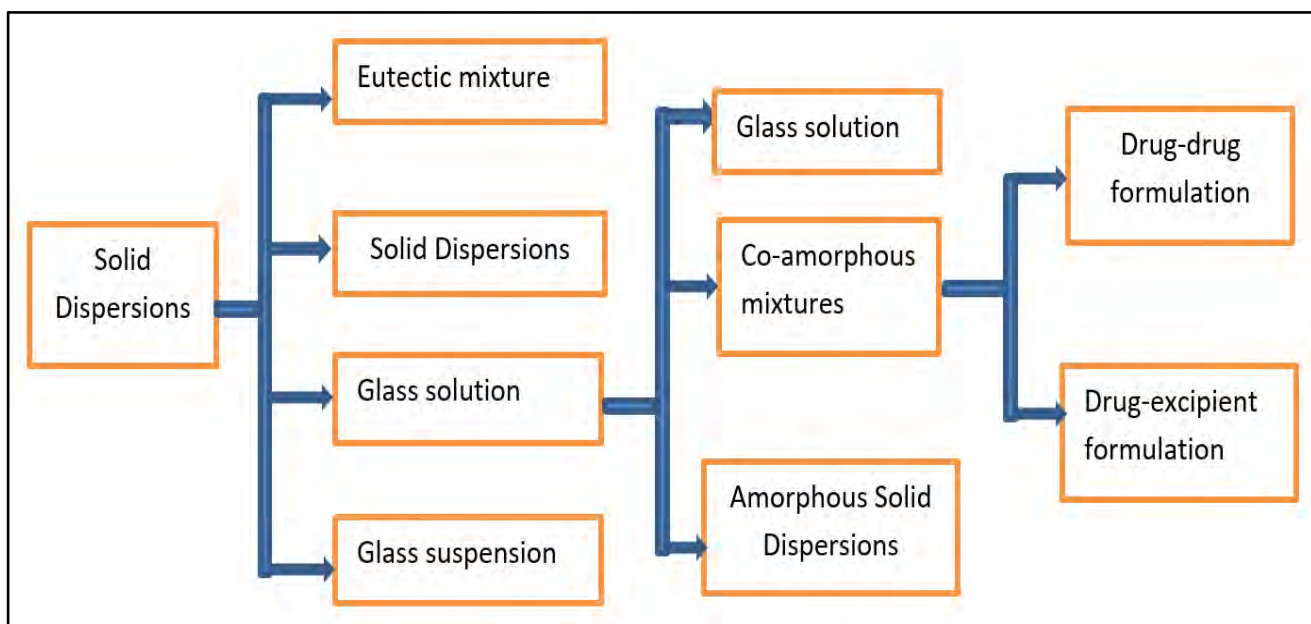
Figure 3.2: Representation of possible forms of final products during formulations (Karagianni *et al*., 2018).

Amorphous drugs or compounds are known for their inherent improved solubility properties as opposed to the crystalline forms. This being due to the higher degree of available free energy allowing amorphous forms to go into solution at a faster rate. A study conducted by Aucamp *et al*, (2016) confirmed that SUL can be prepared as an amorphous solid-state form (Aucamp *et al*., 2016). Past literature also indicated that a stable amorphous form of AZI is possible to prepare by hot melt extrusion and quench cooling methods (Aucamp *et al*., 2015; Jaiswar *et al*., 2016; Montejo-Bernardo *et al*., 2005) and this can be employed co-amorphous with other APIs or a polymer as a stabilizer. The amorphous form of poorly aqueous soluble drugs play an important alternative for improved solubility and bioavailability but pose risk of stability due to recrystallization to their stable solid form- crystalline (Chavan *et al*., 2016b; Newman *et al*., 2018). To combat this, attempts have been made to prepare co-amorphous forms with either drug-drug or drug-polymer combinations to stabilise the amorphicity of the solid-state throughout manufacturing, storage, transportation and shelf life, refer to (**Figure.3.1)** (Jensen *et al*., 2016; Karagianni *et al*., 2018; Moinuddin *et al*., 2017). Key questions every researcher and drug developer have to frequently ask are; firstly, can a solid amorphous form be formulated from a drug compound? Secondly, how will the stability issue be addressed through the process? This current study will attempt to answer the above concerns in malaria medications prescribed for IPTp in Sub-Saharan Africa.
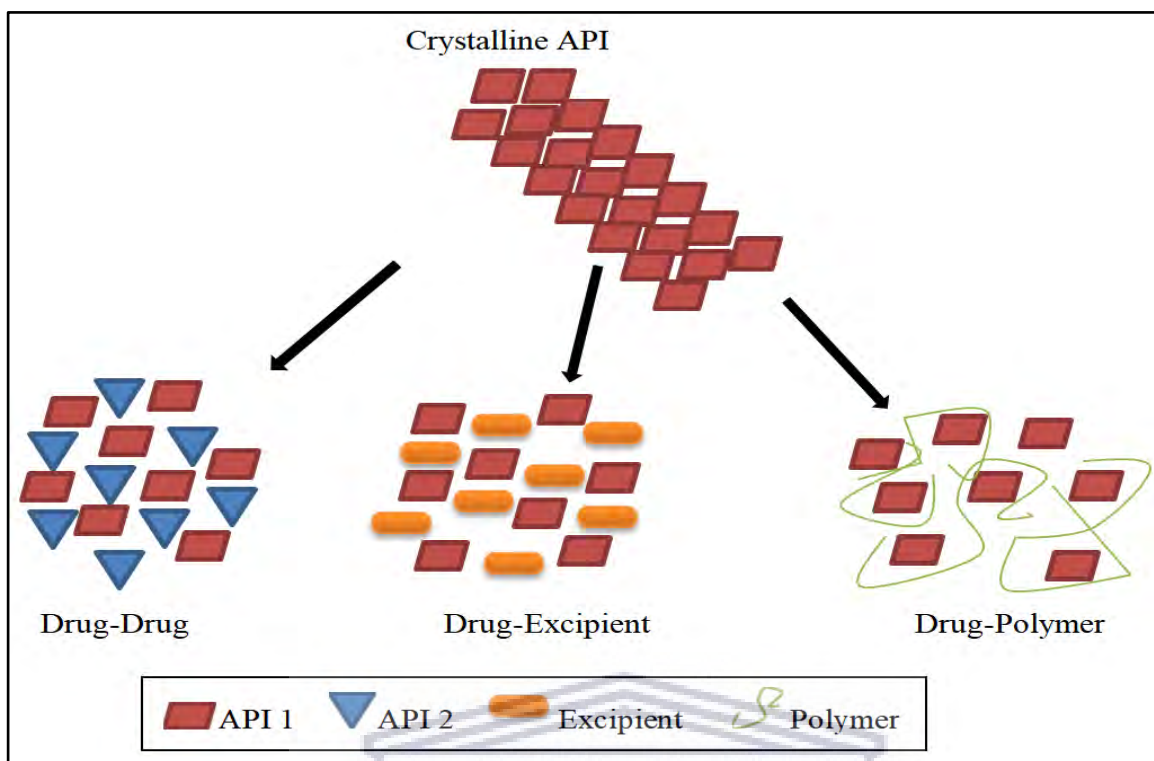
Figure 3.3: Showing three possible Co-amorphous solid forms (Shi *et al.*, 2019).

3.5.6 Solid-State phase transformation

A solid-state phase transformation is an interfacial change occurring between two different solid phases, the chemical and physical conditions must favour an interchange of a material (Qi *et al.*, 2018). The general perspective in pharmaceutical product solid-state phase transformation lies within the Gibbs free energy a compound possesses, this is in accordance with the principle of energy conservation, materials are stable where there is low internal energy. As mentioned early on in this chapter, many APIs can exist in different solid-state physical forms, such as co-crystal, amorphous, solvates, hydrates, or as polymorph solid forms. They may have different physico-chemical properties, including among others, density, melting point, electrical and optical profiles, dissolution rate and solubility (Jug *et al.*, 2010; Milne *et al.*, 2015; Santana *et al.*, 2021). These activity variations of the APIs can have a direct impact on their processability, quality and/or the ultimate performance of final drug products marketed for use. The design, manufacturing processes, transportation and storage conditions can alter the physical form of drugs in the final products through the mechanism of their solid-state phase transformations. As seen in (**Figure 3.4**), these transformations, including hydrates formation, dehydration of hydrates, polymorphic interconversion, de-

solvation of solvates or conversion of the crystalline to amorphous form, can be facilitated via various pharmaceutical processes, such as wet granulation, hot melt extrusion, milling, spray drying, compression, solvent evaporation procedures just to mention the few. Some of these mechanisms may be directly intended in the formulation of a dose, however, an unplanned conversion may occur affecting the final product's efficacy (Lin, 2015). The typical example was the withdrawal of ritonavir from the market following its solid-state phase trans-formation where a semisolid formulation transformed into an unexpected polymorph of ritonavir during storage (Chemburkar *et al.*, 2000). Thus, the most appropriate preventive measure is to formulate the stable form of the APIs in the case of polymorphs or amorphous forms that have limited chance of solid-state transformation during the drug entire life period, to achieve this, an early intervention and intensive study of physico-chemical properties of an API during dosage development is required to elucidate and detect possible transformations of solid-dosage forms (Lin, 2015).

.
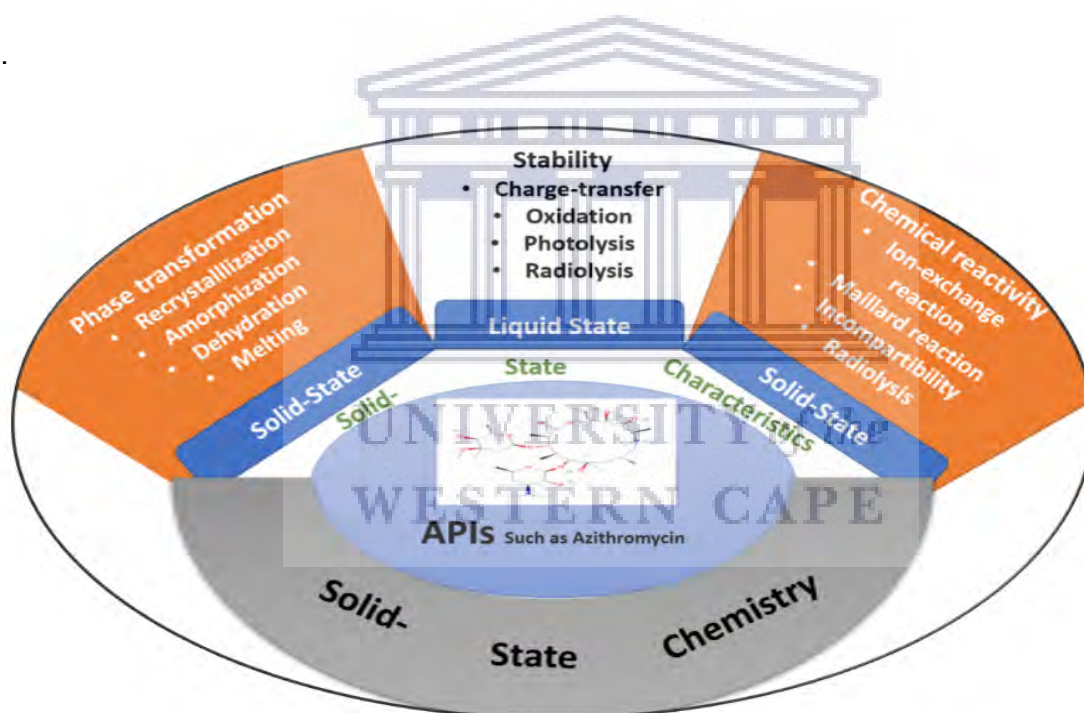
Figure 3.4: Summary of solid-state phase transformation (Lin, 2015).

3.5.7 Preparation methods

Amorphous drugs can be formulated by many methods, however the choice and applicability of the method depends on resources and production quantitative process status. The following methods have been applied and yielded results.

Melt method, under this method, the solid crystalline drug(s) are heated above the melting point and mixture depending on the nature of preparation, whether co-amorphous design with drug-drug or drug excipient (polymer) mixture or single conversion of a drug into its amorphous form, once the homogenous liquid state is reached, the cooling process commences following either room temperature cooling process, ice bath agitation, spray congealing, liquid nitrogen, dry ice or by use of a desiccator **(Figure 3.5)**. Cooling is one essential step that facilitates solid packing pattern, the speed at which energy is lost from the molten preparation dictates the level of disorganisation in the final solid lattice, hence resulting in amorphous solid state properties (Chavan *et al*., 2016a; Jaiswar *et al*., 2016; Schittny *et al*., 2018).
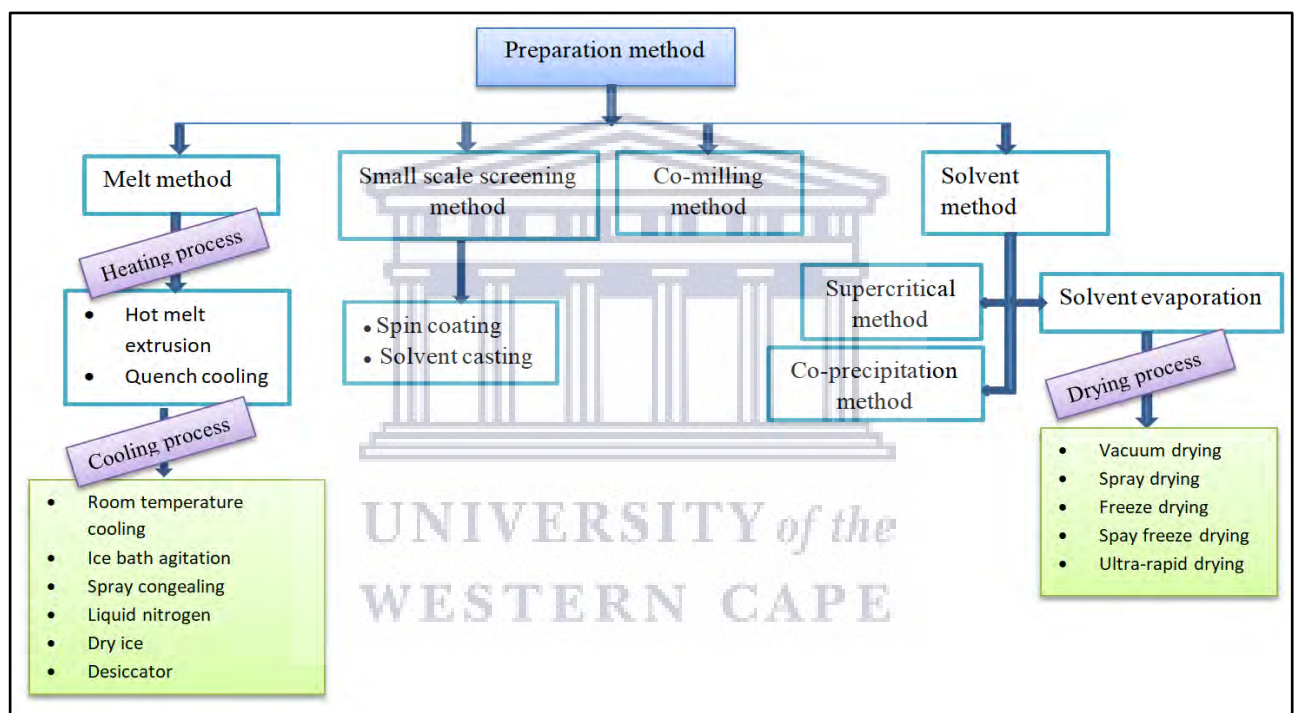
Figure 3.5: Summary of amorphous (Co-amorphous) preparation methods (Meng *et al*., 2015).

Table 3.2 : shows examples of drugs and methods used for preparation

Co-amorphous drugs	Type of co-amorphous	Formulation methods	Outcome of the study
Valsartan-L-arginine + L-lysine	Co-Amorphous Dispersions with Salt Formation	Vibrational ball milling	Solubility increased approximately 1000 folds compared to crystalline form (Huang *et al*., 2017).
Indomethacin- Arginine	Drug-Amino Acids	Spray drying	Immediate drug release through erosion with similar dissolution property (Shi *et al*., 2019).
Olanzapine-ascorbic acid	Drug-Carboxylic Acids	Solvent evaporation	600 folds increase in solubility, 95% dissolution rate in 10 minutes (Maher *et al*., 2016)
Indomethacin-Naproxen	Drug-drug	Melt Quenching	Increased stability and dissolution 7.6 folds (Shi *et al*., 2019).
Lacidipine-Spironolactone	Drug-drug	Solvent evaporation	Increased stability and solubility (Wang *et al*., 2019).
Nateglinide -Metformin hydrochloride	Drug-drug	Solvent evaporation	Increased release rate and synergistic action (Wairkar & Gaud, 2016).
Atenolol-hydrochlorothiazide	Drug-drug	Cryomilling	Improved physical stability compared to the individual amorphous forms (Moinuddin *et al*., 2017).

The three methods that were applied in this study included, quench cooling of the melt, solvent evaporation and spray drying.

Solvent Evaporation

The drug will be dissolved under suitable conditions and solvent allowed to slowly evaporate, this leads to formation of new solid drugs mass (Newman *et al*., 2018) are prepared in this technology (Kawakami, 2009).

Spray dry method

This is a technique intensively used in the chemical, food, pharmaceutical and biopharmaceutical industry, it involves spraying a solution containing the API(s) into a chamber of hot air that dries the droplets of solution instantly. The resulting particles are collected as a powder consisting of small particles (Jain *et al*., 2012).

Quench Cooling During this preparation technique the drug or combination of drugs is heated until all crystalline drug particles have dissolved. The molten product is then removed from the heating plate or oven and quenched on a cold surface.

3.6 Dissolution

Oral dosage forms undergo diversified mechanisms to reach the target site and deliver the required pharmacological effects. The process the solid drug gets into solution with a solvent is referred to as dissolution. This is a kinetic phenomenon and often measured in rates at which it occurs (dissolution rate). It can also be expressed mathematically according to Noyes-Whitney equation as:

$dm/dt = A \ (D/d) \ (C_s - C_b)$ (Equation 3.2)

where;

- Dm/dt = drug solute dissolution rate (gram per second)
- m = mass of dissolved drug (gram)
- t = time (second)
- A = surface area of drug solute particle (meter)
- D = diffusion coefficient (meter/second)
- d = thickness of the concentration gradient (m)
- C_s = drug particle surface concentration (gram or mole/Litre)
- C_b = drug concentration in the bulk solvent (gram or mole/Litre) (Byrn, *et al*,. 2017).

This equation provides information on how dissolution is affected over time, the concentration at the solute surface is higher than that in solution, as time progresses and depending on the

sink condition, the dissolution rate will reduce. The physiological system of gastrointestinal tract (GIT) has wide range of pH (0.8-7.4), more basic in the mouth due to salivary amylase, strongly acidic in the stomach as a result of gastric juice and hydrochloric acid and again more basic in the intestinal area due to bile content (Patricia and Dhamoon, 2020). To accurately predict the *in vivo* results, factors such as pH, drug physico-chemical properties and the solubility of the drug in both aqueous and lipids are of paramount importance (Mudie *et al.*, 2020). Poor bioavailability of oral drugs are linked to their solubility and dissolution plays a key role in ensuring drugs break apart from the mass dosage form within the gastrointestinal tract (GIT) and are freely available for absorption (Zaborenko *et al.*, 2019).

3.7 Absorption

This process involves movement of drug compounds that are not metabolised from the site of administration to the circulatory system. Examples of routes of drug administration include, intravenous (IV) system, intramuscular (IM), oral, intradermal, subcutaneous, inhalation to mention but a few. In the case of oral dosage form, drugs must manoeuvre through and across the GIT barriers, its content fluids mixed and cross intestinal cellular membrane to reach circulation and get distributed to target sites. There are possible two forms of drug molecules in the GIT, the ionised and unionised, this happens because of individual physico-chemical properties and physiological conditions (pH) of the person exposed to the drug compound and this guides the prediction for absorption mechanism and route the compound will traverse across membranes. There are two mechanisms for absorption, passive diffusion and carrier-mediated transport system (Alagga & Gupta, 2020; Montoto, 2018).

Passive diffusion is based on concentration gradient, molecules cross membrane from areas of high concentration to areas of low concentration, the process continues until equilibrium is achieved, in medication, attaining equilibrium is almost impossible since drugs are given at interval dosing frequency and the blood circulation is in constant flow, driving away the absorbed molecules. It occurs via aqueous medium and lipid system, aqueous diffusion system happens from the GI fluids compartment via intestinal pores or may take place in the endothelial spaces in the blood vessels; meanwhile, the lipid diffusion happens particularly on larger molecule bound to proteins or albumin crossing through the lipid compartment. The latter is the most applicable route of permeation as large sections of the body parts consist of lipid units. On the other hand, carrier-mediated transport system is facilitated by specialised transporters particularly for ions and nutrients, vast majority of these transporters are found in the small intestine where most absorptions are favoured by large surface area, microvilli and villi availability and longer transient time of about 3-4 hours, these factors allow more

interactions between drug molecules and carrier-mediated transporters. Carrier-mediated transport systems can be subdivided into active and facilitated diffusion; in active diffusion the drug moves from an area of low concentration to an area of high concentration, against concentration gradient, it consumes energy. Drug molecules form complexations with specific carriers and are transported across the membrane where it dislodges leaving free carriers for the next pick up. The process is suitable for water soluble drugs that mimic the intrinsic physiological compounds such as 5-fluorouracil found in the GIT (Alagga & Gupta, 2020). Because of the fewer number of these specialized transporters, the amount of drug absorbed is limited to the number the available carrier-mediated is capable of transporting; increasing the concentration may not affect the ultimate drug in circulation. Other limiting factors include energy dependent transporters such as P-glycoprotein (P-gp) that facilitates efflux of drug molecules to the GIT. Facilitated active diffusion is similar to active diffusion in that both are selective to particular drug molecules and are limited to availability of carriers (saturation) the key difference is that no energy is required, hence it cannot transport against concentration gradient. Typical example of this transporter is organic cation transporter1 (OCT1) useful for transportation of metformin (Alagga & Gupta, 2020; Dujic et al., 2016).

Other factors that play a significant role in absorption are drug specific physicochemical and dosage content variations, typically, pH, pKa, ionisation of drugs are variables that may need critical understanding before designing an oral dosage form of any drug compound. Non-ionised are often lipophilic and may permeate cell membranes easily as opposed to ionised counterparts that require some form of mediation. Furthermore, the surface area, particle size, nature of the dosage form and solid structural differences such as amorphous, crystalline, polymorphism, contribute to a diversified amount and extent of absorption which ultimately affects drug plasma concentration and bioavailability (Martinez & Amidon, 2002).

3.8 Bioavailability

The drug administered into biological components has an intended target and sites of action for the realization of its therapeutic effect; the measure of the available fraction that reaches such a biological unit is referred to as drug bioavailability. The term is commonly applied to active drug molecules found in the systemic circulation following the administration, assuming its distribution is impeded 100% internal body fluids system, it should be noted that topical medication may not necessarily reach such a compartment and to determine its bioavailability a separate approach has to be applied (Price & Patel, 2020). Depending on the route of administration, different fraction of active pharmaceutical compounds may reach the target implying that dosage variation is required, for example, IV route provides 100% bioavailability,

the rest of other routes require absorption hence, some portions of the drug are negatively affected. Taking oral route as the main focus of this study, only a limited fraction of drugs may gain systemic circulation due to factors mentioned early in this chapter, intestinal and first pass metabolic effects (Alagga & Gupta, 2020; Price & Patel, 2020).

In addition, factors such as clearance and distribution also affect bioavailability. Clearance refers to the rate and extent the body eliminates drugs from the systemic circulation, it occurs via numerous excretory routes such as bile system, renal system, skin, respiratory system. Drugs may be eliminated unaltered or as metabolites, the rate depends on either of the two common kinetic mechanisms; zero order and first order kinetic. In zero order, a constant fraction of drug is removed from the biological system per unit time until a completion independent of drug plasma concentration, it also takes inconsideration saturation brought about by absorption and elimination rate, the effect may lead to drug toxicity in situation where drugs have long half-life and shorter dosing frequency is recommended. First order kinetic, a constant amount of drug is eliminated over time through intrinsic half-life, the fraction of the drug is removed in an exponential manner, the higher the plasma concentration, the more the drug gets eliminated from the system (Currie, 2018; Price & Patel, 2020). Understanding of bioavailability in conjunction to factors affecting it, helps to determine a therapeutic steady state for a particular drug, guiding the dosage strength and frequency, the implication of varied bioavailability of a drug have drawbacks such as; in case of low plasma concentration it may lead to therapeutic failure and possible risk of resistance for antimicrobial while higher concentration results in toxicity and sides effects (Currie, 2018).

3.9 Conclusion

In conclusion, the drug molecular properties, their dosage forms, routes of administration and the physiological system of the intended user have implications on bioavailability and therapeutic outcomes. Although the required knowledge for successful drug delivery is complex, applying critical studies on each section may produce desired results.

References

Alagga, A. A., & Gupta, V. (2020). Drug Absorption, Definition / Introduction. 1–4. NCBI Bookshelf. A service of the National Library of Medicine, National Institutes of Health. StatPearls [Internet]. Treasure Island (FL): StatPearls Publishing; Jan 2020.

Alexander Taylor Florence, A. T. F. and D. A. (2015). Solids 1.1. Physicochemical Principles of Pharmacy*, In Manufacture, Formulation and Clinical Use.* 6th ed. 510. *Pharmaceutical Press.* Royal Pharmaceutical Society, Landon, UK.

Amidon, G. L., Lennernäs, H., Shah, V. P., & Crison, J. R. (1995). A Theoretical Basis for a Biopharmaceutic Drug Classification: The Correlation of in Vitro Drug Product Dissolution and in Vivo Bioavailability. In *Pharmaceutical Research: An Official Journal of the American Association of Pharmaceutical Scientists* (Vol. 12, Issue 3, pp. 413–420). https://doi.org/10.1023/A:1016212804288.

Aucamp, M., Milne, M., & Liebenberg, W. (2016). Amorphous Sulfadoxine: A Physical Stability and Crystallization Kinetics Study. *AAPS PharmSciTech*, *17*(5), 1100–1109. https://doi.org/10.1208/s12249-015-0436-4.

Aucamp, M., Odendaal, R., Liebenberg, W., & Hamman, J. (2015). Amorphous azithromycin with improved aqueous solubility and intestinal membrane permeability. *Drug Development and Industrial Pharmacy*, *41*(7), 1100–1108. https://doi.org/10.3109/03639045.2014.931967.

Benet, L. Z. (2013). The role of BCS (biopharmaceutics classification system) and BDDCS (biopharmaceutics drug disposition classification system) in drug development. *Journal of Pharmaceutical Sciences*, *102*(1), 34–42. https://doi.org/10.1002/jps.23359

Bertone, J. J. (2020). *Basic pharmacological principles*. World Small Animal Veterinary Association World Congress Proceedings, 2011. College of Veterinary Medicine, Western University of Health Sciences, Pomona, CA, USA.

Bi, M., Hwang, S. J., & Morris, K. R. (2003). Mechanism of eutectic formation upon compaction and its effects on tablet properties. *Thermochimica Acta*, *404*(1–2), 213–226. https://doi.org/10.1016/S0040-6031(03)00185-0.

Brittain, H. G. (2009). Developing an appropriate salt form for an active pharmaceutical ingredient. *American Pharmaceutical Review*, *12*(7), 62–65.

Byrn, S. R., Zografi, G., & Chen, X. S. (2017). Solubility and Dissolution. *Solid State Properties of Pharmaceutical Materials*, 249–264. https://doi.org/10.1002/9781119264408.ch17.

Censi, R., & Di Martino, P. (2015). Polymorph impact on the bioavailability and stability of poorly soluble drugs. *Molecules*, *20*(10), 18759–18776. https://doi.org/10.3390/molecules201018759.

Chadha, R., Kuhad, A., Arora, P., & Kishor, S. (2012). Characterisation and evaluation of pharmaceutical solvates of Atorvastatin calcium by thermoanalytical and spectroscopic studies. *Chemistry Central Journal*, *6*(1), 1–15. https://doi.org/10.1186/1752-153X-6-114.

Chavan, R. B., Thipparaboina, R., Kumar, D., & Shastri, N. R. (2016a). Co amorphous systems: A product development perspective. *International Journal of Pharmaceutics*, *515*(1–2), 403–415. https://doi.org/10.1016/j.ijpharm.2016.10.043.

Chavan, R. B., Thipparaboina, R., Kumar, D., & Shastri, N. R. (2016b). Co amorphous systems: A product development perspective. In *International Journal of Pharmaceutics* (Vol. 515, Issues 1–2, pp. 403–415). https://doi.org/10.1016/j.ijpharm.2016.10.043.

Chemburkar, S. R., Bauer, J., Deming, K., Spiwek, H., Patel, K., Morris, J., Henry, R., Spanton, S., Dziki, W., Porter, W., Quick, J., Bauer, P., Donaubauer, J., Narayanan, B. A., Soldani, M., Riley, D., & McFarland, K. (2000). Dealing with the impact of ritonavir polymorphs on the late stages of bulk drug process development. *Organic Process Research and Development*, *4*(5), 413–417. https://doi.org/10.1021/op000023y.

Cherukuvada, S., Kaur, R., & Guru Row, T. N. (2016). Co-crystallization and small molecule crystal form diversity: From pharmaceutical to materials applications. *CrystEngComm*, *18*(44), 8528–8555. https://doi.org/10.1039/c6ce01835a.

Chistyakov, D., & Sergeev, G. (2020). The polymorphism of drugs: New approaches to the synthesis of nanostructured polymorphs. *Pharmaceutics*, *12*(1), 1–9. https://doi.org/10.3390/pharmaceutics12010034.

Craig, D. Q. M., Royall, P. G., Kett, V. L., & Hopton, M. L. (1999). The relevance of the amorphous state to pharmaceutical dosage forms: Glassy drugs and freeze dried systems. *International Journal of Pharmaceutics*, *179*(2), 179–207. https://doi.org/10.1016/S0378-5173(98)00338-X.

Currie, G. M. (2018). Pharmacology, part 2: Introduction to pharmacokinetics. *Journal of Nuclear Medicine Technology*, *46*(3), 221–230. https://doi.org/10.2967/jnmt.117.199638.

Descamps, M. (2016). Amorphous Pharmaceutical Solids. *Advanced Drug Delivery Reviews*, *100*(3), 1–2. https://doi.org/10.1016/j.addr.2016.04.011.

Dhobale, A. v, & Dhembre, G. (2018). *Solubility enhancement techniques-a review. June*. https://doi.org/10.5281/zenodo.1226729.

Dujic, T., Causevic, A., Bego, T., Malenica, M., Velija-Asimi, Z., Pearson, E. R., & Semiz, S. (2016). Organic cation transporter 1 variants and gastrointestinal side effects of metformin in patients with Type 2 diabetes. *Diabetic Medicine*, *33*(4), 511–514. https://doi.org/10.1111/dme.13040.

Gupta, D., Bhatia, D., Dave, V., Sutariya, V., & Gupta, S. V. (2018). Salts of therapeutic agents: Chemical, physicochemical, and biological considerations. *Molecules*, *23*(7), 1–15. https://doi.org/10.3390/molecules23071719.

Homayun, B., Lin, X., & Choi, H. J. (2019). Challenges and recent progress in oral drug delivery systems for biopharmaceuticals. *Pharmaceutics*, *11*(3). https://doi.org/10.3390/pharmaceutics11030129.

Huang, Y., Zhang, Q., Wang, J.-R., Lin, K.-L., & Mei, X. (2017). Amino acids as co-amorphous excipients for tackling the poor aqueous solubility of valsartan. *Pharmaceutical Development and Technology*, *22*(1), 69–76. https://doi.org/10.3109/10837450.2016.1163390.

Hubs, C. (2020). *Pharmaceutical salts of small molecule drugs*. 1–13.

Jagtap, S., Magdum, C., Jadge, D., & Jagtap, R. (2018). Solubility enhancement technique: A review. *Journal of Pharmaceutical Sciences and Research*, *10*(9), 2205–2211.

Jain, M., Lohare, G., Bari, M., Chavan, R., Barhate, S., & Shah, C. (2012). Spray Drying in Pharmaceutical Industry: A Review. *Research Journal of Pharmaceutical Dosage Forms and Technology*, *4*(2), 74–79.

Jaiswar, D. R., Jha, D., & Amin, P. D. (2016). Preparation and characterizations of stable amorphous solid solution of azithromycin by hot melt extrusion. *Journal of Pharmaceutical Investigation*, *46*(7), 655–668. https://doi.org/10.1007/s40005-016-0248-x.

Janssens, S., & Van den Mooter, G. (2009). Review: physical chemistry of solid dispersions. *Journal of Pharmacy and Pharmacology*, *61*(12), 1571–1586. https://doi.org/10.1211/jpp/61.12.0001.

Jensen, K. T., Larsen, F. H., Löbmann, K., Rades, T., & Grohganz, H. (2016). Influence of variation in molar ratio on co-amorphous drug-amino acid systems. *European Journal of Pharmaceutics and Biopharmaceutics*, *107*, 32–39. https://doi.org/10.1016/j.ejpb.2016.06.020.

Jug, M., Maestrelli, F., Bragagni, M., & Mura, P. (2010). Preparation and solid-state characterization of bupivacaine hydrochloride cyclodextrin complexes aimed for buccal delivery. *Journal of Pharmaceutical and Biomedical Analysis, 52*(1), 9–18. https://doi.org/10.1016/j.jpba.2009.11.013.

Justin, J. P., Amit, S. D. (2020). Physiology, Digestion. StatPearls. Treasure Island (FL): StatPearls Publishing; Upstate Medical University and SUNY Upstate Medical University. September 18, 2020.

Karagianni, A., Kachrimanis, K., & Nikolakakis, I. (2018). Co-amorphous solid dispersions for solubility and absorption improvement of drugs: Composition, preparation, characterization and formulations for oral delivery. *Pharmaceutics*, *10*(3). https://doi.org/10.3390/pharmaceutics10030098.

Kawakami, K. (2009). Current status of amorphous formulation and other special dosage forms as formulations for early clinical phases. *Journal of Pharmaceutical Sciences*, *98*(9), 2875–2885. https://doi.org/10.1002/jps.21816.

Lakshmi Prasanthi, N., Sudhir, M., Jyothi, N., & vajrapriya, V. S. (2016). A Review on Polymorphism Perpetuates Pharmaceuticals. *American Journal of Advanced Drug Delivery*, *04*(05). https://doi.org/10.21767/2321-547x.1000002.

Lin, S. Y. (2015). Molecular perspectives on solid-state phase transformation and chemical reactivity of drugs: Metoclopramide as an example. *Drug Discovery Today*, *20*(2), 209–222. https://doi.org/10.1016/j.drudis.2014.10.001.

Maher, E. M., Ali, A. M. A., Salem, H. F., & Abdelrahman, A. A. (2016). In vitro/in vivo evaluation of an optimized fast dissolving oral film containing olanzapine co-amorphous dispersion with selected carboxylic acids. *Drug Delivery*, *23*(8), 3088–3100. https://doi.org/10.3109/10717544.2016.1153746.

Manallack, D. (2011). The pKa Distribution of Drugs: Application to Drug Discovery. *Dyes and Drugs*, 80–102. https://doi.org/10.1201/b13128-7.

Martinez, M. N., & Amidon, G. L. (2002). A mechanistic approach to understanding the factors affecting drug absorption: A review of fundamentals. *Journal of Clinical Pharmacology*, *42*(6), 620–643. https://doi.org/10.1177/00970002042006005.

Meng, F., Gala, U., & Chauhan, H. (2015). Classification of solid dispersions: Correlation to (i) stability and solubility (II) preparation and characterization techniques. *Drug Development and Industrial Pharmacy*, *41*(9), 1401–1415. https://doi.org/10.3109/03639045.2015.1018274.

Milne, M., Liebenberg, W., & Aucamp, M. (2015). The Stabilization of Amorphous Zopiclone in an Amorphous Solid Dispersion. *AAPS PharmSciTech*, *16*(5), 1190–1202. https://doi.org/10.1208/s12249-015-0302-4.

Moinuddin, S. M., Ruan, S., Huang, Y., Gao, Q., Shi, Q., Cai, B., & Cai, T. (2017). Facile formation of co-amorphous atenolol and hydrochlorothiazide mixtures via cryogenic-milling: Enhanced physical stability, dissolution and pharmacokinetic profile. *International Journal of Pharmaceutics*, *532*(1), 393–400. https://doi.org/10.1016/j.ijpharm.2017.09.020.

Montejo-Bernardo, J., García-Granda, S., Bayod-Jasanada, M., Llorente, I., & Llavona, L. (2005). An easy and general method for quantifying Azithromycin dihydrate in a matrix of amorphous Azithromycin. *Arkivoc*, *2005*(9), 321–331. https://doi.org/10.3998/ark.5550190.0006.927.

Montoto, S. S. (2018). ADME Processes in Pharmaceutical Sciences. In *ADME Processes in Pharmaceutical Sciences* (Issue December). https://doi.org/10.1007/978-3-319-99593-9.

Mudie, D. M., Samiei, N., Marshall, D. J., Amidon, G. E., & Bergström, C. A. S. (2020). Selection of In Vivo Predictive Dissolution Media Using Drug Substance and Physiological Properties. *AAPS Journal*, *22*(2), 1–13. https://doi.org/10.1208/s12248-020-0417-8.

Newman, A., Reutzel-Edens, S. M., & Zografi, G. (2018). Coamorphous Active Pharmaceutical Ingredient–Small Molecule Mixtures: Considerations in the Choice of Coformers for Enhancing Dissolution and Oral Bioavailability. *Journal of Pharmaceutical Sciences*, *107*(1), 5–17. https://doi.org/10.1016/j.xphs.2017.09.024.

Patole Tanvee, & Deshpande Ashwini. (2014). Co-Crystallization- a Technique for Solubility Enhancement | International Journal of Pharmaceutical Sciences and Research. *International Journal of Pharmaceutical Sciences and Research*, *5*(9), 3566–3576.

Paulekuhn, G. S., Dressman, J. B., & Saal, C. (2007). Trends in active pharmaceutical ingredient salt selection based on analysis of the orange book database. *Journal of Medicinal Chemistry*, *50*(26), 6665–6672. https://doi.org/10.1021/jm701032y.

Prashantha Kumar, B. R., Soni, M., Bharvi Bhikhalal, U., Kakkot, I. R., Jagadeesh, M., Bommu, P., & Nanjan, M. J. (2010). Analysis of physicochemical properties for drugs from nature. *Medicinal Chemistry Research*, *19*(8), 984–992. https://doi.org/10.1007/s00044-009-9244-2.

Price, G., & Patel, D. A. (2020). *Drug Bioavailability Definition / Introduction*. 1–6.

Qi, S. Y., Tian, Y., Zou, W. B., & Hu, C. Q. (2018). Characterization of solid-state drug polymorphs and real-time evaluation of crystallization process consistency by near-infrared spectroscopy. *Frontiers in Chemistry*, *6*(OCT), 1–7. https://doi.org/10.3389/fchem.2018.00506.

Ranjan, S., Devarapalli, R., Kundu, S., Saha, S., Deolka, S., Vangala, V. R., & Reddy, C. M. (2020). Isomorphism: "Molecular similarity to crystal structure similarity" in multicomponent forms of analgesic drugs tolfenamic and mefenamic acid. *IUCrJ*, *7*, 173–183. https://doi.org/10.1107/S205225251901604X.

Raza, K. (2014). Polymorphism: The Phenomenon Affecting the Performance of Drugs. *SOJ Pharmacy & Pharmaceutical Sciences*. https://doi.org/10.15226/2374-6866/1/2/00111.

Saifee, M., Inamdar, N., Dhamecha, D. L., & Rathi, A. A. (2009). Drug polymorphism: A review. *International Journal of Health Research*, *2*(4), 291–306. https://doi.org/10.4314/ijhr.v2i4.55423.

Santana, N. S., Gomes, A. F., Santana, H. S., Saraiva, G. D., Ribeiro, P. R. S., Santos, A. O., Nogueira, C. E. S., & De Sousa, F. F. (2021). Phase Transformations of Azithromycin Crystals Investigated by Thermal and Spectroscopic Analyses Combined with Ab Initio Calculations. *Crystal Growth and Design*, *21*(6), 3602–3613. https://doi.org/10.1021/acs.cgd.1c00375.

Savjani, K. T., Gajjar, A. K., & Savjani, J. K. (2012). Drug Solubility: Importance and Enhancement Techniques. *ISRN Pharmaceutics*, *2012*(July), 1–10. https://doi.org/10.5402/2012/195727.

Schittny, A., Ogawa, H., Huwyler, J., & Puchkov, M. (2018). A combined mathematical model linking the formation of amorphous solid dispersions with hot-melt-extrusion process

parameters. *European Journal of Pharmaceutics and Biopharmaceutics*, *132*, 127–145. https://doi.org/10.1016/j.ejpb.2018.09.011.

Shi, Q., Moinuddin, S. M., & Cai, T. (2019). Advances in coamorphous drug delivery systems. *Acta Pharmaceutica Sinica B*, *9*(1), 19–35. https://doi.org/10.1016/j.apsb.2018.08.002.

Singh, G., Kaur, L., Gupta, G. D., & Sharma, S. (2017). Enhancement of the Solubility of Poorly Water Soluble Drugs through Solid Dispersion: A Comprehensive Review. *Indian Journal of Pharmaceutical Sciences*, *79*(5), 1–41. https://doi.org/10.4172/pharmaceutical-sciences.1000279.

Stott, P. W., Williams, A. C., & Barry, B. W. (1998). Transdermal delivery from eutectic systems: Enhanced permeation of a model drug, ibuprofen. *Journal of Controlled Release*, *50*(1–3), 297–308. https://doi.org/10.1016/S0168-3659(97)00153-3.

Thayyil, A. R., Juturu, T., Nayak, S., & Kamath, S. (2020). Pharmaceutical Co-crystallization: Regulatory aspects, design, characterization, and applications. *Advanced Pharmaceutical Bulletin*, *10*(2), 203–212. https://doi.org/10.34172/apb.2020.024.

Vogel, H. G., Maas, J., Hock, F. J., & Mayer, D. (2013). Drug Discovery and evaluation: Safety and pharmacokinetic assays, second edition. *Drug Discovery and Evaluation: Safety and Pharmacokinetic Assays, Second Edition*, 1–1402. https://doi.org/10.1007/978-3-642-25240-2.

Wairkar, S., & Gaud, R. (2016). Co-Amorphous Combination of Nateglinide-Metformin Hydrochloride for Dissolution Enhancement. *AAPS PharmSciTech*, *17*(3), 673–681. https://doi.org/10.1208/s12249-015-0371-4.

Wang, Z., Sun, M., Liu, T., Gao, Z., Ye, Q., Tan, X., Hou, Y., Sun, J., Wang, D., & He, Z. (2019). Co-amorphous solid dispersion systems of lacidipine-spironolactone with improved dissolution rate and enhanced physical stability. *Asian Journal of Pharmaceutical Sciences*, *14*(1), 95–103. https://doi.org/10.1016/j.ajps.2018.11.001.

Zaborenko, N., Shi, Z., Corredor, C. C., Smith-Goettler, B. M., Zhang, L., Hermans, A., Neu, C. M., Alam, M. A., Cohen, M. J., Lu, X., Xiong, L., & Zacour, B. M. (2019). First-Principles and Empirical Approaches to Predicting In Vitro Dissolution for Pharmaceutical Formulation and Process Development and for Product Release Testing. *AAPS Journal*, *21*(3). https://doi.org/10.1208/s12248-019-0297-y.

CHAPTER 4

The physico-chemical properties and solid-state forms of sulfadoxine, pyrimethamine and azithromycin

4.1 Introduction

Oral bioavailability of any drug is an important aspect in attaining the therapeutic goal for that particular drug. Dosage form designs are linked to the therapeutic goal and play a significant role in the effective treatment of patients. It is a well-known fact that the larger part of available marketed drugs are formulated into oral dosage forms (capsules, tablets, powder, suspension), this being due to the ease of administration that oral dosage forms provide (Dhobale & Dhembre, 2018; Jagtap *et al.*, 2018; Savjani *et al.*, 2012). Considering this, it is clear to see how the physico-chemical characteristics of a drug plays an important role in achieving optimal bioavailability (Zaborenko *et al.,* 2019). This chapter will elucidate the physicochemical properties associated with SUL, PYR and AZI.

4.2.1 Sulfadoxine (SUL)

This drug belongs to the sulfonamide group of drugs and is a synthetic analog of para-aminobenzoic acid (PABA) **(Figure 4.1)**, with a pyrimidine moiety having a 4-aminobenzenesulfonamide group at the 4th position and methoxy substituents at the 5th and 6th positions. SUL is classified as a broad-spectrum sulphanilamide and has been used in management of bacterial conditions (respiratory infections, urinary infection) and in combination with the antiprotozoal (pyrimethamine) for treating uncomplicated malaria for years. The mechanism of action of SUL is rendered by competing with PABA for the bacterial enzyme dihydropteroate synthase, inhibiting addition of PABA into dihydrofolic acid, the precursor of folic acid. This process interferes with the synthesis of parasitic folic acid, synthesis of purines and pyrimidines, which ultimately leads to cellular growth inhibition and cell death of the susceptible parasite (PubChem, 2021a).

Currently, SUL is marketed in oral dosage forms as fixed dose combinations (FDC) with PYR or as FDC with PYR and amodiaquine for malaria treatment in children in areas with parasitic chloroquine resistance. As discussed in Chapter 2 the SUL:PYR FDC has application in adult, pregnant women as an intermittent preventive therapy (IPTp-SP) with this FDC containing 500 mg SUL and 25mg PYR.

4.2.2 Physico-chemical properties of SUL

Sulfadoxine is a crystalline yellowish compound with chemical formula: $C_{12}H_{14}N_4O_4S$, with a molar weight of 301.33g.mol^{-1}. Literature reports a melting point of 190 - 194℃, a logP of 0.70 and pKa of 6.30 (PubChem, 2021a). Even though this compound falls outside the Lipinski's rule of 5 briefly described in chapter 1.1 *paragraph one*, it has been reported to have a very slight solubility profile in aqueous media (Holtzkamp *et al*., 2016 and Badehorst *et a*l., 2017). Badehorst *et al*., (2017) studied the solubility of FDC of sulfadoxine and pyrimethamine, comparing with 1:1 molar and mass ratios and obtained an equilibrium solubility of 269 µg/ml after 24 hours. Further reports in literature indicate that sulfadoxine solubility is enhanced in natural buffered media in an acidic pH, however this is negatively affected when in combination with pyrimethamine (Holtzkamp *et al*., 2016). SUL is slightly soluble in organic solvent such as methanol and ethanol (PubChem, 2021a). Additionally, the presence of hydrogen acceptors and donors' functional groups on the chemical structure of SUL **(Figure. 4.1**) and (**Table 4.1**) provides an interesting physico-chemical property that can be optimised during solid-state dose formulation to enhance its poor aqueous solubility habit. Solid-state modification discussed in chapter 3.5, such as co-crystals, solid dispersion, co-amorphous, cyclodextrin, solvate are some of the methods intensively studied in an attempt to improve aqueous solubility of drugs. The chemical interaction by H bonding, covalent or charge transfer dictated by a molecule in question and such bonds are stabilised by the amide nitrogen atom (ANH) as H acceptor and amine nitrogen atom (ANH$_2$) as H donor, under specific pH conditions (Sandhiya & Senthilkumar, 2014). There has been no report indicating any possibility of other forms of SUL beside the crystalline form, a study by (Aucamp *et al*., 2016) on a stability form of amorphous yielded an amorphous that re-crystallises to most stable form, this does not rule out the possibility of formulating SUL as co-amorphous, especially with a stabilizer such polymers or APIs with good glass forming properties.
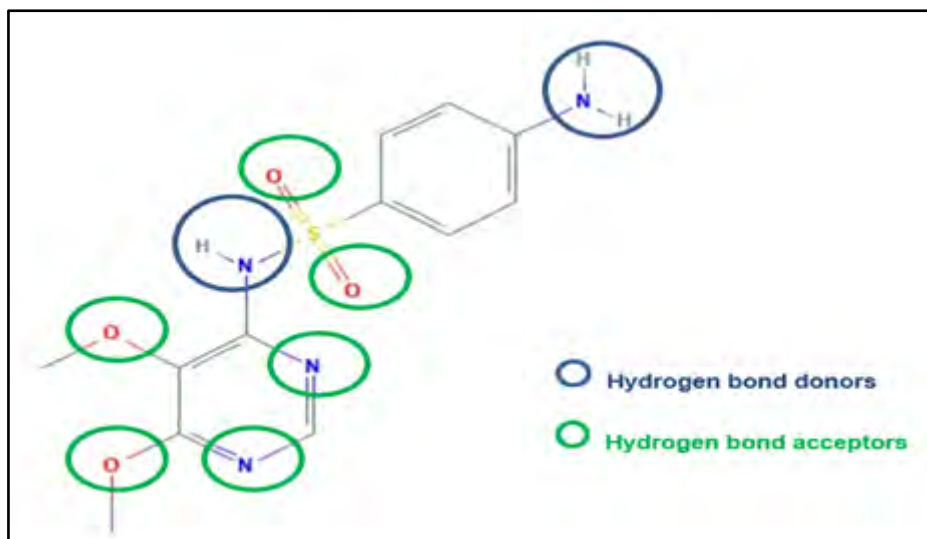
Figure 4.1: The chemical structure of sulfadoxine as adapted from (PubChem, 2021a).

4.2.3 Pharmacokinetics of SUL

SUL belongs to the BCS II class, its oral bioavailability is over 90% due to good intestinal absorptive properties and attained peak plasma concentration within 2-8 hours following oral administration of the drug. Previous studies indicate that SUL are bound to plasma protein leading to lower concentration in red blood cells as opposed to plasma and mainly cleared via the renal pathway through glomerular filtration. It has been noted that approximately 70% of filtrated SUL is reabsorbed along the tubular section of the kidney, these characteristics are perceived to contribute to its longer elimination half-life of 8.33 days in healthy adults (De Kock *et al.,* 2017; Mikomangwa *et al* 2020; Liu *et al.,* 2012). Only a small fraction of this drug is affected by phase II metabolism into more water soluble metabolites which include; acetylate metabolites (5%) that is further metabolised by N-acetyltransferase 2 (NAT2) and glucuronide (2–3%). SUL and its metabolites are primarily eliminated through the renal system and a small fraction through the GIT in stool (De Kock *et al.,* 2017) . In pregnancy however, various physiological factors are altered, such as fluid volume and metabolic enzyme capacity that may have different impacts on the pharmacokinetic profile of a drug (De Kock *et al.,* 2017). The above positive attributes of SUL may be misleading as its poor aqueous solubility would mean a high dose concentration is required to achieve a therapeutic plasma concentration. There have been many attempts to solve low water solubility and this study focused on formulating its amorphous form with other combinations to counter the mentioned challenge.

4.3.1 Pyrimethamine (PYR)

PYR is a synthetic derivative of ethyl-pyrimidine classified as a folic acid antagonist and has potent antimalarial properties. PYR is commonly used in combination with sulfadoxine for chemoprophylaxis or treatment of uncomplicated malaria. It may also be prescribed in conjunction with dapsone or other sulphonamides to treat toxoplasmosis and prevention of *Pneumocystis jiroveci*, formerly known as *Pneumocystis carinii* pneumonia (PCP). PYR acts by competitively inhibiting dihydrofolate reductase (DHFR), an essential enzyme in the redox cycle necessary for the synthesis of tetrahydrofolate, DHFR is a required cofactor for the production of DNA and proteins (Agomo *et al*., 2011; Pearson and Hewlett, 1987). Its application is limited to areas with low resistance and in areas of chloroquine resistance, *P. falciparum* malaria. This activity is highly selective against plasmodium and *Toxoplasma gondii* (Dunay *at el*., 2018), especially the erythrocytic schizonticidal and tissue schizonticidal potency in malaria parasites has been identified, this property is associated to the 4-amino-quinoline compounds on its structure. However, PYR does not have positive activity against gametocytes, but it is capable of inhibiting sporogony (asexual spore formation) in the mosquito life cycle phase. The activity of both SUL and PYR given as combination therapy has been found not to clear parasites completely from the placenta and the peripheral system but rather through suppression of multiplication (Mikomangwa *at el*., 2020).

4.3.2 Physico-chemical properties of PYR

Pyrimethamine (PYR) exist as an odourless, white crystalline powder drug and has chemical formula: $C_{12}H_{13}N_4Cl$, chemical name (2,4-diamino-5-(p-chlorophenyl)-6-methylpyrimidine), molar weight of 248.71g.mol^{-1} , it exhibits a sharp melting point at 233℃ -234°C. PYR is a weak basic drug with logP of 2.69 and pKa of 7.34 (PubChem, 2021b). The drug is classified under BSC II, meaning it has poor aqueous solubility property with good cellular membrane permeability. It has a low solubility profile in acetone, chloroform, ethanol and dilute hydrochloric acid (HCl) and soluble in dimethyl sulfoxide (DMSO) and dimethyl formamide (DMF) (PubChem, 2021b), practically insoluble in water. In fact, approximately 40 µg/ml has been attributed to its water solubility at 25. The LogP 2.69 may predict pH dependency of its dissolution and solubility is lower in gastric fluids as opposed to gastrointestinal pH 6.8, however, plasma concentration has been found to vary markedly due to patients' physiological variations (Khatri *et al*., 2018). Furthermore, studies have proven that PYR's dissolution and solubility are enhanced through binary or combination formulation and this dependent on the nature of preparation such complexation in cyclodextrins cavitation, and co-crystallization (Onyeji *et al*., 2009). Another factor of influence is the existence of hydrogen bond donor and acceptors exhibited by PYR (**Figure 4.2**) and (**Table 4.1**) this is important in new bond

formation that has benefit in dissolution and solubility, high electron density increases the chance of intermolecular interaction commonly through pi-pi bonding (Onah & Odeiani, 2002).
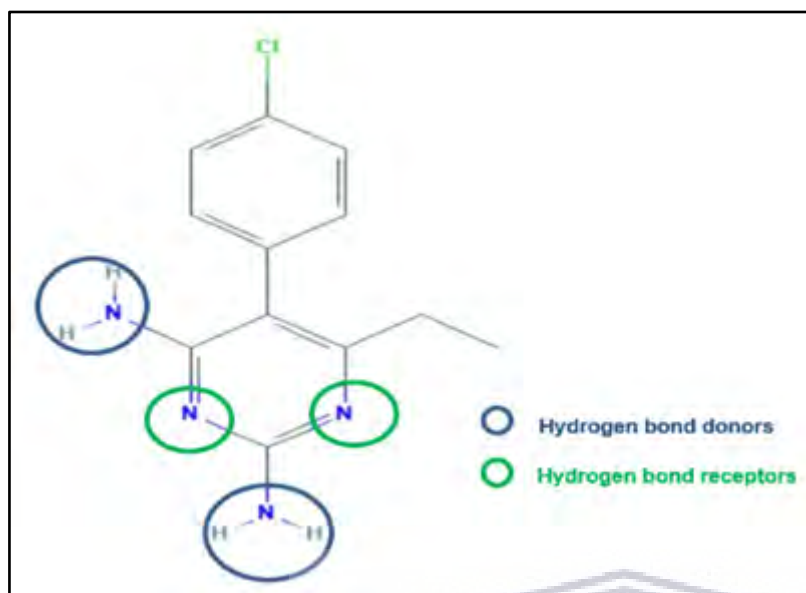
Figure 4.2: Molecular structure of pyrimethamine (PubChem 2021b).

4.3.3 Pharmacokinetics of PYR

Pyrimethamine exhibits poor aqueous solubility although with good cellular permeability properties, thus being classified as a BCS II drug. It is typically well absorbed in the gastro-intestinal tract and reaches maximum systemic circulation concentration of over 90% bioavailability following the oral route of administration. PYR is metabolized by liver enzymes into multiple unknown metabolites and it is still unclear whether some of these metabolites are active against parasitaemia or not (De Kock *at el*., 2017). Over 80% of this drug compound is highly bound to plasma proteins resulting in its longer clearance half-life of 100 hours and approximately 15-30% of the drug in the plasma drug is eliminated unchanged in urine(Aucamp *at el*., 2016).

4.4.1 Azithromycin (AZI)

Azithromycin is classified as azalide and a subclass of macrolide antibiotics, derived from parent drug- erythromycin with bactericidal, bacteriostatic and anti parasitaemia activities (Wilson *et al.,* 2015). AZI reversibly binds to the 23S ribosomal subunit of the 50S ribosome of susceptible microorganisms, inhibiting the translational process in protein synthesis, as newly synthesized peptidyl transfer ribonucleic acid (tRNA) molecule is stopped from

penetrating the acceptor site on the ribosome to the peptidyl (donor) site, and ultimately inhibiting ribonucleic acid (RNA) responsible for protein synthesis resulting to cell growth inhibition and eventually cell death (Kshirsagar *et al* 2017; Oldenburg *et al.,* 2019). AZI is commonly recommended for treatment of respiratory infections (bacterial pathogens), urinary tract infections, STDs and in combination with other antimalarial drugs for less severe malaria management (Sandman and Iqbal, 2020).

4.4.2 Physico-chemical properties of AZI

Azithromycin (AZI) is a white crystalline powder that exhibits chemical formula of $C_{38}H_{72}N_2O_{12}$, molar weight of 748.51g.mol-1 and melts between 113℃ -115 °C, its logP is 4.02 and pKa of 8.50. AZI's mass, number of hydrogen receptors and hydrogen donors (**Figure 4.3**) and (**Table 4.1**) (PubChem, 2021c) is a typical example of compound exhibiting the lipophilic habit as described by Lipinski's rule of 5 in chapter 1.1 paragraph one, this confirms its poor aqueous solubility, approximately 100 µg/mL. AZI is soluble in organic solvent such as Ethanol, (DMSO), (DMF). The drug has been reported to have various physical forms such as monohydrate, dehydrates, hydrates (Odendaal, 2012) and an amorphous form was formulated via hot-melt demonstrating possible additional solid-state (Aucamp *et al.*, 2015), these forms may have completely different physico-chemical characteristics presented in chapter 3, choosing amorphous form in formulating an oral dose may curb down the oral bioavailability challenge. The fundamental challenge of poor solubility has been studied on possible amorphous form and found enhanced aqueous solubility and dissolution rate in pH 6 and pH 7.2, also miscibility with hydrophilic polymers pointed positive direction towards mitigating this behaviour compared to crystalline AZI dihydrate form. (Aucamp *et al.*, 2015; Jaiswar, *et al.*, 2016).
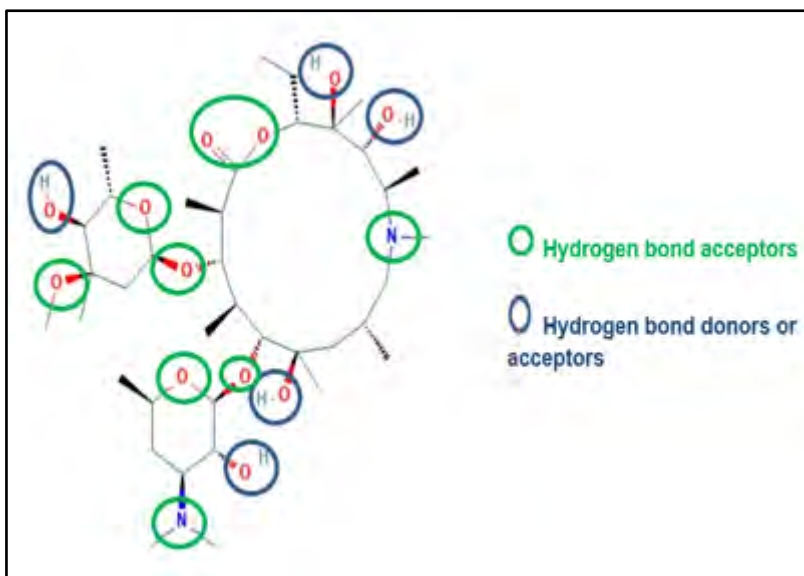
Figure 4.3 Azithromycin chemical structure (PubChem, 2021c)

4.4.3 Pharmacokinetics of AZI

AZI is poorly but readily absorbed within the small intestine after oral ingestion and extensively distributed to the central compartment including the tissue. The pKa of 8.5 greatly impact on the drug ionisation that impede on absorption along the GIT, a higher basic environment of above pH 8.5 would increase the fraction of unionised drug molecule and enhance permeation across intestinal membrane but due to the physiological pH within the system, only a limited amount gets absorbed (Lode, 1991; Villarino and Martín-Jiménez, 2013; Kong *et al*., 2017). It attains the peak systemic circulation concentration within 2-3 hours and has an absolute bioavailable of approximately 37% in healthy adults (Kong *et al*., 2017). Studies have proven that AZI concentrates on phagocytic cells that transports the drug to target site and distributed more in the tissue than in plasma protein that may portray its long half-life due to slow redistribution from tissue to systemic circulation before finally getting metabolised and cleared from the central compartment (Lode, 1991). It should be noted that a loading dose is required to reach faster steady state bioavailability than use of lower dose, especially when long treatment is recommended. AZI undergoes very limited hepatic metabolism as opposed to other macrolides. Its elimination pathway is primarily through the biliary system in the stool unchanged and about 6% in urine (Pharmgkb *at el*., 2020; Drew and Gallis, 1992). The pharmacokinetic characteristic of AZI has led to its favourability in clinical practice as opposed to the first-generation macrolides (erythromycin); fewer doses are prescribed, such as a two day dose of 1 gram each per day, which improves patients' compliance.

In malaria management, a study conducted in Malawi has attracted new focus in the inclusion of AZI in the intermittent preventive treatment (IPTp_SP) in pregnancy (Chico and Chandramohan, 2011). Although the clinical trial registered good outcomes used in combination with SP, AZI has very poor aqueous solubility and that limits its bioavailability, the drug has been reported to have various physical forms such as monohydrate, dehydrates, hydrates and an amorphous solid-state form (Aucamp *at el*., 2016), choosing amorphous form in formulating an oral dose may curb down the oral bioavailability challenge. These three active pharmaceutical ingredients (APIs) have some characteristics of interest to this study; they all structurally have H-bond donors and receptors needed for co-amorphous intermolecular interactions, poor aqueous solubility properties limiting their oral bioavailability, safety profile in pregnancy from second trimester and active against plasmodium parasite species.

Table 4.1 Summary of physico-chemical characteristics of sulfadoxine, pyrimethamine and azithromycin (PubChem, 2021a, 2021b, 2021c)

API	Chemical formula	Molar mass (g/mol)	Melting Point (°C)	Rotatable bond count	Number of H-receptor	Number of H-donor
Sulfadoxine	$C_{12}H_{14}N_4O_4S$	310.33	192-194	5	8	2
Pyrimethamine	$C_{12}H_{13}N_4Cl$	248.71	233-234	2	4	2
Azithromycin	$C_{38}H_{76}N_2O_{14}$	785.02	192-194	7	16	7

4.5 Conclusion

Based on the attributes of SUL, PYR and AZI presented in this chapter, malaria associated challenges in pregnancy and its effects to children less than 5 years, and solid state physicochemical properties dealt with in chapter 3; there is need to find a solution from the formulation perspective, the oral dosage form with an improved solubility to enhance bioavailability, reduce the high dose strength required, minimise side effects and possibly delay risk of resistance to these drugs, combined amorphous for oral dosage form may be one of the possible options. Malaria is a reality and still with us, the cost of control and management continues to torment the global economy, continuous care with affordable medicine is a long term plan each endemic region has to embrace.

4.6 Reference

Acheampong, A., Gyebi, A., Darko, G., Apau, J., Owusu Gyasi, W., & Addai-Arhin, S. (2018). Development and validation of RP-HPLC method for simultaneous estimation of sulfadoxine and pyrimethamine in tablet dosage form using diclofenac as internal standard. *Cogent Chemistry*, *4*(1), 1472198. https://doi.org/10.1080/23312009.2018.1472198.

Agomo, C. O., Oyibo, W. A., & Odukoya-Maije, F. (2011a). Parasitologic Assessment of Two-Dose and Monthly Intermittent Preventive Treatment of Malaria during Pregnancy with Sulphadoxine-Pyrimethamine (IPTP-SP) in Lagos, Nigeria. *Malaria Research and Treatment*, *2011*, 1–6. https://doi.org/10.4061/2011/932895.

Aucamp, M., Milne, M., & Liebenberg, W. (2016). Amorphous Sulfadoxine: A Physical Stability and Crystallization Kinetics Study. *AAPS PharmSciTech*, *17*(5), 1100–1109. https://doi.org/10.1208/s12249-015-0436-4.

Aucamp, M., Odendaal, R., Liebenberg, W., & Hamman, J. (2015). Amorphous azithromycin with improved aqueous solubility and intestinal membrane permeability. *Drug Development and Industrial Pharmacy*, *41*(7), 1100–1108. https://doi.org/10.3109/03639045.2014.931967.

Bagalkoti, J. T., Joshi, S. D., & Nandibewoor, S. T. (2019). Spectral and molecular modelling studies of sulfadoxine interaction with bovine serum albumin. *Journal of Photochemistry and Photobiology A: Chemistry*, *382*(May), 111871. https://doi.org/10.1016/j.jphotochem.2019.111871.

Chico, R. M., & Chandramohan, D. (2011). Azithromycin plus chloroquine: Combination therapy for protection against malaria and sexually transmitted infections in pregnancy. *Expert Opinion on Drug Metabolism and Toxicology*, *7*(9), 1153–1167. https://doi.org/10.1517/17425255.2011.598506.

De Kock, M., Tarning, J., Workman, L., Nyunt, M. M., Adam, I., Barnes, K. I., & Denti, P. (2017a). Pharmacokinetics of sulfadoxine and pyrimethamine for intermittent preventive treatment of malaria during pregnancy and after delivery. *CPT: Pharmacometrics and Systems Pharmacology*, *6*(7), 430–438. https://doi.org/10.1002/psp4.12181.

Dhobale, A. v, & Dhembre, G. (2018). *Solubility enhancement techniques-a review. June*. https://doi.org/10.5281/zenodo.1226729.

Drew, R. H., & Gallis, H. A. (n.d.). *and Clinical Applications*.

Dunay, I. R., Gajurel, K., Dhakal, R., Liesenfeld, O., & Montoya, J. G. (2018). Treatment of Toxoplasmosis : Historical Perspective , Animal. *Clinical Microbiology and Infection*, *31*(4), 1–33.

Jagtap, S., Magdum, C., Jadge, D., & Jagtap, R. (2018). Solubility enhancement technique: A review. *Journal of Pharmaceutical Sciences and Research*, *10*(9), 2205–2211.

Jaiswar, D. R., Jha, D., & Amin, P. D. (2016). Preparation and characterizations of stable amorphous solid solution of azithromycin by hot melt extrusion. *Journal of Pharmaceutical Investigation*, *46*(7), 655–668. https://doi.org/10.1007/s40005-016-0248-x.

Khatri, P., Shah, M. K., Patel, N., Jain, S., Vora, N., & Lin, S. (2018). Preparation and characterization of pyrimethamine solid dispersions and an evaluation of the physical nature of pyrimethamine in solid dispersions. *Journal of Drug Delivery Science and Technology*, *45*(March), 110–123. https://doi.org/10.1016/j.jddst.2018.03.012.

Kong, F. S., Rupasinghe, T. W., Simpson, J. A., Vodstrcil, L. A., Fairley, C. K., McConville, M. J., & Hocking, J. S. (2017). Pharmacokinetics of a single 1g dose of azithromycin in rectal tissue in men. *PLoS ONE*, *12*(3), 1–14. https://doi.org/10.1371/journal.pone.0174372.

Kshirsagar, N., Gogtay, N., Moran, D., Utz, G., Sethia, A., Sarkar, S., & Vandenbroucke, P. (2017). Treatment of adults with acute uncomplicated malaria with azithromycin and chloroquine in India, Colombia, and Suriname. *Research and Reports in Tropical Medicine*, *Volume 8*, 85–104. https://doi.org/10.2147/rrtm.s129741.

Liu, Y. M., Zhang, K. E., Liu, Y., Zhang, H. C., Song, Y. X., Pu, H. H., Lu, C., Liu, G. Y., Jia, J. Y., Zheng, Q. S., Zhu, J. M., & Yu, C. (2012). Pharmacokinetic Properties and Bioequivalence of Two Sulfadoxine/Pyrimethamine Fixed-Dose Combination Tablets: A Parallel-Design Study in Healthy Chinese Male Volunteers. *Clinical Therapeutics*, *34*(11), 2212–2220. https://doi.org/10.1016/j.clinthera.2012.10.001.

Lode, H. (1991). The pharmacokinetics of azithromycin and their clinical significance. *European Journal of Clinical Microbiology & Infectious Diseases*, *10*(10), 807–812. https://doi.org/10.1007/BF01975832.

Mikomangwa, W. P., Minzi, O., Mutagonda, R., Baraka, V., Mlugu, E. M., Aklillu, E., & Kamuhabwa, A. A. R. (2020). Effect of sulfadoxine-pyrimethamine doses for prevention of malaria during pregnancy in hypoendemic area in Tanzania.. *Malaria Journal*, *19*(1), 1–11. https://doi.org/10.1186/s12936-020-03234-4.

National Center for Biotechnology Information (2021a). PubChem Compound Summary for CID 17134, Sulfadoxine. Available at: https://pubchem.ncbi.nlm.nih.gov/compound/Sulfadoxine [Accessed 20, Oct, 2021].

National Center for Biotechnology Information (2021b). PubChem Compound Summary for CID 4993, Pyrimethamine. Available at: https://pubchem.ncbi.nlm.nih.gov/compound/Pyrimethamine [Accessed 20, Oct, 2021].

National Center for Biotechnology Information (2021c). PubChem Compound Summary for CID 447043, Azithromycin. Available at: https://pubchem.ncbi.nlm.nih.gov/compound/Azithromycin [Accessed 20, Oct, 2021].

Odendaal, R., n.d. 2012. *Amorphism and polymorphism of azithromycin*. North-West University, Boloka Institutional Repository.

Oldenburg, C. E., Amza, A., Kadri, B., Cotter, S. Y., Stoller, N. E., West, S. K., Robin, L., Porco, T. C., Keenan, J. D., Lietman, T. M., & Gaynor, B. D. (2019). Annual Versus Biannual Mass Azithromycin Distribution and Malaria Parasitemia During the Peak Transmission Season Among Children in Niger. *Pediatr Infect Dis J.*, *37*(6), 506–510. https://doi.org/10.1097/INF.0000000000001813.Annual.

Onah, J. O., & Odeiani, J. E. (2002). Physico-chemical studies on the charge-transfer complex formed between sulfadoxine and pyrimethamine with chloranilic acid. *Journal of Pharmaceutical and Biomedical Analysis*, *29*(4), 639–647. https://doi.org/10.1016/S0731-7085(02)00102-4.

Onyeji, C. O., Omoruyi, S. I., Oladimeji, F. A., & Soyinka, J. O. (2009). Physicochemical characterization and dissolution properties of binary systems of pyrimethamine and 2-hydroxypropyl-β-cyclodextrin. *African Journal of Biotechnology*, *8*(8), 1651–1659. https://doi.org/10.4314/ajb.v8i8.60360.

Pearson, R. D., & Hewlett, E. L. (1987). Use of pyrimethamine-sulfadoxine (Fansidar) in prophylaxis against chloroquine-resistant plasmodium falciparum and Pneumocystis carinii. *Annals of Internal Medicine*, *106*(5), 714–718. https://doi.org/10.7326/0003-4819-106-5-714.

Pharmgkb, S., Available, N., Pathways, R., & Literature, R. (2020). *Macrolide Antibiotic Pathway , Pharmacokinetics / Pharmacodynamics*. 9–11.

Sandhiya, L., & Senthilkumar, K. (2014). A theoretical probe on the non-covalent interactions of sulfadoxine drug with pi-acceptors. *Journal of Molecular Structure*, *1074*, 157–167.

https://doi.org/10.1016/j.molstruc.2014.05.064.

Sandman, Z., Iqbal, O. A. & Sciences, H. Azithromycin. A service of the National Library of Medicine, National Institutes of Health. StatPearls [Internet]. Treasure Island (FL): StatPearls Publishing; 2020 Jan- 1–7 (2020).

Savjani, K. T., Gajjar, A. K., & Savjani, J. K. (2012). Drug Solubility: Importance and Enhancement Techniques. *ISRN Pharmaceutics*, *2012*(July), 1–10. https://doi.org/10.5402/2012/195727.

Villarino, N., & Martín-Jiménez, T. (2013). Pharmacokinetics of macrolides in foals. *Journal of Veterinary Pharmacology and Therapeutics*, *36*(1), 1–13. https://doi.org/10.1111/jvp.12010.

Wang, P., Sims, P. F. G., & Hyde, J. E. (1997). A modified in vitro sulfadoxine susceptibility assay for Plasmodium falciparum suitable for investigating Fansidar resistance. *Parasitology*, *115*(3), 223–230. https://doi.org/10.1017/S0031182097001431.

Wilson, D. W., Goodman, C. D., Sleebs, B. E., Weiss, G. E., de Jong, N. W. M., Angrisano, F., Langer, C., Baum, J., Crabb, B. S., Gilson, P. R., McFadden, G. I., & Beeson, J. G. (2015). Macrolides rapidly inhibit red blood cell invasion by the human malaria parasite, Plasmodium falciparum. *BMC Biology*, *13*(1), 1–19. https://doi.org/10.1186/s12915-015-0162-0.

Zaborenko, N., Shi, Z., Corredor, C. C., Smith-Goettler, B. M., Zhang, L., Hermans, A., Neu, C. M., Alam, M. A., Cohen, M. J., Lu, X., Xiong, L., & Zacour, B. M. (2019). First-Principles and Empirical Approaches to Predicting In Vitro Dissolution for Pharmaceutical Formulation and Process Development and for Product Release Testing. *AAPS Journal*, *21*(3). https://doi.org/10.1208/s12248-019-0297-y.

CHAPTER 5

Materials and methods

5.1 Introduction

As discussed in Chapter 3 the investigation of the solid-state chemistry of APIs can be an involved process which requires the utilisation of many complementing analytical techniques. In the science of solid-state chemistry it is important to combine several analytical techniques to allow the accurate characterisation of specific solid-state forms of a given API. This chapter will therefore outline and discuss all the materials and methods used in the preparation and characterisation of sulfadoxine, pyrimethamine, azithromycin crystalline and associated amorphous forms.

5.2 Materials

Sulfadoxine (Batch number: 20200601) with a purity of 99.94% and azithromycin (Batch number: 20190606) with a purity of 99.80% was purchased from DB Fine chemicals (Johannesburg, South Africa). Pyrimethamine (Batch number: 201107013 was purchased from Sigma-Aldrich (Johannesburg, South Africa). Chromatography grade acetone, acetonitrile, chloroform, butanone, methanol and ethanol were purchased from Labchem (Johannesburg, South Africa). Hydrochloric acid (HCl), sodium hydroxide (NaOH), glacial acetic acid, ammonium acetate, sodium hydrogen orthophosphate, disodium hydrogen orthophosphate, anhydrous sodium acetate, dipotassium hydrogen phosphate, dihydrogen potassium phosphate, were sourced from Sigma Aldrich (Johannesburg, South Africa). Distilled water was obtained from a Milli-Q Elix® Essential 3 water purification system from Merck® (Johannesburg, South Africa) and ultrapure water with resistivity of 18.2 MΩ.cm^{-1} was obtained from a Lasec® Purite (Johannesburg, South Africa) laboratory water system.

5.3 Solid-state form preparation methods

The main objective of this study was to improve the aqueous solubility of sulfadoxine, pyrimethamine and azithromycin through the potential preparation of a co-amorphous or a ternary amorphous solid-state system. In order to achieve this, two well-known preparation methods, namely; quench cooling of the melt and solvent evaporation methods were investigated as preparation methods. These two preparation methods will be discussed in detail in the subsequent paragraphs. The ternary amorphous system, termed SPA throughout this study was prepared by firstly weighing the individual crystalline drugs to obtain the

required ratios of 20:20:1 % w/w, for sulfadoxine, azithromycin and pyrimethamine respectively. This ratio was used as it is firstly, the ratio as per available fixed dose combination (FDC) for sulfadoxine and pyrimethamine (SP) commonly used for malarial prophylaxis in pregnancy, and secondly, it includes the required amount of azithromycin currently prescribed by the WHO as additional malaria prophylaxis (Chapter 2, paragraph 2.5).

5.3.1. Preparation of SPA-C

The crystalline forms of all three APIs (SPA-C) were pre-mixed by spatulation method. Each API was accurately weighed in the w/w/w ratio of 1:1:0.05 for sulfadoxine, azithromycin and pyrimethamine respectively, followed by mixing it thoroughly using a mortar and pestle and the final constitution was termed SPA-C.

5.3.2 Quench cooling of the melt

Quench cooling of the melt method is also known as hot melt. This method involves exposing the material, in this case the APIs to elevated temperature until the fusion point is achieved followed by the rapid cooling of the molten product (Aucamp *et al.*, 2016; Aucamp *et al*., 2015; Lodagekar *et al.*, 2019). In this study, in particular, the quench cooling of the melt method is presented diagrammatically in **Figure 5.1** and involved setting a hot plate (Dragon Lab, Beijing, China) to 150.0°C ± 3.0°C. Subsequently, an aluminium pan was placed onto the hot surface and crystalline azithromycin dihydrate was added to the pan. Once azithromycin dihydrate achieved a molten state crystalline sulfadoxine was added and the temperature was raised gradually to 200.0°C ± 3.0°C, upon melting of the second API, crystalline pyrimethamine was added and the hot molten liquid facilitated the melting of the third API while stirring to a homogeneous solution. The resultant product was removed and placed on a cool surface at room temperature. The subsequent, sudden change in temperature resulted in the quenching of the molten mixture. The resulting preparation was collected into a container and sealed.
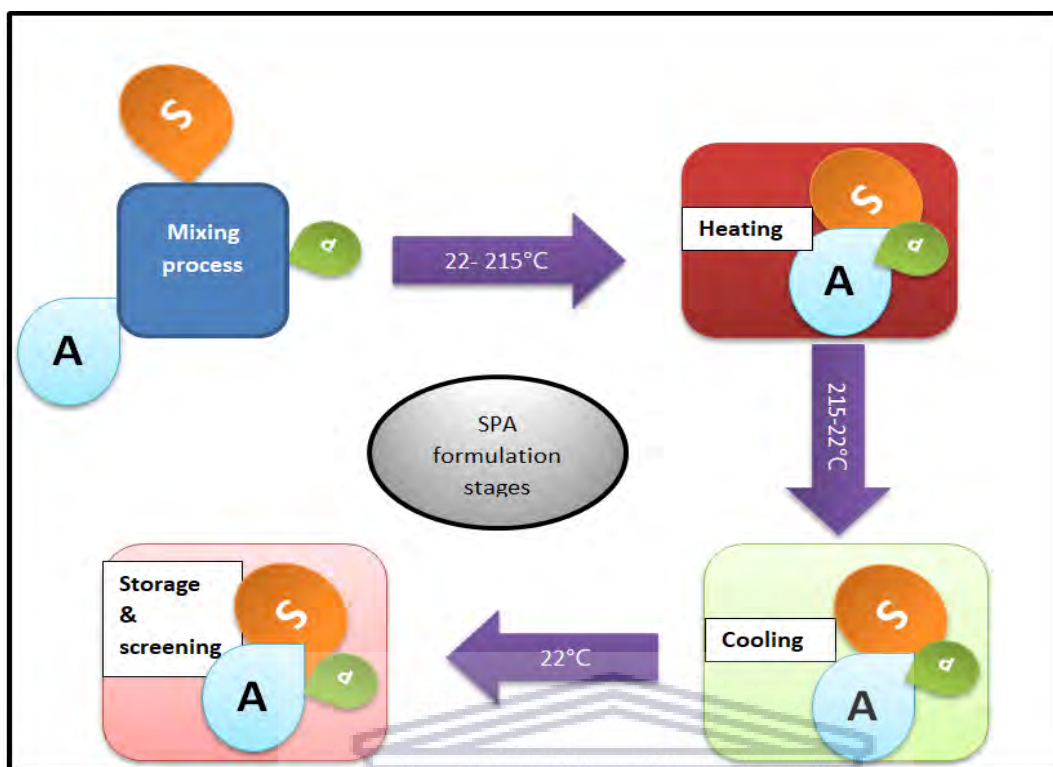
Figure 5.1: Diagrammatic representation of the quench cooling of the melt preparation method. Where: S = crystalline sulfadoxine, P = crystalline pyrimethamine and A= crystalline azithromycin and together is denoted as SPA.

5.3.3 Solvent evaporation

Solid-state formation through solvent evaporation is a method that takes into consideration the solubility of a compound in a given solvent (Dengale *et al*., 2016; Newman *et al*., 2018). The SPA-C mixture was accurately prepared. Subsequently, 20 ml of solvent was added to a 100 ml clean, dried glass beaker and placed on a magnetic stirrer hot plate (Dragon Lab, Beijing, China) set 5 ℃ below the boiling point of the particular solvent. The powder and solvent were agitated through stirring resulting in approximately 100 rotations per minute. Using a clean spatula, a small amount of the pre-weighed and prepared SPA-C (paragraph 5.3.1) was added to the solvent and time was allowed for it to dissolve. The addition of SPA-C was repeated multiple times until saturation of the solution was reached. The beaker was removed and placed on the bench to cool to room temperature (22 ± 3.0℃); the content was filtered through a 0.22 μm syringe filter into a clean beaker. Subsequently, two procedures were further conducted **(Figure 5.2)**, namely:

(a) *Slow evaporation process:* where the filtered solution was kept in the glass beaker and sealed with Parafilm® (Bemis Company Inc., Neenah, USA) which was perforated with small

holes to enhance evaporation of the organic solvent The glass beakers were placed in a secured fume hood until solid-state formation was observed.

(b) Rapid evaporation process: where the solvent was rapidly removed using a Büchi RII rotary evaporator (Flawil, Switzerland), equipped with a temperature controlled water bath at 40 ℃ and a circulating cooling unit a new solid product formed in under 15 minutes. The entire process was repeated with all the solvents investigated and products collected and sealed ready for analysis.
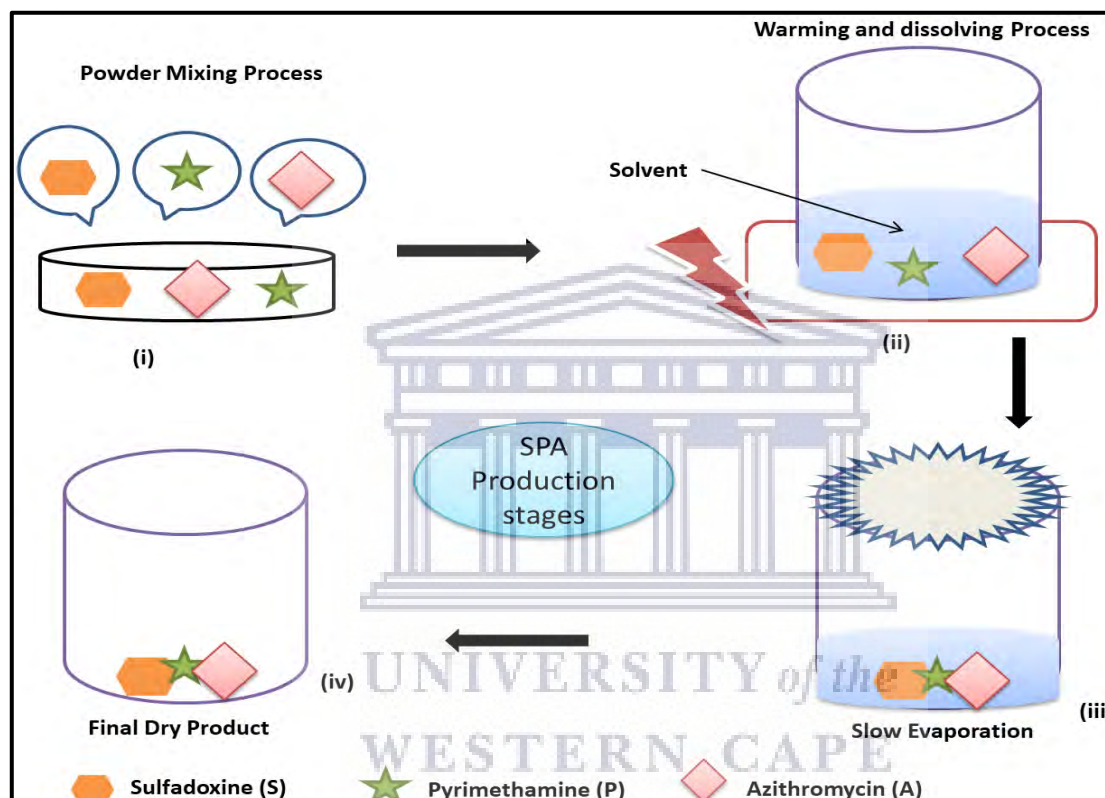
Figure 5.2: Diagrammatic representation of slow solvent evaporation formulation method. Where S=Sulfadoxine, P=Pyrimethamine, A=Azithromycin.

5.4. Physico-chemical characterisation methods

5.4.1 Hot-stage microscopy (HSM)

This method uses a combination of microscopy and thermal analysis to analyse materials as a function of temperature and time. HSM is extensively employed in the pharmaceutical industry since it enables a unique way to visually follow thermal changes in the sample (Šimek *et al.*, 2014). HSM allows the visual observation of solid-state phase transformations, melting point, sublimation, protein denaturation, dehydration, to mention but just a few. The equipment

used was an Olympus SZX7 (Japan) microscope equipped with a Linkam THMS600 heating stage (Surrey, UK). Micrographs were captured using a real-time Olympus UC30 (Tokyo, Japan) camera and the Stream Essentials software® (Olympus, Tokyo, Japan). A small amount of material was placed on a microscope slide with a small drop of silicone oil added to the sample. The sample was subsequently covered with a cover slip and mounted on the heating stage. The clear visibility of the sample particles was obtained by adjusting the focus of the microscope. Heating was initiated from ambient temperature at 10℃/minute. Data in the form of micrographs was captured as changes in the sample were observed and recorded against the specific temperature at which a thermal event was observed. The data obtained from HSM aided decision-making on the appropriate temperature range required for subsequent thermal analyses such as thermogravimetric analysis (TGA) and differential scanning calorimetry (DSC) (Aucamp, Milne, *et al.*, 2015).

5.4.2 Thermogravimetric analysis (TGA)

TGA is employed to determine the volatile property, thermal stability and other physical characteristics such as adsorption, absorption, and desorption, as well as chemical phenomena which may include: decomposition, solid-gas reactions, oxidation and reduction, to mention a few (Ghaderi, 2015). The equipment measures the change in mass of the sample over time as temperature changes when a constant heating rate is being applied. A sample weighing between 1 - 5 mg was placed into a porcelain crucible and heated from ambient temperature to 600°C, using a TGA 4000 (PerkinElmer Waltham, USA) system. The obtained thermograms were analysed, using Pyris™ software to evaluate the thermal behaviour of the sample under investigation.

5.4.3 Differential scanning calorimetry (DSC):

This is a thermal technique that uses the molar heat capacity of a sample against the temperature difference obtained through comparison with a reference. It determines melting point (thermal transition temperature), enthalpy (ΔH), heat capacity (ΔC_p), entropy (ΔS), Gibbs free energy (ΔG) and energy needed to change the structure of a material (Byrn *et al.*, 2017).

The heat transfer to the sample is measured in correlation to the reference in a temperature-controlled, inert environment. An equal amount of energy is supplied to both the sample and reference simultaneously but the amount that will increase the temperature of the sample will be different based on the chemical or structural composition of the item analysed. This difference in temperature is measured as it relates to specific thermodynamic properties of each sample and includes thermal stability and at some point facilitate structural "fingerprint" evaluation of a compound (Durowoju *et al.*, 2017). During this study, the sample was weighed

(2 – 4 mg) into an aluminium sample pan, sealed, and placed into the furnace of a Perkin Elmer DSC 8000 (Waltham, USA). A heating rate of 10°C/minute was used and the furnace was heated from ambient to 50℃ below the sample degradation temperature, as determined from HSM and TGA. Pyris™ software was used to analyse the generated thermograms..

5.4.4 Fourier-transform infrared (FTIR)

This technique analyses and identifies the functional groups of organic and polymeric compounds and rarely that of inorganic compounds. A small quantity of sample was mounted on the sample stage of a Perkin Elmer Spectrum 400 FTIR Spectrometer (Perkin Elmer, USA). Infrared light was subsequently passed through it, with some IR radiation being absorbed and some passed through undisturbed. The absorbance enables the molecules in the sample to convert the radiation to vibrational or rotational energy and is observed as peaks on a resulting infrared spectrum. The changes in the solid state such as hydrogen bonding or π-π interactions which were reflected as peak shifts of functional groups were studied and also showed the fingerprint peaks of the molecules (Hofko *et al*., 2018).

5.4.5 Powder X-ray diffraction (PXRD)

PXRD is an analytical method commonly used for the identification of crystalline substances in their powder (solid) form. The crystalline structural information is analysed and the basic atomic spacing in a molecule or compound can also be observed. A small amount of sample was lightly grinded using an agate mortar and pestle. The grinded sample was packed to form a thin layer on a suitable sample holder. The sample holder was subsequently placed into the sample holder of a Bruker D8 Advance (Massachusetts, USA) powder X-ray diffractometer. An X-ray beam was generated at 40kV and 40mA and diffraction of the sample was measured across a range of 4 – 40°2θ. The interaction of the incident ray and sample created diffraction ray and peak intensity when Bragg's law conditions were met**:**

nλ = 2d sin θ   **Equation 5.1**

Bragg's law states that when an incident ray comes into contact with a crystalline sample, the angle of incidence (θ) will reflect back with the same angle of scattering. When the path distance (d) is equal to a whole number (n) of a wavelength (λ) then a constructive interference will occur. The identification of the sample is based on the diffracted ray (the constructive interference), through determination of the unit cell dimensions, atoms and spaces in between them in a crystalline sample (Dutrow and Clark, 2016; Rajeswari, *et al*., 2020).

5.4.7 High Performance Liquid Chromatography

A Knauer Azura HPLC system equipped with a photodiode array detector, autosampler and column temperature controller, (Berlin, Germany) was used to develop a simple but robust method to accurately detect and simultaneously quantify SPA.

Chromatographic conditions: The column used was an ACE$^®$ 3µm C$_{18}$ (250 x 4.6 mm) (Aberdeen, Scotland), (Zubata *et al*., 2002) . Mobile phase solutions constituted an HPLC grade acetonitrile and di-potassium phosphate buffer in the ratio 60:40 v/v. The 0.038 M di-potassium phosphate buffer was prepared by accurately weighing 6.7 g, dissolving in ultra-pure water added to 200 ml beaker, sonicated and filtered through 0.2 µm nylon membrane to 1000 ml volumetric flask and made to volume with distilled water to obtain the required concentration (Ghari *et al*., 2013; Singh *et al*., 2019; Waghule *et al*., 2013). The pH of the mobile phase was adjusted to pH 8.2 using either 2 N hydrochloric acid (HCl) and or 1 N sodium hydroxide (NaOH). the detection wavelength set at 210 nm. A controlled column temperature of 30°C, mobile phase flow rate of 1.0 ml/min and an injection volume of 10 µl showed the best chromatographic response for each compound.

5.4.8 Vapour Sorption

Vapour sorption technique is an essential tool that provides information regarding the interaction of moisture with compounds. Adsorption and desorption of water molecules measured at constant temperature and pressure may provide significant information in terms of the morphology of a solid-state form. The amorphous forms of drugs can drastically be affected by moisture that facilitates their recrystallisation to the most stable solid-state form of a given drug, the crystalline (Aucamp *et al*., 2016; Punčochová *et al*., 2014). Solid-state forms. As part of a physical stability study, vapour sorption analyses were performed utilising a Q5000-SA vapor sorption analyser (TA Instruments, Delaware, USA). The calibration of the microbalance was done prior to each vapor sorption run with a 50 mg standard weight. For each sample, the microbalance was set to zero before placing the sample into a metallised quartz sample pan. Each vapour sorption experiment consisted of a percentage relative humidity (% RH) increase from 5% to 95% RH, a desorption phase during which the %RH was decreased from 95% to 5% and a second adsorption phase from 5% - 95% RH. Throughout the absorption-desorption phases the humidity chamber was accurately controlled at 25°C.

5.5 Solubility

Solubility of a drug is of paramount importance since the most popular dosage forms on the market are oral dosage forms due to the overwhelming advantages it offers to patients (Homayun *et al*., 2019). Understanding the phenomenon of drug solubility requires procedures such as dissolution testing, a prerequisite for all solid oral dosage forms and normally employed to establish the product release and stability testing throughout the development life-cycle (Byrn *et al*., 2017; Mudie et al., 2020; Ojarinta *et al*., 2017; Zaborenko *et al*., 2019). Dissolution is a pivotal analytical test applied in detecting physical changes that may occur in an active pharmaceutical ingredient (API) and any solid formulated product. This process also guides the optimisation of drug release from a given formulation during the early stages of the drug development process, where *in vitro* dissolution testing is done (Mudie *et al*., 2020). The therapeutic outcome of an oral dosage form depends on the plasma concentration of a drug obtained after absorption which is primarily determined by the drug's intrinsic ability to dissolve in the gastrointestinal tract (GIT) fluids after ingestion. Hence, the rate of dissolution of the drug is eminent to this overall process. The exact dissolution technique employed is determined by the dosage form characteristics and the intended route of administration. For solid dosage forms, the industry standard dissolution testing methodologies are the United States Pharmacopoeia (USP) Apparatus I (basket) and USP Apparatus 2 (paddle) (USP, 2018). The current study employed an USP Apparatus 2 (paddle) setup using a SRII 6 Hanson Research Corporation (Chatsworth, California USA) dissolution bath, equipped with a circulating temperature controller.

5.5.1 Dissolution

Dissolution experiments were conducted in distilled water or pH 1.2 using a paddle rotation of 100 rpm. Prior to each dissolution experiment, each of six dissolution vessels were filled with 900 ml of the relevant dissolution medium which was subsequently heated to 37.5 ± 2℃. To each vessel the SPA-C mixture or resulting ternary amorphous solid-state form was added after it was suspended utilising glass beads, ≥ 60 µm (Sigma-Aldrich, Johannesburg, South Africa) in an aliquot of pre-warmed dissolution medium. The drug – glass bead suspensions were respectively transferred to each dissolution vessel. At predetermined time intervals (5, 10, 20, 40 and 60 minutes) 5 ml of dissolution medium was withdrawn from each vessel, subsequently filtered through a 0.2 µm nylon filter into HPLC sample vials for analysis. The pH 1.2 buffered solution was prepared by adding 12 grams of sodium chloride with 42 ml hydrochloric acid to 6 litres of water followed by sufficient stirring to allow adequate mixing of the solution. For the acetate buffered solution (pH 4.5), 7.721 g of sodium acetate and 0.353 g of acetic acid were added to a 1 litre volumetric flask and 800 ml of distilled water was added.

The phosphate buffered solution (pH 6.8) was prepared by adding 28.2 g of disodium hydrogen phosphate and 11.45 g of potassium hydrogen phosphate to 1 litre of distilled water (Beynon & Easterby, 2018). All these buffers were adjusted to standard value by adding either few drops of 1 N sodium hydroxide or 2 N hydrochloric acid.

5.5.2 Equilibrium solubility

This test was carried out using small glass vials of an approximate volume of 4 ml. The test vials were placed into a stirrer, heating block maintained at $37 \pm 0.5°C$ with the stirring speed set at 380 rpm. Approximately 2 ml of solvent was added to each vial and a magnetic stirrer bar was placed into each vial to facilitate a continuous stirring process. Using a small spatula the sample under investigation was transferred to the vial containing the relevant solvent. The sample was observed for a few minutes and in instances where complete sample solubility was observed additional sample was added until saturation was attained. The vials were left *in situ* for the stipulated test period. Subsequently, the samples were filtered through a 0.2 µm nylon filter into HPLC sample vials. Samples were withdrawn at intervals of 0.5, 1, 2 , 4 , and finally 24 hours. The above procedures were applied for all biological gastro-intestinal pH conditions (pH 1.2, pH 4.5, pH 6.8 and distilled water). Samples were investigated using HPLC to elucidate solubility performance (drug concentration quantification) and any possible degradation (stability).

5.6 Conclusion

The solid-state form preparation methods and characterisation techniques described in this chapter facilitated the understanding of the study hypothesis and concept as stipulated in Chapter 1. During the course of this study, challenges in terms of methodology were addressed through making multiple attempts, especially on the solid-state form preparation approach in an effort to ensure sample purity. Significant attention was placed on the development of a suitable HPLC method due to the fact that limited research has been published on ternary APIs but specifically on the combination of these three drugs together into one solid-state form. From a literature search it became apparent that a suitable HPLC method didn't exist and the analytical success of this project hinged on the accurate quantification of the concentrations of the three drugs during equilibrium solubility and dissolution testing. Inevitably, this resulted in the development and validation of an appropriate HPLC method. Furthermore, from the observations and data collected, it became
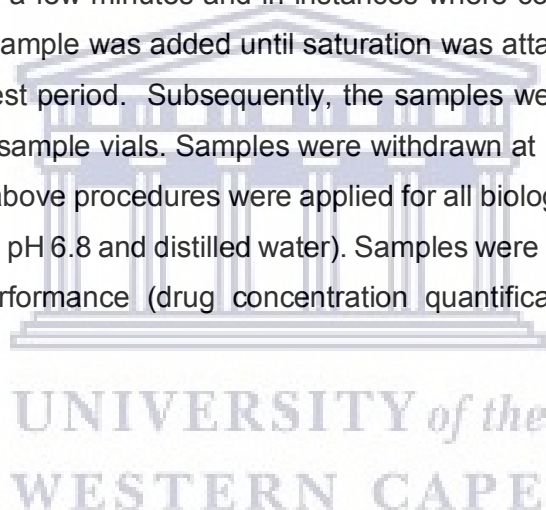
apparent that not all approaches could yield significant positive data and as such an intensive screening was necessary for a successful accomplishment of the objectives.

5.7 References:

Aucamp, M., Milne, M., & Liebenberg, W. (2016). Amorphous Sulfadoxine: A Physical Stability and Crystallization Kinetics Study. *AAPS PharmSciTech*, *17*(5), 1100–1109. https://doi.org/10.1208/s12249-015-0436-4.

Aucamp, M., Odendaal, R., Liebenberg, W., & Hamman, J. (2015). Amorphous azithromycin with improved aqueous solubility and intestinal membrane permeability. *Drug Development and Industrial Pharmacy*, *41*(7), 1100–1108. https://doi.org/10.3109/03639045.2014.931967.

Banerjee, D. (1993). Experimental Techniques in Thermal Analysis Thermogravimetry (TG) & Differential Scanning Calorimetry (DSC). *Analytical Proceedings*, *12*, 469–508.

Beynon, R. J., & Easterby, J. S. (2018). Preparation of buffer solutions. *Buffer Solutions*, 45–62. https://doi.org/10.4324/9780203494691-5.

Byrn, S. R., Zografi, G., & Chen, X. S. (2017). Solubility and Dissolution. *Solid State Properties of Pharmaceutical Materials*, 249–264. https://doi.org/10.1002/9781119264408.ch17.

Dengale, S. J., Grohganz, H., Rades, T., & Löbmann, K. (2016). Recent advances in co-amorphous drug formulations. *Advanced Drug Delivery Reviews, 100*(2016), 116–125. https://doi.org/10.1016/j.addr.2015.12.009.

Durowoju, I. B., Bhandal, K. S., Hu, J., Carpick, B., & Kirkitadze, M. (2017). Differential scanning calorimetry — A method for assessing the thermal stability and conformation of protein antigen. *Journal of Visualized Experiments*, *2017*(121), 1–8. https://doi.org/10.3791/55262.

Dutrow, B. L. & Clark, C. M. (2016). *Geochemical Instrumentation and Analysis X-ray Powder Diffraction (XRD) What is X-ray Powder Diffraction Fundamental Principles of X-ray Powder Diffraction (XRD) X-ray Powder Diffraction (XRD) Instrumentation - How Does It Work ?* 1–8.

Formulary, T. H. E. N. (2018). *2018 the United States Pharmacopeia* (Vol. 2).

Ghaderi F, M. F. (2015). Thermal Analysis Methods in Pharmaceutical Quality Control. *Journal of Molecular Pharmaceutics & Organic Process Research*, *03*(01), 1–2. https://doi.org/10.4172/2329-9053.1000e121.

Ghari, T., Kobarfard, F., & Mortazavi, S. A. (2013). Development of a simple RP-HPLC-UV method for determination of azithromycin in bulk and pharmaceutical dosage forms as an

alternative to the USP method. *Iranian Journal of Pharmaceutical Research*, *12*(SUPPL.), 55–61. https://doi.org/10.22037/ijpr.2013.1272.

Hofko, B., Porot, L., Falchetto Cannone, A., Poulikakos, L., Huber, L., Lu, X., Mollenhauer, K., & Grothe, H. (2018). FTIR spectral analysis of bituminous binders: reproducibility and impact of ageing temperature. *Materials and Structures/Materiaux et Constructions*, *51*(2). https://doi.org/10.1617/s11527-018-1170-7.

Homayun, B., Lin, X., & Choi, H. J. (2019). Challenges and recent progress in oral drug delivery systems for biopharmaceuticals. *Pharmaceutics*, *11*(3). https://doi.org/10.3390/pharmaceutics11030129.

Jaiswar, D. R., Jha, D., & Amin, P. D. (2016). Preparation and characterizations of stable amorphous solid solution of azithromycin by hot melt extrusion. *Journal of Pharmaceutical Investigation*, *46*(7), 655–668. https://doi.org/10.1007/s40005-016-0248-x.

Karagianni, A., Kachrimanis, K., & Nikolakakis, I. (2018). Co-amorphous solid dispersions for solubility and absorption improvement of drugs: Composition, preparation, characterization and formulations for oral delivery. *Pharmaceutics*, *10*(3). https://doi.org/10.3390/pharmaceutics10030098.

Karmwar, P., Graeser, K., Gordon, K. C., Strachan, C. J., & Rades, T. (2011). Investigation of properties and recrystallisation behaviour of amorphous indomethacin samples prepared by different methods. *International Journal of Pharmaceutics*, *417*(1–2), 94–100. https://doi.org/10.1016/j.ijpharm.2010.12.019.

Löbmann, K., Laitinen, R., Grohganz, H., Gordon, K. C., Strachan, C., & Rades, T. (2011). Coamorphous drug systems: Enhanced physical stability and dissolution rate of indomethacin and naproxen. *Molecular Pharmaceutics*, *8*(5), 1919–1928. https://doi.org/10.1021/mp2002973.

Lodagekar, A., Chavan, R. B., Mannava, M. K. C., Yadav, B., Chella, N., Nangia, A. K., & Shastri, N. R. (2019). Co amorphous valsartan nifedipine system: Preparation, characterization, in vitro and in vivo evaluation. *European Journal of Pharmaceutical Sciences*, *139*(August), 105048. https://doi.org/10.1016/j.ejps.2019.105048.

Mudie, D. M., Samiei, N., Marshall, D. J., Amidon, G. E., & Bergström, C. A. S. (2020). Selection of In Vivo Predictive Dissolution Media Using Drug Substance and Physiological Properties. *AAPS Journal*, *22*(2), 1–13. https://doi.org/10.1208/s12248-020-0417-8.

Newman, A., Reutzel-Edens, S. M., & Zografi, G. (2018). Coamorphous Active Pharmaceutical Ingredient–Small Molecule Mixtures: Considerations in the Choice of Coformers for Enhancing Dissolution and Oral Bioavailability. *Journal of Pharmaceutical Sciences*, *107*(1), 5–17. https://doi.org/10.1016/j.xphs.2017.09.024.

Ojarinta, R., Heikkinen, A. T., Sievänen, E., & Laitinen, R. (2017). Dissolution behavior of co-amorphous amino acid-indomethacin mixtures: The ability of amino acids to stabilize the supersaturated state of indomethacin. *European Journal of Pharmaceutics and Biopharmaceutics*, *112*, 85–95. https://doi.org/10.1016/j.ejpb.2016.11.023.

Punčochová, K., Heng, J. Y. Y., Beránek, J., & Štěpánek, F. (2014). Investigation of drug-polymer interaction in solid dispersions by vapour sorption methods. *International Journal of Pharmaceutics*, *469*(1), 159–167. https://doi.org/10.1016/j.ijpharm.2014.04.048.

Rajeswari, A. E. Jackcina, S. C, Sreerag, G. K. Jayaraj, A.P ,9 - Characterization studies of polymer-based composites related to functionalized filler-matrix interface, Editor(s): Kheng, L. G, Aswathi M.K., Rangika, T. L, Sabu. T, In Woodhead Publishing Series in Composites Science and Engineering, Interfaces in Particle and Fibre Reinforced Composites, Woodhead Publishing, 2020, Pages 219-250, ISBN 9780081026656, https://doi.org/10.1016/B978-0-08-102665-6.00009-1.
(https://www.sciencedirect.com/science/article/pii/B9780081026656000091).

Šimek, M., Grünwaldová, V., & Kratochvíl, B. (2014). Hot-stage microscopy for determination of API particles in a formulated tablet. *BioMed Research International*, *2014*. https://doi.org/10.1155/2014/832452.

Singh, A. P., Chauhan, I., Bhardwaj, S., Gaur, P., Kumar, S. S., & J, J. (2019). Hplc Method Development and Validation for Azithro-Mycin in Oral Suspension. *Journal of Applied Pharmaceutical Sciences and Research*, *April*, 7–12. https://doi.org/10.31069/japsr.v2i1.2.

Towers, M. (2009). British Pharmacopoeia 2009. *British Pharmacopia*, *1–4*, 1–1000. https://doi.org/10.3788/AOS201232.1231003.

Waghule, S. N., Jain, N. P., Patani, C. J., & Patani, A. C. (2013). Method development and validation of HPLC method for determination of azithromycin. *Der Pharma Chemica*, *5*(4), 166–172.

Wood, S., Hollis, J. R., & Kim, J.-S. (2016). *Reports on Progress in Physics Related content Raman spectroscopy as an advanced structural nanoprobe for conjugated molecular semiconductors*.

Yee, P. Y., Scholes, D. T., Schwartz, B. J., & Tolbert, S. H. (2019). Dopant-Induced Ordering of Amorphous Regions in Regiorandom P3HT [Rapid-communication]. *Journal of Physical Chemistry Letters*, *10*(17), 4929–4934. https://doi.org/10.1021/acs.jpclett.9b02070.

Zaborenko, N., Shi, Z., Corredor, C. C., Smith-Goettler, B. M., Zhang, L., Hermans, A., Neu, C. M., Alam, M. A., Cohen, M. J., Lu, X., Xiong, L., & Zacour, B. M. (2019). First-Principles and Empirical Approaches to Predicting In Vitro Dissolution for Pharmaceutical Formulation and Process Development and for Product Release Testing. *AAPS Journal*, *21*(3). https://doi.org/10.1208/s12248-019-0297-y.

Zubata, P., Ceresole, R., Rosasco, M. A., & Pizzorno, M. T. (2002). A new HPLC method for azithromycin quantitation. *Journal of Pharmaceutical and Biomedical Analysis*, *27*(5), 833–836. https://doi.org/10.1016/S0731-7085(01)00554-4.

CHAPTER 6

The preparation and physico-chemical characterisation of a ternary amorphous system consisting of sulfadoxine, pyrimethamine and azithromycin

6.1 Introduction

As discussed in preceding chapters malaria is still a life-threatening disease. Two drugs typically used in the treatment of malaria, sulfadoxine (SUL) and pyrimethamine (PYR) are still considered essential in areas with low resistance to SUL and PYR, with the World Health Organisation (WHO) recommending at least three doses of SUL and PYR (1500 mg + 75 mg) available as a fixed dose combination (FDC), in a monthly interval from the second trimester during pregnancy (Chapter 2, paragraph *2.5*). Furthermore, due to other pregnancy related complications arising from sexually transmitted diseases, (STDs) and urinary tract infections (UTIs), such as low birth weight and premature birth; the third drug, azithromycin (AZI) is currently recommended for inclusion in the abovementioned regimen to reduce the aforementioned risks and any negative impact to both the fetus (baby) and mother (Chapter 2, *paragraph 2.5*). As literature dictates, SUL, PYR and AZI are all poorly soluble in aqueous media (Chapter 4). The aim of this study was to improve the aqueous solubility of SUL, PYR and AZI through the potential preparation of a ternary amorphous system. As described in Chapter 1, *paragraph 1.3*, specific aims for this study were to firstly characterise the physico-chemcial properties of the three APIs to provide an experimental foundation which would facilitate accurate data interpretation and inform amorphous solid-state formation methods. The study progressed further towards investigating different co-amorphous preparation techniques and finally thorough physico-chemical characterisation of prepared solid-state forms were conducted. This chapter will be discussing all experimental work conducted towards achieving the overall aim of the study.

6.2 The physico-chemical characterisation of SUL, PYR, AZI and the physical mixture SPA-C

An integral part of any solid-state chemistry study involving APIs is the initial physico-chemical characterisation of the compounds under investigation. For this study it was important to firstly investigate the thermal behaviour of the crystalline solid-state forms of the three APIs, especially to inform potential incompatibility of the three APIs in combination with one another but also to allow decision-making on the most appropriate preparation method of a potential new amorphous solid-state form. Furthermore, thorough analysis using Fourier-transform infrared spectroscopy (FTIR), powder X-Ray diffraction (PXRD), moisture sorption analysis, equilibrium solubility and dissolution rate studies involving the individual compounds as well

as the physical mixture, termed SPA-C, was necessary to allow the collection of a thorough set of baseline data.

6.2.1 Thermal analysis

Thermal analyses form the cornerstone of any solid-state chemistry and solid-state form modification study. The reason being the differences in the internal energy (enthalpy and entropy) associated with different solid-state forms of a drug (Lipatov *et al*., 1976; Psimadas *et al*., 2012). All three crystalline drugs were analysed using the thermo-analytical techniques of DSC, TGA and HSM, as described in Chapter 5. Data generated using these three techniques were interpreted together and in comparison, with another to form a thorough understanding of not only the thermal behaviour of the individual compounds but also that of a physical mixture of SPA-C prior to any solid-state modification.

Visual observation of SUL using the HSM setup as described in Chapter 5, paragraph 5.4.1) confirmed an off-white to yellowish, crystalline habit which correlated with that described in literature Cimellaro and Marasco, (2018). Figure 6.1 depicts the DSC thermogram obtained for SUL when heated from 40 – 250°C. A single, sharp melting endotherm was observed with a peak melting temperature (T_m) of 201.36°C. HSM confirmed the results obtained during DSC analysis with the onset of degradation at ≈223°C being visible as discolouration of the molten sample (Figure 6.1(c)). These results correlated with previous studies (Holtzkamp, 2016; Aucamp et al., 2016; Badenhorst, 2017).
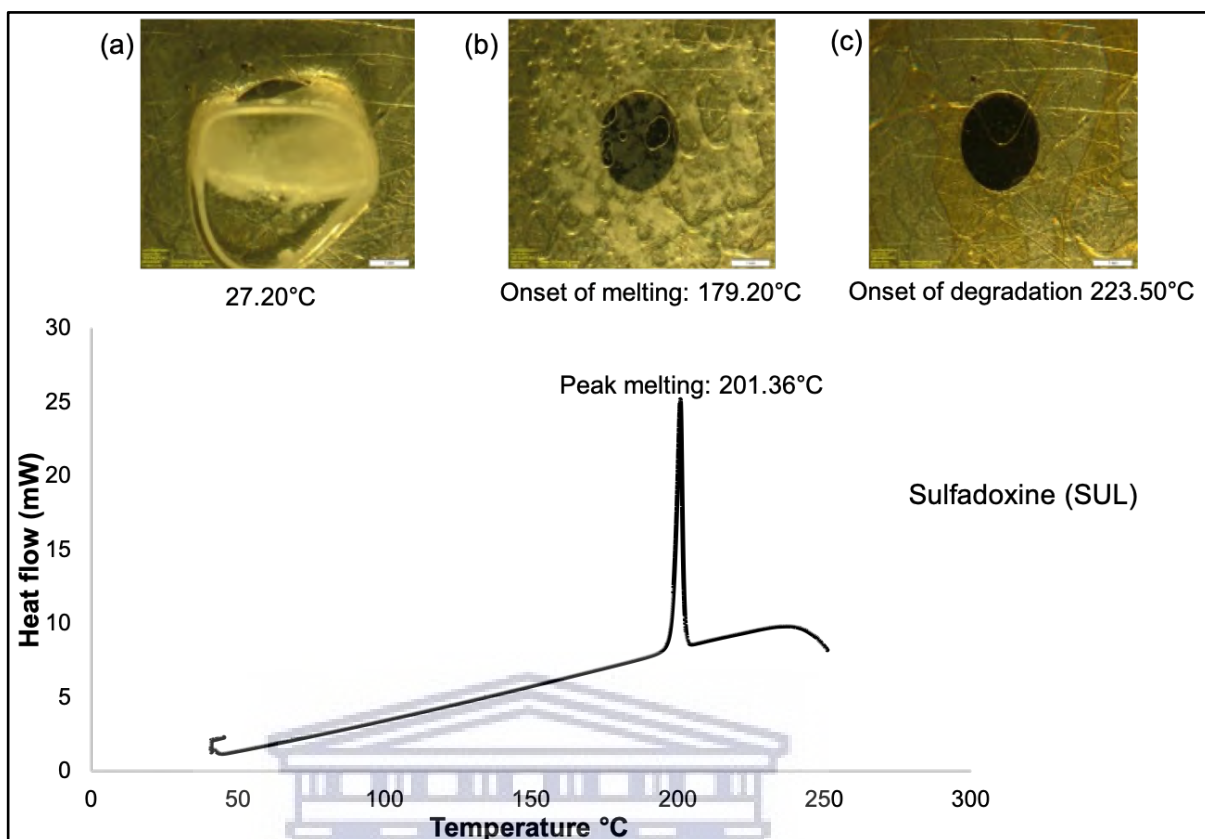
Figure 6.1: DSC thermogram obtained for SUL during heating from 40 – 250°C applying a heating rate of 10°C/min. Insets (a) depicts an HSM micrograph of SUL at ambient temperature, (b) onset of melting and (c) onset of degradation.

The DSC analysis of PYR showed a single, sharp melting endotherm at a peak temperature of 242.06°C with HSM showing onset of melting at ≈230°C. This confirms results reported from previous studies (Holtzkamp, 2016; Badenhorst, 2017).
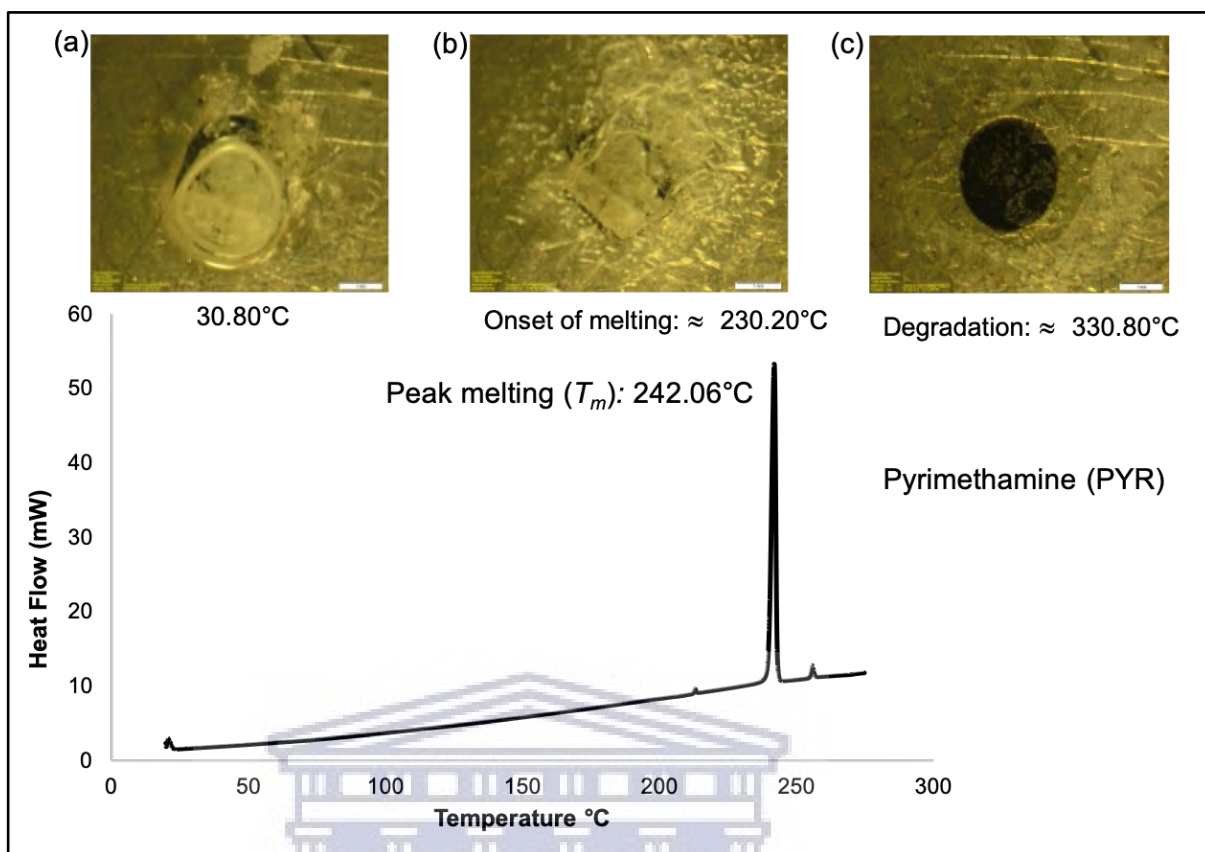
Figure 6.2: DSC thermogram obtained for PYR during heating from 30 – 280 °C applying a heating rate of 10°C/min. Insets (a) depicts an HSM micrograph of SUL at ambient temperature, (b) onset of melting and (c) onset of degradation.

The DSC analysis of AZI showed an endothermic shift in the baseline from ≈75 - 100°C followed by a small and broad endothermic event. Using HSM analysis it was noted that the initial thermal event is attributed to dehydration, which correlates with the fact that the solid-state form used in this study was the dihydrate form of AZI. The second thermal event was confirmed to be melting of the compound with a peak melting temperature (T_m) of 119.67°C.

In a previous study by Aucamp *et al*. (2015), DSC analysis of AZI dihydrate showed two endothermic peaks at 76.4 and 86.5°C, respectively, confirming the dehydration of the compound. Due to equipment limitations and the fact that DSC analysis couldn't be performed using a pierced DSC sample pan lid the two dehydration events were observed as an endothermic baseline drift. The small melting endotherm observed in this study corresponds to that reported by Aucamp *et al*. (2015).
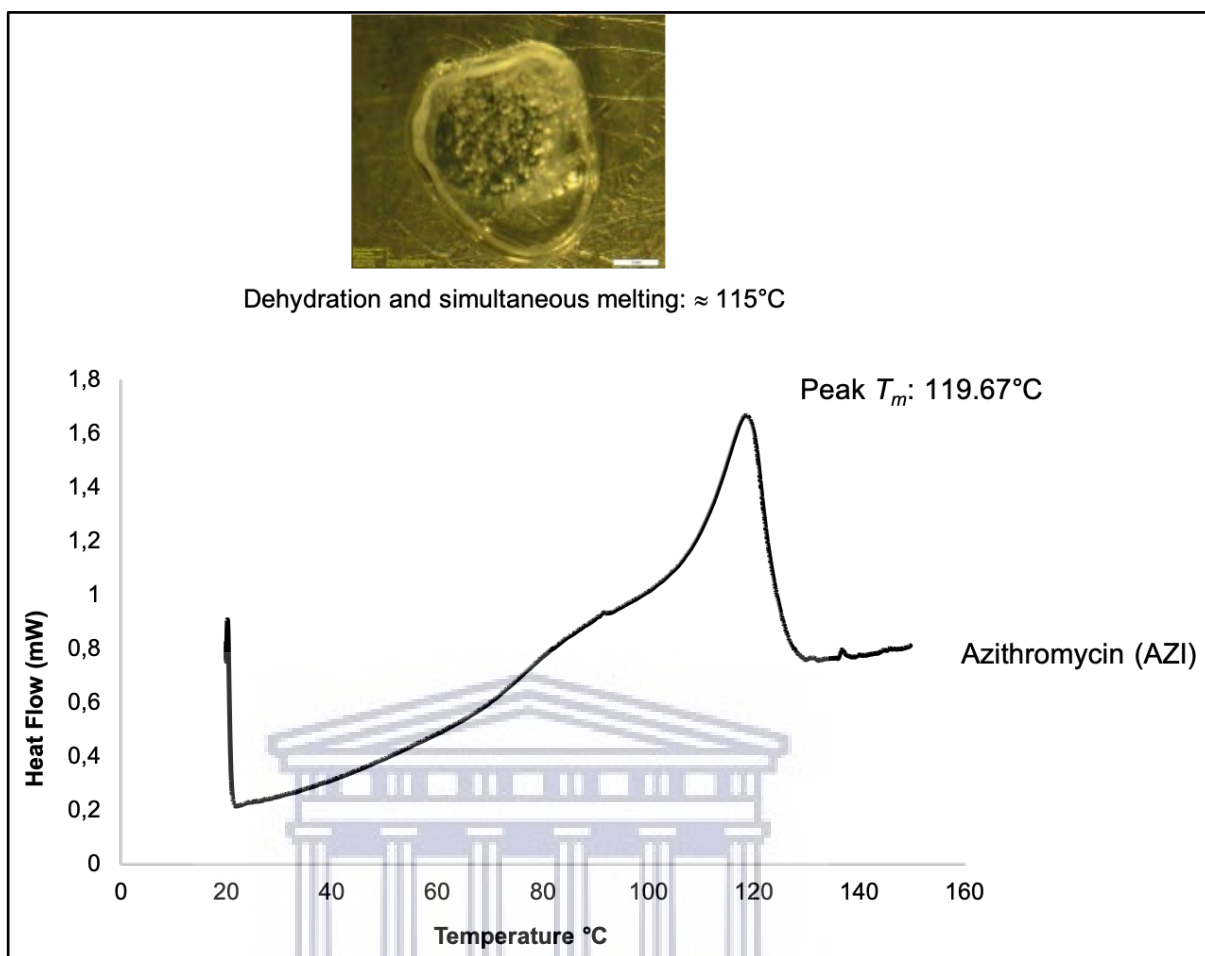
Figure 6.3: DSC thermogram obtained for AZI during heating from 20 – 150°C applying a heating rate of 10°C/min. Inset (a) HSM micrograph depicting the onset of melting visually observed at ≈115°C.

Since the aim of this study was to improve the aqueous solubility of all three compounds through molecular modification, rendering the three compounds in an amorphous solid dispersion or a ternary amorphous system, the three compounds were subsequently combined and mixed as a physical mixture in the following ratios 1:0.05:1 w/w/w for SUL, PYR and AZI. This physical mixture was subsequently termed SPA-C and thermal analysis thereof followed.
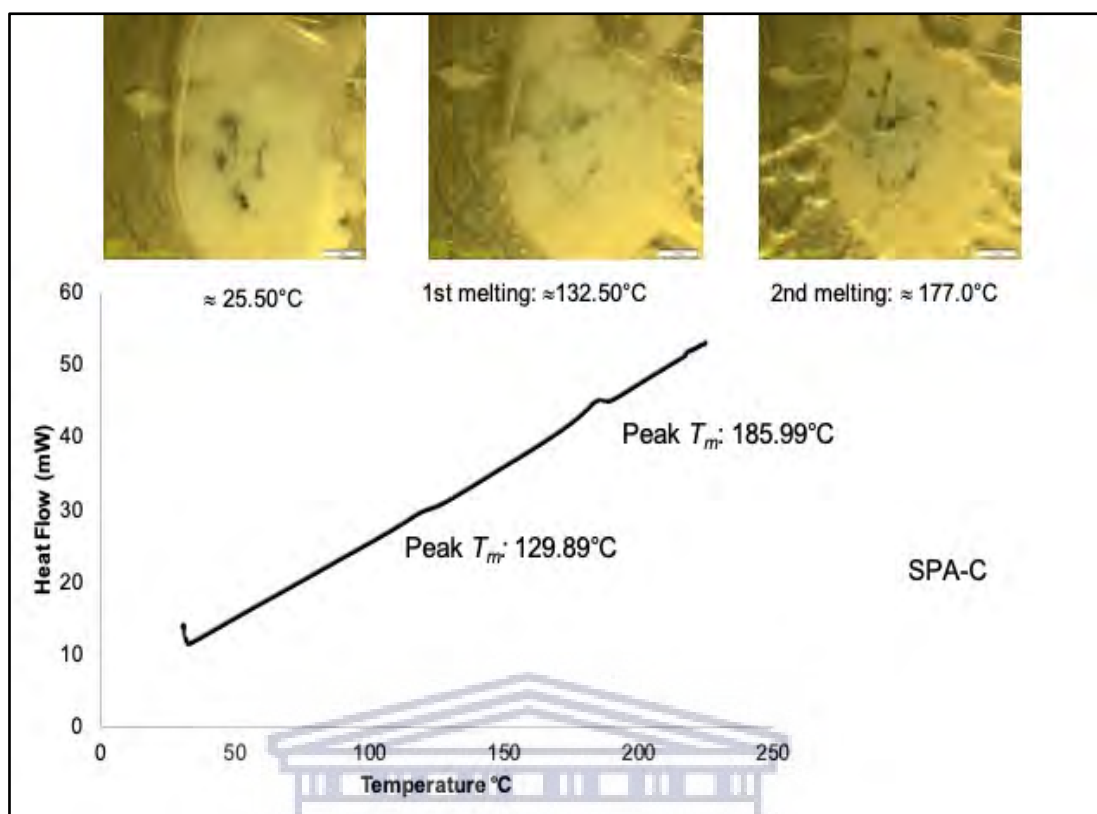
Figure 6.4: DSC thermogram obtained for SPA-C during heating from 20 - 250°C with a heating rate of 10°C/min applied.

The DSC thermogram obtained with SPA-C showed the onset of a thermal event at 122.49℃ which could be considered as a combination of thermal events associated with AZI. HSM proved the dehydration of AZI in the temperature range of 82.2 - 130.0°C inferring to the loss of molecular water of azithromycin dihydrate. Based on the visual observations made using HSM the melting of AZI was occurring simultaneously with dehydration. Referring to the DSC thermogram under discussion, the peak temperature (Peak T_m) for the first thermal event was observed at 129.89°C which is approximately 10°C higher than the Peak T_m observed for AZI **(Figure 6.3)** but correlating with that observed using HSM **(Figure 6.4 inset)**. It is hypothesised that this is due to the mixing of the three APIs, resulting in a reduction in the heat of fusion of AZI, especially since the melting of AZI could also result in the solubilisation of SUL and PYR in the molten part of the sample. Following this thermal event, a second event was observed at a peak temperature of 185.99°C, this confirmed the HSM observation of a second onset of melting at ≈177.0°C. It was thus deduced that this thermal event is linked to the melting of SUL which showed an onset of melting at 179.20°C **(Figure 6.1)**. Once again this endothermic event was significantly smaller than that observed with the individual APIs and it was further concluded that this is due to the miscibility of the compounds. This second endotherm does however confirm that the miscibility of the three compounds is not complete

since should there exist complete miscibility of the compounds only one endothermic event would've been observed. This being said, it should be highlighted that this second endotherm was 15.37°C and 55.67°C lower than that of SUL and PYR, respectively.

TGA of the single crystalline compounds as well as the physical mixture (SPA-C) was conducted to determine if any dehydration, desolvation or interaction of the individual compounds in SPA-C will occur during heating of the samples. TGA was also utilised to investigate the degradation temperature of the mentioned samples. TGA data of PYR and SUL, **Figure 6.5(a)** and **(c)** showed no weight loss from 30°C to approximately 200°C. Loss in weight was observed above 240°C and 260°C, respectively as the drugs started to degrade. AZI, however, behaved differently with approximately 4.3% loss of mass quantified at ≈90-110°C **(Figure 6.5 (b))**, this value conferred to the theoretical percentage (4.5%) and linked to dehydration of two molecules of water that is part of the molecular structure of AZI, confirming that the dihydrate form of AZI was used in this study. During the TGA of the physical mixture (SPA-C), depicted in **Figure 6.5(d)**, an initial weight loss between 95 - 110 °C was observed which was quantified to 3.5%. This weight loss % correlated with the relative amount of AZI present in SPA-C and was thus ascribed to the presence of AZI in the mixture. Further analysis of the TGA trace demonstrated a significant weight loss of 84.8% with an onset temperature of 230°C. The onset of degradation observed with SPA-C was not lower than that obtained with any of the individual compounds, with the onset temperature determined to be 245°C and thus it was concluded that the three compounds are compatible with one another.
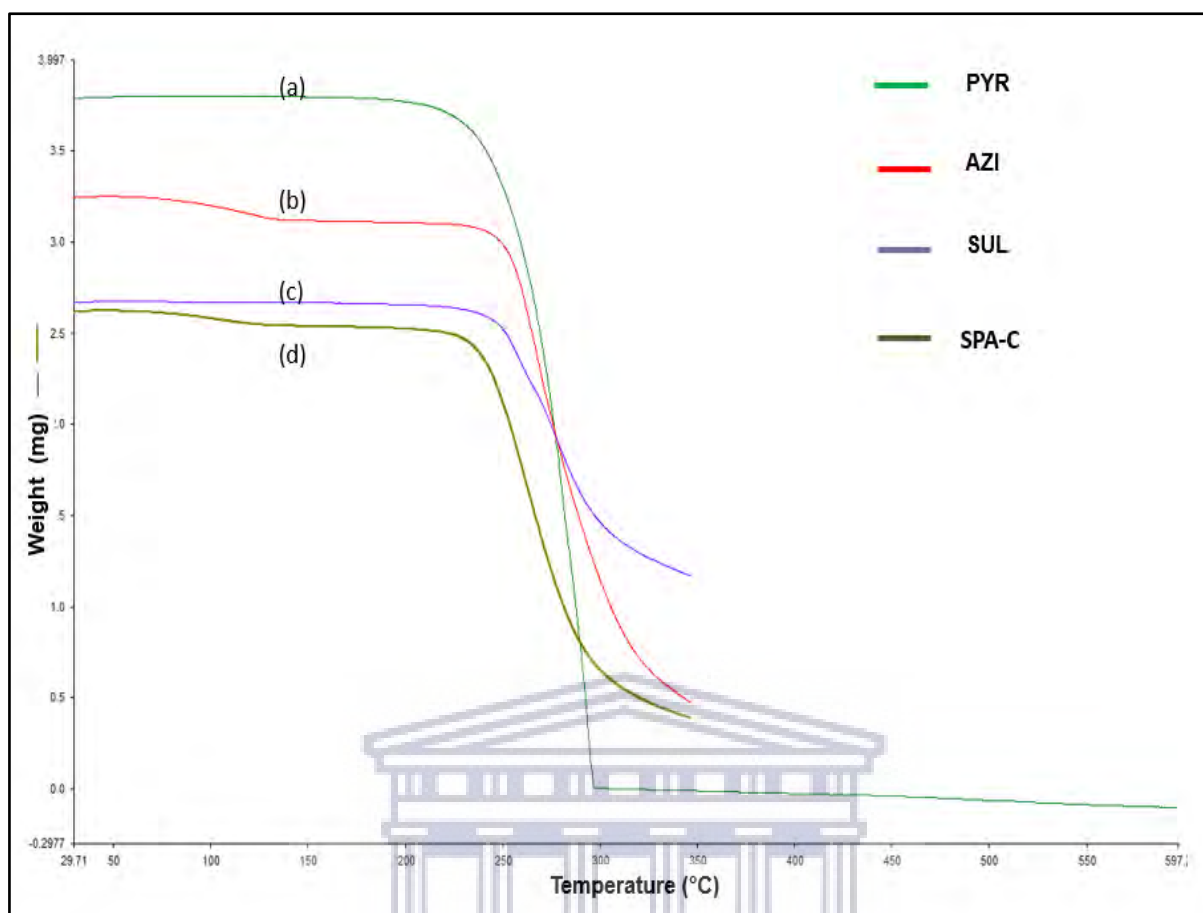
Figure 6.5: Overlay of TGA obtained for (a) PYR, (b) AZI, (c) SUL and (d) SPA-C during heating from 30 – 600°C for PYR and 30 – 350 °C for SUL, AZI and SPA-C; applying a heating rate of 10°C/min.
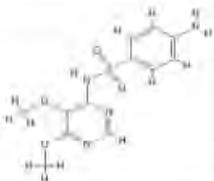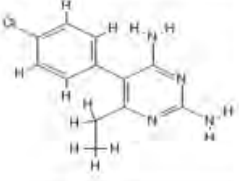
6.2.2 Fourier-transform infrared spectroscopy (FTIR)
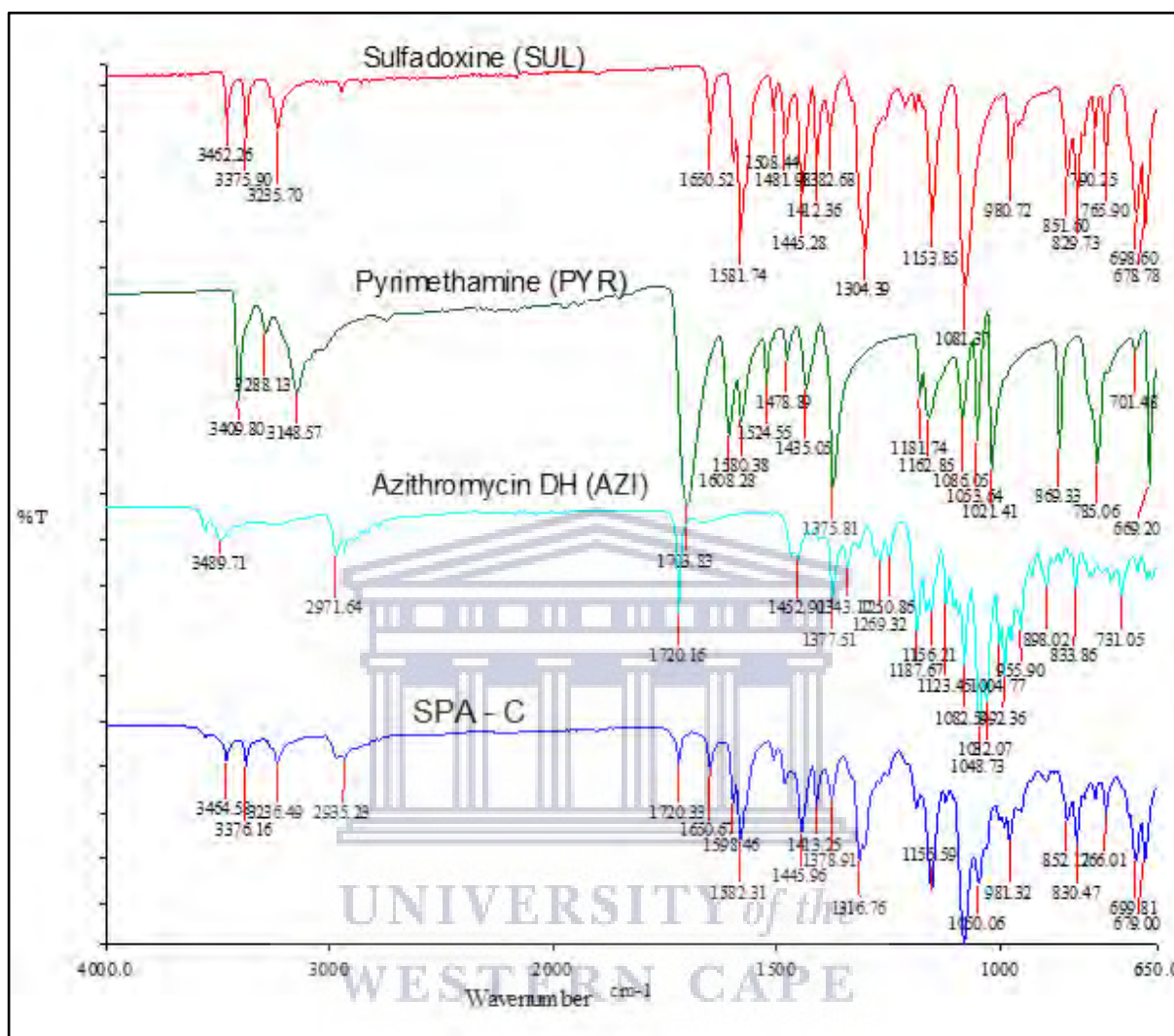
Figure 6.6: Overlay of FTIR spectra obtained for SUL, PYR, AZI and SPA-C.

The FTIR spectra of pure crystalline SUL, PYR, AZI and SPA-C (**Figure 6.6**) and (**Table 6.1**), depict the IR absorption bands obtained for the individual compounds in comparison with that of the physical mixture (SPA-C). For SUL characteristic absorbance bands were observed at 3462.21 and 3375.88 cm^{-1}, corresponding to stretching vibrations of N-H and C-H of the aromatic ring; peaks at 1650.39 and 1581.68 cm^{-1} are due to vibrational stretching of C=N and C=C, respectively (Braschi *et al*., 2013). Other peaks below 1480 cm^{-1} indicate vibrational stretching of C-H from the CH_3- groups and C-N, S=0. Distinctive IR absorbance bands for PYR were observed at 3466.15 and 3133.82 cm^{-1} (**Figure 6.6**) which are associated with stretching vibrations of the N-H and aromatic ring C-H functional groups, respectively

Table 6.1: Table of SUL, PYR and AZI chemical structures describing the wavenumbers obtained from FTIR analysis with correlating functional groups (El-Badry, 2011; Mallah *et al.*, 2011; Braschi *et al.*, 2013; Aucamp *et al.*, 2015; Jaiswar, Jha and Amin, 2016; Santana *et al.*, 2021)

SUL		PYR		AZI		SPA-C	
Wavenumber (cm⁻¹)	Functional group	Wavenumber (cm⁻¹)	Functional group	Wavenumber (cm⁻¹)	Functional group	Wavenumber (cm⁻¹)	Functional group
-	-	-	-	3559.52	-OH	-	-
-	-	-	-	3497.27	-OH	-	-
3462.21	N-H	3466.15	N-H	-	-	3464.58	N-H
3375.88	C-H	3133.82	C-H	-	-	3376.16	C-H
						3236.49	C-H
2948.41	C-H	-	-	2971.44	C-H	-	-
-	-					2935.23	C-H
-	-	-	-	1720.18	C=O	1720.33	C=O
1650.39	C=N	1625.87	C=N			1650.67	C=N
-	-	-	-	-	-	1598.46	C=C
1581.68	C=C	1556.2	C=C			1582.31	C=C
1445.29	CH	1436.22	CH	1457.62	CH	1445.96	CH
1304.38	C≡N			1377.42	C≡N	1378.91	C≡N
					C-O-C		

(**Table 6.1**) (El-Badry, 2011). The absorption bands between 1625.87 and 1556.2 cm^{-1} of PYR correspond to the stretching vibrations of C=N and C=C on the aromatic rings of the chemical structure. The peaks displayed at 1436.22 and 1278.28 cm^{-1} of the spectrum indicate C-H bending vibration from CH$_3$ and C-N stretching vibration, respectively (El-Badry, 2011). The spectrum of pure AZI (**Figure 6.6**) showed peaks at 3559.52 cm^{-1} and 3497.27 cm^{-1} indicating free and bound –OH-groups (**Table 6.1**) which is associated to the two molecules of water of crystallisation found in the dihydrate structure of AZI (Mallah *et al.*, 2011). Other sharp IR absorbance bands of AZI were observed at 2971.44 indicating C-H stretching and at 1720.18 cm^{-1} indicative of a C=O stretch. Furthermore, IR absorption bands at 1457.62 cm^{-1} and 1377.42 cm^{-1} are related to the vibrational stretching of the CH$_3$ and C≡N functional groups. A

sharp peak at 1187.53 cm^{-1} indicates asymmetrical stretching of C–O–C whereas the

absorbance peak at 1052 cm^{-1} is linked to C–O–C symmetrical stretching (Santana *et al.*, 2021). To elucidate a comprehensive compatibility profile of the combination of SUL, PYR and AZI as in SPA-C, FTIR data was collected for SPA-C as well and the infrared absorbance characteristics showed no significant change in peaks, affirming no strong and lasting intermolecular interactions between the three APIs when existing in a mere physical mixture (**Figure 6.6**)

6.2.3 Powder X-ray diffraction (PXRD)

The PXRD patterns of SUL, PYR, AZI and SPA-C illustrated characteristic, sharp diffraction peaks detected at multiple scattering angles from 4 - 40 °2θ with variable peaks intensities known for crystalline compounds. Peaks observed for SPA-C confirmed the presence of all the individual components with no significant interference or shifts in the diffraction angles. This was considered as an indication of compatibility of the individual compounds forming SPA-C. A study by Aucamp, et. al, (2016), confirms a similar habit of sulfadoxine. The finding from (Onyeji, et al., 2009) on physicochemical characterisation of pyrimethamine and 2-hydroxypropyl-β-cyclodextrin, depicted an identical sharp peak for pure crystalline PYR as obtained in the current study. The PXRD patterns observed for pure crystalline AZI in the studies by (Aucamp et al., 2015 and Jaiswar et al., 2016) confirmed a similar diffraction profile of the crystalline AZI.

Table 6.2: Summary of PXRD diffraction peaks observed with SUL, PYR, AZI and SPA-C

SUL (°2θ)	PYR (°2θ)	AZI (°2θ)	SPA-C (°2θ)
		7.96	8.18
9.78	-	9.87	9.88
		11.25	11.41
		11.93	-
-	12.15	-	12.18
		12.83	12.80
-	-	15.99	15.81
-	-	16.55	16.55
-	-	16.63	-
-	-	16.96	16.90
17.82	-	-	17.91
18.35	-	-	18.41
-	18.74	-	18.80
-	19.49	-	-
19.63	-	19.85	19.67
-	20.26	-	-
25.00	-	-	-
-	25.52	-	25.54
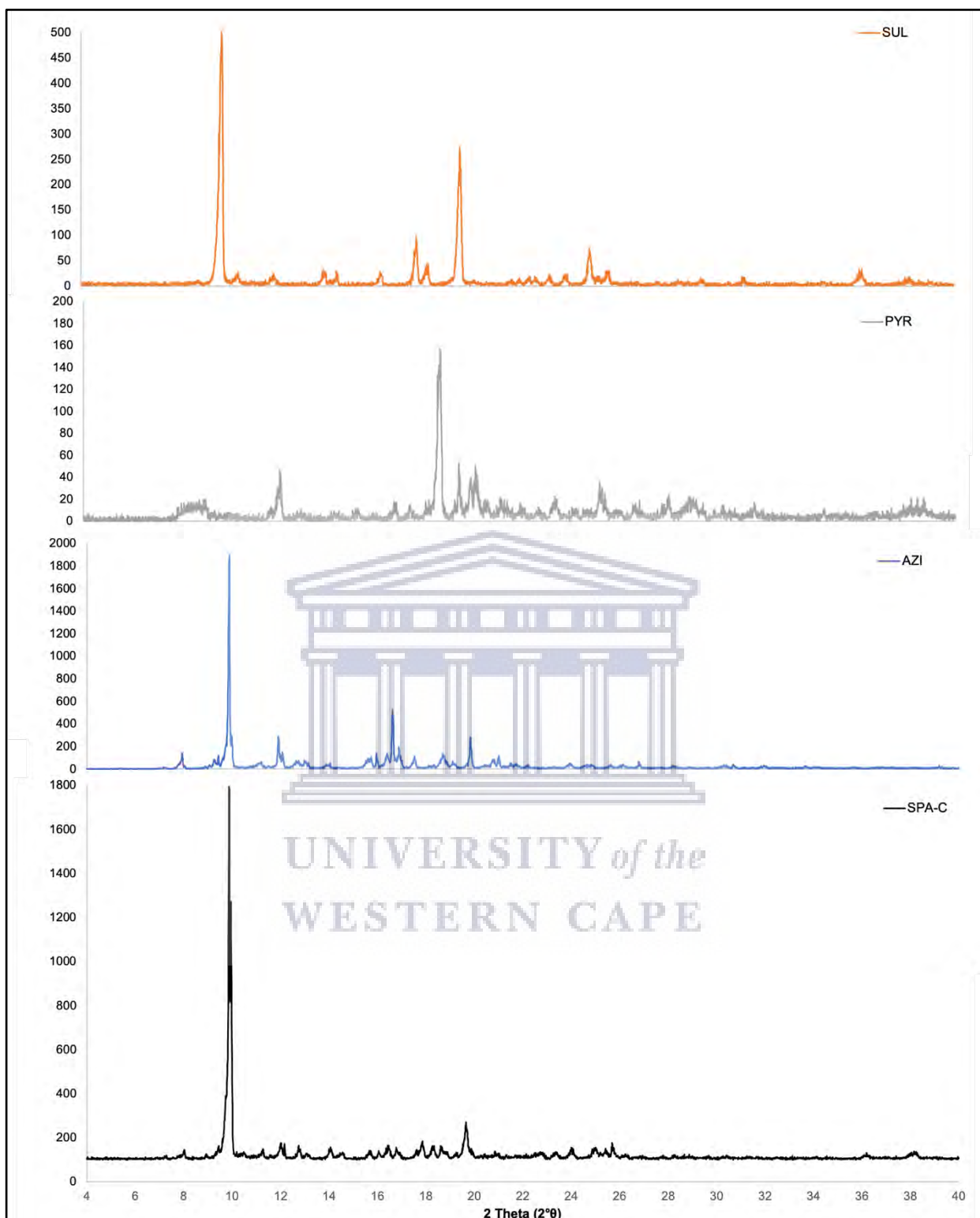
Figure 6.7: An overlay of the PXRD patterns obtained for SUL, PYR, AZI and SPA-C, across a scanning range of 4-40°2θ, collected at ambient temperature.

6.2.4 Vapour sorption analysis

Vapour sorption analysis is an important gravimetric analytical tool used to determine the amount of moisture as well as the kinetics involved during vapour sorption of a compound. Different compounds and specifically different solid-state forms of the same drug may adsorb vapour in varying amounts and following varying kinetics during exposure to isothermal and elevated relative humidity conditions (Sheokand, Modi and Bansal, 2014). These observed vapour sorption differences allow one to understand the specific solid-state form under investigation better in terms of physical stability. When investigating different solid-state forms of a drug or even combinations of amorphous drugs such as co-amorphous forms or solid dispersions vapour sorption analysis may be used to investigate the physical stability of these solid-state forms. Thus, to aid in further investigation it was therefore imperative to firstly investigate the vapour sorption behaviour of the individual compounds.
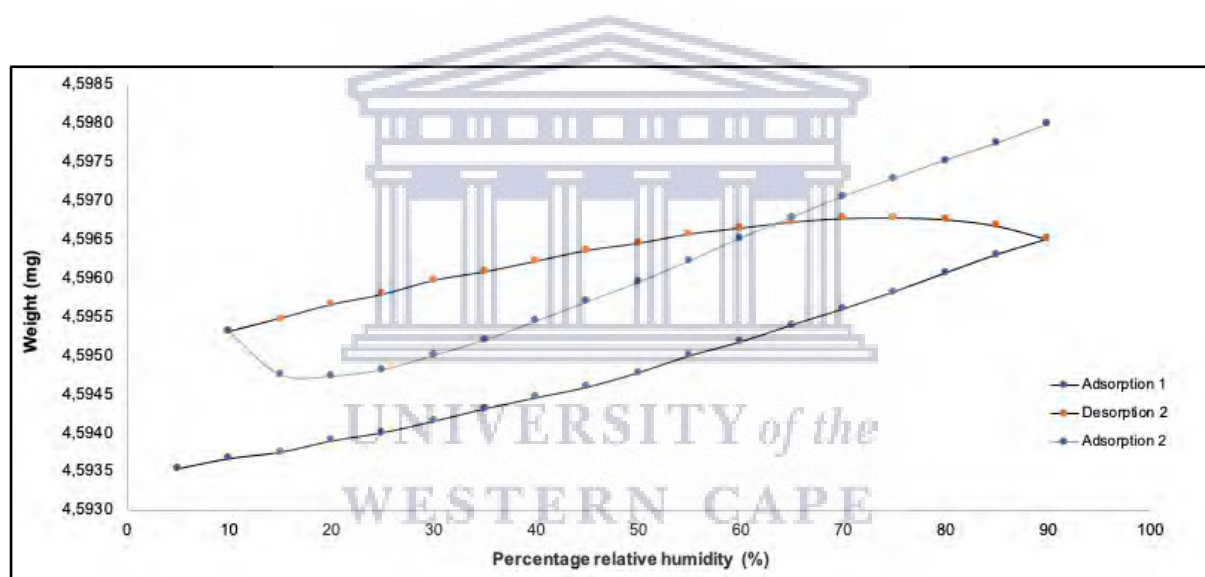
Figure 6.8: Moisture sorption isotherms obtained for SUL during exposure to increasing percentage relative humidity (%RH) (5 - 90 %RH), decreasing, 90 - 5 %RH and finally a second increase in %RH from 5 - 90 %RH.

The moisture sorption isotherm obtained for SUL **(Figure 6.8)** showed that this crystalline compound adsorbed a total of 0.003 mg water during the first adsorption phase (5 - 90% RH). The moisture sorption isotherm showed to be a Type III moisture sorption isotherm based on the fact that low levels of moisture is adsorbed at low %RH levels, however a significant increase in moisture adsorption was not observed when %RH levels increased. It can therefore be stated that the SUL adsorption isotherm doesn't fit a typical moisture sorption isotherm as described in literature (Thielmann and Burnett, 2012; Mathlouthi and Rogé, 2003; Andrade, Lemus and Pèrez, 2011). The isotherm plots obtained during the adsorption and

desorption phase may show significant differences in terms of weight adsorbed or desorbed at a specific %RH. This phenomenon is termed hysteresis and based on the difference between observed adsorption - desorption - adsorption isotherms the moisture sorption behaviour of a compound may be either characterised as reversible or irreversible (Aviara, 2020). The more pronounced hysteresis is between adsorption - desorption - adsorption measurements for a single sample the higher the likelihood is to conclude that a structural change occurred in the sample under investigation. During the desorption phase of SUL a weight loss of 0.001 mg was quantified and it should be mentioned that the desorption phase was only conducted until 10% RH with a possibility of more weight loss should the experiment be conducted to 5% RH. From the second adsorption phase conducted with SUL it can be concluded that the initial adsorbed moisture and subsequent desorption of the moisture didn't lead to any structural changes in the SUL molecule, this being ascribed to the similar shape of the second adsorption isotherm and the hysteresis is characterised to be reversible. Furthermore, just as with the first adsorption phase, 0.003 mg of moisture adsorption was quantified during the second adsorption phase.

Figure 6.9: Moisture sorption isotherms obtained for PYR during exposure to increasing percentage relative humidity (%RH) (0 - 90 %RH), decreasing, 90 - 5 %RH and finally a second increase in %RH from 5 - 90 %RH.

The first adsorption isotherm obtained for PYR during exposure to relative humidity from 5 - 90 %RH showed an isotherm that resembles a Type III isotherm **(Figure 6.9)**, just as was observed with SUL **(Figure 6.8)**. The first adsorption isotherm resulted in the adsorption of 0.003 mg of moisture. A small level of hysteresis was observed between the subsequent desorption isotherm and the first adsorption isotherm but it is the second adsorption isotherm

that is indicative that the sorbed amount of water is not structurally bound to the molecular structure of PYR. This conclusion is based on the fact that the second sorption isotherm showed the same Type III isotherm shape and that only 0.002 mg of water was adsorbed which is correlated with the 0.001 mg of water which got desorbed during the %RH decrease phase.
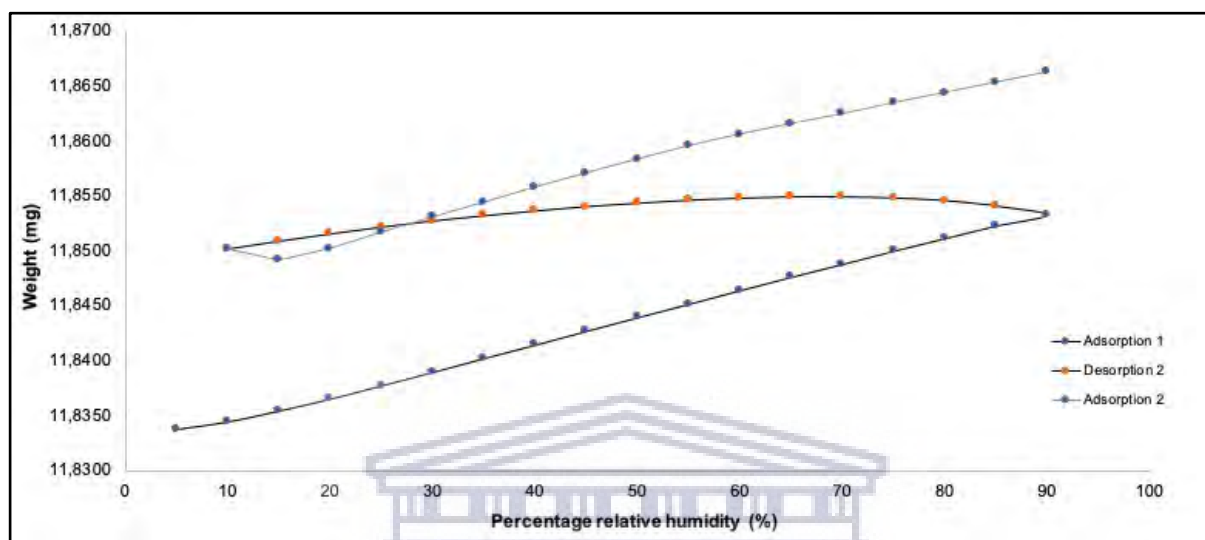
Figure 6.10: Moisture sorption isotherms obtained for AZI during exposure to increasing percentage relative humidity (%RH) (0 - 90 %RH), decreasing, 90 - 5 %RH and finally a second increase in %RH from 5 - 90 %RH.

The moisture sorption behaviour observed for AZI showed that this molecule doesn't exhibit any sensitivity towards elevated relative humidity conditions. This may be attributed to the fact that AZI dihydrate already possesses two water molecules as part of the molecular structure. The quantity of moisture adsorbed during the vapour sorption studies was low and the adsorption process proved to be reversible due to the lack of significant hysteresis observed during the first adsorption phase and the subsequent desorption phase **(Figure 6.10)**. The second adsorption phase showed to follow the same pattern as the first adsorption phase and therefore it was concluded that exposure of AZI to high levels of relative humidity didn't have a significant impact on the molecule with no solid-state form transformations observed.

On the other hand, the moisture sorption isotherms obtained during the exposure of SPA-C to increasing relative humidity levels showed interesting results. **Figure 6.11** depicts the moisture sorption isotherms obtained, with the first adsorption phase being signified by a sharp increase in the adsorbed moisture from 70%RH. The desorption phase showed that this

significant increase in the adsorbed moisture is a fully reversible process but interestingly a slight weight increase was observed during the desorption phase from 70%RH. No hysteresis was observed between the first and second adsorption phases and the same vapour sorption behaviour was observed. This shows that the desorption process didn't result in a permanent solid-state modification or transformation. From this observed phenomena it was concluded that the mere mixing of SUL, PYR and AZI resulted in a powder mixture that exhibits enhanced moisture sorption ability and it was clear that this ability could only be ascribed to the mixing of the compounds since none of the individual drugs showed this behaviour.
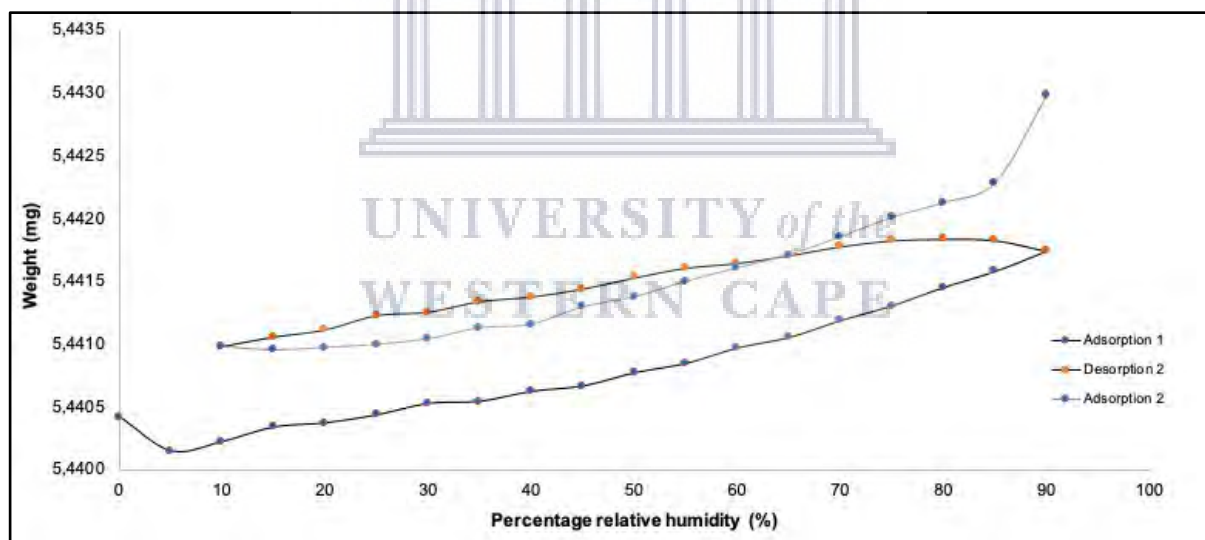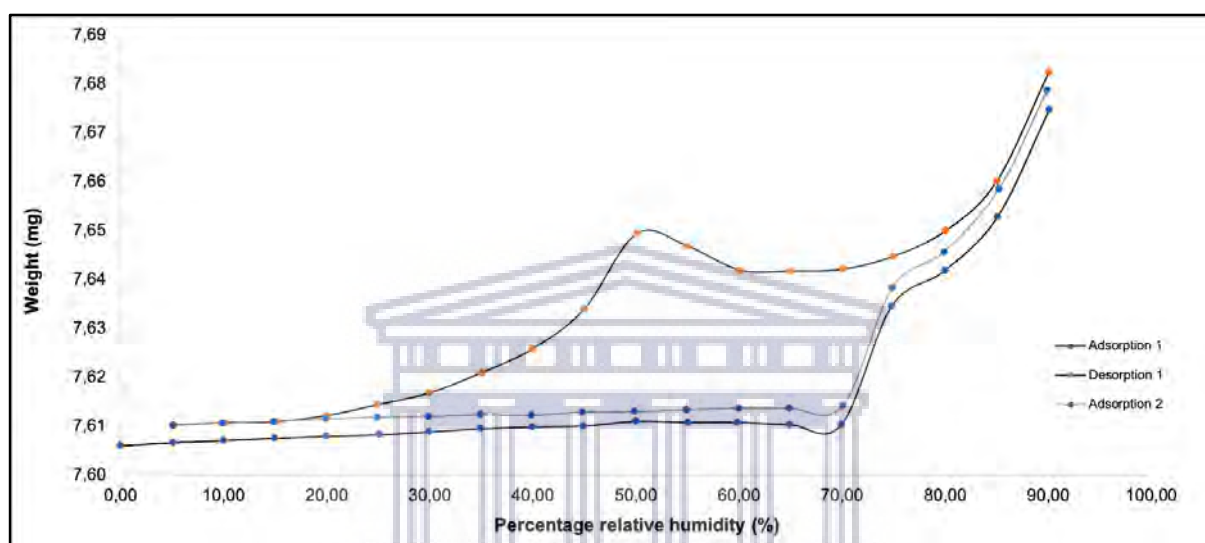

Figure 6.11: Moisture sorption isotherm obtained for SPA-C during exposure to increasing percentage relative humidity (%RH) (0 - 90 %RH), decreasing, 90 - 5 %RH and finally a second increase in %RH from 5 - 90 %RH.

6.2.5 Equilibrium solubility testing of SUL, PYR, AZI and SPA-C

6.2.5.1 Equilibrium solubility of SUL alone and SUL in SPA-C in various solubility media

Equilibrium solubility testing was conducted using the method described in Chapter 5, paragraph 5.5 to determine the equilibrium solubility of SUL, PYR, AZI and SPA-C in distilled water, pH 1.2 and pH 6.8 buffered aqueous solutions. **Figure 6.12** depicts the quantified solubility concentrations obtained for pure SUL and SUL in the SPA-C combination at 0.5, 1, 2, 4 hours and then finally equilibrium solubility after 24 hours. The equilibrium solubility concentration for SUL after 24 hours was quantified to 0.34 ± 0.02 mg/ml in distilled water and when SUL formed part of SPA-C the equilibrium solubility after 24 hours was determined to be 1.18 ± 0.05 mg/ml. This is a 347.06% increase in the solubility of SUL in distilled water. Similar equilibrium solubility behaviour was previously reported by Holtzkamp (2016), where

an equilibrium solubility concentration of 464 µg/ml was reported. However, in that study the solubility of SUL and PYR in combination with one another in a weight ratio of 500:25 w/w SUL:PYR was investigated, whilst in this current study it is expected that the presence of AZI in the SPA-C mixture will either positively or negatively affect the solubility of each individual compound. Results obtained in this study using the SPA-C combination showed a slower onset of solubility, in comparison with pure SUL since no SUL was detected in the 30 minutes solubility sample of SPA-C. Upon comparison of the results obtained in this study with that reported by Holtzkamp (2016) a 2.5-fold solubility increase for SUL in distilled water was observed. It was therefore concluded that AZI played an additional synergistic role in terms of equilibrium solubility of SUL.
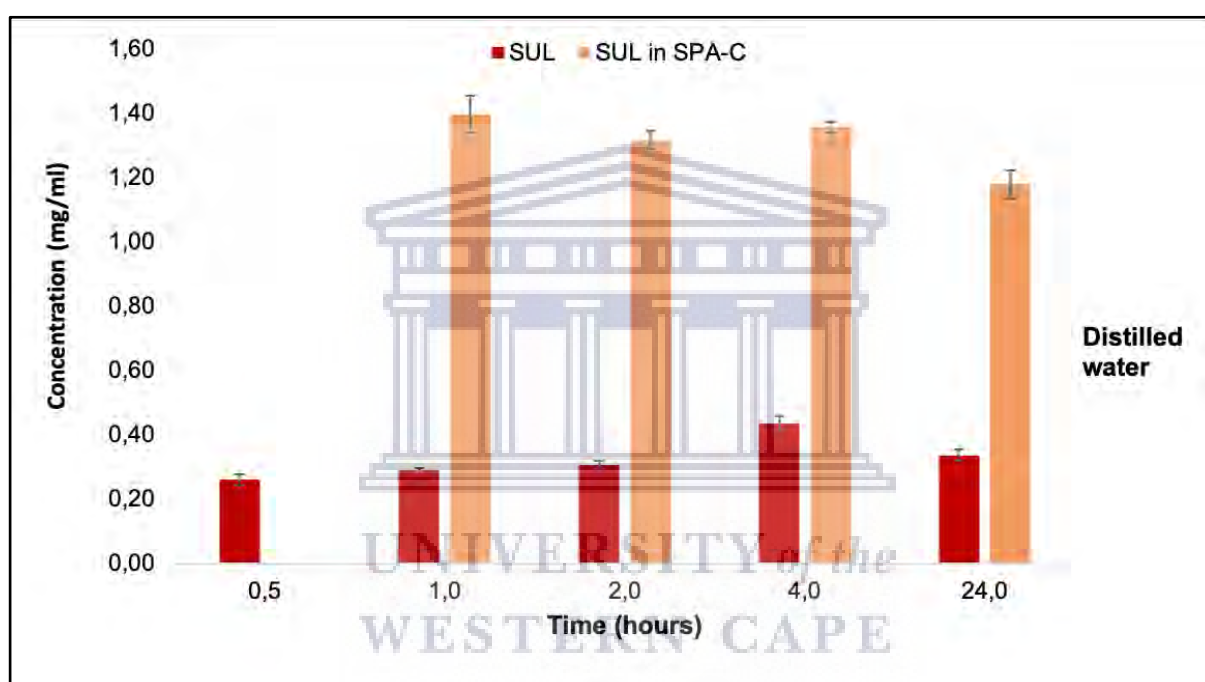
Figure 6.12: Equilibrium solubility concentration (mg/ml) of pure SUL and SUL in SPA-C in distilled water, with samples analysed at 0.5, 1, 2, 4 and 24 hours agitated and maintained at 37.0 ± 0.5°C.
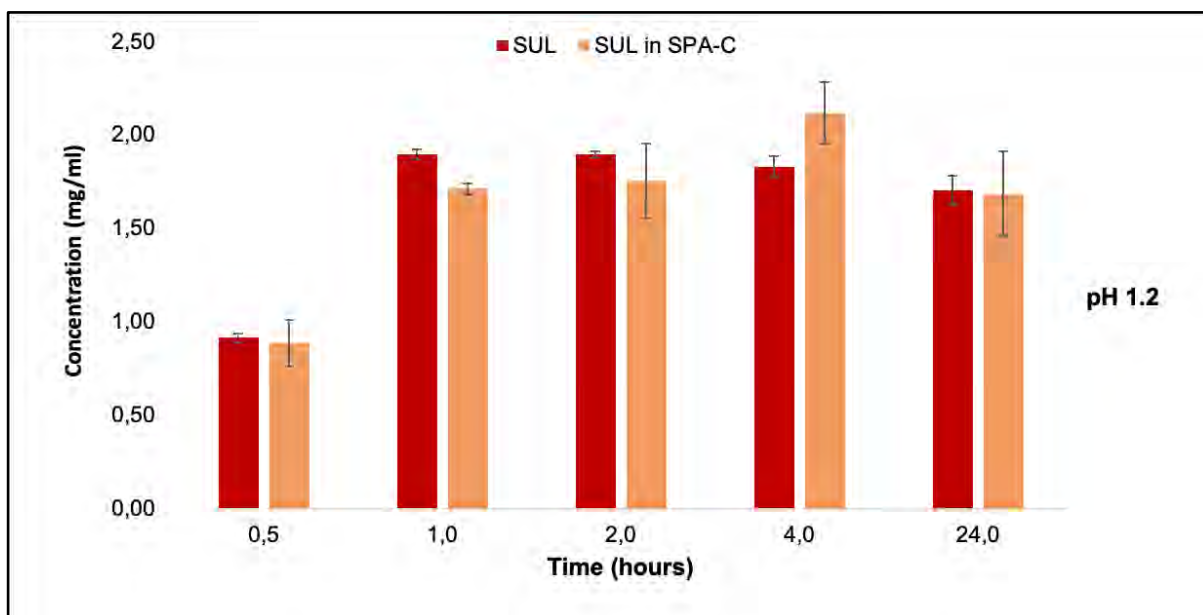
Figure 6.13: Equilibrium solubility concentration (mg/ml) of pure SUL and SUL in SPA-C in pH 1.2, with samples analysed at 0.5, 1, 2, 4 and 24 hours agitated and maintained at 37.0 ± 0.5°C.

Equilibrium solubility testing of pure SUL and SUL in the SPA-C combination in pH 1.2 aqueous solubility medium showed a solubility concentration of 1.71 ± 0.08 mg/ml and 1.69 ± 0.06 mg/ml, respectively **(Figure 6.13)** after a period of 24 hours. These results were in excellent correlation with that obtained in the equilibrium solubility testing study conducted by Holtzkamp (2016), where a concentration of 1.19 mg/ml SUL was reported for pure SUL and SUL in combination with PYR in the 1 : 0.05 %w/w combination.

Figure 6.14 depicts the equilibrium solubility of SUL and SUL in SPA-C when solubilised in pH 6.8. The equilibrium concentration obtained for SUL alone in pH 6.8 after 24 hours was 0.06 ± 0.02 mg/ml and when in the SPA-C combination it was quantified to be 0.71 ± 0.20 mg/ml. These results were found to be in fair correlation with that reported by Holtzkamp (2016) who reported an equilibrium solubility concentration of 1.02 mg/ml in pH 6.8 for SUL alone, whilst in the 1 : 0.05 %w/w combination with PYR a concentration of 1.13 mg/ml was documented.

Figure 6.14: Equilibrium solubility concentration (mg/ml) of pure SUL and SUL in SPA-C in pH 6.8, with samples analysed at 0.5, 1, 2, 4 and 24 hours agitated and maintained at 37.0 ± 0.5°C.

6.2.5.2 Equilibrium solubility of PYR alone and PYR in SPA-C in various solubility media

Figures 6.15, 6.16 and 6.17 depict the equilibrium solubility data obtained for PYR and PYR in SPA-C in distilled water, buffer media at pH 1.2 and pH 6.8, respectively. PYR alone showed better solubility in distilled water and pH 1.2 as opposed to PYR in SPA-C in corresponding solubilisation media. Maximum concentrations of 0.35 ± 0.023 mg/ml and 3.55 ± 0.20 mg/ml in distilled water and pH 1.2 were obtained within 2 hours whereas for PYR in SPA-C maximum solubility concentration were determined to be 0.13 ± 0.02 mg/ml 1.46 ± 0.27 mg/ml in the same conditions. The same synergistic effect as discussed in the section of SUL equilibrium solubility was only observed in pH 6.8 where a concentration of 0.95 ± 0.13 mg/ml at 0.5 hours versus 0.39 ± 0.03 mg/ml was achieved for PYR in SPA-C, this high solubility concentration reduces over time with equilibrium solubility of PYR in pH 6.8. The equilibrium solubility results of PYR in pH 1.2, distilled water and pH6.8 reported by Holtzkamp (2016) showed a decrease in PYR solubility when in combination with SUL. However, the results obtained here with PYR in combination with SUL and AZI showed a similar trend as reported by Holtzkamp (2016), except in pH 6.8 where an increase in PYR solubility was observed hence, this study elucidates new data that shows that the presence of a third drug, AZI facilitates improved solubility of PYR when existing in a mere physical mixture.
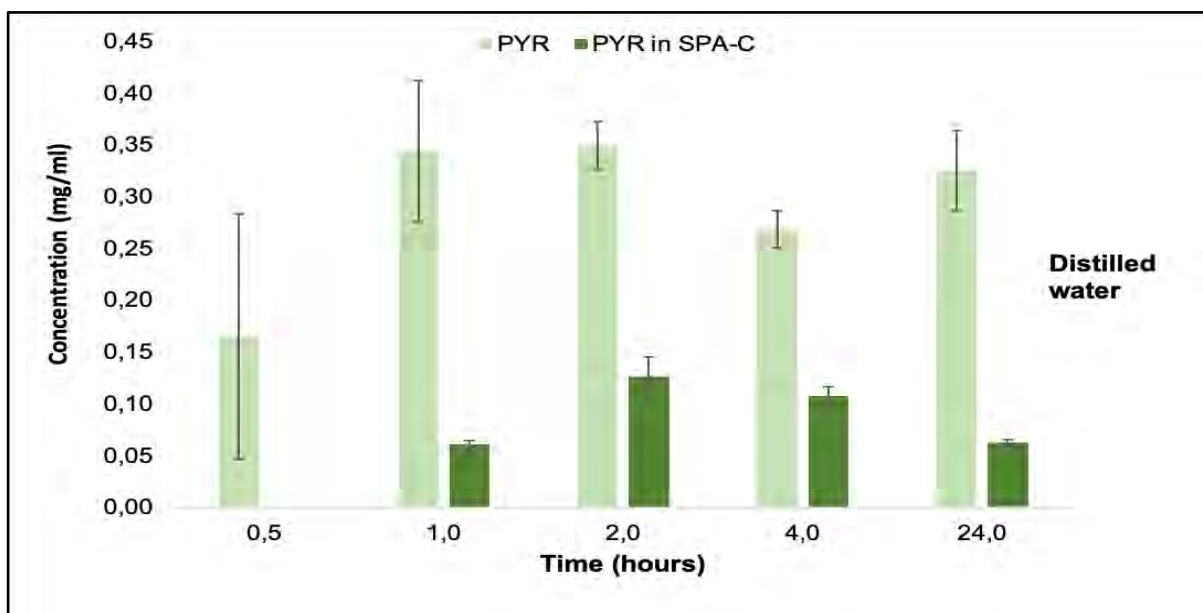
Figure 6.15: Equilibrium solubility concentration (mg/ml) of pure PYR and PYR in SPA-C in distilled water, with samples analysed at 0.5, 1, 2, 4 and 24 hours agitated and maintained at 37.0 ± 0.5°C.

Figure 6.16: Equilibrium solubility concentration (mg/ml) of pure PYR and PYR in SPA-C in pH 1.2, with samples analysed at 0.5, 1, 2, 4 and 24 hours agitated and maintained at 37.0 ± 0.5°C.
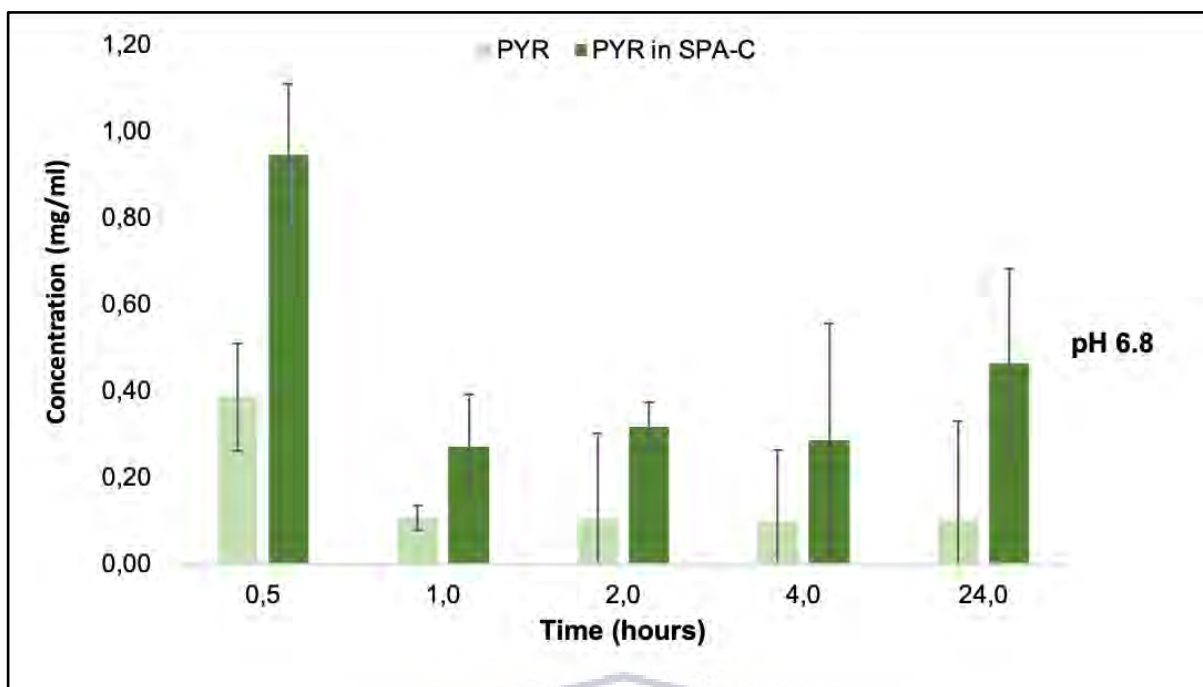
Figure 6.17: Equilibrium solubility concentration (mg/ml) of pure PYR and PYR in SPA-C in pH 6.8, with samples analysed at 0.5, 1, 2, 4 and 24 hours agitated and maintained at 37.0 ± 0.5°C.

6.2.5.3 Equilibrium solubility of AZI alone and AZI in SPA-C in various solubility media

Solubility of AZI was investigated in a similar manner as for SUL and PYR. **Figure 6.18** depicts the equilibrium solubility graph obtained for pure AZI and AZI in SPA-C solubilised in distilled water. The equilibrium solubility of AZI increased with time and the maximum concentration of 0.05 ± 0.02 mg/ml was attained in 24 hours, compared with AZI in SPA-C, a maximum concentration of 0.05 ± 0.003 mg/ml was achieved within 2 hours.
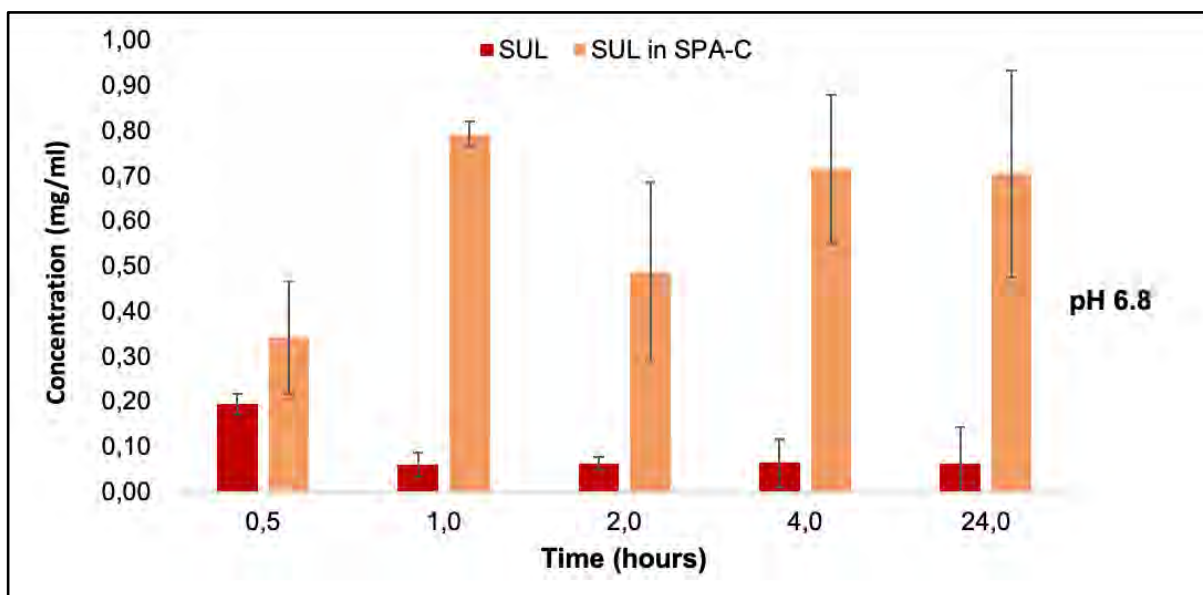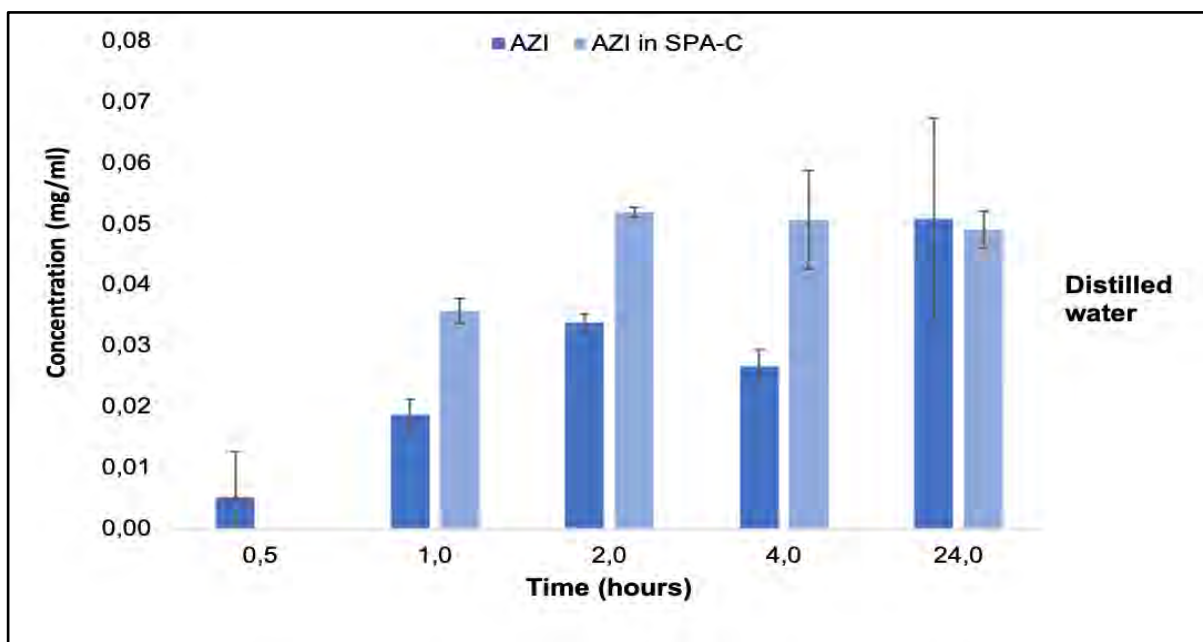
Figure 6.18: Equilibrium solubility concentration (mg/ml) of pure AZI and AZI in SPA-C in distilled water, with samples analysed at 0.5, 1, 2, 4 and 24 hours agitated and maintained at 37.0 ± 0.5°C.

The result from solubilisation in pH 1.2 depicted a similar trend (**Figure 6.19**), a concentration of 1.15 ± 0.94 mg/ml in 24 hours was obtained and in SPA-C, 1.39 ± 0.09 mg/ml was observed after 2 hours, this is over 20-folds higher than the equilibrium solubility concentration obtained in distilled water. When comparing the equilibrium solubility quantified for AZI in pH 6.8 **(Figure 6.20)**, a result contrary to the above observations was obtained, where pure AZI had better equilibrium dissolution (3.40 ± 0.23 mg/ml) after 4 hours as opposed to AZI present in the SPA-C mixture at the same time interval. However, despite this observed spike in the equilibrium solubility of pure AZI after a 4 hour period in pH 6.8, the solubility concentration stabilised at 0.93 ± 0.10 mg/ml. This was a 2.6 - fold solubility increase compared to AZI present in the SPA-C physical mixture for which the equilibrium solubility of AZI was quantified as 0.35 ± 0.21 mg/ml.

These findings are closely related to the finding from a study by Adeli, (2016), where solubility of AZI was investigated via formulation of a co-crystal with paracetamol, they reported a solubility concentration of 0.05 mg/ml for pure AZI and achieved an improvement of 60% with co-crystal sample. Arora *et al* (2010), studied AZI in a solid dispersion using urea and documented 0.068 mg/ml of pure AZI after 48 hours in pH 6.8. An increase registered in SPA-C indicates a probable synergistic effect in combination with SUL and PYR, however that enhancement is interrupted at pH 6.8. The reason for increased equilibrium solubility in pH

1.2 could be linked to the pKa of AZI being 8.7 and being a basic compound, decreasing the pH would increase the fraction of ionised drug and facilitate increased solubility (Aucamp *et al.*, 2015).
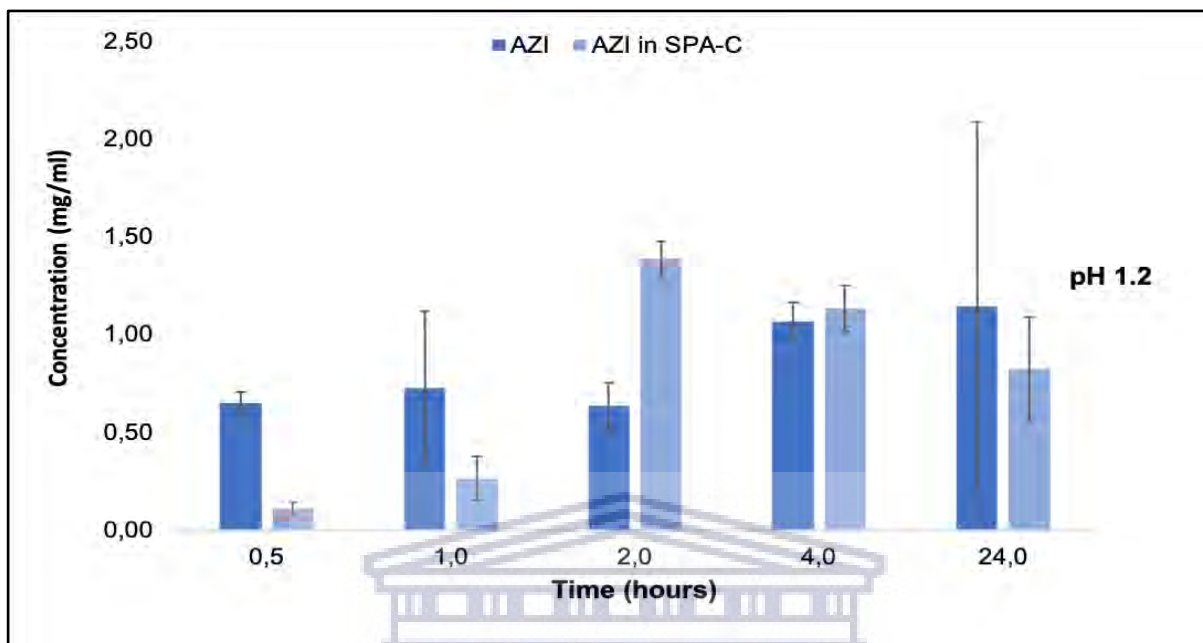
Figure 6.19: Equilibrium solubility concentration (mg/ml) of pure AZI and AZI in SPA-C in pH 1.2, with samples analysed at 0.5, 1, 2, 4 and 24 hours agitated and maintained at 37.0 ± 0.5°C.
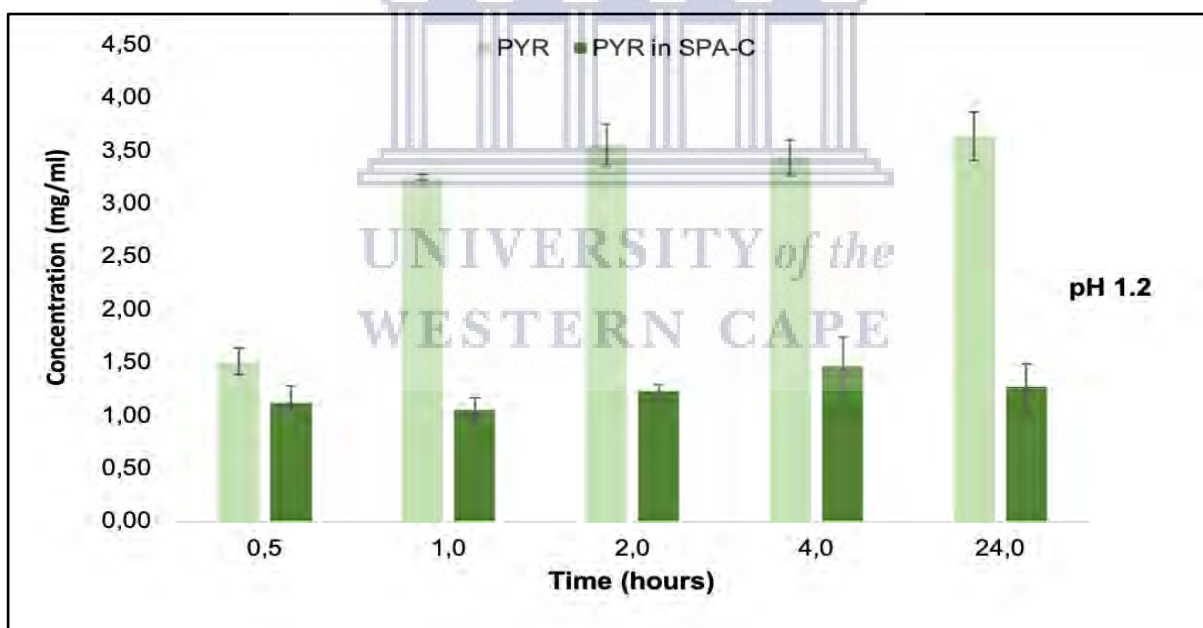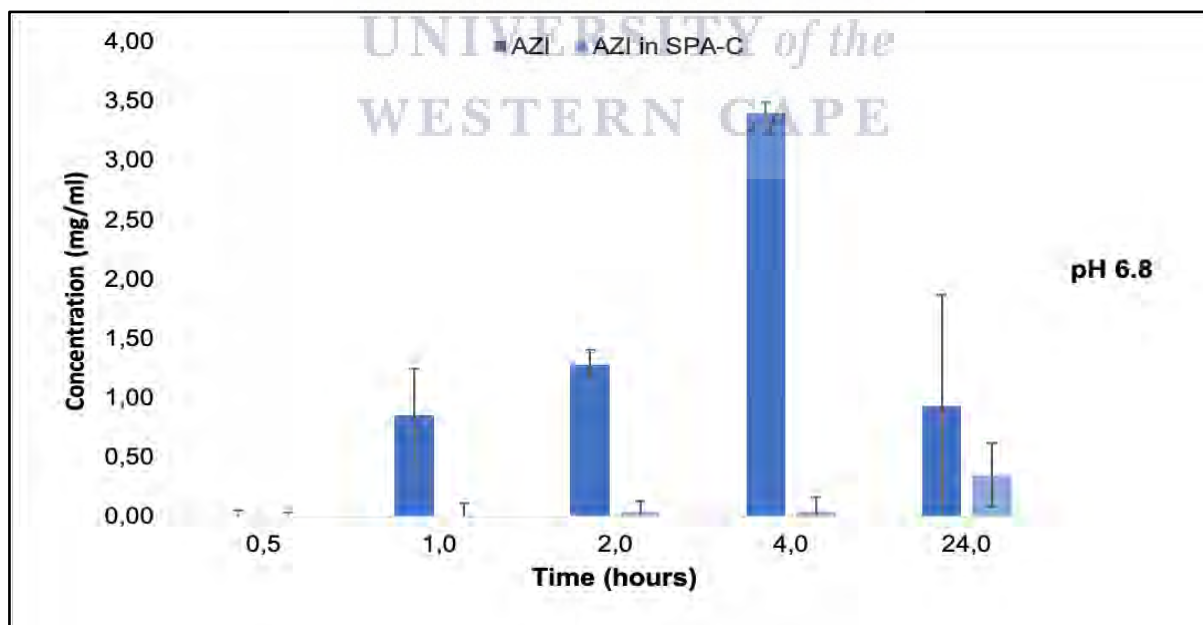

Figure 6.20: Equilibrium solubility concentration (mg/ml) of pure AZI and AZI in SPA-C in pH 6.8, with samples analysed at 0.5, 1, 2, 4 and 24 hours agitated and maintained at 37.0 ± 0.5°C.

6.2.6 Dissolution rate determination of SUL, PYR, AZI and SPA-C

Drug dissolution rate testing is an essential experiment normally employed to determine the rate at which a drug will enter a state of solubilisation within the gastro-intestinal fluids which will ultimately assist in the prediction of the bioavailability and therapeutic outcomes thereof. As discussed in literature (Chapter 3), several factors such as the API physico-chemical properties, formulation or dosage form design and patient's physiological conditions, among others, may facilitate or hinder the process. Investigating the dissolution rate of SPA-C in comparison with the individual compounds SUL, PYR and AZI as stated in Chapter 5, paragraph 5.5.1 was one of the objectives of this study which would facilitate an understanding towards potential dissolution rate increase or retardation due to solid-state form manipulation.

The dissolution rate of SUL **(Figure 6.21)** and **(Table 6.3)**, PYR **(Figure 6.22)** and **(Table 6.4)** and AZI **(Figure 6.23)** and **(Table 6.5)** were firstly performed in distilled water. Samples were extracted at various intervals of 5, 10, 20, 40 and 60 minutes to elucidate the change in concentration of the drugs over time. It became apparent that these drugs reach their potential maximum dissolution within the first 10 minutes of exposure to the dissolution medium. Pure crystalline form of these drugs performed poorly with SUL reaching a maximum drug dissolution of not more than 38%, PYR not more than 26% and AZI not more than 5%, thus confirming slow dissolution rate exhibited by all three compounds which could also be directly linked with the low equilibrium solubility concentrations observed (**Figures 6.12, 6.15 and 6.18**).

It is worth mentioning a gradual increase in drug dissolution concentration of PYR as the dissolution time progressed, whilst on the other hand the dissolution rates for both SUL and AZI stabilised at 10 minutes during the testing period. This data is in line with the literature, the poor aqueous solubility of these drugs may require some kind of formulation intervention to maximise the drug's potential and also curb down the toxicity associated with taking higher dose concentrations aimed to meet the therapeutic efficacy (Aucamp, *et al*., 2015; Kaur, *et al.*, 2012; Pacult, *et al*., 2019; Wairkar & Gaud, 2016; Weuts, *et al*., 2011).

During the dissolution rate testing of all three drugs as part of the physical mixture, SPA-C, significant increases in the dissolution rate of SUL, PYR and AZI were observed. As outlined in **Tables 6.3 - 6.5** and graphically demonstrated in **Figures 6.21 - 6.23**, SUL reached the highest dissolved percentage of 56.35 ± 3.19% after only 5 minutes. PYR and AZI reached drug dissolved percentages of 41.36 ± 4.84% and 23.14 ± 2.00% after 5 minutes, respectively. The main cause of this tremendous improvement is not clearly understood, however, as mentioned in literature, it's possible that combining these drugs results in an enhancement in physico-chemical or bulk material characteristics that favours their dissolution rates.

Table 6.3: Summary of dissolution rate results obtained for SUL in distilled water maintained at 37 ± 0.5 °C

Time (min)	SUL percentage dissolved (%)	STDEV	SUL in SPA-C percentage dissolved (%)	STDEV
0	0.00	0.00	0.00	0.00
5	33.33	1.42	56.35	3.19
10	35.97	1.43	66.58	0.84
20	36.73	1.77	74.76	0.52
40	37.37	1.50	81.19	1.27
60	36.86	1.87	83.19	1.29
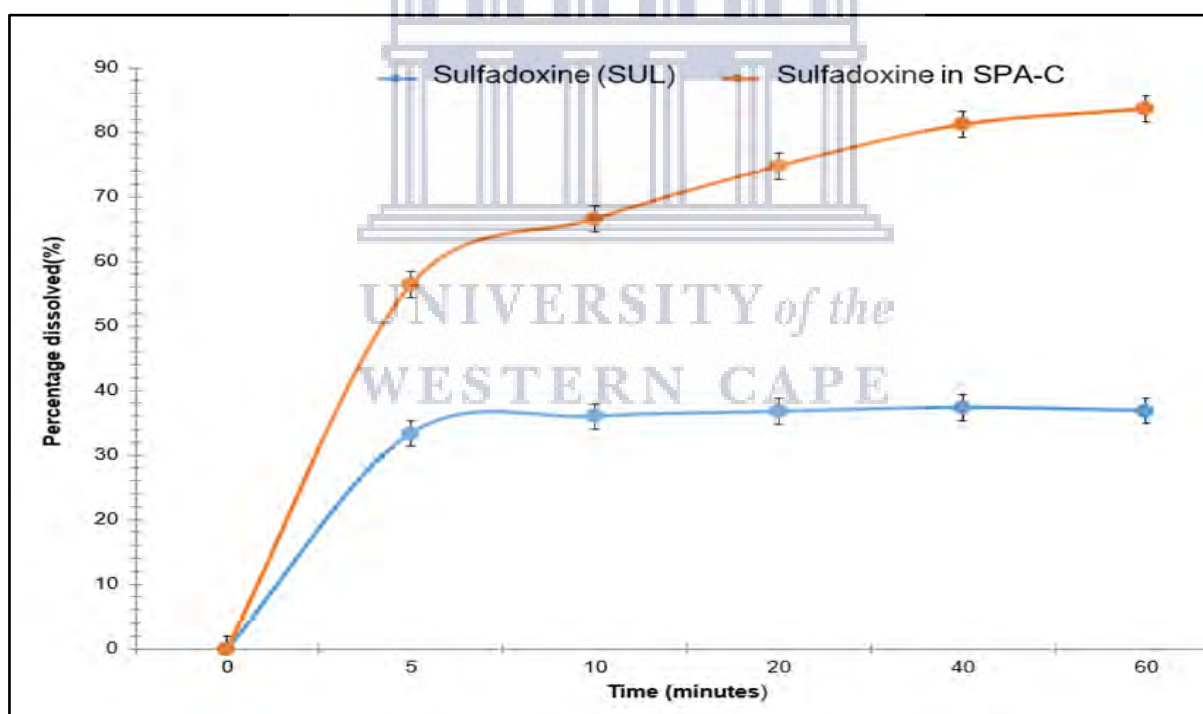
Figure 6.21: Dissolution rate obtained for SUL and SUL in SPA-C in distilled water maintained at 37 ± 0.5 °C

Table 6.4: Summary of dissolution rate results obtained for PYR in distilled water maintained at 37 ± 0.5 °C

Time (min)	PYR percentage dissolved (%)	STDEV	PYR in SPA-C percentage dissolved (%)	STDEV
0	0.00	0.00	0.00	0.00
5	7.56	1.44	41.36	4.84
10	11.02	2.97	37.39	5.09
20	16.74	2.97	44.95	9.72
40	22.38	3.60	47.56	2.10
60	25.75	3.92	53.49	3.25
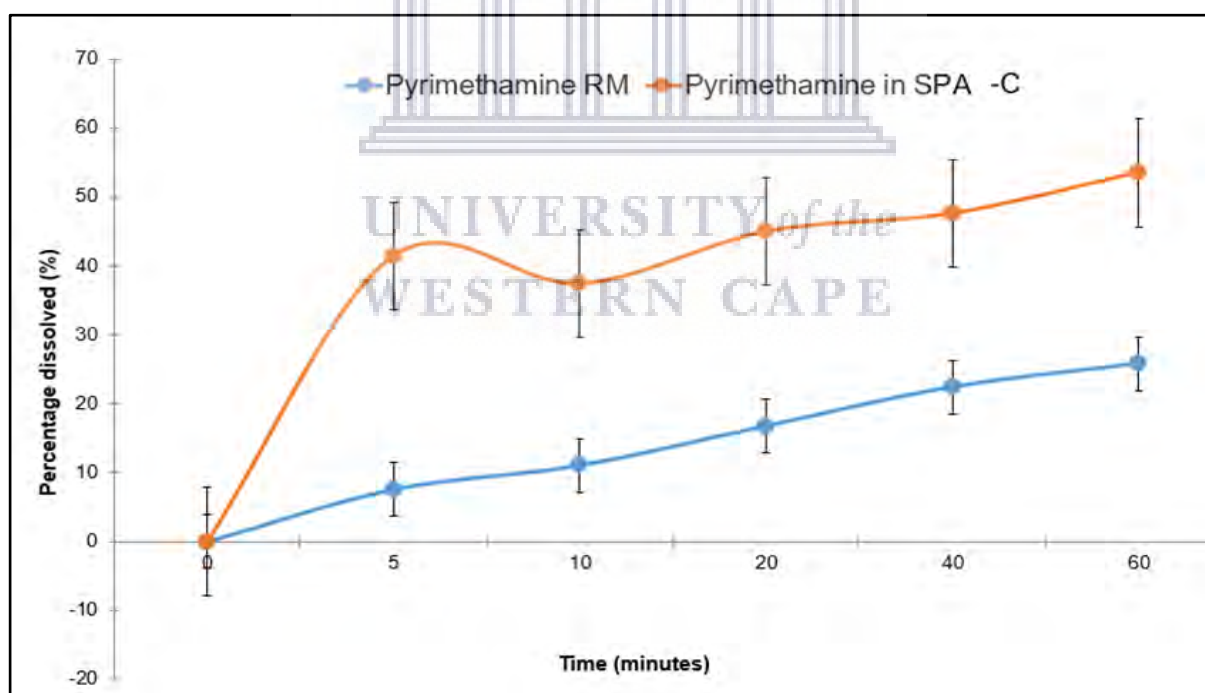
Figure 6.22: Dissolution rate obtained for PYR and PYR in SPA-C in distilled water maintained at 37 ± 0.5 °C.

Table 6.: Summary of dissolution rate results obtained for AZI in distilled water maintained at 37 ± 0.5 °C

Time (min)	AZI percentage dissolved (%)	STDEV	AZI in SPA-C percentage dissolved (%)	STDEV
0	0.00	0.00	0.00	0.00
5	4.94	2.18	23.14	2.00
10	3.82	0.74	32.70	1.51
20	4.51	0.62	43.24	4.36
40	4.55	0.90	49.78	3.88
60	4.57	0.86	48.24	1.75
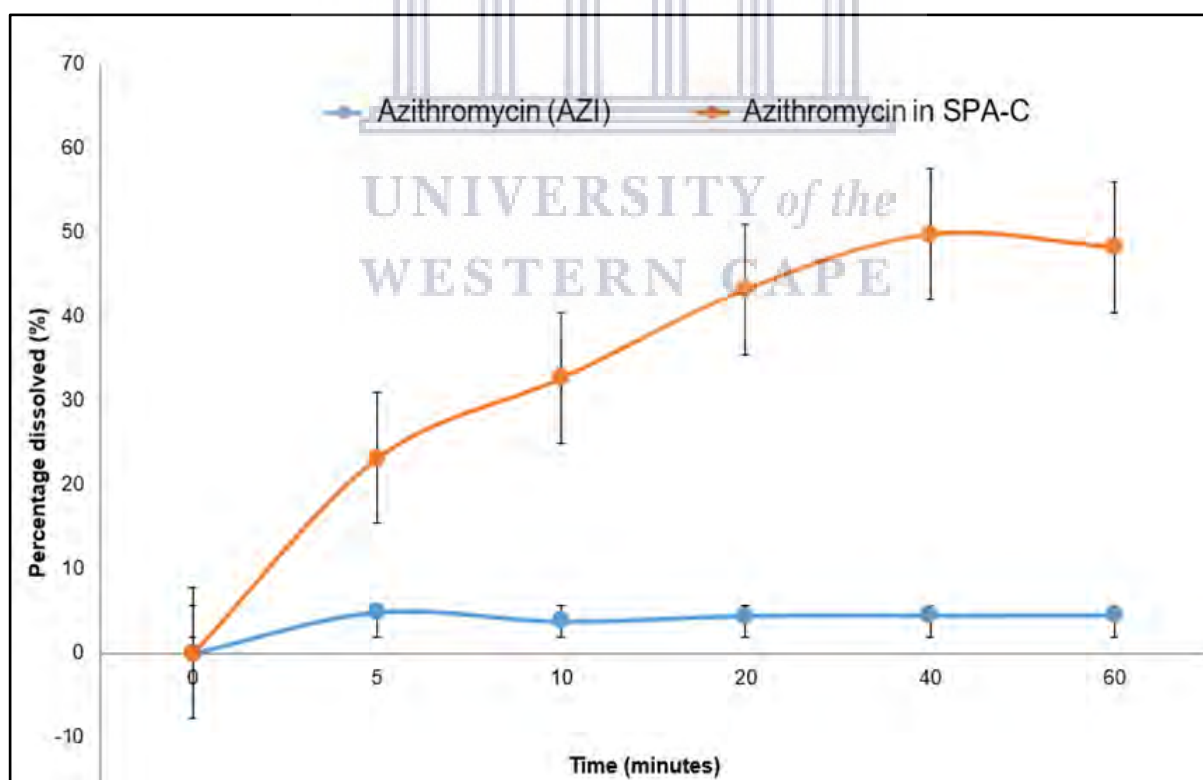
Figure 6.23: Dissolution rate obtained for AZI and AZI in SPA-C in distilled water maintained at 37 ± 0.5 °C.

6.3 Preparation and characterisation of potential co-amorphous or ternary solid-state forms consisting of SUL, PYR and AZI using different preparation techniques

Using the characterisation data collected during this initial experimental phase the study continued towards the preparation of an amorphous or perhaps several amorphous solid-state forms consisting of all three APIs. As discussed in Chapter 5, three methods, which included slow solvent evaporation, rapid solvent evaporation and quench cooling of the melt, were used to investigate the possibility of preparing a ternary amorphous system. The results obtained during this phase of the study will be discussed in the following paragraphs.

6.3.1 Slow solvent evaporation

Solvent evaporation has been well described in literature as an acceptable method for the preparation of amorphous solid-state forms of drugs, whether it is co-amorphous systems or amorphous solid dispersions (Weuts et al., 2011; Baird and Taylor, 2012; Van Den Mooter, 2012; Singh et al., 2017; Karagianni, Kachrimanis and Nikolakakis, 2018). As described in Chapter 5, paragraph 5.3.3, using the well-known technique of solvent evaporation, SPA-C was dissolved in either acetone, acetonitrile, chloroform, butanone, or methanol. Removal of solvent plays a key role in amorphous solid-state formation. Samples prepared using the slow evaporation method were investigated and characterised using DSC, TGA, FTIR, vapour sorption analysis and only for the most promising preparations PXRD. This was done to determine the crystallinity or amorphicity of the prepared samples to inform whether amorphous solid forms were successfully prepared.

Figure 6.24 depicts the DSC thermograms obtained for the samples prepared from the slow evaporation method. **Figure 6.24(a)** depicts the DSC trace obtained with SPA-C subjected to slow solvent evaporation from acetone. A melting endotherm with peak temperature (T_m) 187.23°C was observed. The same thermal behaviour was observed for the samples obtained from slow evaporation from (b) acetonitrile (T_m = 187.43°C), (c) butanone (T_m = 198.01°C), (d) chloroform (T_m = 186.99°C) and (e) methanol (T_m = 186.33°C). It was hypothesised that the slow solvent evaporation method rendered SPA-C into an amorphous solid-state form, especially since only one thermal event was observed. This being said, a very small step in the measured heat flow was observed in the DSC thermograms obtained for the SPA-C samples evaporated from acetone (119.88°C - 125.61°C) and methanol (62.98°C - 85.56°C)
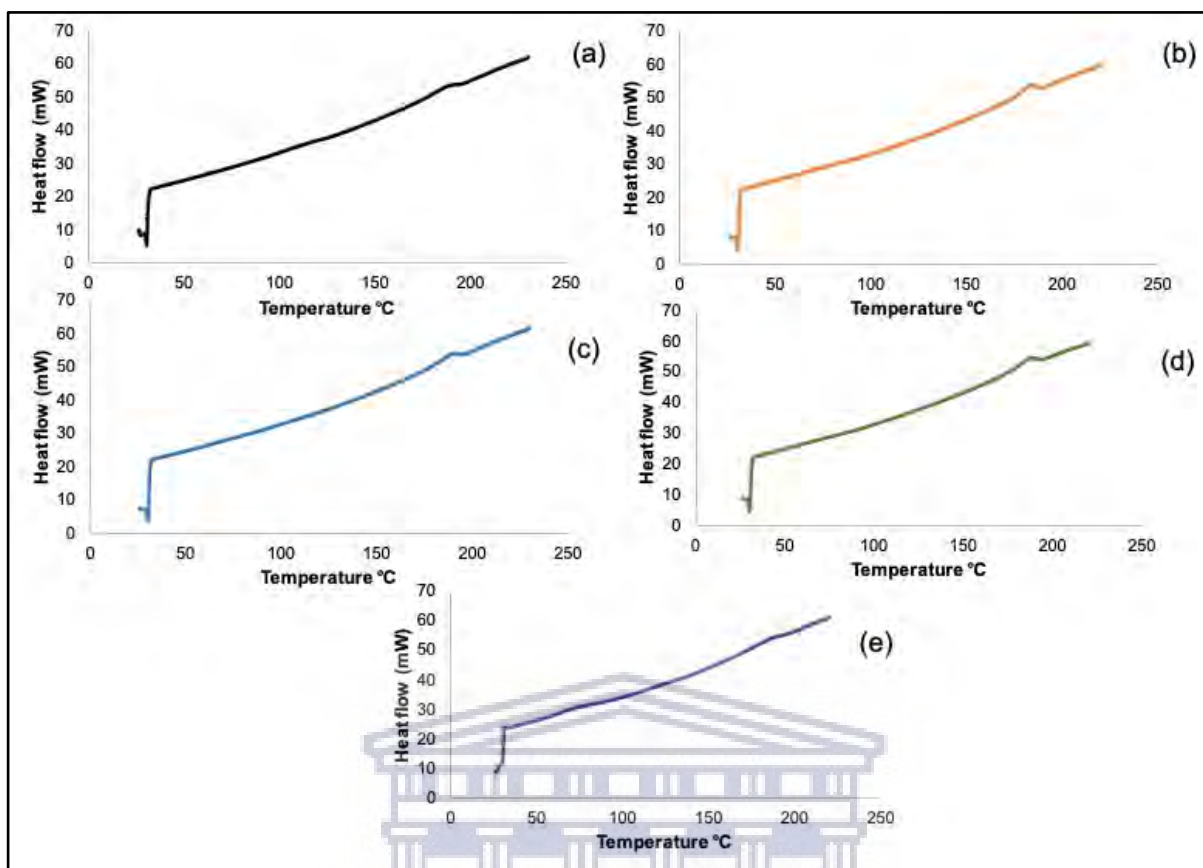
Figure 6.24: DSC thermograms obtained from the slow evaporation process using (a) acetone, (b) acetonitrile, (c) butanone, (d) chloroform and (e) methanol.

It was however noted that the DSC traces appeared very similar to that obtained with SPA-C and therefore at this point of the experimental process it was challenging to conclude whether ternary amorphous systems were prepared *via* slow solvent evaporation. Further investigation was therefore necessary. **Figure 6.25** depicts the TGA traces obtained with the slow solvent evaporation preparations. The traces obtained with the preparations from butanone and chloroform showed weight loss in the temperature range of 95 - 130°C and 90 - 120°C, respectively. This weight loss was quantified as 3.9% and 5.7% respectively and it was concluded that this weight loss may be ascribed to residual solvent which remained in the sample. Interestingly however, no desolvation was observed for these two samples during DSC analysis but it was concluded that this might be due to the fact that the samples could be analysed using a pierced DSC pan lid.

The onset of degradation for each slow evaporated preparation was determined to be: (a) 220°C (butanone), (b) 225°C (acetone), (c) 225°C (chloroform), (d) 220°C (methanol) and (e) 222°C (acetonitrile). Weight loss observed in these preparations were higher than that quantified for SPA-C prior to subjecting it to the slow solvent evaporation process and in all instances the onset of degradation was also lower in comparison with that obtained with SPA-

C prior to the slow solvent evaporation process (245°C). This was considered to be an indication of some level of molecular interaction which might have occurred between the three compounds but whether all three drugs exist now in an amorphous state was still not evident.
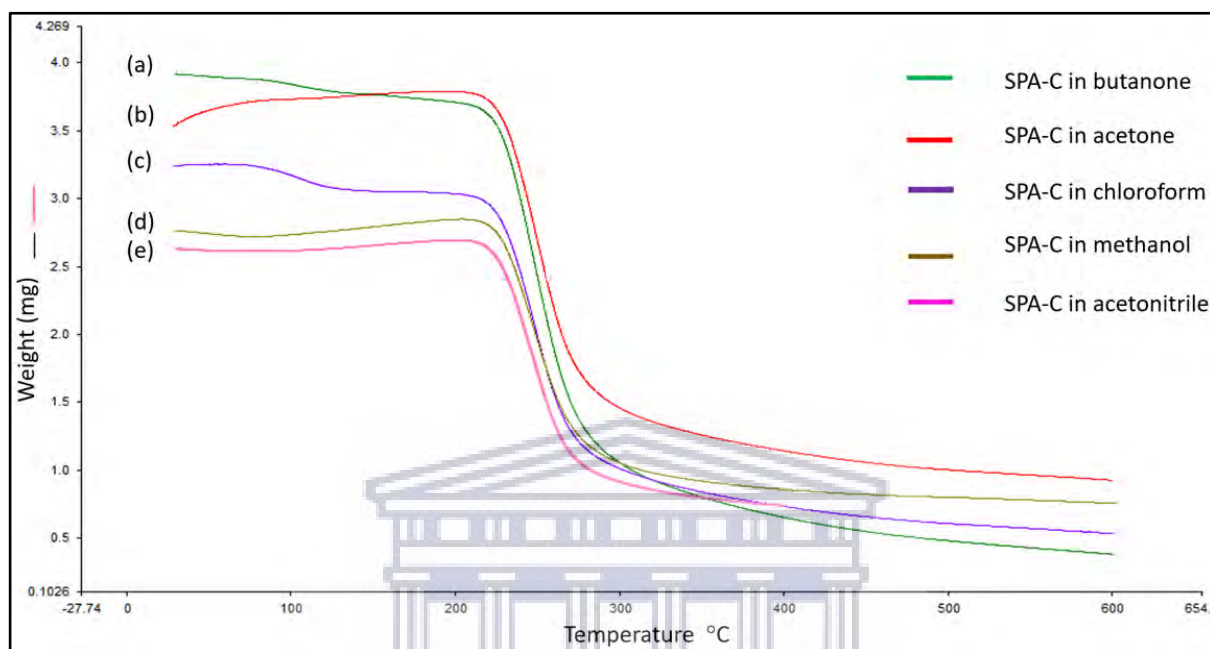
Figure 6.25: Overlay of TGA traces obtained for samples prepared *via* slow solvent evaporation (a) butanone, (b) acetone, (c) chloroform, (d) methanol and (e) acetonitrile followed by slow evaporation, heated from 30 – 600 °C at a heating rate of 10°C/min.

The preparations were further investigated using FTIR analysis. **Figure 6.26** depicts an overlay of the individual FTIR spectrums and **Table 6.6** outlines the observed wavenumbers with corresponding functional groups. Based on the FTIR data obtained it was concluded that no solid-state form modification occurred due to the slow solvent evaporation process, since all absorbance bands associated with crystalline SPA-C were still identifiable in all the samples obtained through the slow solvent evaporation process, with the only observable difference being in the region of 1720 cm⁻¹ where no absorbance was detected for the samples evaporated from acetonitrile, butanone, chloroform, and methanol. However, upon closer inspection of the obtained spectra it was noticed that the mentioned absorbance band was identifiable on the individual spectra but was most probably too small for the FT-IR software to quantify the peaks associated with that absorbance band for the mentioned samples. This being said, it was however noted that the FT-IR absorbance spectrum obtained for SPAC-C

evaporated from acetone exhibited significant smaller absorbance bands in the region of 3500 - 2800 cm^{-1} which was a phenomenon considered to be worth investigating further.
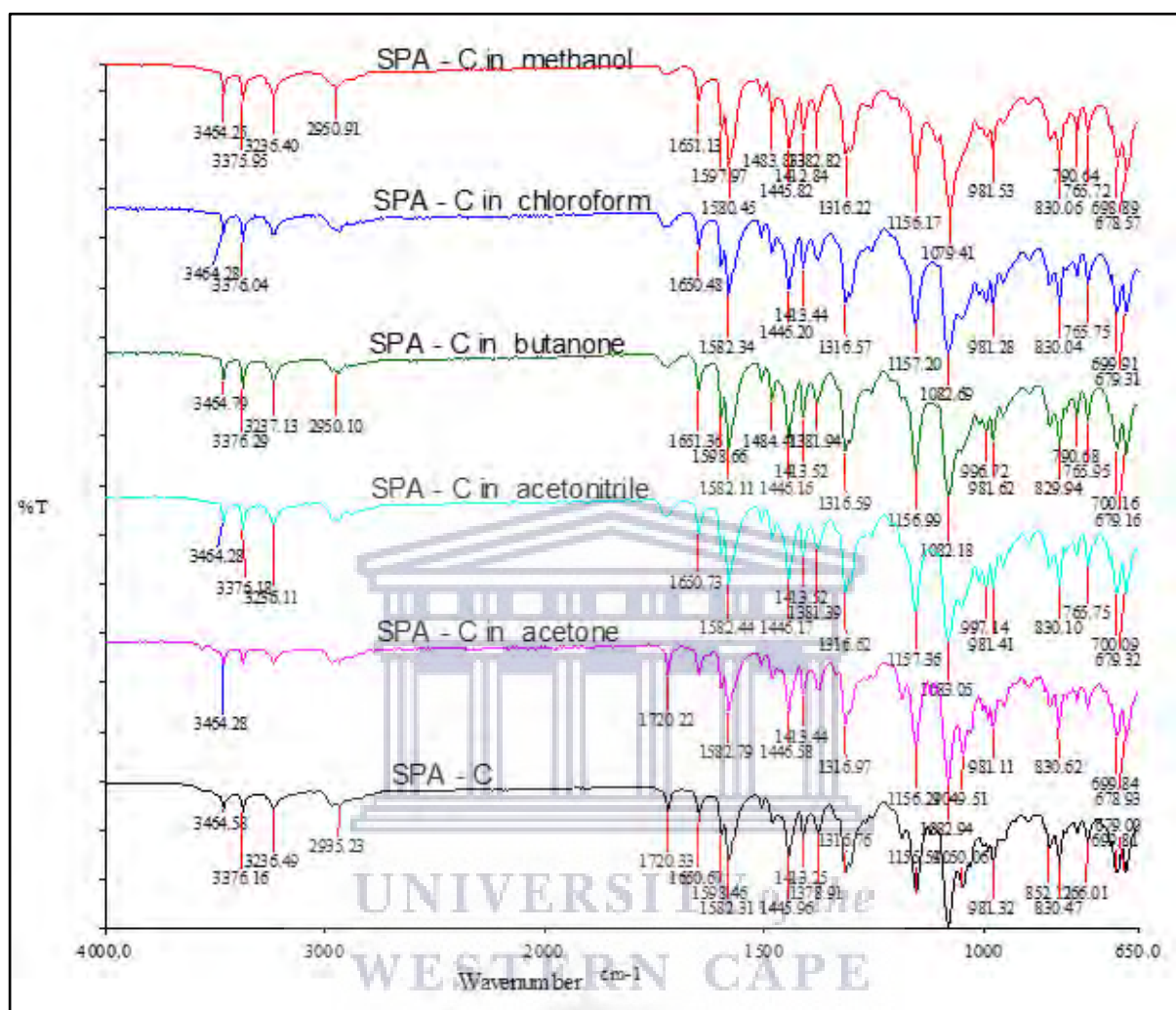
Figure 6.26: An overlay of the FTIR spectra obtained for samples prepared by dissolving SPA-C in either acetone, acetonitrile, chloroform, butanone and methanol followed by slow evaporation of the solvent.

Table 6.6: Table of SPA-C prepared by slow solvent evaporation in acetone, acetonitrile, butanone, chloroform and methanol; describing the wavenumbers obtained from FTIR analysis with correlating functional groups.

SPA-C		Acetone		Acetonitrile		Butanone		Chloroform		Methanol	
Wavenumber (cm^{-1})	Functional group	Wavenumber (cm^{-1})	Functional group	Wavenumber (cm^{-1})	Functional group	Wavenumber (cm^{-1})	Functional group	Wavenumber (cm^{-1})	Functional group	Wavenumber (cm^{-1})	Functional group
3464.58	N-H	3464.28	N-H	3464.28	N-H	3464.79	N-H	3464.28	N-H	3464.25	N-H
3376.16	C-H	3376.29	C-H	3376.18	C-H	3376.29	C-H	3376.04	C-H	3375.95	C-H
3236.49	C-H	3237.13	C-H	3236.11	C-H	3237.13	C-H	3236.40	C-H	3236.40	C-H
2935.23	C-H	2950.10	C-H	2950.73	C-H	2950.10	C-H	-	-	2950.91	C-H
1720.33	C=O	1720.22	C=O	-	-	-	-	-	-	-	-
1650.67	C=N	1651.36	C=N	1650.73	C=N	1651.36	C=N	1650.48	C=N	1651.13	C=N
1598.46	C=C	1598.66	C=C	1589.66	C=C	1598.66	C=C	1597.97	C=C	1597.97	C=C
1582.31	C=C	1582.79	C=C	1582.44	C=C	1582.11	C=C	1583.24	C=C	1580.45	C=C
1482.41	CH$_3$	1482.41	CH$_3$	1482.41	CH$_3$	1482.41	CH$_3$	1483.80	CH$_3$	1483.80	CH$_3$
1445.96	CH$_3$	1446.58	CH$_3$	1446.58	CH$_3$	1448.41	CH$_3$	1446.20	CH$_3$	1445.82	CH$_3$
1413.25	CH$_3$	1413.44	CH$_3$	1413.44	CH$_3$	1413.52	CH$_3$	1413.44	CH$_3$	1412.84	CH$_3$
1378.91	C≡N	1316.97	C≡N	1316.97	C≡N	1316.59	C≡N	1316.57	C≡N	1316.22	C≡N

The preparation obtained through slow evaporation from acetone showed at this point the most promise to exist as a ternary amorphous system and therefore the solid-state habit was confirmed using PXRD. **Figure 6.27** depicts an overlay of the PXRD diffraction pattern obtained with the preparation in comparison with that of SPA-C. Although the diffraction peaks were found to be low in intensity, diffraction peaks at: 10.03, 11.30, 11.94, 14.23, 14.64, 15.87, 18.36, 22.9 and 25.58°2θ were observed and therefore it was concluded that this preparation resulted in a mixture of the three drugs but existing at a lower crystallinity level. **Table 6.7** lists all the significant diffraction peaks obtained with SPA-C evaporated from acetone and it clearly shows the correlation between the diffraction peaks obtained with SPA-C. It was there concluded that this preparation method did not render the drugs into a ternary amorphous system, although some reduced crystallinity was observed, the individual phases observed in SPA-C were still observable in the preparation obtained from slow evaporation of acetone.
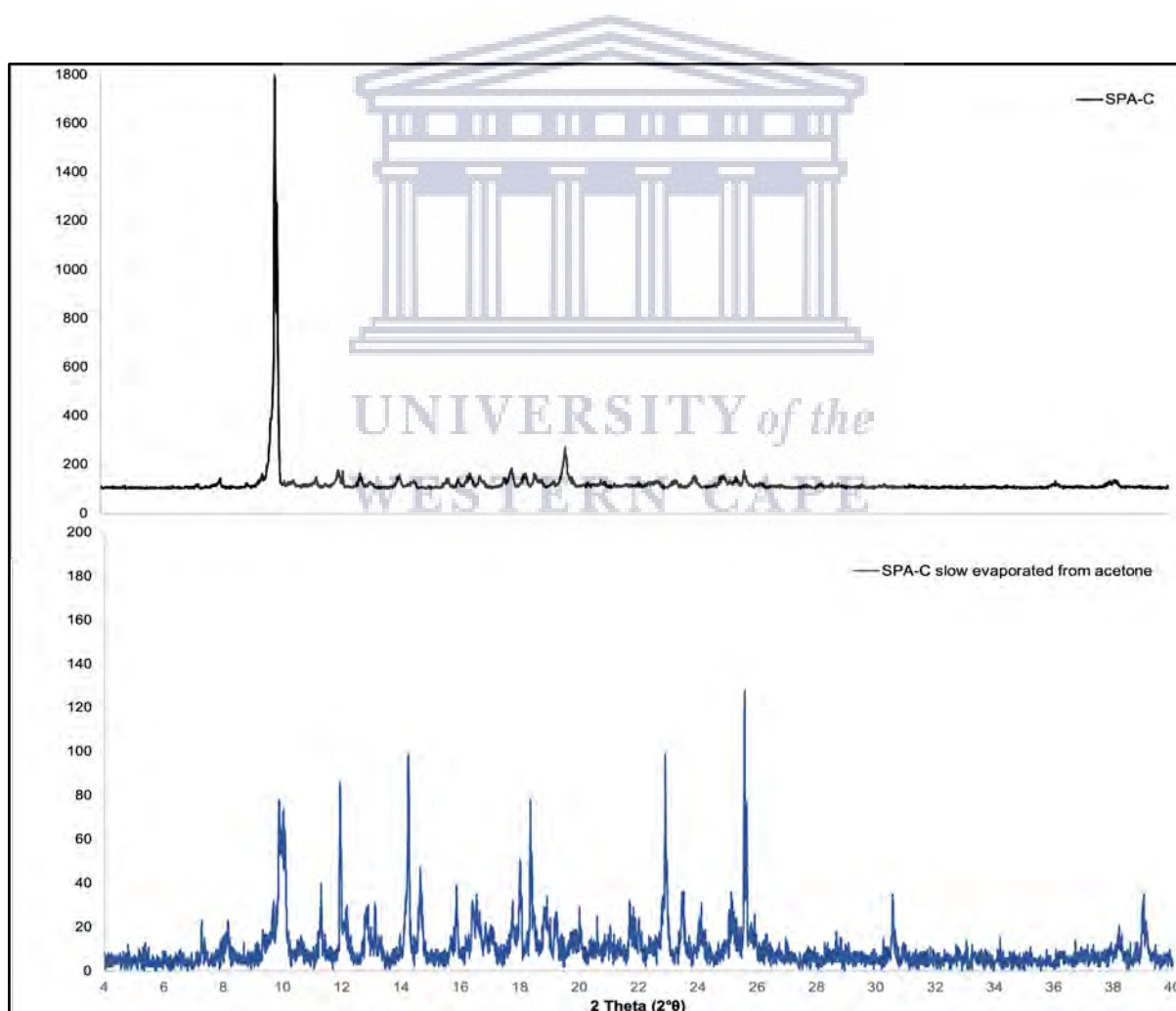
Figure 6.27: Overlay of the PXRD obtained for SPA-C and prepared via slow solvent evaporation

Table 6.7: Summary of PXRD diffraction peaks obtained with the acetone slow evaporation sample in comparison with SPA-C and SPA-C

Acetone slow evaporation	SPA-C
(°2θ)	(°2θ)
7.29	7.29
9.94	9.88
11.29	11.25
11.95	12.18
12.83	12.80
14.23	-
14.65	-
15.86	15.81
16.46	-
16.56	16.55
18.01	17.90
18.32	18.41
18.87	18.80
19.21	19.67
22.91	-
23.49	-
24.10	-
25.16	-
25.59	25.54
30.58	-

6.3.2 Rapid solvent evaporation

DSC analysis of the samples obtained from the rapid solvent evaporation process (**Figure 6.28**) denoted single melting endotherms for sample (a) acetone (T_m = 187.99°C), (b) acetonitrile (T_m = 184.18°C), (c) butanone (T_m = 183.53°C), (d) chloroform (T_m = 184.73°C) and (e) methanol (T_m = 184.93°C). These thermal patterns were also observed in samples obtained during the slow solvent evaporation process (**Figure 6.24**), the most notable for a

ternary amorphous form however was the sample obtained from (a) acetone. This was due to the size of the endothermic event at 187.99°C, while the rest of the DSC thermograms followed the same trend for slow solvent evaporation and the conclusion derived under the above section can equally be deduced hereof.
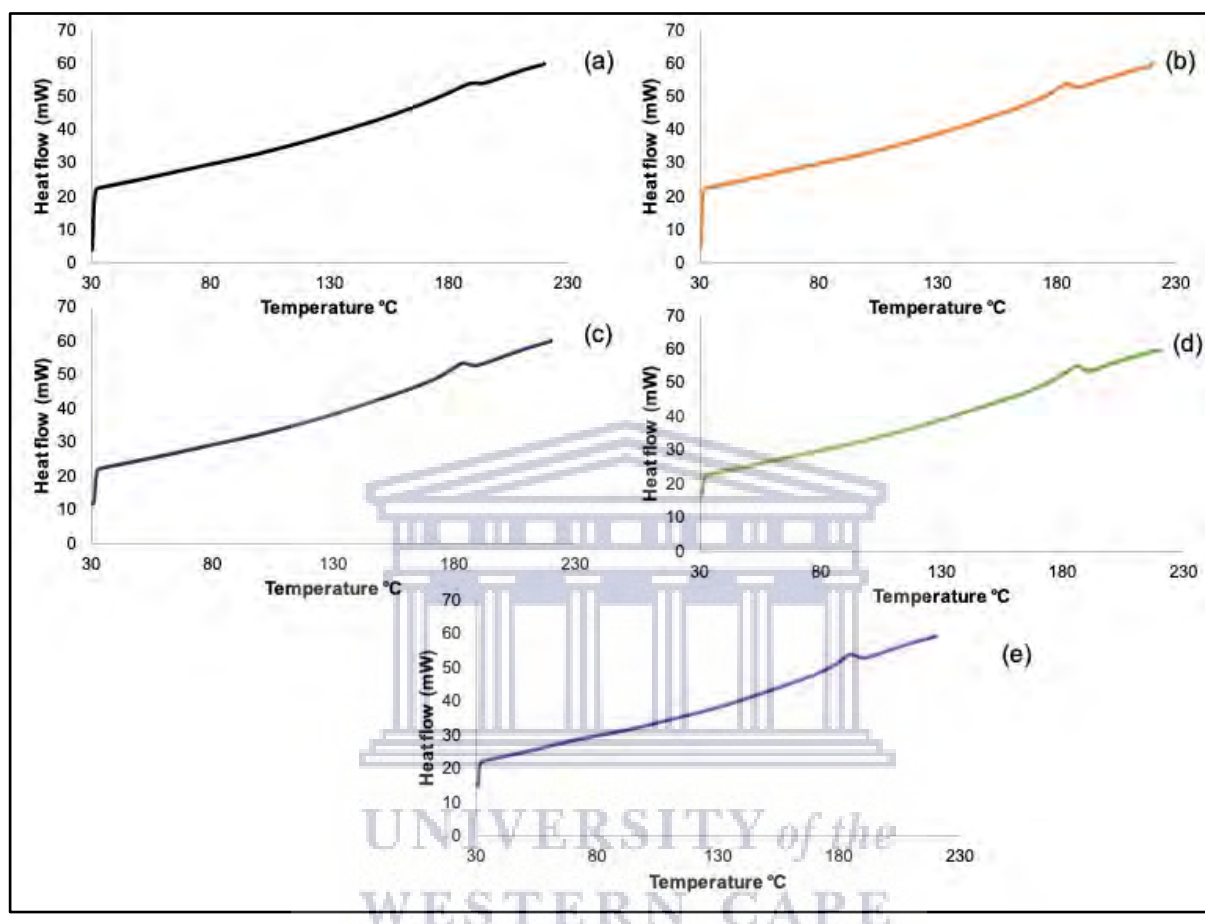
Figure 6.28: DSC thermograms obtained with SPA-C subjected to rapid solvent evaporation with (a) evaporation form acetone, (b) evaporation from acetonitrile, (c) evaporation from butanone, (d) evaporation from chloroform and (e) evaporation from methanol.

The samples obtained from the rapid solvent evaporation process were further subjected to TGA analysis to ascertain whether any differences in the prepared samples could be observed. **Figure 6.29** provides an overlay of the TGA results obtained for these samples. The degradation observed in samples prepared *via* rapid solvent evaporation showed similar trends as obtained with the slow evaporated samples and their onset temperatures were determined to be: (a) 225°C (acetonitrile), (b) 225°C (methanol), (c) 222°C (chloroform), (d) 222°C (butanone) and (e) 220°C (acetone). Weight loss observed in these preparations were higher than that quantified for SPA-C prior to subjecting it to the rapid solvent evaporation and

demonstrated lower onset of degradation in comparison with that obtained with SPA-C (prior solvent evaporation).
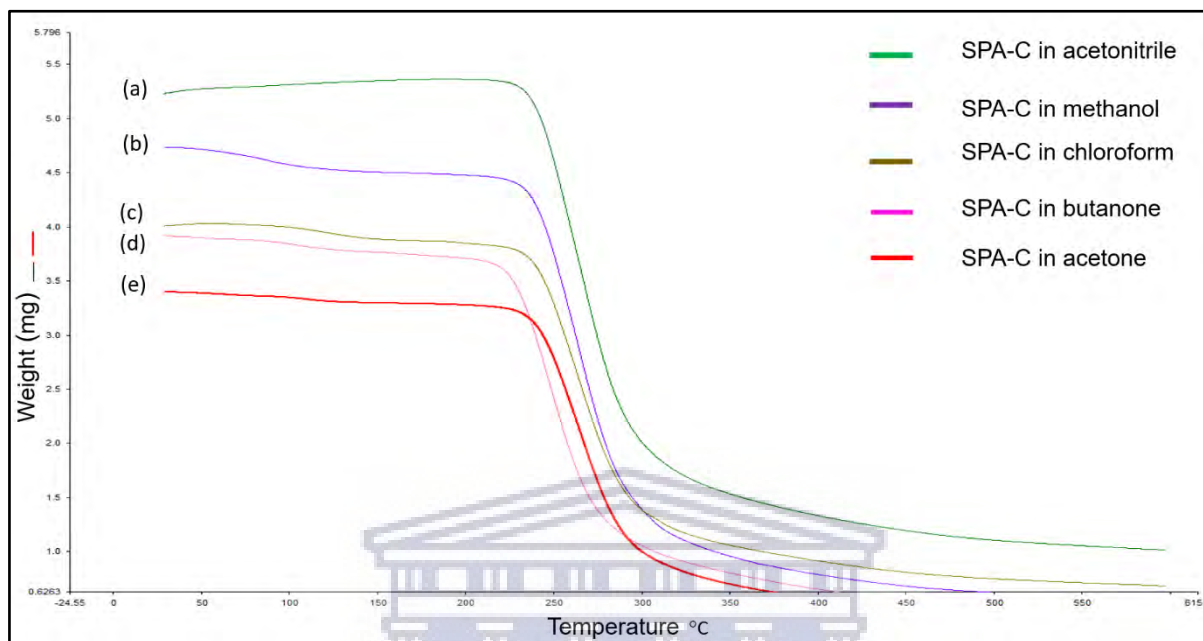
Figure 6.29: Overlay of TGA obtained for SPA-C dissolved in either (a) acetonitrile, (b) methanol, (c) chloroform, (d) butanone and (e) acetone; followed by rapid evaporation, heated (a) and (c) from 30 – 600 °C, (b) from 30 – 500 °C, (c) from 30 – 410 °C and (d) 30 – 370 °C at a heating rate of 10°C/min.

To determine whether samples prepared *via* rapid solvent evaporation rendered any promising ternary amorphous systems, further investigation using FTIR analysis was done. **Figure 6.30** depicts an overlay of the individual FTIR spectrums and **Table 6.8** outlines the observed wavenumbers with corresponding functional groups. The data indicated few changes in the spectrum, the peak shapes and intensity were not fully convincing for possible new strong intermolecular bond formation, however all the preparations exhibited broadened peaks at wavenumber 1720 cm^{-1}. The preparation obtained from rapid evaporation from acetone, once again, showed the most promise with significant peak broadening and disappearance of absorbance bands in the region of 3500 - 3000 cm^{-1}. This resulted in further investigation of this sample using PXRD.

Figure 6.31 depicts an overlay of the PXRD data obtained with SPA-C rapidly evaporated from acetone versus that of SPA-C. Two diffraction peaks at 9.79 and 31.65 °2θ were observed for the solvent evaporated sample. The sample was characterised as amorphous, partly crystalline with a diffraction peak attributed to either SUL or AZI still identifiable in the sample.
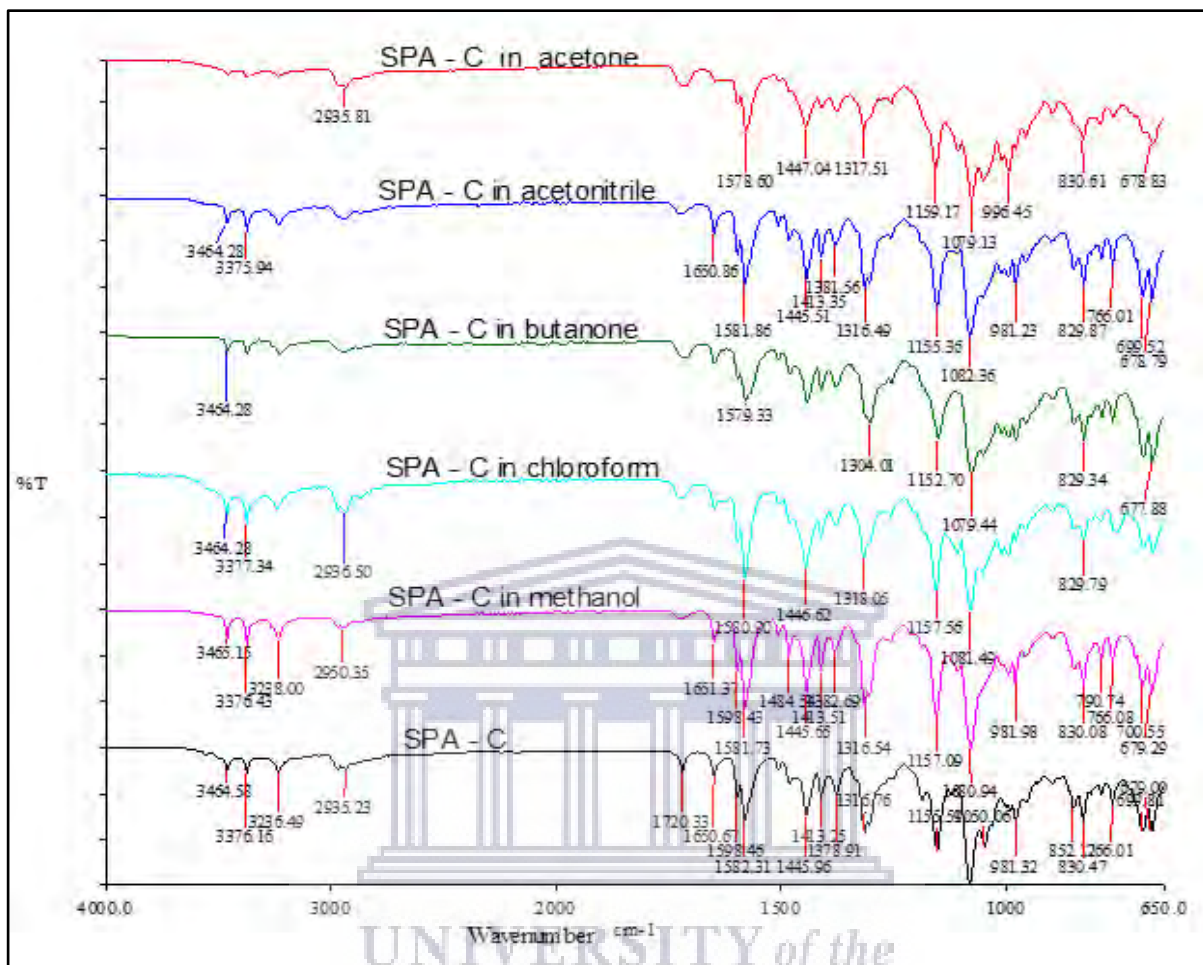
Figure 6.30: An overlay of the FTIR spectra obtained for samples prepared by dissolving SPA-C in either acetone, acetonitrile, chloroform, butanone and methanol followed by rapid evaporation of the solvent

Table 6.8: Table of SPA-C prepared by rapid solvent evaporation in acetone, acetonitrile, butanone, chloroform, and methanol; describing the wavenumbers obtained from FTIR analysis with correlating functional groups.

SPA-C		Acetone		Acetonitrile		Butanone		Chloroform		Methanol	
Wavenumber (cm⁻¹)	Functional group	Wavenumber (cm⁻¹)	Functional group	Wavenumber (cm⁻¹)	Functional group	Wavenumber (cm⁻¹)	Functional group	Wavenumber (cm⁻¹)	Functional group	Wavenumber (cm⁻¹)	Functional group
3464.58	N-H	-	-	3464.28	N-H	3464.79	N-H	3464.28	N-H	3455.15	N-H
3376.16	C-H	-	-	3375.94	C-H	-	-	3377.34	C-H	3376.43	C-H
3236.49	C-H	-	-	3238.00	C-H	-	-	-	-	3238.00	C-H
2935.23	C-H	2935.81	C-H	2950.86	C-H	-	-	2936.50	C-H	2935.33	C-H
1720.33	C=O	-	-	-	-	-	-	-	-	-	-
1650.67	C=N	-	-	1650.73	C=N	-	-	-	-	1651.37	C=N
1598.46	C=C	-	-	1589.66	C=C	-	-	-	-	1598.43	C=C
1582.31	C=C	1578.60	C=C	1581.86	C=C	1579.33	C=C	1580.90	C=C	1581.73	C=C
1482.41	CH₂	-	-	-	-	-	-	-	-	1484.54	CH₂
1445.96	CH₂	1447.04	CH₂	1445.51	CH₂	1447.04	CH₂	1446.62	CH₂	1445.65	CH₂
1413.25	CH₂	-	-	-	-	-	-	-	-	1413.51	CH₂
1378.91	C≡N	1317.51	C≡N	1316.97	C≡N	1304.04	C≡N	1318.05	C≡N	1316.54	C≡N
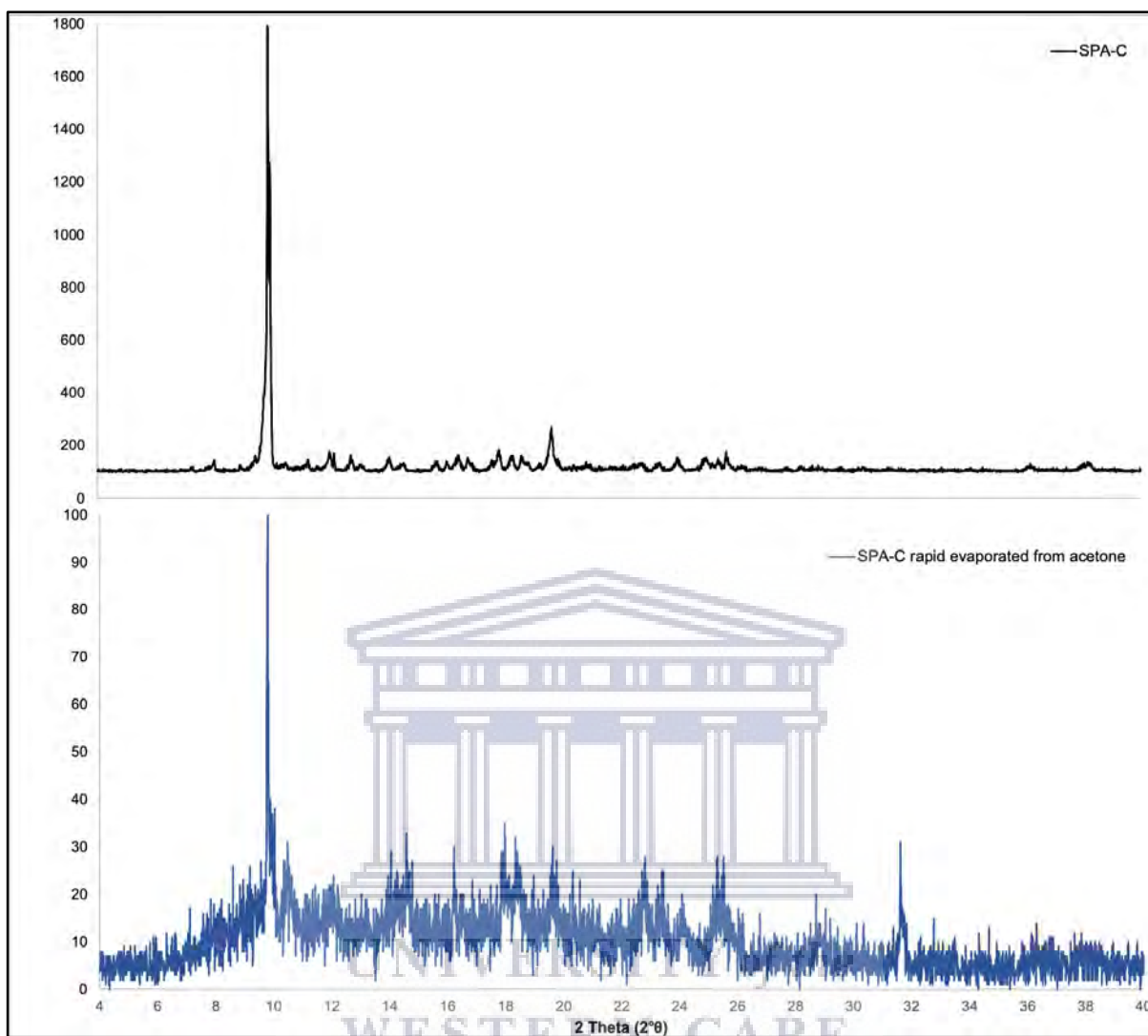
Figure 6.31: An overlay of the PXRD depicting SPA-C and SPA-C prepared via rapid solvent in acetone.

Based on the results presented in this section it was concluded that the rapid solvent evaporation from acetone resulted in the preparation of a partly amorphous solid-state form, however since it was not completely amorphised during this preparation method it was decided to investigate the process of quench cooling of the melt further.

6.3.3 Quench cooling of the melt

The next phase of the study was to investigate the possibility of a complete amorphous solid-state form using the well-known method of quench cooling of the melt. **Figure 6.32** depicts the DSC thermogram obtained with SPA-C subjected to melting followed by quench cooling of the melting phase. Interestingly, two glass transition temperatures were observed with the

http://etd.uwc.ac.za/

obtained preparation during DSC analysis. The first T_g was observed at 74.65 °C and it was signified by a clear step in the heat flow baseline. The second T_g was observed at 183.22 °C, which is. Initially, it was considered that this prepared solid-state form exhibited the same thermal behaviour as that observed for the samples obtained from slow and rapid solvent evaporation (**Figures 6.24 and 6.28**). However, further investigation, which will be discussed in the subsequent paragraphs, allowed a conclusion to be drawn that this solid-state form presents with two transition temperatures.
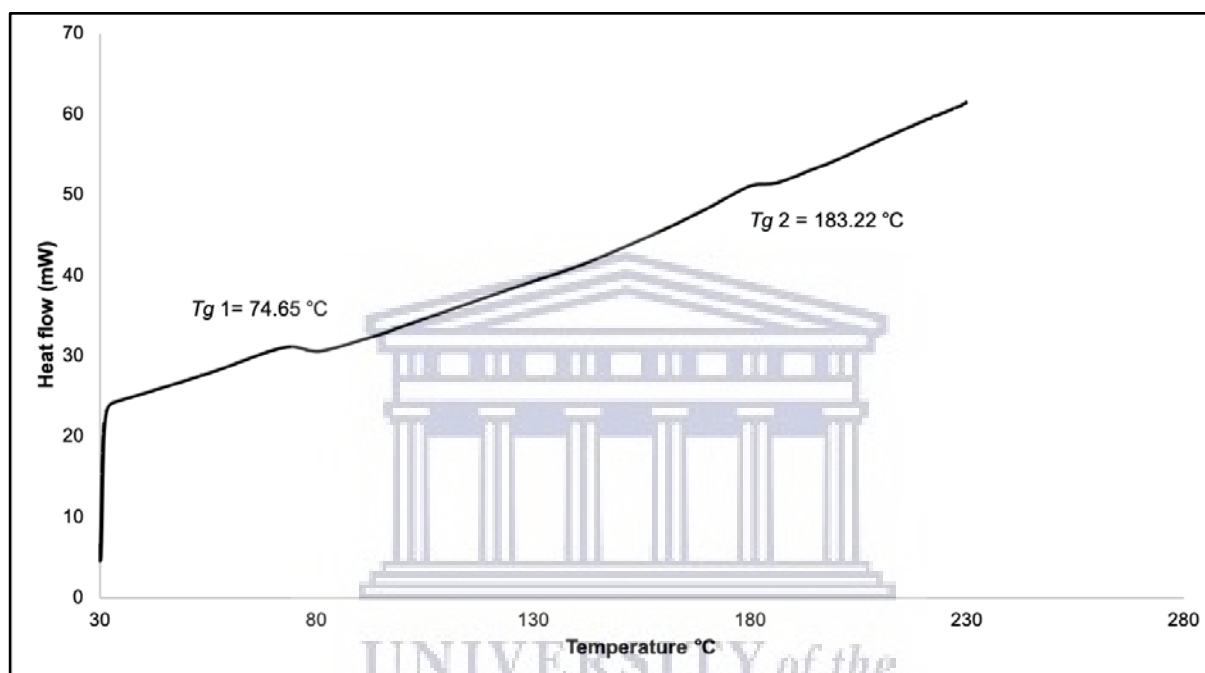
Figure 6.32: DSC thermogram depicting the heat flow trace obtained during the quench cooling of the melt of SPA-C.

TGA analysis was subsequently used to ascertain whether any difference in terms of weight loss could be observed between SPA-C and SPA-A. The result obtained showed no significant weight loss throughout until the degradation point and no difference in the onset of degradation was observed **(Figure 6.33)**. The only difference was in terms of moisture content, with SPA-C showing weight loss in the temperature range of 95 - 110 °C which was quantified to 3.5%. As described in paragraph 6.21 this was confirmed to be associated with the loss of two molecules of water since the dihydrate form of AZI was used. However, this dehydration step was not observed during the TGA of SPA-A and this was ascribed to the fact that during the melting process AZI dehydrated and thus no residual molecular water is present in SPA-A.
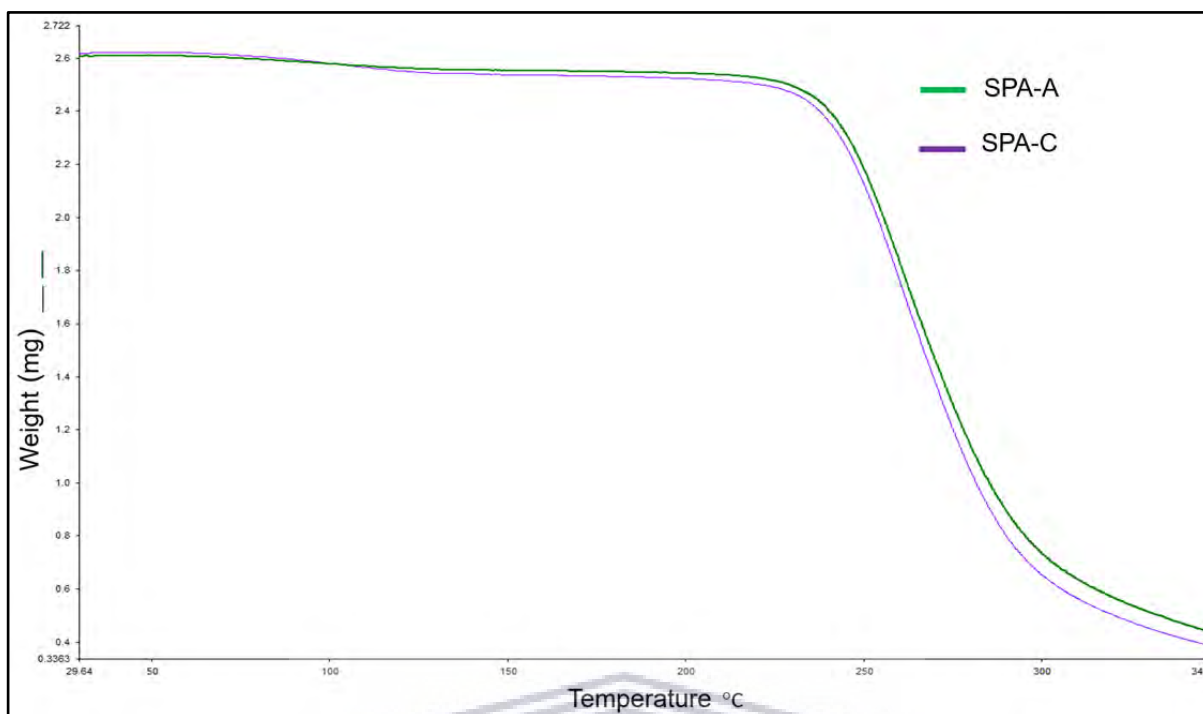
Figure 6.33: Overlay of TGA obtained for SPA-C and SPA-A heated from 30 –345 °C at a heating rate of 10°C/min.
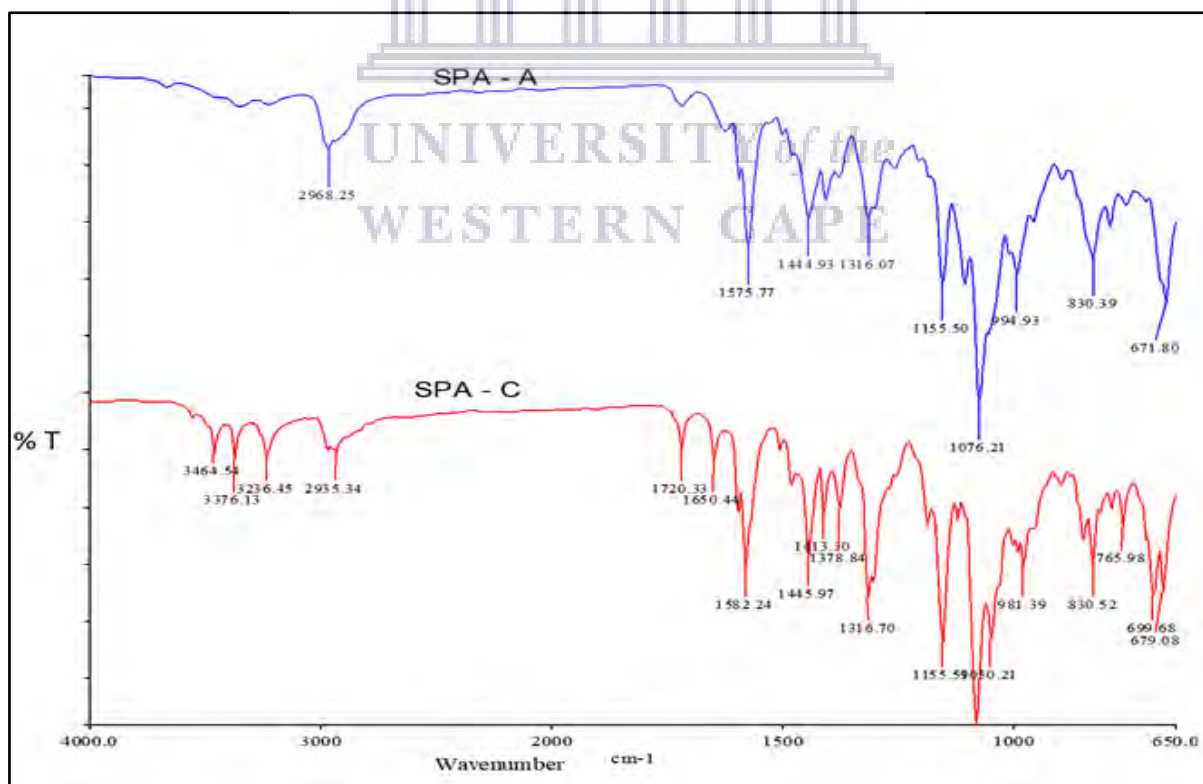
Figure 6.34: An overlay of the FTIR spectra obtained for a sample prepared by hot-melt (SPA-A) in comparison with SPA-C.

The FTIR spectrum of SPA-A and associated absorbance bands are shown in **(Figure 6.34)** and **(Table 6.9)**. Here an investigation of SPA-A was studied in comparison with SPA-C. The SPA-A spectrum exhibited significant differences in the peaks; either there was complete loss of peaks or broadening and shifts in the vibrational frequencies. The IR spectrum showed notable peak broadening related to the -OH, N-H, C-H, C=O, C≡N, and C-O-C functional groups, as opposed to SPA-C. The chemical structures of SUL, PYR and AZI all possess hydrogen bond (H-bond) receptors and H-bond donors, these functional groups have inherent affinity of forming H-bonding when suitable conditions capable of altering the physico-chemical properties of the compounds are attained (Braschi, *et al.*, 2013). The hot-melt method provided additional energy during the heating process that interrupted the molecular bond resulting in molecular packing re-arrangement and with a good glass forming property of AZI (Mahlin and Bergström, 2013), the rapid loss of this energy when quench cooled, facilitated a disorganised and short-range packing lattice. Furthermore, an investigation of a glass forming capacity of AZI has been widely studied (Aucamp, *et al.*, 2015; Jaiswar, Jha, and Amin, 2016), which confirms the characteristic changes obtained. This change in spectrum characteristics provides diagnostic evidence of new intermolecular bond formation. Subsequently, PXRD was further employed to confirm whether this solid-state form preparation resulted in a ternary amorphous form. **Figure 6.35** depicts the PXRD pattern obtained for SPA-A in comparison with SPA-C. This pattern exhibited the typical halo-like diffraction pattern which is characteristic of completely amorphous solid-state forms. This pattern therefore confirmed that all three drugs, SUL, PYR and AZI, existed in the amorphous state.

Table 6.9: Table of SPA-C prepared by hot-melt (SPA- A) describing the wavenumbers obtained from FTIR analysis with correlating functional groups.

SPA-C		SPA- A	
Wavenumber (cm⁻¹)	Functional group	Wavenumber (cm⁻¹)	Functional group
3464.58	N-H	-	-
3376.16	C-H	-	-
3236.49	C-H	-	-
2938.23	C-H	2968.25	C-H
1720.33	C=O	-	-
1650.67	C=N	-	-
1598.46	C=C	-	-
1582.41	C=C	1575.77	C=C
1445.96	CH_2	1444.93	CH_2
1413.25	CH_2	-	-
1378.84	CH_3	-	-
1316.70	C≡N	1316.07	C≡N
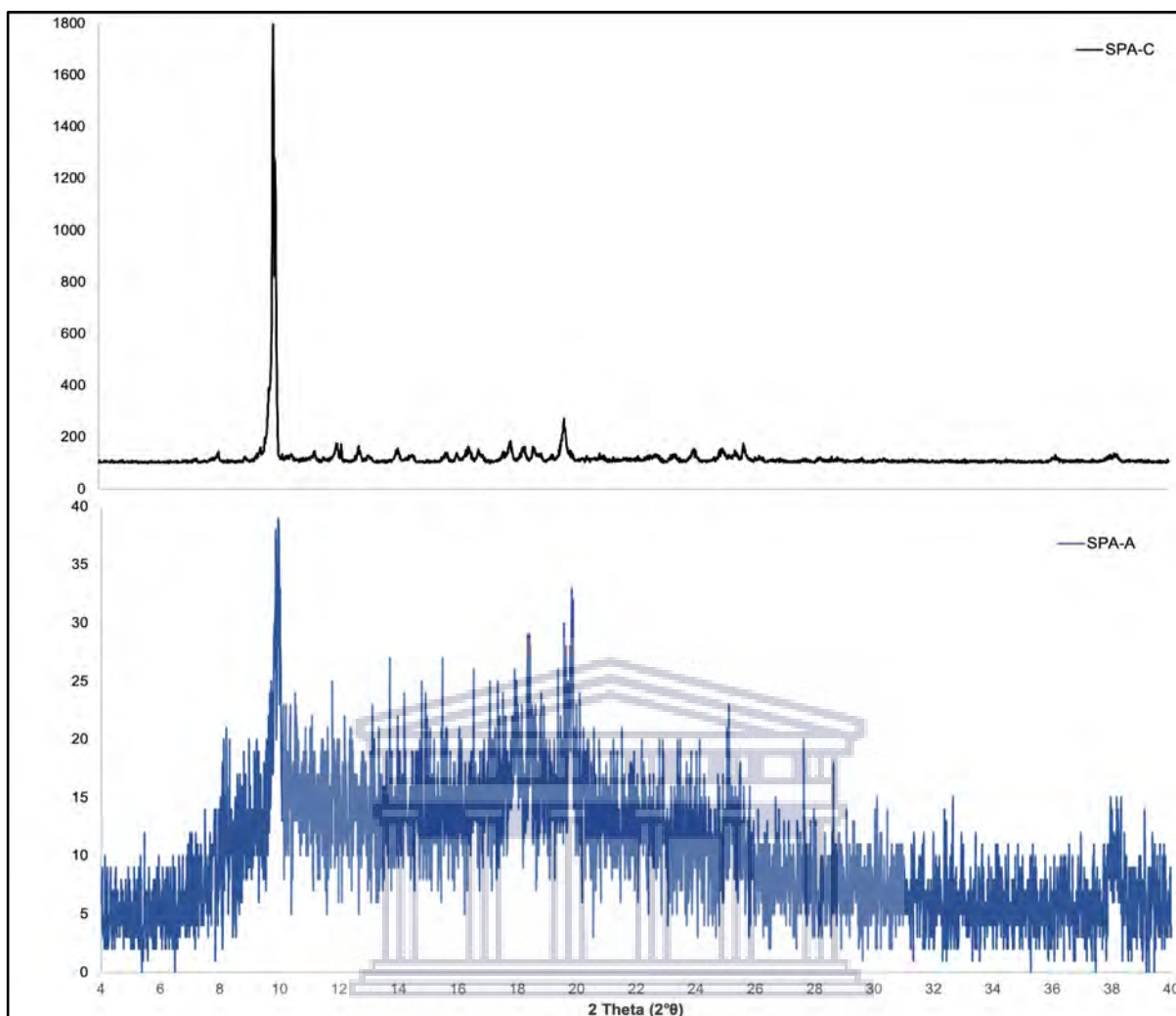
Figure 6.35: An overlay of the PXRD patterns obtained for SPA-A and SPA-C, across a scanning range of 4-40°2θ, collected at ambient temperature.

Based on the thermal, spectroscopic and PXRD investigations conducted on the samples prepared using the three described preparation methods it was concluded that quench cooling of the melt resulted in a completely amorphous solid-state form that consists of all three APIs. It was therefore decided to continue further physico-chemical characterisation of this ternary amorphous system prepared *via* quench cooling of the melt (SPA-A). Further investigation included determining the impact the amorphous solid form would have on the equilibrium solubility and dissolution rate of each of the APIs and finally it was important to ascertain the ability of this solid-state form to remain stable during processing and storage conditions.

Equilibrium solubility of SUL in SPA-A was investigated and compared to that of pure SUL and SUL in SPA-C, in distilled water, pH 1.2 and pH 6.8 (**Figure 6.36, Figure 6.37 and Figure 6.38**). SUL in SPA-A had the highest solubility across experimented media with distilled water being the most favourable solvent. Maximum concentration was obtained within an hour of operation with concentrations of 7.66 ± 0.39 mg/ml, 2.59 ± 0.39 mg/ml and 7.14 ± 0.1.3 mg/ml for distilled water, pH 1.2 and pH 6.8, respectively. This was over 16-folds higher in comparison to SUL. The obtained data typically reflects the impact of an amorphous form on the solubility of a compound. No previous literature exists that investigated enhanced SUL aqueous solubility when existing in an amorphous solid-state form. A study by Aucamp *et al,* (2016) revealed that it is possible to prepare SUL as an amorphous solid-state form, however this form had to be stabilised it with a polymer to ensure reversion to the stable crystalline form is hindered.
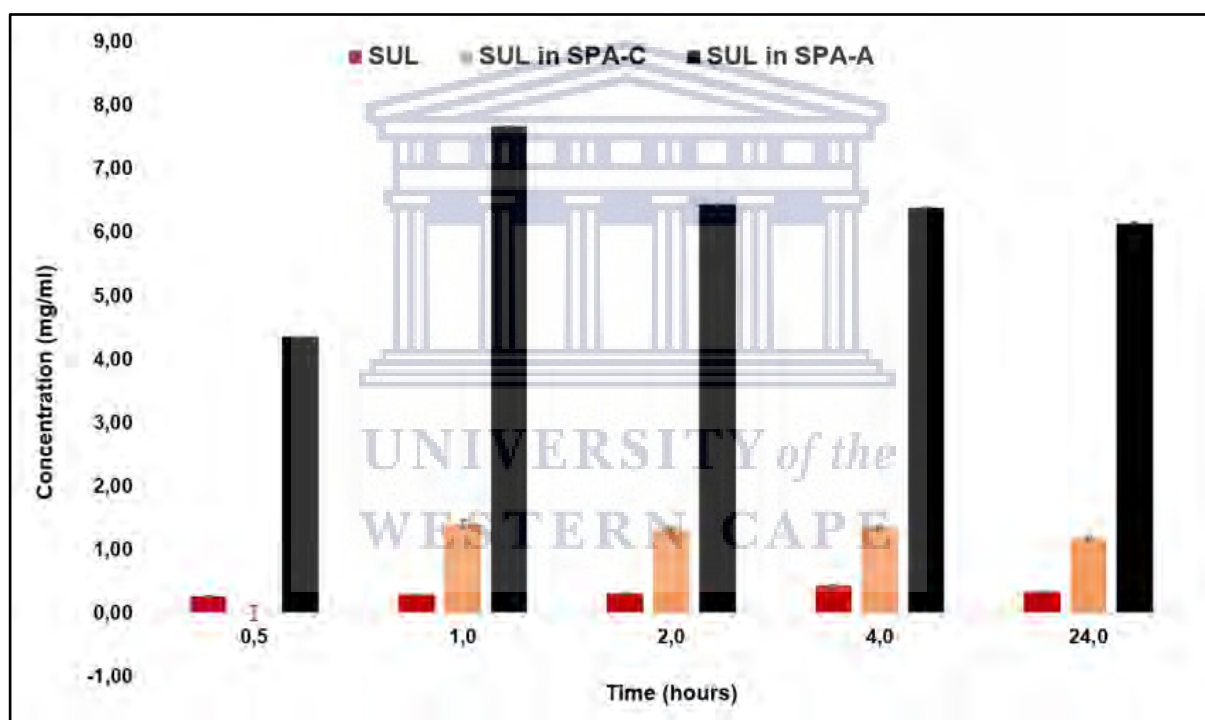
Figure 6.36: Equilibrium solubility concentration (mg/ml) of pure SUL, SUL in SPA-C and SUL in SPA-A in distilled water, with samples analysed at 0.5, 1, 2, 4 and 24 hours agitated and maintained at 37.0 ± 0.5°C.
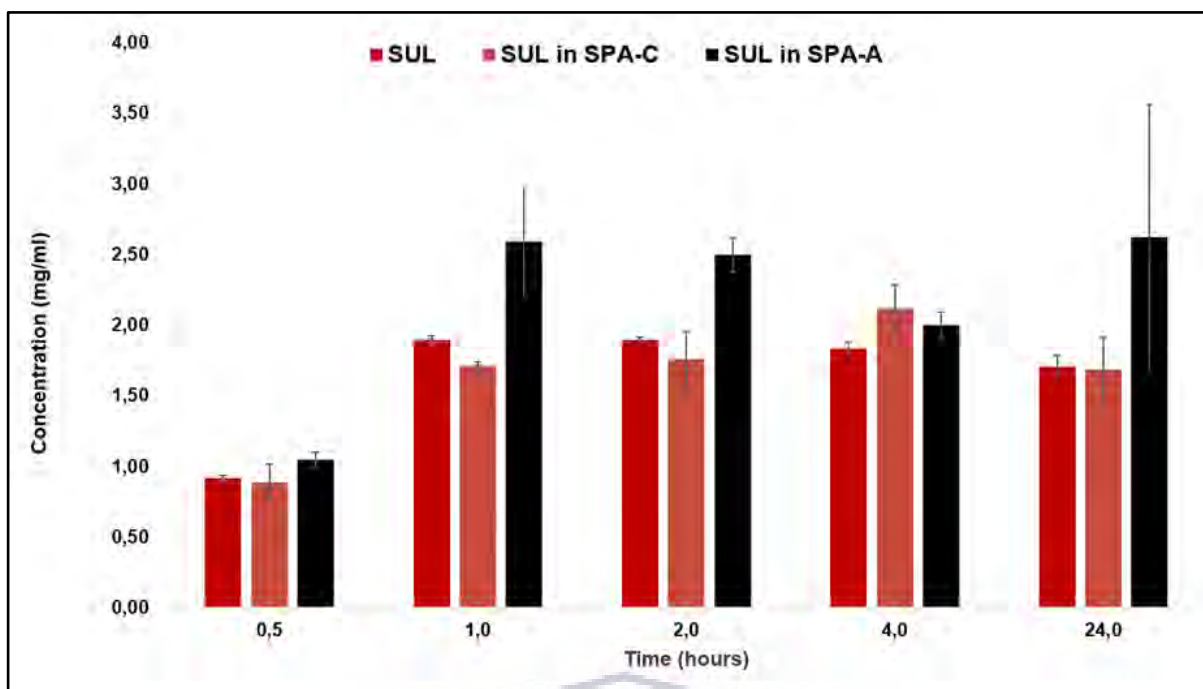
Figure 6.37: Equilibrium solubility concentration (mg/ml) of pure SUL, SUL in SPA-C and SUL in SPA-A in pH 1.2, with samples analysed at 0.5, 1, 2, 4 and 24 hours agitated and maintained at 37.0 ± 0.5°C.

Figure 6.38: Equilibrium solubility concentration (mg/ml) of pure SUL, SUL in SPA-C and SUL in SPA-A in pH 6.8, with samples analysed at 0.5, 1, 2, 4 and 24 hours agitated and maintained at 37.0 ± 0.5°C.

The comparisons of the solubilities of PYR in SPA-A with its crystalline counterparts, solubilised in distilled water, pH 1.2 and pH 6.8 are presented in **Figure 6.39**, Figure **6.40**and **Figure 6.41**. SPA-A performed better than SPA-C and single PYR in distilled water and pH 6.8 with quantified concentrations of 0.48 ± 0.04 mg/ml and 2.56 ± 0.34 mg/ml respectively. These concentrations are over 37% and 66% higher in comparison to pure PYR. Interestingly, when solubilised in pH 1.2, pure PYR still showed the highest equilibrium solubility than when combined as part of SPA-C or as an amorphous form as part of SPA-A. This varied trend exhibited by PYR could possibly be explained by the fact that when in combination with SUL and AZI, PYR needs to compete for solubilising solvent, since this is governed by the amount of solvent which is available to accommodate solubilised molecules. Thus, when only PYR is being solubilised, no need exists for it to compete to be solubilised. This is however just a hypothesis and further investigation of this phenomena utilising solution-state nuclear magnetic resonance studies might shed light on this observation.

Another interesting phenomenon observed during the determination of PYR equilibrium solubility from the SPA-A solid-state form was the decrease in the solubilised PYR concentration in pH 6.8 buffered medium across the testing period. A significantly high solubilised concentration (2.56 ± 0.24 mg/ml) was observed for PYR after the first 30 minutes of solubilisation of SPA-A. Thereafter, gradually lower PYR concentrations were quantified up until 24 hours upon which an equilibrium solubility of 0.39 ± 0.11 mg/ml was obtained. This proved that the SPA-A solid-state form may undergo solution-mediated phase transformation.

And again, there has been limited or no studies for amorphous forms or any co-amorphous solid-state form of PYR to relate this finding. Thus far, the current study has elucidated the impact that each of the three drugs may play in enhancing the solubility profile of one another; however further investigations may be necessary to fully comprehend the extent of this improved equilibrium solubility impact in bioavailability.

Figure 6.39: Equilibrium solubility concentration (mg/ml) of pure PYR, PYR in SPA-C and PYR in SPA-A in distilled water, with samples analysed at 0.5, 1, 2, 4 and 24 hours agitated and maintained at 37.0 ± 0.5°C.
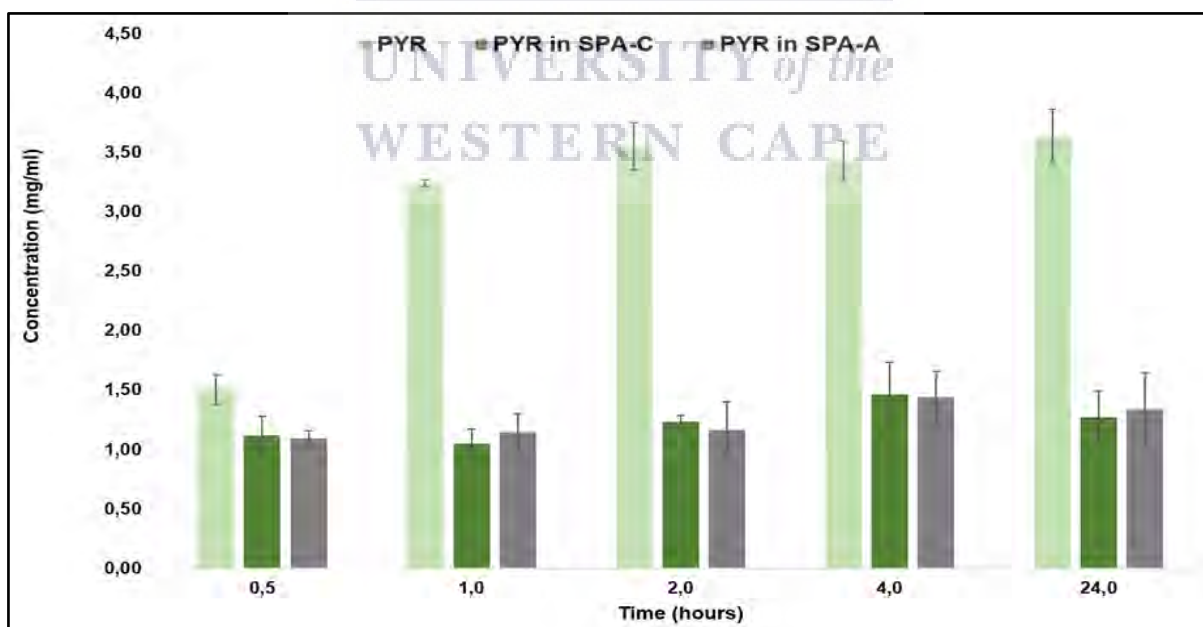
Figure 6.40: Equilibrium solubility concentration (mg/ml) of pure PYR, PYR in SPA-C and PYR in SPA-A in pH 1.2, with samples analysed at 0.5, 1, 2, 4 and 24 hours agitated and maintained at 37.0 ± 0.5°C.
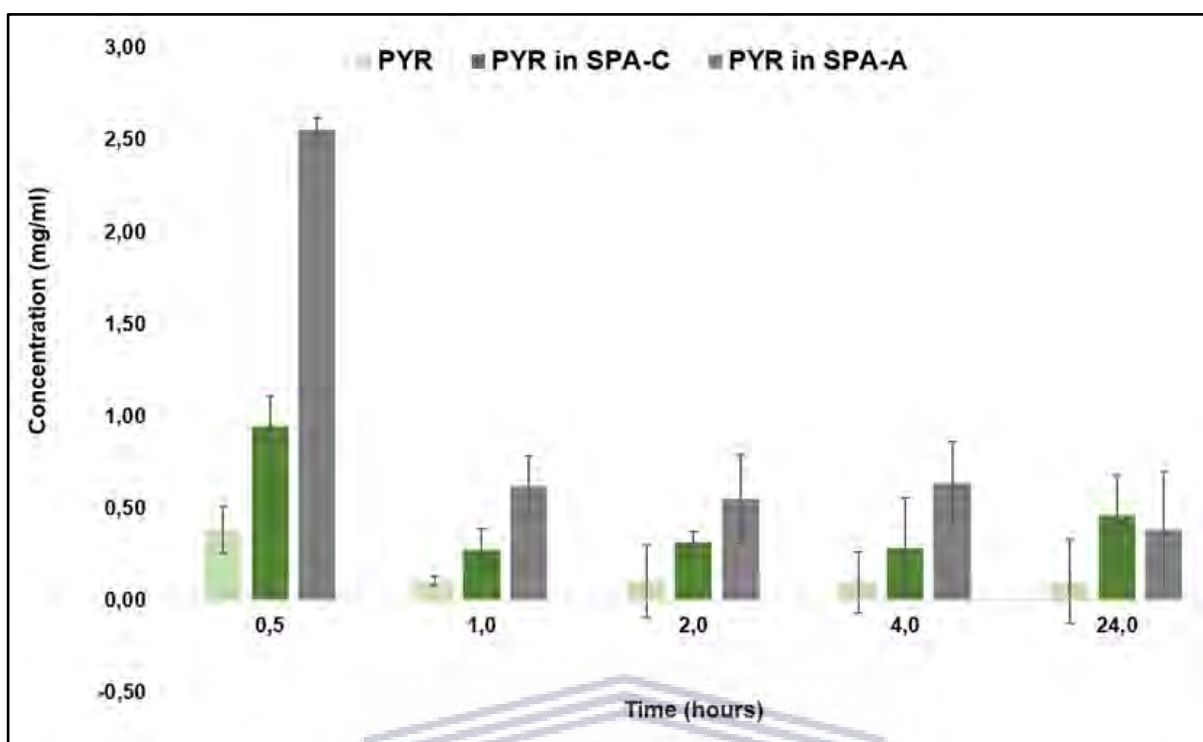
Figure 6.41: Equilibrium solubility concentration (mg/ml) of pure PYR and PYR in SPA-C and PYR in SPA-A in pH 6.8, with samples analysed at 0.5, 1, 2, 4 and 24 hours agitated and maintained at 37.0 ± 0.5°C.

To evaluate the impact of SPA-A on the equilibrium solubility of AZI, investigation was done in distilled water **(Figure 6.42)**, buffered pH 1.2 **(Figure 6.43)** and buffered solution pH 6.8 **(Figure 6.44)**. This data was compared to pure AZI and AZI in SPA-C, it was evident that the amorphous habit of SPA-A resulted in increased AZI solubility in all the experimented solubilisation media. The maximum concentrations quantified were 0.41 ± 0.03 mg/ml, 2.26 ± 1.26 mg/ml, and 7.14 ± 0.05 mg/ml for samples in distilled water, pH 1.2 and pH 6.8 respectively. In summary this showed approximately an 8-folds solubility improvement in distilled water and a 2-fold improvement in solubility in pH 1.2 and pH 6.8. This corroborates with the literature highlighted in this study that state the positive impact that amorphous forms of drugs may have on the aqueous solubility of poorly soluble drugs (Aucamp *et al.*, 2015; Chavan *et al.*, 2016b; Jaiswar *et al.*, 2016; Liu *et al.*, 2018; Montejo-Bernardo *et al.*, 2005; Milne *et al.*, 2015; Newman *et al.*, 2012).
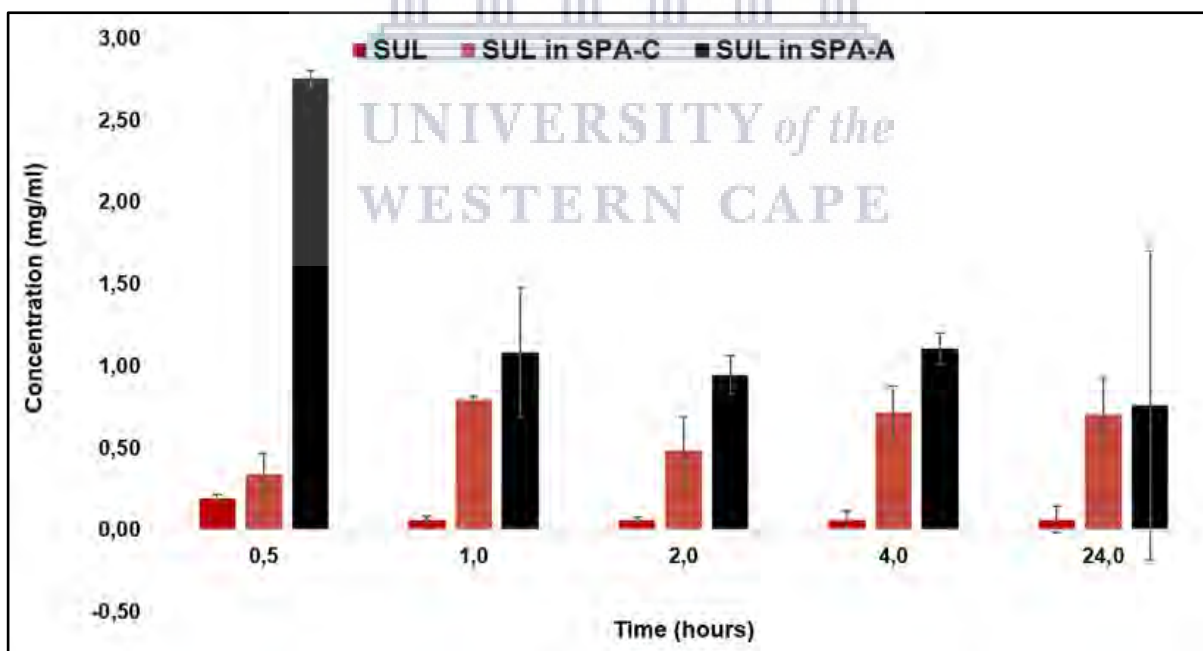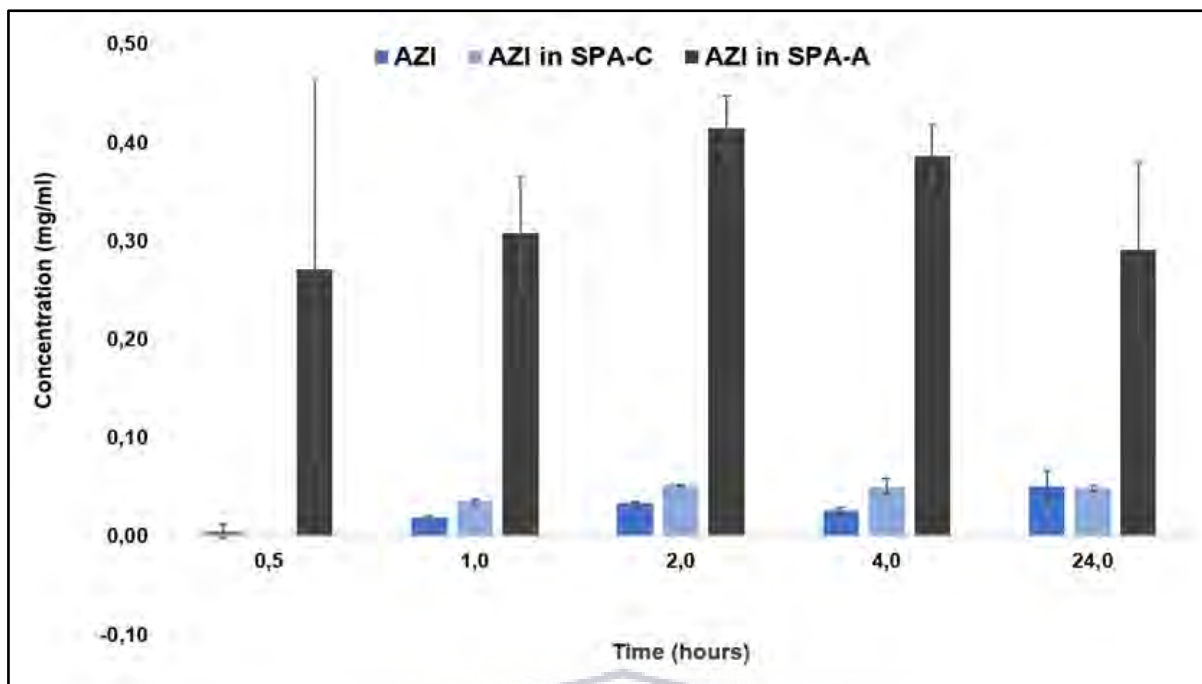
Figure 6.42: Equilibrium solubility concentration (mg/ml) of pure AZI and AZI in SPA-C and AZI in SPA-A in distilled water, with samples analysed at 0.5, 1, 2, 4 and 24 hours agitated and maintained at 37.0 ± 0.5°C.
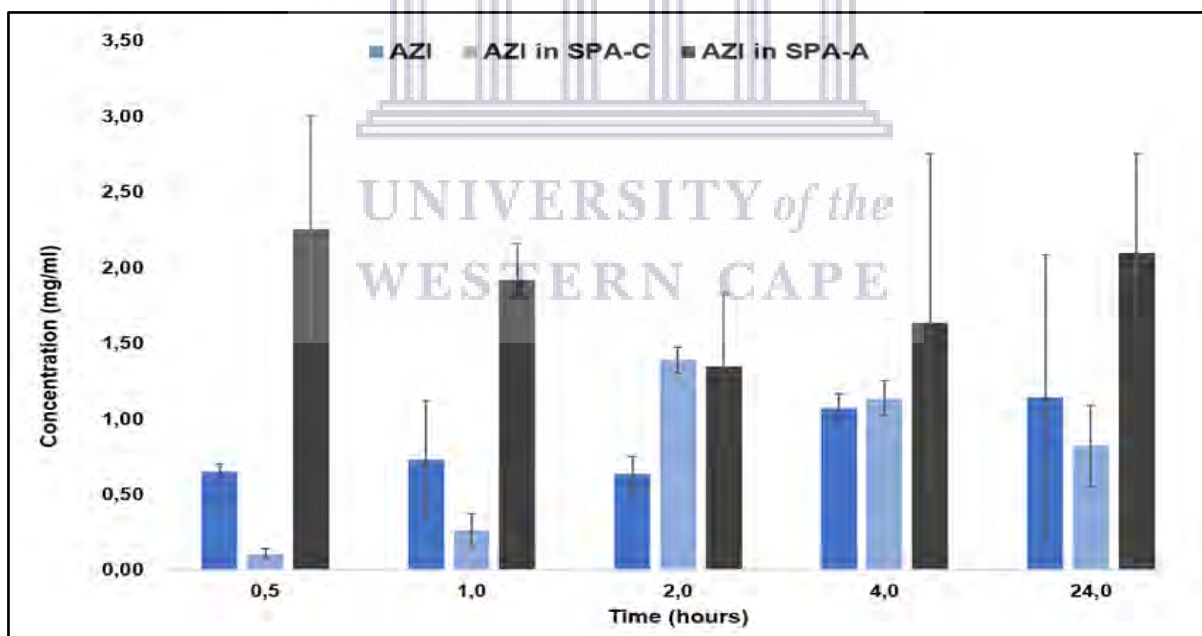
Figure 6.43: Equilibrium solubility concentration (mg/ml) of pure AZI and AZI in SPA-C and AZI in SPA-A in pH 1.2, with samples analysed at 0.5, 1, 2, 4 and 24 hours agitated and maintained at 37.0 ± 0.5°C.
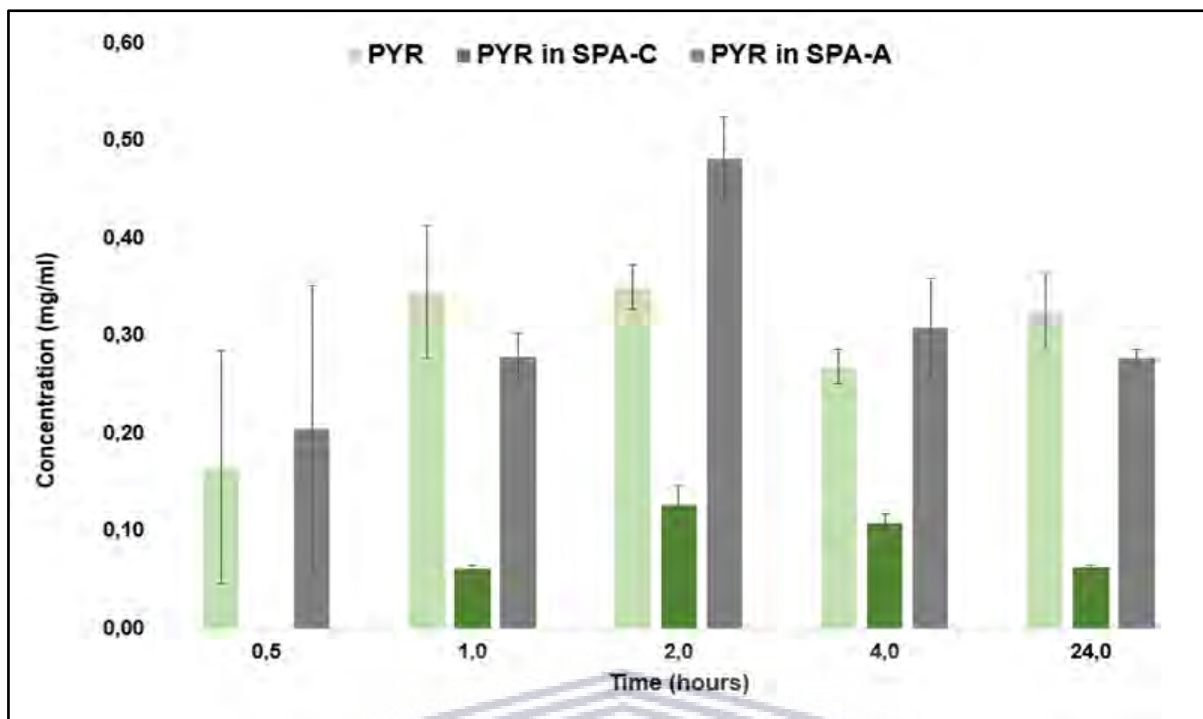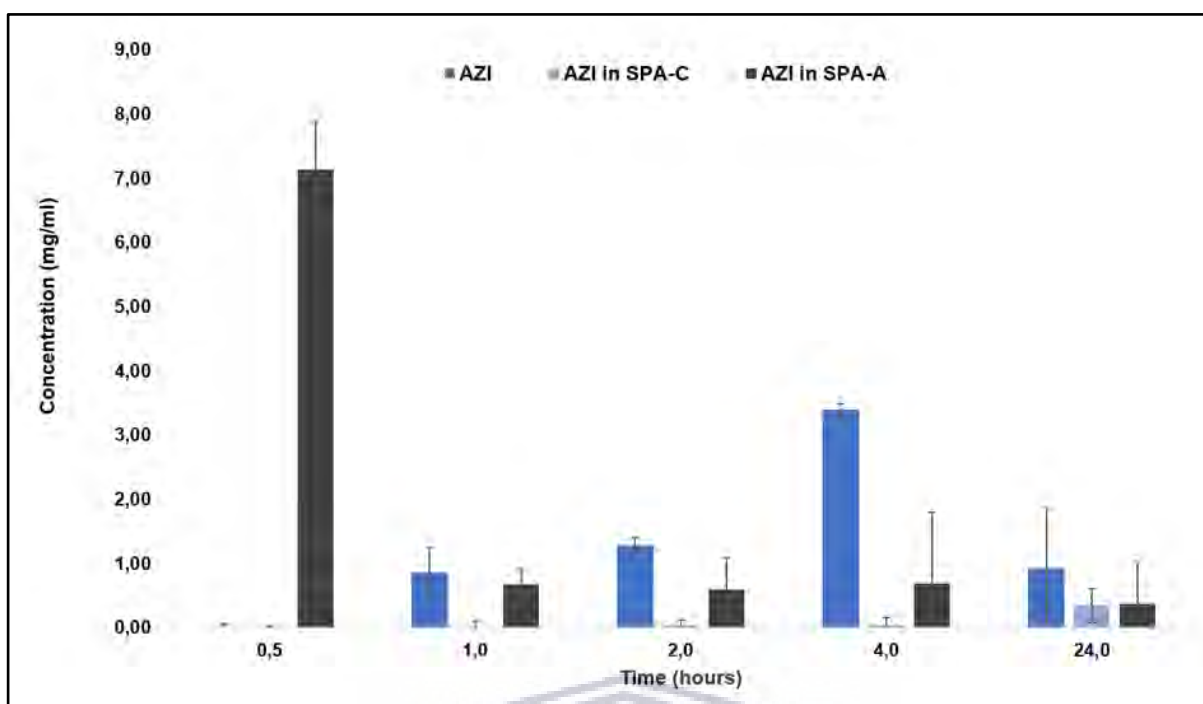
Figure 6.44: Equilibrium solubility concentration (mg/ml) of pure AZI and AZI in SPA-C and AZI in SPA-A in pH 6.8, with samples analysed at 0.5, 1, 2, 4 and 24 hours agitated and maintained at 37.0 ± 0.5°C.

To investigate the impact of the ternary amorphous form on the dissolution rate of SUL, PYR and AZI, the dissolution rate studies were conducted, and data obtained for SUL is presented in **Figure 6.45** and **Table 6.10**. The dissolution rate data for PYR as part of SPA-A is presented in **Figure 6.46** and **Table 6.11**, and that obtained for AZI is outlined in **Figure 6.46**. and **Table 6.12**. It was apparent that dissolution generally increased in the order of single APIs, physical mixture (SPA-C) and highest was with SPA-A. The amorphous solid-state form outperformed the other counterparts, a confirmation to literature that, the amorphous forms of drugs have better dissolution and solubility property as opposed to their individual crystalline counterparts (Wang *et al*., 2019; Kasten *et al*., 2017; Pacult, *et al*., 2019; Sai Krishna Anand *et al.*, 2018; Kawakami *et al.*, 2018; Schittny, Huwyler and Puchkov, 2019; Melzig, Finke, Schilde and Kwade, 2018). The maximum dissolution rate percentages for SPA-A were: 77.3% (**Figure 6.45**), 68.5% (**Figure 6.46**) and 52.8%, **(Figure 6.47)** for SUL, PYR and AZI respectively. As aforementioned under section for SPA-C dissolution, the exact explanation for improved dissolution rate of SPA-C observed in this experiment remains unclear, the effects related to co-amorphous formation are noted in literature examples in chapter 3, (**Table 3.1**). Furthermore, this data deduced an improvement of over two folds, sulfadoxine and pyrimethamine and over nine folds, azithromycin. Dissolution rate increase may not

conclusively entail an enhanced solubility and bioavailability, more investigation related to physiological conditions are necessary to draw reliable conclusions.

Table 6.10: Summary of dissolution rate results obtained for SUL in distilled water maintained at 37 ± 0.5 °C.

Time (min)	SUL percentage dissolved (%)	STDEV	SUL in SPA-C percentage dissolved (%)	STDEV	SUL in SPA-C percentage dissolved (%)	STDEV
0	0.00	0.00	0.00	0.00	0.00	0.00
5	33.33	1.42	56.35	3.19	71.13	2.82
10	35.97	1.43	66.58	0.84	75.25	2.48
20	36.73	1.77	74.76	0.52	76.23	1.67
40	37.37	1.50	81.19	1.27	76.66	1.76
60	36.86	1.87	83.19	1.29	77.35	2.76
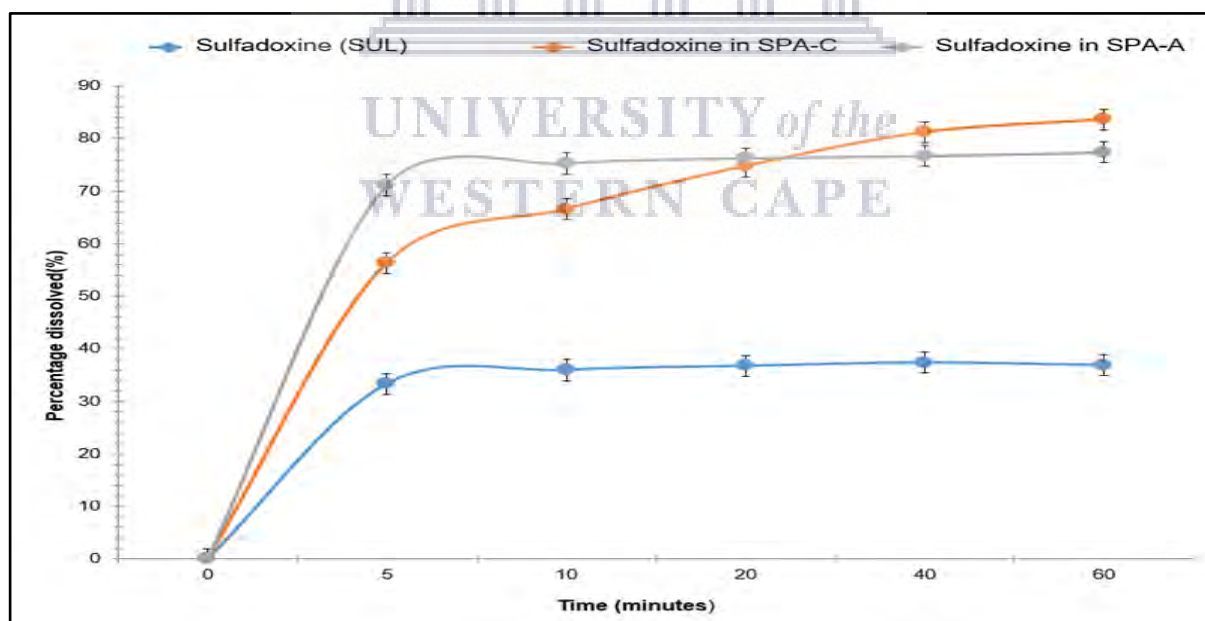
Figure 6.45: Dissolution rate obtained for SUL, SUL in SPA-C and SUL in SPA-A in distilled water maintained at 37 ± 0.5 °C.

Table 6.11: Summary of dissolution rate results obtained for PYR in distilled water maintained at 37 ± 0.5 °C

Time (min)	PYR percentage dissolved (%)	STDEV	PYR in SPA-C percentage dissolved (%)	STDEV	PYR in SPA-C percentage dissolved (%)	STDEV
0	0.00	0.00	0.00	0.00	0.00	0.00
5	7.56	1.44	41.36	4.84	64.48	2.73
10	11.02	2.97	37.39	5.09	67.24	2.71
20	16.74	2.97	44.95	9.72	67.27	2.29
40	22.38	3.60	47.56	2.10	68.34	1.91
60	25.75	3.92	53.49	3.25	66.54	4.20
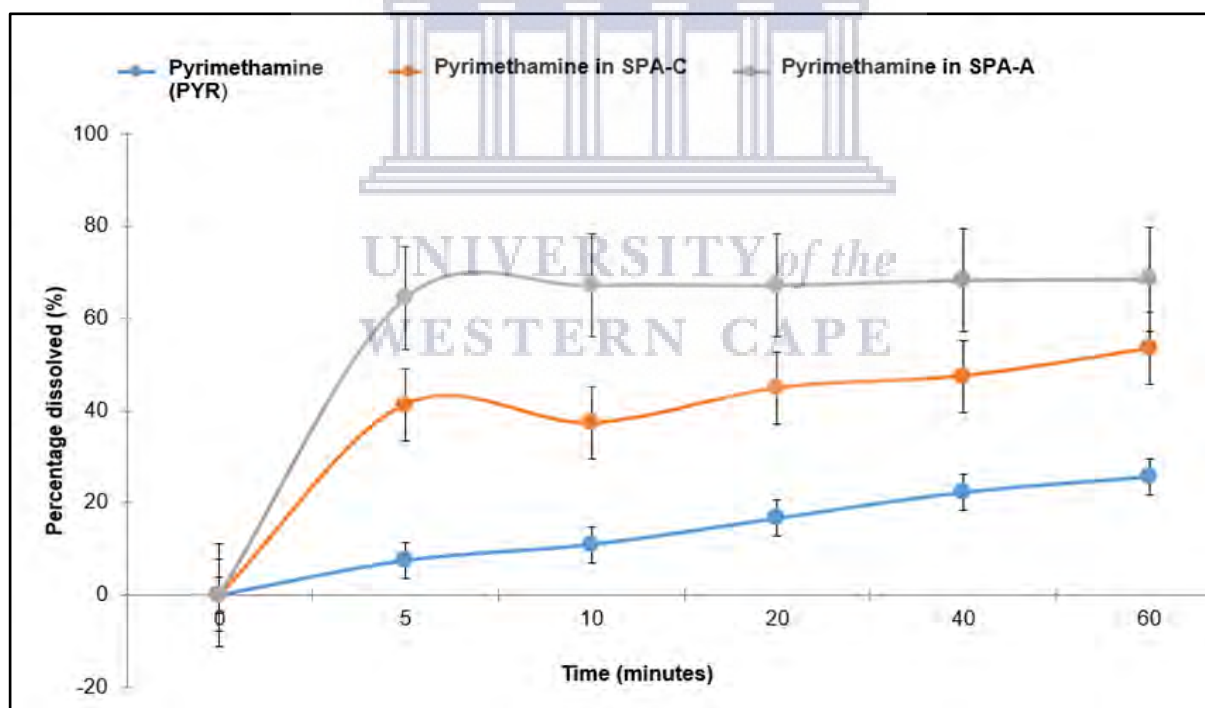
Figure 6.46: Dissolution rate obtained for PYR, PYR in SPA-C and PYR in SPA-A in distilled water maintained at 37 ± 0.5 °C.

Table 6.12: Summary of dissolution rate results obtained for AZI in distilled water maintained at 37 ± 0.5 °C

Time (min)	AZI percentage dissolved (%)	STDEV	AZI in SPA-C percentage dissolved (%)	STDEV	AZI in SPA-A percentage dissolved (%)	STDEV
0	0.00	0.00	0.00	0.00	0.00	0.00
5	4.94	2.18	23.14	2.00	44.44	1.75
10	3.82	0.74	32.70	1.51	46.89	2.78
20	4.51	0.62	43.24	4.36	49.18	4.47
40	4.55	0.90	49.78	3.88	48.84	2.46
60	4.57	0.86	48.24	1.75	52.80	4.04
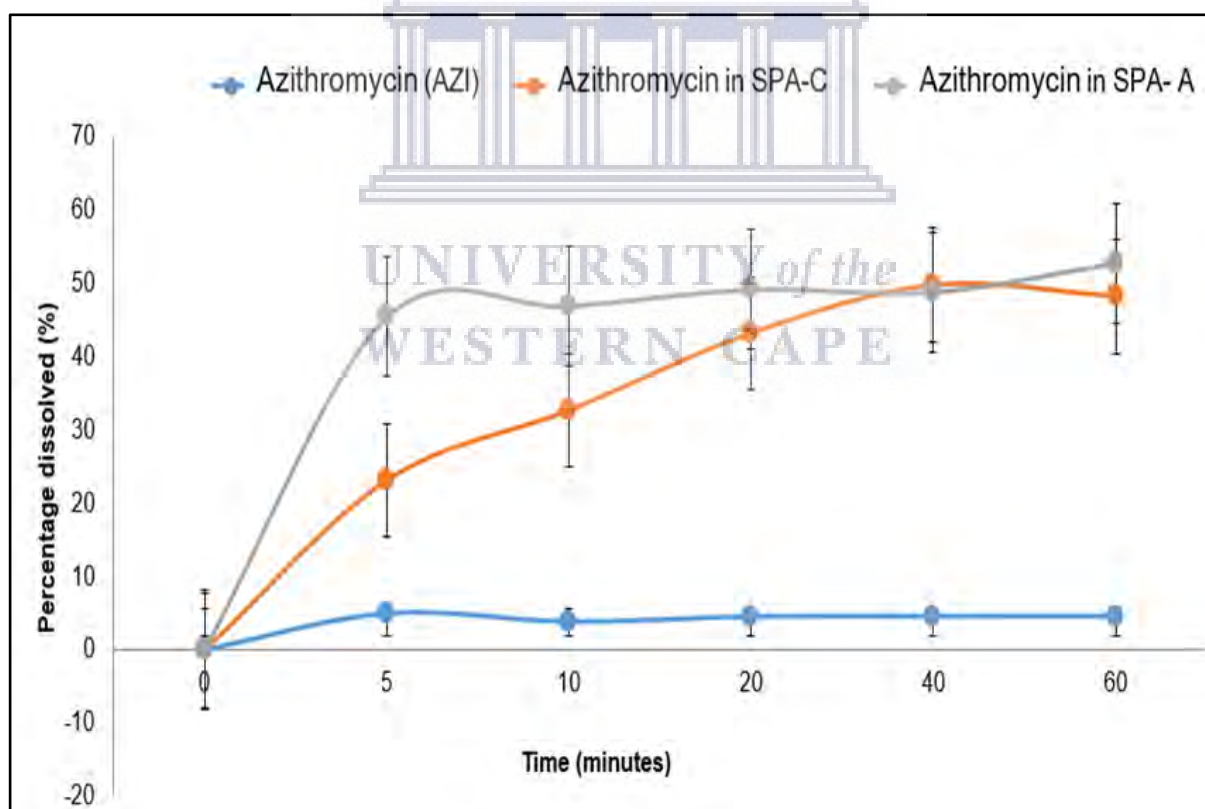
Figure 6.47: Dissolution rate obtained for AZI, AZI in SPA-C and AZI in SPA-A in distilled water maintained at 37 ± 0.5 °C.

6.4 Physical stability of SPA-A

Physical stability of amorphous solid-state forms is a significant challenge and an important aspect that negatively affects application of amorphous compounds in dosage form design. As previously alluded in proceeding chapters, an amorphous exhibits higher intermolecular energy that improves on its physico-chemical behaviours of pharmaceutical importance (Aucamp *et al*., 2016; Beyer *et al*., 2016; Chavan *et al*., 2016; Descamps, 2016; Liu *et al*., 2018; Milne *et al*., 2015; Ojarinta *et al*., 2017; Ueda *et al*., 2016). To evaluate this impediment, an investigation was done on SPA-A where samples were stored at 5 °C ± 2 °C, 22 °C ± 2 °C and 60 °C ± 3 °C for a period of 6 months, results were obtained at 2-month intervals and are shown in **Figures 6.48, 6.49 and 6.50**. The FTIR data didn't show any significant changes in the physical stability of the stored samples over the 4-month storage period for all the investigated conditions.

Similarly, the sample stored at room temperature showed physical stability after storage of six months. However, a notable difference was observed in the FTIR data collected for the samples stored at 5 °C ± 2 °C and 60 °C ± 3 °C after 6 months. With more pronounced absorbance peaks appearing which corresponds greatly with that observed for SPA-C, although these peaks could not compare definite exact intensities as for SPA-C. This could possibly mean the recrystallisation onset was cropping in along the way at these storage conditions.

Additionally, to confirm this solid behaviour, an PXRD was conducted and presented in Figure 6.51, Figure 6.52, and Figure 6.53, for storage at 60 °C ± 3 °C, 5 °C ± 2 °C and 25 °C ± 2 °C respectively, it was evident enough that no storage conditions negatively affected SPA-A during stability study period, all the data demonstrated characteristic peaks diffraction of amorphous forms other than crystalline. From this finding, it was deduced that the ternary amorphous was stable.
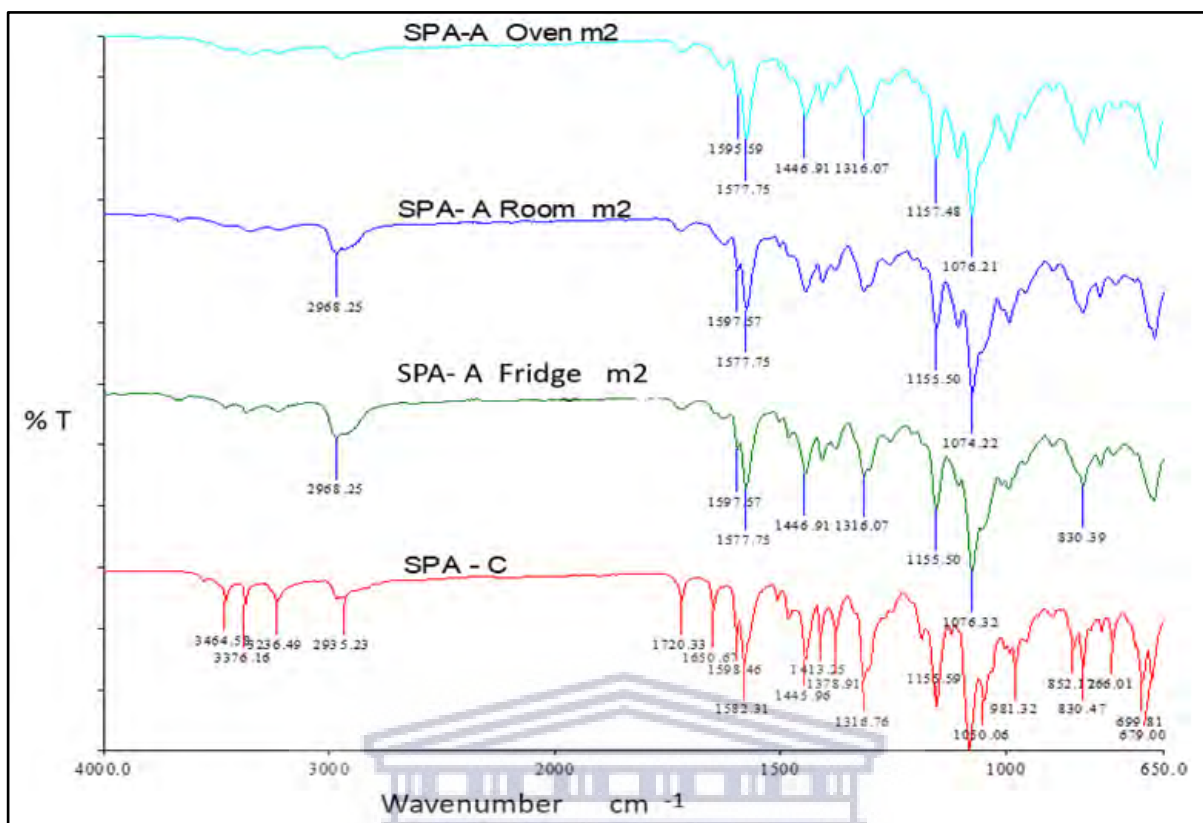
Figure 6.48: An overlay of the FTIR spectra obtained for SPA-A stored for a period of 2 months at 5 °C ± 2 ℃, ambient temperature (22 C ± 3 ℃) and 60 °C ± 3 ℃, in comparison with SPA-C.

Figure 6.49: An overlay of the FTIR spectra obtained for SPA-A stored for a period of 4 months at 5 °C ± 2 °C, ambient temperature (22 °C ± 3 °C) and 60 °C ± 3 °C, in comparison with SPA-C.
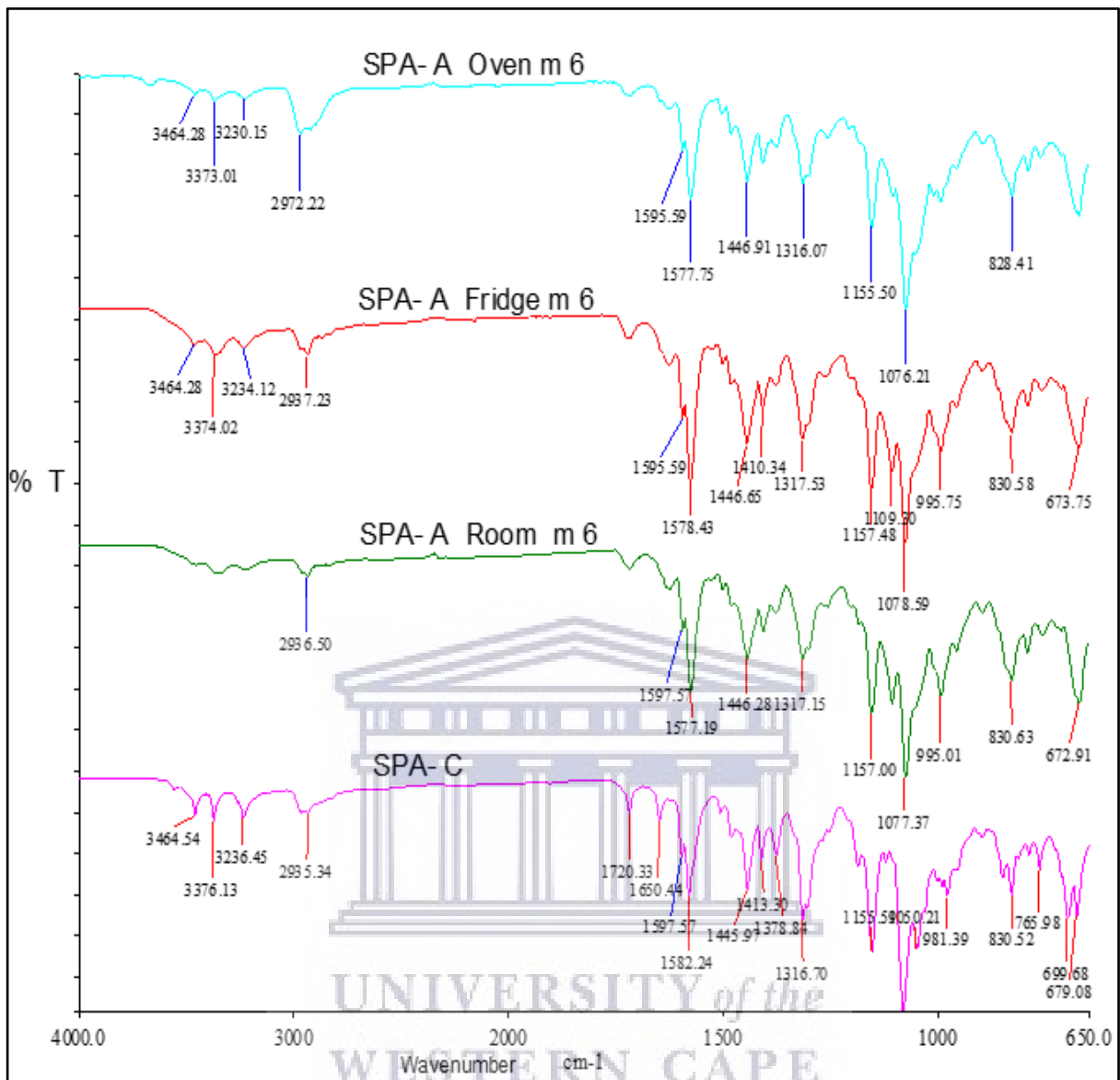
Figure 6.50: An overlay of the FTIR spectra obtained for SPA-A stored for a period of 6 months at 5 °C ± 2 ℃, ambient temperature (22 °C ± 3 ℃) and 60 °C ± 3 ℃, in comparison with SPA-C.
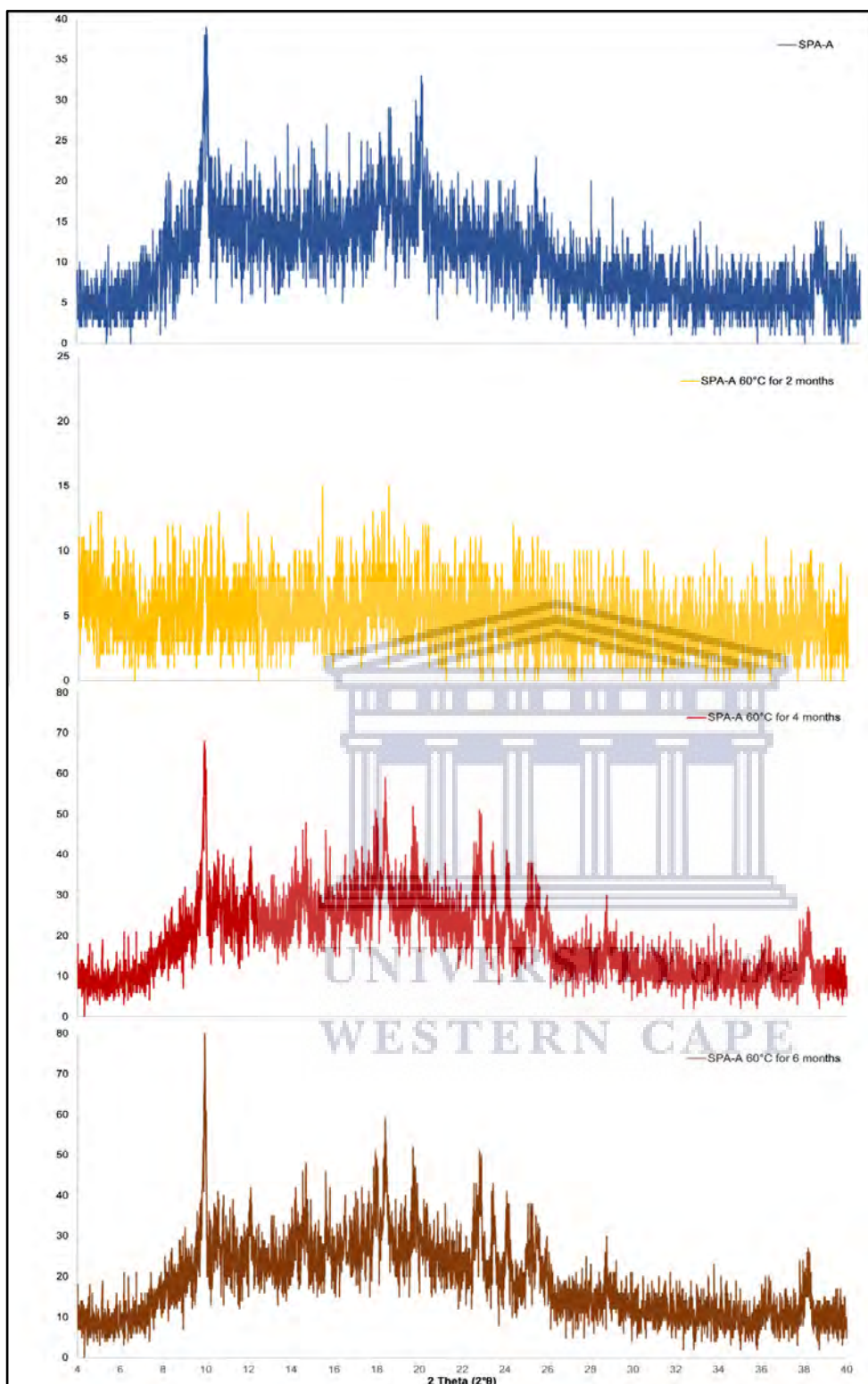
Figure 6.51: An overlay of the PXRD diffraction patterns obtained during the storage of SPA-A at 60 °C ± 3 ℃ for a period of 6 months.
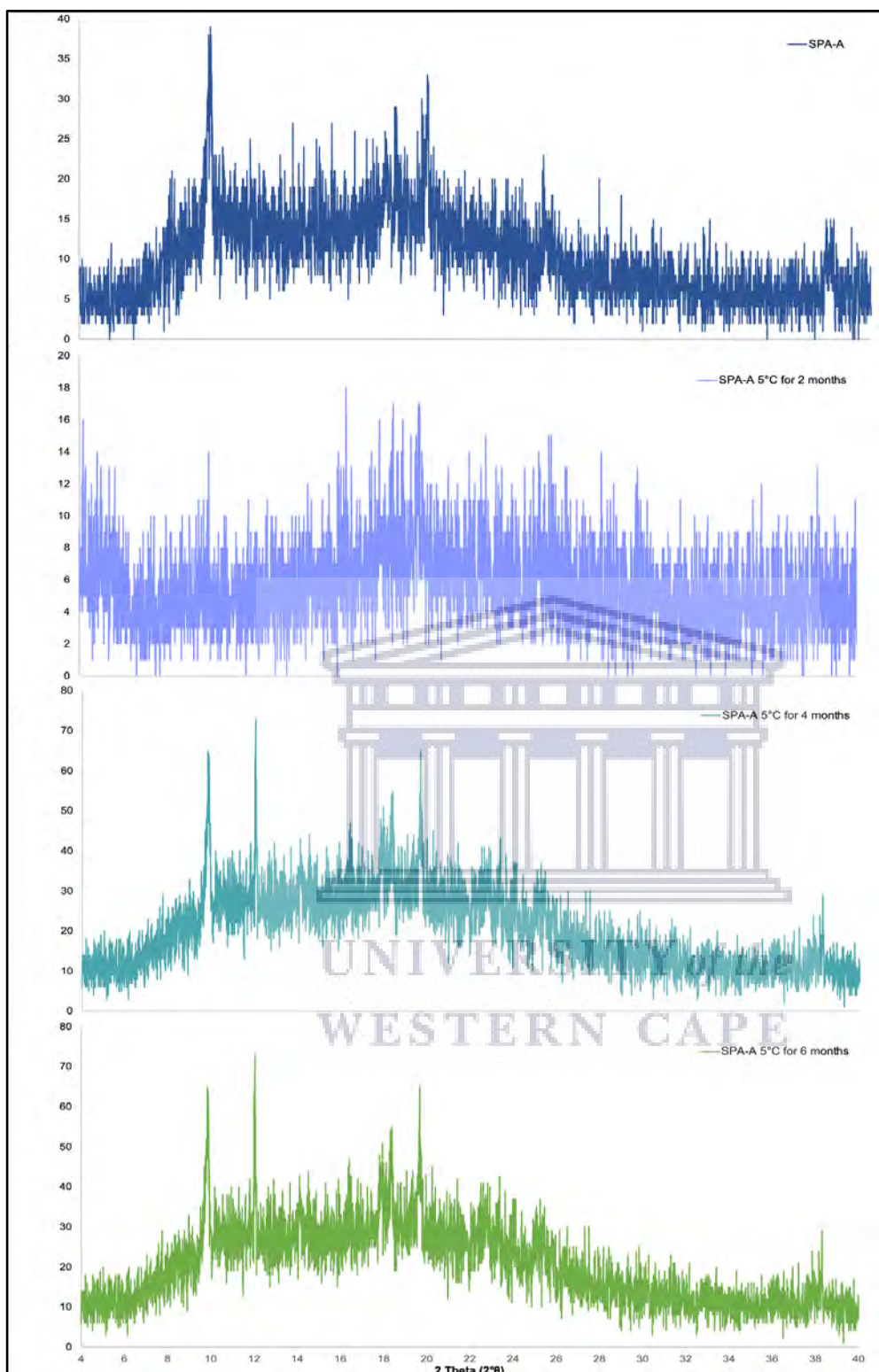
Figure 6.52: An overlay of the PXRD diffraction patterns obtained during the storage of SPA-A at 5 °C ± 2 ℃ for a period of 6 months.
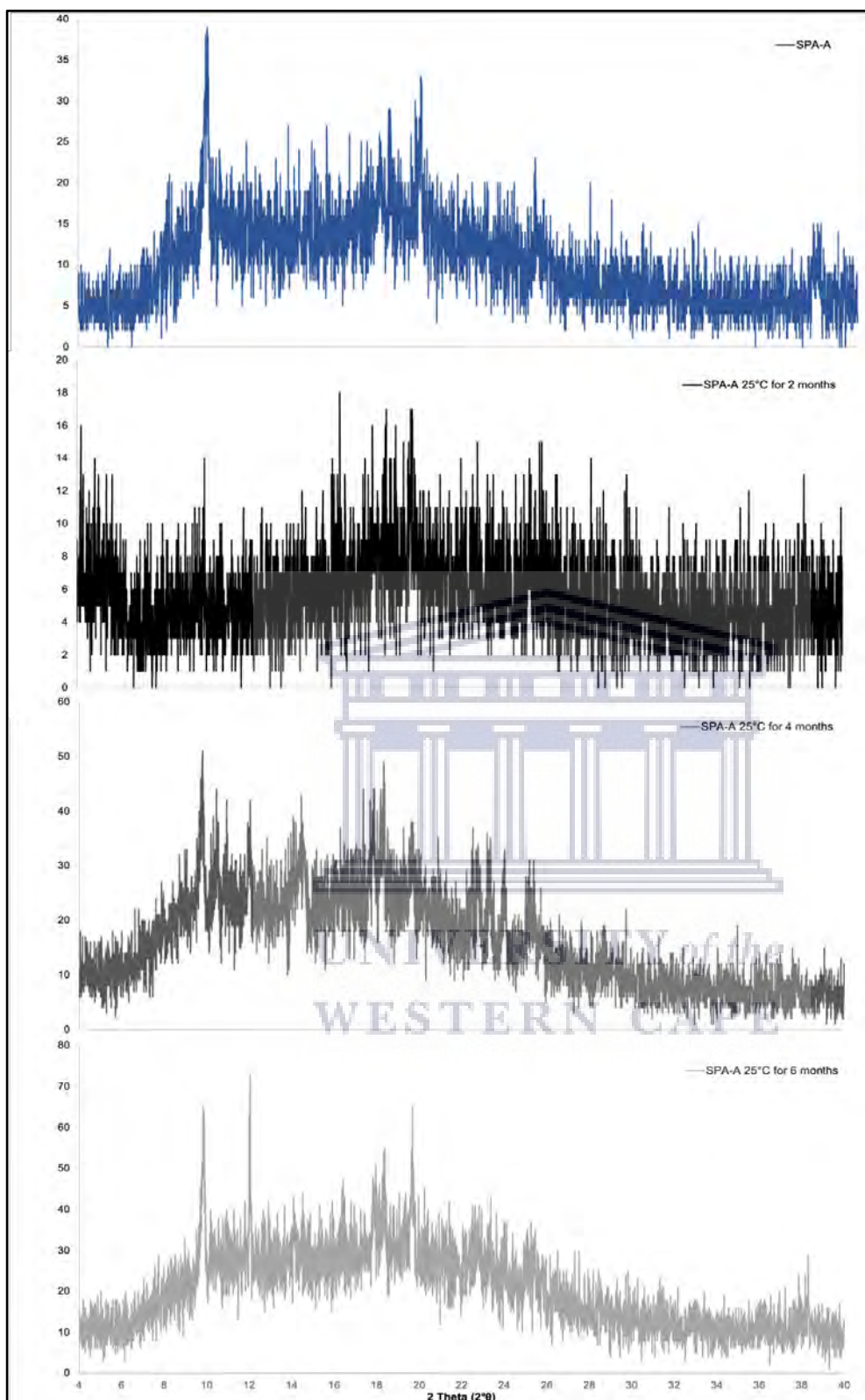
Figure 6.53: An overlay of the PXRD diffraction patterns obtained during the storage of SPA-A at 25 °C ± 2 ℃ for a period of 6 months.

6.5 Conclusion

The results were obtained and presented in the most summarised forms in tables and figures to facilitate insightful findings in the study. Thermal, FTIR and PXRD data signified differences in all three forms of APIs, pure crystalline, physical mixture, and ternary amorphous samples. An amorphous form with improved stability was formulated *via* quench cooling of the melt and solvent evaporation, with the quench cooling of the melt being the most promising method. This preparation method resulted in a novel ternary amorphous system consisting of three drugs combined in the amorphous state. Solubility and dissolution studies proved that the SPA-A solid-state form resulted in improved solubility of over 16-fold for SUL, 1.3-fold for PYR and 8-fold for AZI in distilled water and equally so with other experimented media as opposed to their counterparts. These solubility improvements are considered to be significant. Further to this the physical stability of this ternary amorphous solid-state form is exceptional with proven stability thereof when subjected to even high storage temperatures for a period of 6 months. The time frame of this study only allowed the investigation of stability for a 6 month period but future investigations should include more elaborate stability testing for longer time periods and at various pharmaceutically relevant storage conditions. Currently, in literature ternary amorphous systems only report on drug-drug-polymer systems, with a polymer added to such a solid-state form preparation as a means to stabilise the two co-amorphous drugs. From the stability study conducted on SPA-A it became apparent that the addition of a polymer to this solid-state form may not be necessary and it is hypothesised that the combination of the three drugs in their amorphous states may actually present a stabilising effect.

In this study a novel amorphous solid-state form consisting of three well-known compounds have been successfully prepared and this novel solid-state form may positively impact the bioavailability of these drugs.

6.6 Reference

Andrade, R.D.P., Roberto, L.M., & Pérez, C.E.C. (2011). Models of sorption isotherms for food: Uses and limitations | Modelos de isotermas de sorcion para alimentos: Usos y limitaciones. *Vitae*, *18*(3), pp.325–334.

Adeli, E. (2016). Preparation and evaluation of azithromycin binary solid dispersions using various polyethylene glycols for the improvement of the drug solubility and dissolution rate. *Brazilian Journal of Pharmaceutical Sciences*, 52(1), pp.1–13.

Arora, S., Sharma, P., Irchhaiya, R., Khatkar, A., Singh, N. and Gagoria, J. (2010). Development, characterization and solubility study of solid dispersions of cefuroxime axetil by the solvent evaporation method. *Journal of Advanced Pharmaceutical Technology & Research*, 1(3), p.326.

Aucamp, M., Milne, M., & Liebenberg, W. (2016). Amorphous Sulfadoxine: A Physical Stability and Crystallization Kinetics Study. *AAPS PharmSciTech*, *17*(5), 1100–1109. https://doi.org/10.1208/s12249-015-0436-4.

Aucamp, M., Odendaal, R., Liebenberg, W., & Hamman, J. (2015). Amorphous azithromycin with improved aqueous solubility and intestinal membrane permeability. *Drug Development and Industrial Pharmacy*, *41*(7), 1100–1108. https://doi.org/10.3109/03639045.2014.931967.

Badenhorst, L. (2017). Investigation of solubility and permeability of sulfadoxine and pyrimethamine mixtures. (May).

Baird, J. A., & Taylor, L. S. (2012). Evaluation of amorphous solid dispersion properties using thermal analysis techniques ☆. *Advanced Drug Delivery Reviews*, *64*(5), 396–421. https://doi.org/10.1016/j.addr.2011.07.009.

Beyer, A., Radi, L., Grohganz, H., Löbmann, K., Rades, T., & Leopold, C. S. (2016). Preparation and recrystallization behavior of spray-dried co-amorphous naproxen-indomethacin. European Journal of Pharmaceutics and Biopharmaceutics, 104, 72–81. https://doi.org/10.1016/j.ejpb.2016.04.019.

Braschi, I., Paul, G., Gatti, G., Cossi, M., & Marchese, L. (2013). Embedding monomers and dimers of sulfonamide antibiotics into high silica zeolite Y: An experimental and computational study of the tautomeric forms involved. *RSC Advances*, *3*(20), 7427–7437. https://doi.org/10.1039/c3ra22290j.

Cimellaro, G. P., & Marasco, S. (2018). Methods of analysis. *Geotechnical, Geological and Earthquake Engineering*, *45*, 331–351. https://doi.org/10.1007/978-3-319-72541-3_14.

Chavan, R. B., Thipparaboina, R., Kumar, D., & Shastri, N. R. (2016). Co amorphous systems: A product development perspective. In International Journal of Pharmaceutics (Vol. 515, Issues 1–2, pp. 403–415). https://doi.org/10.1016/j.ijpharm.2016.10.043.

El-Badry, M. (2011). Physicochemical characterization and dissolution properties of meloxicam-gelucire 50/13 binary systems. *Scientia Pharmaceutica*, *79*(2), 375–386. https://doi.org/10.3797/scipharm.1101-22.

Descamps, M. (2016). Amorphous Pharmaceutical Solids. *Advanced Drug Delivery Reviews*, *100*(3), 1–2. https://doi.org/10.1016/j.addr.2016.04.011.

Holtzkamp, I. (2016). Solubility and dissolution testing of selected sulfadoxine/pyrimethamine mixtures. (November).

Jaiswar, D. R., Jha, D., & Amin, P. D. (2016). Preparation and characterizations of stable amorphous solid solution of azithromycin by hot melt extrusion. *Journal of Pharmaceutical Investigation*, *46*(7), 655–668. https://doi.org/10.1007/s40005-016-0248-x

Karagianni, A., Kachrimanis, K., & Nikolakakis, I. (2018). Co-amorphous solid dispersions for solubility and absorption improvement of drugs: Composition, preparation, characterization and formulations for oral delivery. Pharmaceutics, 10(3). https://doi.org/10.3390/pharmaceutics10030098

Kasten, G., Nouri, K., Grohganz, H., Rades, T. and Löbmann, K., 2017a. Performance comparison between crystalline and co-amorphous salts of indomethacin-lysine. *International Journal of Pharmaceutics*, 533(1), pp.138-144.

Kaur, J., Aggarwal, G., Singh, G. & Rana, A. C. Improvement of drug solubility using solid dispersion. *Int. J. Pharm. Pharm. Sci.* **4**, 47–53 (2012).

Kawakami, K., Sato, K., Fukushima, M., Miyazaki, A., Yamamura, Y. and Sakuma, S., 2018. Phase separation of supersaturated solution created from amorphous solid dispersions: Relevance to oral absorption. *European Journal of Pharmaceutics and Biopharmaceutics*, 132, pp.146-156.

Lipatov, Y. S., Privalko, V. P., Kercha, Y. Y., Krafchik, S. S., & Kuz'mina, V. A. (1976). Thermodynamics and kinetics of phase transitions in linear polyurethanes from

hexa(methylene diisocyanate) and low molecular weight glycoles. *Colloid and Polymer Science Kolloid Zeitschrift & Zeitschrift Für Polymere*, *254*(7), 615–627. https://doi.org/10.1007/BF01753690.

Liu, X., Feng, X., Williams, R. O., & Zhang, F. (2018). Characterization of amorphous solid dispersions. *Journal of Pharmaceutical Investigation*, *48*(1), 19–41. https://doi.org/10.1007/s40005-017-0361-5.

Mahlin, D. and Bergström, C.A.S. (2013). Early drug development predictions of glass-forming ability and physical stability of drugs. *European Journal of Pharmaceutical Sciences*, 49(2), pp.323–332.

Mallah, M. A., Sherazi, S. T. H., Mahesar, S. A., & Rauf, A. (2011). *Assessment of Azithromycin in Pharmaceutical Formulation by Fourier-transform Infrared (FT- IR) Transmission Spectroscopy Assessment of Azithromycin in Pharmaceutical Formulation by Fourier-transform Infrared (FT-IR) Transmission Spectroscopy. 12*(January), 61–67.

Mathlouthi, M., & Rogé, B. (2003). Water vapour sorption isotherms and the caking of food powders. *Food Chemistry*, *82*(1), 61–71. https://doi.org/10.1016/S0308-8146(02)00534-4.

Melzig, S., Finke, J., Schilde, C. and Kwade, A., 2018. Formation of long-term stable amorphous ibuprofen nanoparticles via antisolvent melt precipitation (AMP). *European Journal of Pharmaceutics and Biopharmaceutics*, 131, pp.224-231.

Milne, M., Liebenberg, W., & Aucamp, M. (2015). The Stabilization of Amorphous Zopiclone in an Amorphous Solid Dispersion. *AAPS PharmSciTech*, *16*(5), 1190–1202. https://doi.org/10.1208/s12249-015-0302-4.

Montejo-Bernardo, J., García-Granda, S., Bayod-Jasanada, M., Llorente, I., & Llavona, L. (2005). An easy and general method for quantifying Azithromycin dihydrate in a matrix of amorphous Azithromycin. Arkivoc, 2005(9), 321–331. https://doi.org/10.3998/ark.5550190.0006.927

Newman, A., Knipp, G., & Zografi, G. (2012). Assessing the performance of amorphous solid dispersions. Journal of Pharmaceutical Sciences, 101(4), 1355–1377. https://doi.org/10.1002/jps.23031

Onyeji, C. O., Omoruyi, S. I., Oladimeji, F. A., & Soyinka, J. O. (2009). Physicochemical characterization and dissolution properties of binary systems of pyrimethamine and 2-hydroxypropyl-β-cyclodextrin. *African Journal of Biotechnology*, *8*(8), 1651–1659. https://doi.org/10.4314/ajb.v8i8.60360.

Ojarinta, R., Heikkinen, A. T., Sievänen, E., & Laitinen, R. (2017). Dissolution behavior of co-amorphous amino acid-indomethacin mixtures: The ability of amino acids to stabilize the supersaturated state of indomethacin. *European Journal of Pharmaceutics and Biopharmaceutics*, *112*, 85–95. https://doi.org/10.1016/j.ejpb.2016.11.023.

Pacult, J., Rams-Baron, M., Chmiel, K., Jurkiewicz, K., Antosik, A., Szafraniec, J., Kurek, M., Jachowicz, R. and Paluch, M., 2019. How can we improve the physical stability of co-amorphous system containing flutamide and bicalutamide? The case of ternary amorphous solid dispersions. *European Journal of Pharmaceutical Sciences*, 136, p.104947.

Psimadas, D., Georgoulias, P., Valotassiou, V., & Loudos, G. (2012). Molecular Nanomedicine Towards Cancer : *Journal of Pharmaceutical Sciences*, *101*(7), 2271–2280. https://doi.org/10.1002/jps

Sai Krishna Anand, V., Sakhare, S., Navya Sree, K., Nair, A., Raghava Varma, K., Gourishetti, K. and Dengale, S., 2018. The relevance of co-amorphous formulations to develop supersaturated dosage forms: In-vitro, and ex-vivo investigation of Ritonavir-Lopinavir co-amorphous materials. *European Journal of Pharmaceutical Sciences*, 123, pp.124-134.

Santana, N. S., Gomes, A. F., Santana, H. S., Saraiva, G. D., Ribeiro, P. R. S., Santos, A. O., … De Sousa, F. F. (2021). Phase Transformations of Azithromycin Crystals Investigated by Thermal and Spectroscopic Analyses Combined with Ab Initio Calculations. *Crystal Growth and Design*, *21*(6), 3602–3613. https://doi.org/10.1021/acs.cgd.1c00375.

Schittny, A., Huwyler, J. and Puchkov, M., 2019. Mechanisms of increased bioavailability through amorphous solid dispersions: a review. *Drug Delivery*, 27(1), pp.110-127.

Sheokand, S., Modi, S.R. and Bansal, A.K. (2014). Dynamic Vapor Sorption as a Tool for Characterization and Quantification of Amorphous Content in Predominantly Crystalline Materials. Journal of Pharmaceutical Sciences, 103 (11):3364-3376. http://doi.org/10.1002/jps.24160.

Singh, G., Kaur, L., Gupta, G. D., & Sharma, S. (2017). Enhancement of the Solubility of Poorly Water Soluble Drugs through Solid Dispersion: A Comprehensive Review. *Indian Journal of*

Pharmaceutical Sciences, *79*(5), 1–41. https://doi.org/10.4172/pharmaceutical-sciences.1000279.

Thielmann, F., & Burnett, D. J. (2006). *Isotherm Types and Adsorption Mechanisms of Solvents on Pharmaceutical Excipients; Dynamic Vapour Sorption Application Note 26*.

Ueda, H., Muranushi, N., Sakuma, S., Ida, Y., Endoh, T., Kadota, K., & Tozuka, Y. (2016). RESEARCH PAPER A Strategy for Co-former Selection to Design Stable Co -amorphous Formations Based on Physicochemical Properties of Non-steroidal Inflammatory Drugs. 1018–1029. https://doi.org/10.1007/s11095-015-1848-2.

Van Den Mooter, G. . (2012). The use of amorphous solid dispersions : A formulation strategy to overcome poor solubility and dissolution rate. *Drug Discovery Today: Technologies*, *9*(2), e79–e85. https://doi.org/10.1016/j.ddtec.2011.10.002.

Wang, Z., Sun, M., Liu, T., Gao, Z., Ye, Q., Tan, X., Hou, Y., Sun, J., Wang, D. and He, Z., 2019. Co-amorphous solid dispersion systems of lacidipine-spironolactone with improved dissolution rate and enhanced physical stability. *Asian Journal of Pharmaceutical Sciences*, 14(1), pp.95-103.

Weuts, I., Van Dycke, F., Voorspoels, J., De Cort, S., Stokbroekx, S., Leemans, R., … Reading, M. (2011). Physicochemical properties of the amorphous drug, cast films, and spray dried powders to predict formu lation probability of success for solid dispersions: Etravirine. *Journal of Pharmaceutical Sciences*, *100*(1), 260–274. https://doi.org/10.1002/jps.2224.lkm.
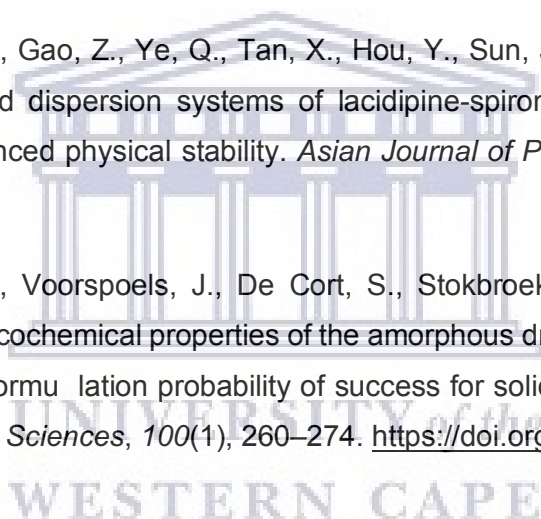
CHAPTER 7

Development and validation of a high-performance liquid chromatography method for the simultaneous detection and analysis of sulfadoxine, pyrimethamine and azithromycin

7.1 Introduction

High-performance liquid chromatography (HPLC) is an essential technique employed in the pharmaceutical industry to detect and quantify chemical compounds intended for pharmaceutical applications. Chemical compounds are often analysed based on the nature (ionisable or non-ionisable) that impact on retention and elution of an analyte *via* a stationary phase (column). Depending on the physico-chemical properties of a compound a multitude of liquid chromatography methods may be used to accurately detect and quantify that specific compound. Reversed-phase chromatography (RP-HPLC) is a very common HPLC method configuration that allows the separation and detection of many and various types of compounds.

As discussed in Chapter 1, the aim of this study was to prepare a combined amorphous solid-state form consisting of SUL, PYR and AZI to increase the aqueous solubility of all three drugs. The preceding chapter detailed the solid-state physico-chemical characteristics not only of the individual three active compounds but also that of the prepared ternary amorphous system (SPA-A). However, to accurately quantify the equilibrium solubility and dissolution rate of SUL, PYR and AZI alone or in the drug combinations SPA-C and SPA-A, it was necessary to have a reliable and accurate analytical method for the simultaneous detection of all three drugs. This resulted in the development of a suitable HPLC method concurrently with the conducted research presented in Chapter 6.

A literature search revealed developed and validated HPLC methods for SUL and PYR (Acheampong et al., 2018; Pai et al., 2016), likewise for AZI as single API (Ghari *et al.*, 2013; Singh *et al.*, 2019; Waghule et al., 2013; Zubata *et al.*, 2002). To date, there are no studies reporting an HPLC method that may be used to simultaneously detect and quantify SUL, PYR, and AZI, in bulk material, as part of solid-state form modifications and during equilibrium solubility and dissolution rate testing in various aqueous buffered media. Thus, it necessitated developing a simple yet robust HPLC method to accomplish the study objectives. To elaborate further, attempts to replicate the above methods failed as different chromatographic conditions could not be harmonised to detect and quantify all the APIs. According to LoBrutto and Patel (2007), it is of paramount importance to validate an analytical method to prove its reliability, reproducibility, and its ability to ensure the method does what it is intended and designed for.

Overall, this chapter disseminates the procedures and steps followed in developing and validating this method. The developed HPLC method was validated in terms of linearity, precision, accuracy, limit of detection (LOD), limit of quantification (LOQ), selectivity, robustness, and solution stability.

7.2 Method development and optimisation

An HPLC instrument is a technically simple to operate instrument and typically allows several chromatographic conditions that permits the purification, identification and quantification of a vast number of compounds (APIs and excipients) in the pharmaceutical industry (Driver and Raynie, 2007). It is commonly employed in pharmaceutical development to investigate drug assays, drug dissolution rates, solubility, as well as drug impurity and stability (Zacharis, 2009). A typical RP-HPLC setup is based on two important aspects, namely; (a) the mobile phase, normally consisting of a mixture of organic and aqueous solvents, and (b) the stationary phase consisting of a packed column with material ranging in levels of polarity bounded with a silica backbone. These are key factors upon which separation of the analytes are determined (Belanger *et al.* 1997). Other factors that need consideration during HPLC method development arise from the analytes. The physio-chemical properties, such as the logP, pKa and solubility influences the selection of a suitable sample preparation solvent, mobile phase, and stationary phase for effective compound elution. Furthermore, the nature of the chemical compound being analysed affects the retention in the column due to intermolecular interactions occurring between the molecule and the packed stationary phase (Böttcher, *et al.*, 2021; Belanger *et al.* 1997; LoBrutto, 2007).

As already mentioned, the analysis of SUL, PYR and AZI as individual drugs is not exclusively new, few literature sources more so for a combination of SUL and PYR have described the development and validation of methods suitable for the detection and quantification of all three compounds. Pai, Dias and Sawant (2016), developed a method to simultaneously separate SUL and PYR and reproducible chromatographic responses were obtained using a Zorbax Eclipse Plus C_{18}, 3.5 µm (4.6×100 mm) column with a mobile phase constituting acetonitrile and 20 mM sodium acetate buffer (80:20% v/v) at pH 6. A flow rate of 1.0 ml/min and UV-detection set at 224 nm was applied. SUL and PYR eluted at 0.9 and 1.2 minutes, respectively. The method was validated following standard procedures and concluded analytical reproducibility (Pai, Dias and Sawan, 2016). Mwalwisi *et al.*, (2016) developed a gradient elution method to detect sulfalene, sulfadoxine, and pyrimethamine using a standard C_{18} column with the mobile phase composed of 60 %v/v of a 0.05 M KH_2PO_4 buffer solution (pH = 2.6) and 40 %v/v methanol, and a detection wavelength of 215 nm. Similarly, a RP-

HPLC method for the simultaneous identification and quantification of SUL and PYR in a tablet dosage form was developed using a Waters µBondapak C_{18} column (3.9 × 300 mm, 3.6 µm particle size) with a combination of acetonitrile and phosphate buffer (75:25 %v/v), pH of 2.5, as the mobile phase. The mobile phase flow rate was set to 1.0 mL/min and a detection wavelength of 230 nm. Sulfadoxine and pyrimethamine eluted at 2.86 and 3.60 minutes, respectively. Validation deemed the method as linear, precise, specific, robust, sensitive, and cost effective (Acheampong *et al.*, 2018).

A literature search conducted on available methods for the detection and quantification of AZI revealed methods from various researchers. Okaru, *et al* (2017), developed an HPLC method suitable to analyse bulk sample, tablets and suspensions containing AZI using a mobile phase consisting of acetonitrile, 0.1 M KH_2PO_4 pH 6.5, 0.1 M tetrabutylammonium hydroxide pH 6.5 and water (25:15:1:59 v/v/v/v) as mobile phase at flow rate of 1.0 mL/min. The stationary phase was a reversed-phase XTerra® (250 mm × 4.6 mm i.d., 5 µm particle size) at a temperature of 43 ℃ with a UV wavelength of 215 nm. Additionally, Singh *et al*, (2019) also developed an HPLC method for quantitative analysis of AZI in an oral suspension, using a Hypersil BDS-C_{18} (250 mm × 4.6 mm i.d.) column, with an isocratic mobile phase setup consisting of methanol, acetonitrile and phosphate buffer (60:30:10; v/v/v) at pH 8 with an employed analytical run time of 15 minutes, a flow rate of 1.0 ml/min, and UV detector set at 212 nm. The method was found to meet international analytical method validation parameters. Other studies conducted reported similar chromatographic conditions. These include an HPLC method to detect AZI in bulk material and pharmaceutical dosage forms using UV-detection at a wavelength of 210 nm and a C_{18} column, 5 µm, 250 mm × 4.6 mm, with methanol/buffer (90:10 v/v) as mobile phase pumped at a flow rate of 1.5 ml/min (Ghari *et al.*, 2013). An HPLC method utilising a mixture of 0.0335 M phosphate buffer (pH 7.5) and methanol in the proportion 20:80, wavelength of 210 nm with a flow rate of 1.2ml/min, was developed too (Waghule *et al.*, 2013).
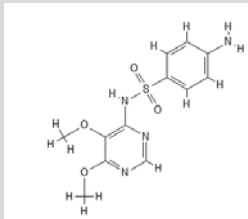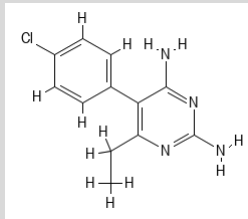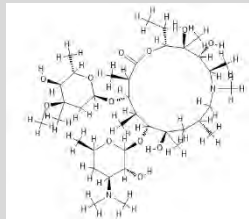
As already mentioned, aspects which influence the successful development of accurate, precise and robust HPLC methods are the physico-chemical characteristics of the compounds, attributes of the stationary phase, the mobile phase composition as well as the detection wavelength of each compound. These were the characteristics and attributes that were considered during the HPLC method development process followed in this study and the subsequent paragraphs will discuss how all these attributes were utilised to develop a suitable analytical method.

7.2.1 Physico-chemical characteristics of SUL, PYR and AZI informing HPLC method development

The described methods in paragraph 7.2 showed few parameters in common, and during replication of these methods to ascertain whether one of these methods with slight modifications may be used for the simultaneous detection of SUL, PYR and AZI proved unsuccessful. Hence, a suitable HPLC method to allow the successful analysis of the compounds in this study became an imperative requirement. The physico-chemical properties of these APIs are described in Chapter 4, and a summary is shown here in **Table 7.1.** Putting in perspective the Lipinski's rule of 5, compounds with a logP above 5, possessing over 5 hydrogen bond donor species, more than 10 hydrogen bond recipient species and molecular weight of over 500 daltons of which AZI exhibits 75 % of these properties, would predict that AZI possess more hydrophobic characteristics (Halberstadt, 2017) as opposed to SUL and PYR and differences in their pKa-values signified that an alteration of the pH of a potential mobile phase will affect detection and elution of all three drugs. In fact, for an ionisable compound, complete ionisation of the compound is achieved at $\pm$ 2 units from the pKa-value. An analyte that is capable of being ionised is found to produce a shift in its retention time during HPLC analysis (Dolan, 2017; LoBrutto, 2007). Considering this, AZI was the compound on which significant focus was placed during the method development stage due to its instability at low pH (Skinner *et al.*, 1993; Saita *et al.*, 2018).
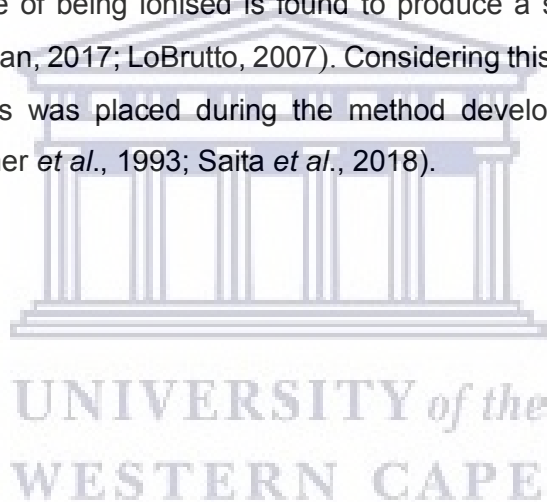
Table 7.1: Summary of physico-chemical properties of SUL, PYR and AZI that may affect HPLC method development.

Physico-chemical property	SUL	PYR	AZI
LogP	0.70	2.69	4.02
pKa	6.30	7.34	8.5
Solubility in water	Poorly soluble	Very poorly	Very poorly
Solubility in organic solvents	Slightly soluble in alcohol, and in methanol. (PubChem, 2021a)	Soluble in dimethyl sulfoxide (DMSO) and dimethyl formamide (DMF). (PubChem, 2021b)	Ethanol, (DMSO), (DMF). (PubChem, 2021c)

7.2.2 Column choice

The column selection is one other critical aspect playing a definite role during HPLC method development. As alluded to at the introduction of this chapter, columns form an integral part of any HPLC system and can impact immensely on resulting chromatography. The key factors to consider when choosing the column are efficiency, selectivity, robustness, loadability, and compatibility with the mobile phase (Ahuja and Rasmussen, 2007). According to Jerkovich and Vivilecchi, (2007), the separation efficiency determines the eluted peak(s) characteristics with peak splitting, tailing and fronting being reported effects due to possible inappropriate column choice (**Figure 7.1**). It is also important to understand the effect of analyte concentration on the resultant peak shapes, with higher analyte concentration leading to potential column capacity overloading observed as a "shark-fin" peak shape as depicted in (**Figure 7.1 C**).

The term symmetry is applied when classifying peak types. When the distance from the onset of compound elution to the peak apex and from the apex to the baseline is equal (symmetry factor (S) = 1), such a peak is termed a symmetric peak (Gaussian peak) (**Figure 7.1 A**). Tailing is diagnosed when the backside of the peak spreads further beyond the normal end point, this is then considered to be an asymmetric peak with a symmetry factor (S) value >1, whereas fronting is an asymmetric peak with a symmetry factor <1 occurring when the front part of the peak is flatter than the back (Meyer, 2004). The selectivity of the column refers to the ability to differentiate analytes being analysed under the same chromatographic condition and method and it is dictated by interactions between analytes and the stationary phase surface. **Figure 7.1 B** illustrates variation in the column efficiency and selectivity. The efficiency of the column is defined as the degree of band-broadening obtained following analyte injection into the column. This depends on the chromatographic kinetic factors such as molecular diffusion, flow rate, mass-flow dynamics, and the column packing. Furthermore, higher efficiency is obtained with smaller particle sizes of packing material resulting in a more uniform packing. The most common column type in the pharmaceutical industry is the silica based packed columns because of its physical characteristics. These columns show high mechanical strength, high column efficiency, wide range of available pore sizes and particle size distribution (Kazakevich and LoBrutto, 2007). The separation of multiple analytes requires narrow peak widths resulting in sharp peaks (**Figure 7.1 A**) to enable effective separation within a particular run time. The distance from the injection point to peak apex is termed as retention time (t_R) and it is an identification parameter for analytes in the chromatographic system (Belanger *et al.,* 1997).

During this HPLC method development study several reversed phase columns were used during preliminary trial runs, as outlined in **Table 7.3.** For the current study, an ACE® 3µm particle size, C_{18} (250 x 4.6 mm) (Advance Chromatography Technologies Ltd., Aberdeen, Scotland) column was employed to develop this RP-HPLC method. This column was chosen as the best option based on observations made during the mentioned trial runs conducted.
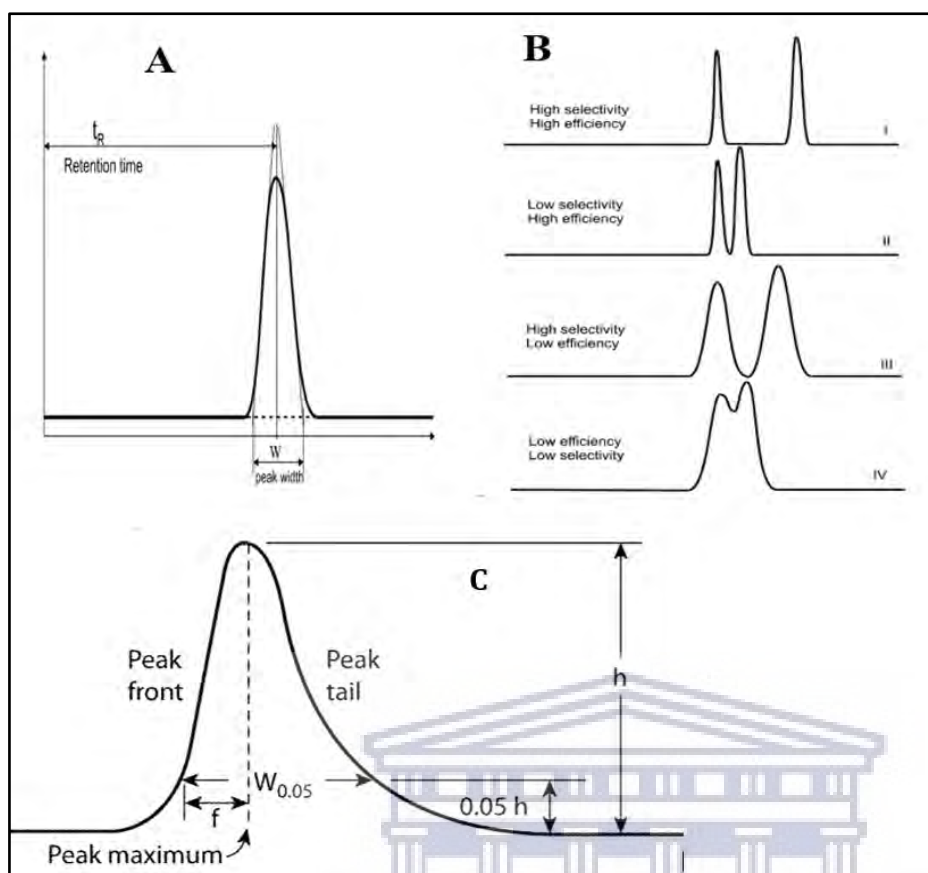
Figure 7.1: Diagrammatic representation of peak types; (A) symmetric peak, (ideal Gaussian), (B) peaks obtained from varying column's efficiency and selectivity and (C) the parts of common peak shapes (Adapted from Kazakevich and LoBrutto, 2007a; USP, 2012).

7.2.3 Mobile phase choice

The physico-chemical characteristics of the analytes is the most influential property to be considered in deciding on the mobile phase composition during HPLC method development. As described above, SUL, PYR and AZI exhibit pKa-values across a wide range. The limiting factor was based on the pKa-value of AZI, since it requires some form of buffering to maintain the mobile phase pH as closely to its pKa as possible. Preliminary mobile phase investigations proved that a pH of 8.2 $\pm$ 1 was found suitable. During these preliminary investigations where different buffer concentrations were investigated it was also noted that AZI elution shows selectivity towards the buffering agent used with a strong concentration above 0.04M phosphate buffer not yielding acceptable peaks, with either peak broadening observed or no peak that could be attributed to AZI was detected. Furthermore, to determine the solvent proportionality, (**Table 7.3**), various attempts were made by altering one variable at a time, acetonitrile : di-potassium hydrogen phosphate (60:40) was confirmed as the most reliable

mobile phase across a 24 hour injection period. Investigations which involved changing the mobile phase pH led to observed shifts in the retention time for AZI to such an extent that the peak attributed to AZI was superimposing on the peak attributed to PYR elution time. On the other hand, both SUL and PYR did not show any peak retention time shifts due to adjustments in the pH of the mobile phase. This confirmed the observation made from the physico-chemical properties of AZI that a change in pH will affect the resulting chromatography of this compound.

7.2.4 Determination of optimal wavelength

A detector is an essential component of an HPLC instrument, and its role is to detect the chemical compound or substance as it elutes from the column. This occurs because of the changes emanating from the contents in the mobile phase that differs from the usual baseline and that information is detected in the form of an electric signal. The most common liquid chromatographic detectors are UV detectors, due to their flexibility in sensitivity, operating temperatures and wide linearity range (Meyer, 2004). Notably, the sensitivity is primarily based on the compound's molecular structure, with higher absorption attained when compounds exhibit aromatic rings and ketone functional groups (Meyer, 2004). The current study investigated wavelengths from 200 - 250 nm (**Table 7.2**). Researched literature found SUL and PYR detectable within a wide UV detection range (Acheampong *et al.,* 2018; Pai *et al*., 2017), however, AZI is detected efficiently only within the range of 205 - 218 nm (Waghule *et al*., 2013; Ghari *et al*., 2013; Singh *et al*., 2019), although the data obtained in Table 7.2 shows best peak intensities at 200 nm. However, due to the impact of acetonitrile signal interference due to the absorbance of acetonitrile in the wavelength range of 190 - 200nm (Rodriguez, 2004), 210 nm was deemed an optimal wavelength which would allow accurate detection of all three compounds.

Table 7.2: Peak areas obtained with varied wavelengths for SUL, PYR and AZI

	SUL (100 µg/ml)	PYR (100 µg/ml)	AZI (2000 µg/ml)
Wavelength (nm)	Peak area (mAU)	Peak area (mAU)	Peak area (mAU)
200	9328.05	8194.88	1720.77
210	4696.38	6017.49	924.31
220	2554.62	4730.27	515.81
230	1277.76	3228.89	136.04
250	2903.38	1634.61	22.45
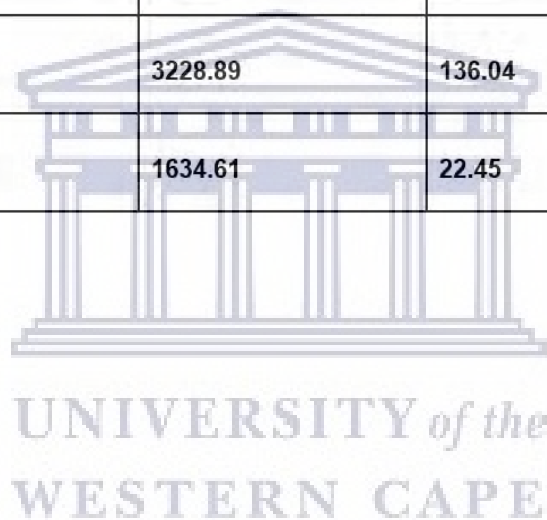
Table 7.3: Mobile phase constitution, different column types used to determine suitable compound detection and quantification with remarks provided on the drug separation and elution with each mobile phase and column combination with wavelength set at 210 nm.

Columns		Luna	Kinetex	ACE	Zorbax Eclipse	
Mobile Phase						Remarks
ACN:MeOH (v/v)	% v/v 80:20	SUL, PYR	SUL, PYR	SUL, PYR	SUL, PYR	No AZI detected
	50:50	SUL, PYR	SUL, PYR	SUL, PYR, ACE	No Peak	Low peak response obtained for AZI
	70:30	SUL, PYR	SUL, PYR	SUL, PYR	No peak	No A detected
	20:80	No peak	No peak	No peak	No peak	Not suitable
ACN: Acetate buffer (v/v)	90:10	No peak	No Peak	No peak	No peak	Not suitable
	80:20	No Peak	No Peak	No peak	No peak	Not suitable
	60:40	SUL, PYR	SUL, PYR	SUL, PYR	SUL, PYR	No A detected
	50:50	SUL, PYR	SUL, PYR	SUL, PYR	SUL, PYR	No AZI
	40:60	SUL, PYR, AZI	SUL, PYR, AZI	SUL, PYR, AZI	X	Despite detection the peak obtained with AZI was very broad
MeOH: phosphate buffer	90:10	SUL, PYR	SUL, PYR	SUL, PYR	X	No AZI
	60:40	SUL, PYR	SUL, PYR	SUL, PYR	X	No AZI
	50:50	No peak	SUL	SUL, PYR	X	No AZI
	40:60	No peak	No peak	No peak	X	Not suitable

Columns		Luna	Kinetex	ACE	Zorbax Eclipse	
Mobile Phase						**Remarks**
	20:30:50	SUL, PYR	SUL, PYR	SUL, PYR	SUL	Broad peaks
	30:20:50	SUL, PYR, AZI	SUL, PYR, AZI	SUL, PYR, AZI	SUL, PYR, AZI	Small AZI
ACN: MeOH: phosphate buffer	20:40:40	SUL, PYR	SUL, PYR	SUL, PYR	SUL, PYR	No AZI
	60:10:30	SUL, PYR	SUL, PYR	SUL, PYR	SUL, PYR	No AZI
	20:20:60	No peak	No peak	No peak	No peak	unsuitable
ACN: MeOH: Water	10:40:50	No peak	No Peak	No peak	No peak	unsuitable
	30:50:20	SUL, PYR	SUL, PYR	SUL, PYR	X	No AZI
	50:20:30	SUL, PYR	SUL, PYR	SUL, PYR	X	No AZI
	20:40:40	SUL, PYR	SUL, PYR	SUL, PYR	X	No AZI
ACN: Phosphate buffer	30:70	No peak	No Peak	No peak	X	unsuitable
	40:60	SUL, PYR	SUL, PYR	SUL, PYR, AZI	X	Broad peaks
	50:50	SUL, PYR, AZI	SUL, PYR, AZI	SUL, PYR, AZI	X	Small AZI
	60:40	SUL, PYR, AZI	SUL, PYR, AZI	SUL, PYR, AZI	X	Best peaks
	70:30	SUL, PYR	SUL, PYR	SUL, PYR, AZI	X	Broad AZI

Where: X- not tried, MeOH- methanol, ACN- Acetonitrile, % mixed- percentage ration mixture, v/v- volume per volume, ▭ Maybe, ▭ Yes, uncoloured cells indicating parameters considered to not be an option.

7.2.5 Optimised RP-HPLC method

The optimisation process resulted in the following chromatographic setup with resulting chromatography depicted in **Figure 7.2;** a mobile phase comprising of acetonitrile (ACN): 0.038M K_2HPO_4 (60:40 v/v) pH 8.2 at a flow rate of 1.0 ml/min, the column was an ACE$^{®}$ 3µm, C_{18} (250 x 4.6 mm) with temperature maintained at 30 ℃, UV wavelength set at 210 nm and the retention times for SUL, PYR and AZI were at 2.46, 4.02 and 9.43 minutes respectively.
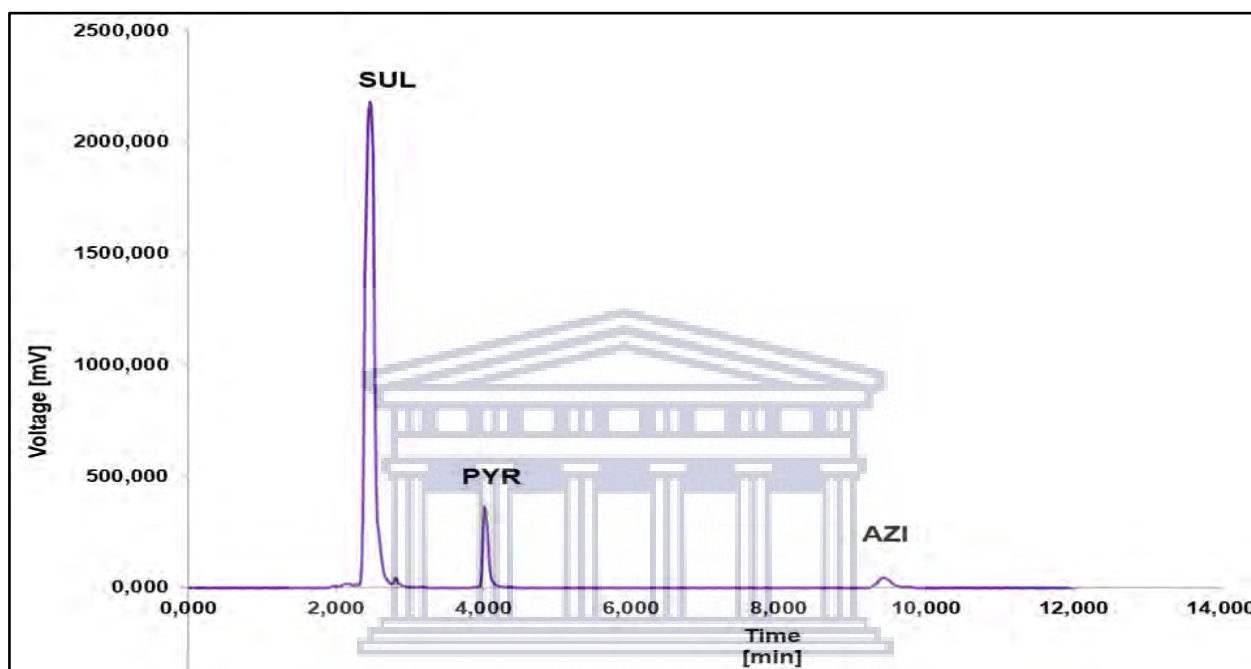
Figure 7.2: Showing the peaks for SUL, PYR and AZI (1:0.05:1%w/v) in SPA-C obtained under final optimised chromatographic conditions.

7.3 Validation of the developed HPLC method

Method validation forms part of analytical method development and plays a key role in ensuring the accuracy and precision of the developed method to allow the generation of trustworthy analytical results. Method validation for this study was performed according to the International Conference for Harmonisation (ICH) analytical method validation guidelines and included the following parameters: linearity and range, accuracy, precision (inter- and intra-day), limit of detection (LOD), limit of quantification (LOQ), system repeatability, robustness, specificity and finally stability (ICH, 2005).

7.3.1 Linearity of response

When the analytical response of an analysis is directly proportional to the concentration of an analyte in the analysed sample, it is termed as linearity of response (ICH, 2005). The procedure requires at least five different concentrations being analysed and a correlation plot of the analytical response versus the sample concentration, also termed a calibration curve, should provide a correlation coefficient (r^2) greater than or equal to 0.99 (EMA, 1995; UNODC, 2021).

The linearity of this method was investigated within a concentration range of 4.00 - 160.00 µg/ml for SUL and PYR (Table 7.3 and Figure 7.3) and 25.00 - 1000.00 µg/ml for AZI (Table 7.4 and Figure 7.4). The concentration differences were based on detection sensitivity with AZI exhibiting low detection sensitivity as opposed to the other two APIs.

Table 7.4: HPLC responses obtained for SUL, PYR, during the linearity testing

Concentration (µg/ml)	SUL peak area (mAU) (% RSD)	PYR peak area (mAU) (%RSD)
4	211.65	271.5
10	591.88	721.14
20	1232.39	1485.02
40	2601.5	2954.77
90	4608.56	5969.56
160	8273.35	10744.56
Regression coefficient (r^2)	0,996	0,999
Slope	50,65	66,41
y-intercept	184,71	104,85

Table 7.5: HPLC responses obtained for AZI, during the linearity testing

Concentration (µg/ml)	AZI peak area (mAU)(%RSD)
25	17.52
50	84.23
100	128.8
200	189.3
500	582.4
1000	948.83
Regression coefficient (r^2)	0,990
Slope	0,96
y-intercept	26,40
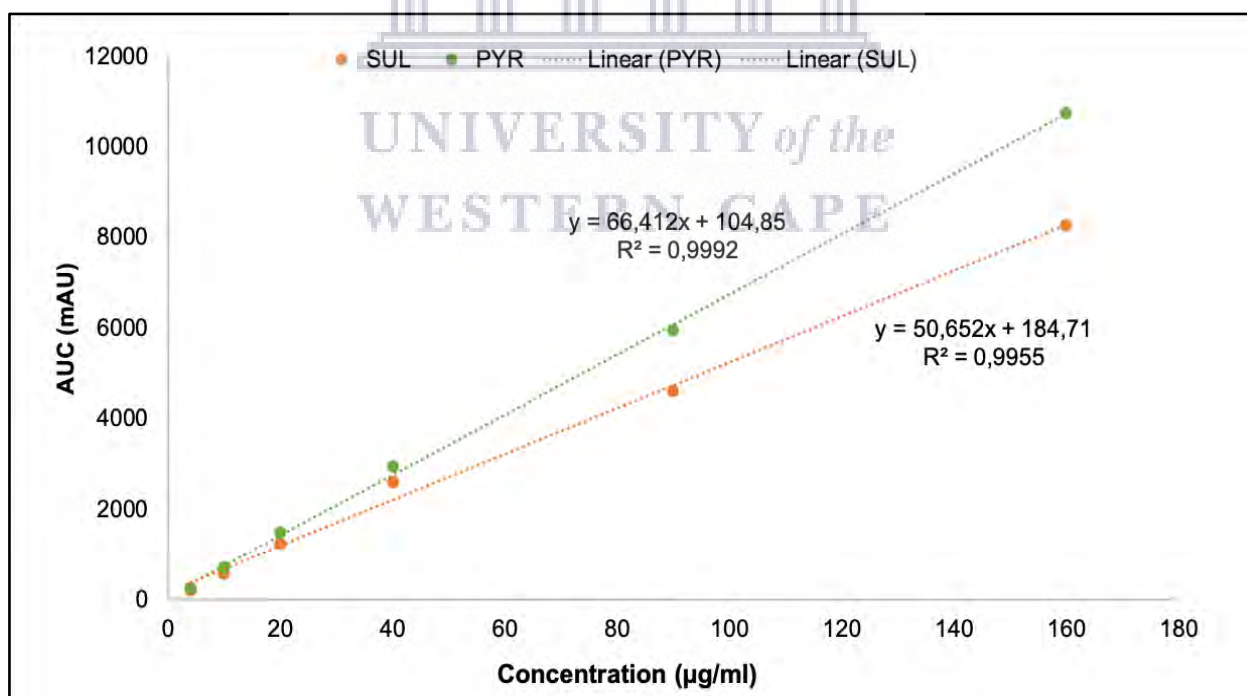
Figure 7.3: Regression plots obtained with SUL and PYR solutions across a concentration range of 4.00 - 160.00 µg/ml.
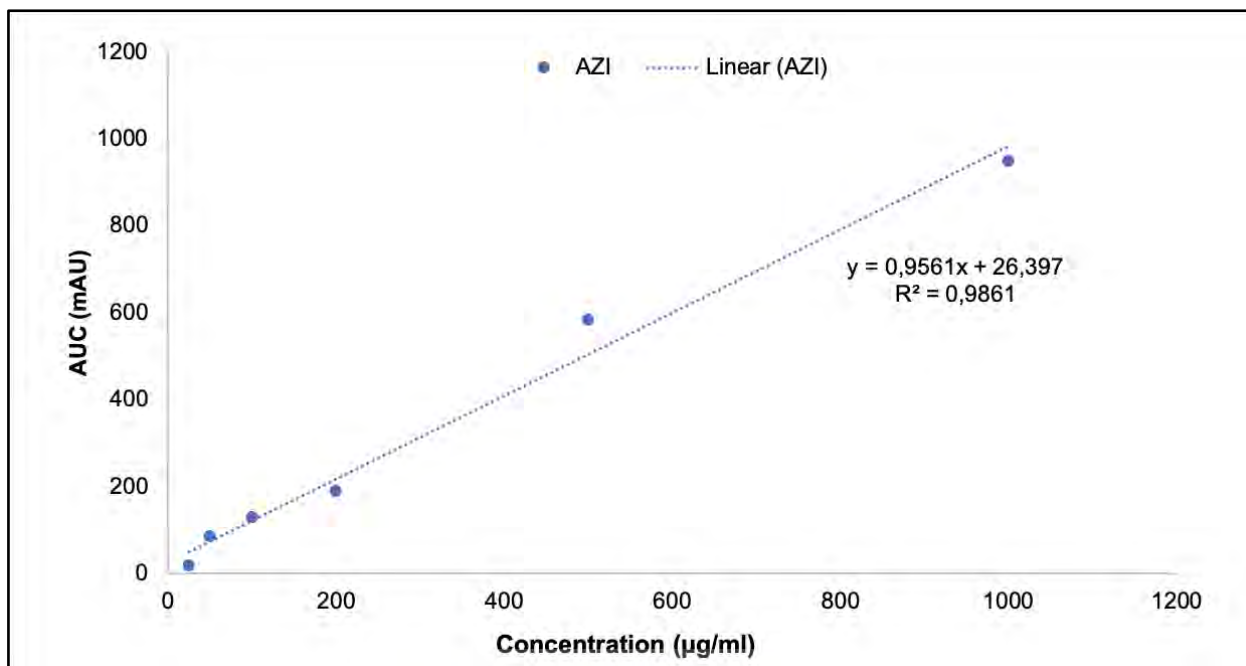
Figure 7.4: Regression plot obtained with of AZI solutions across a concentration range of 25.00 - 1000.00 µg/ml.

7.3.2 Limit of detection (LOD) and limit of quantification (LOQ)

LOD and LOQ form part of an integral component of method validation requirements. LOD is the lowest amount of an analyte the method can accurately detect and identify. An analyte peak should still exhibit a notable peak size differentiating from background noise. It is important to note that LOD can easily be interfered with by any slight change of chromatographic condition and hence may not form part of robust parameters. Whereas LOQ is the lowest quantifiable concentration of an analyte with a certain degree of accuracy and precision. LOQ can also be defined as the calibration concentration of the working range, because its accuracy and precision is verified on a run/batch to batch basis (UNODC, 2009). During this method validation process the LOD and LOQ for each compound was calculated based on the standard deviation of the peak response versus analyte concentration and the slope obtained during linearity testing. This was achieved using ANOVA statistical analysis and applying the following two equations:

$$LOD = 3.3\sigma / b \qquad \text{(Equation 7.1)}$$
$$LOQ = 10\sigma / b \qquad \text{(Equation 7.2)}$$

With σ being the standard deviation of the peak areas across the tested concentration range and b being the slope of the calibration curve. The LOD and LOQ for SUL was calculated to

be 0.72 µg/ml and 2.19 µg/ml, respectively. For PYR both values were determined to be 1.72 µg/ml and 5.21 µg/ml, respectively. Lastly, for AZI LOD and LOQ were calculated to be 0.07 µg/ml and 0.20 µg/ml.

7.3.3 Accuracy

The accuracy of an HPLC method is defined by Paithankar, (2013) as the ability of an analytical method to provide data as closely to the international standard reference analyte's value as possible. There are no known specific set values, however, accuracy should be assessed on analytes with known concentration. It is conventionally recommended to be done with at least nine injections on three different concentration levels and reported as a percentage recovery value within 98.0 - 102.0% (Mahapatra and Sreedhar, 2018; LoBrutto and Patel, 2007; ICH, 2005). In this current study, accuracy was determined at the following concentration levels: SUL 10, 20, 100 µg/ml, PYR 10, 20, 100 µg/ml and AZI 100, 500 and 1000 µg/ml. **Tables 7.6, 7.7 and 7.8** display the spiked concentration used to determine the recovery from a standard solution prepared for each API. From the data obtained, accuracy of this method conforms to the acceptable limit, all recovery percentages with exception of a sample from SUL at concentration of 20.2 (mg/ml) that exceeded the limit by 0.23%.
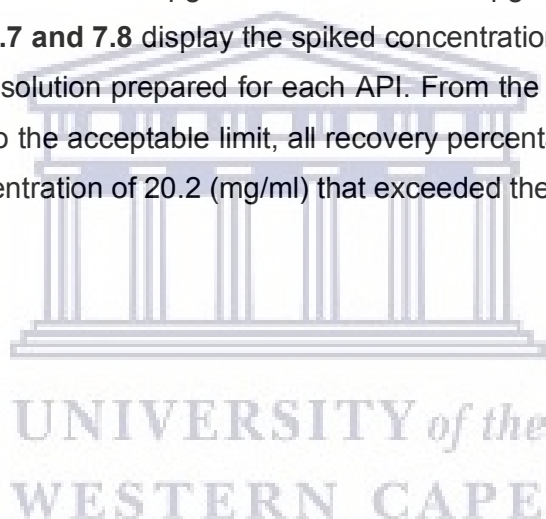
Table 7.6: Outline of the accuracy results obtained for SUL during the method validation process

Expected concentration (µg/ml)	Peak area (mAU) SUL			Recovery	
	Area 1	Area 2	Average	µg/ml	%
101.0	4976.633	4980.924	4978.7785	**100.96**	**99.96**
101.0	5004.949	4990.008	4997.4785	**101.34**	**100.34**
101.0	5000.838	4974.722	4987.78	**101.14**	**100.14**
20.2	1004.586	1012.123	1008.3545	**20.37**	**100.84**
20.2	999.128	1045.501	1022.3145	**20.65**	**102.23**
20.2	1000.955	1000.110	1000.483	**20.21**	**100.05**
10.1	433.437	427.682	430.5595	**10.10**	**100.00**
10.1	433.178	430.458	431.818	**10.13**	**99.31**
10.1	432.682	424.282	428.482	**10.05**	**99.50**

Table 7.7: Outline of the accuracy results obtained for PYR during the method validation process

Concentration (µg/ml)	Peak area (mAU) PYR			Recovery	
	Area 1	Area 2	Average	µg/ml	%
100.2	6003.455	6069.483	6036.469	99.66	99.46
100.2	6088.986	6002.149	6045.568	99.81	99.61
100.2	6017.494	6004.566	6011.03	99.24	99.04
21.5	1385.018	1379.942	1382.48	21.55	100.23
21.5	1388.132	1375.454	1381.793	21.54	100.19
21.5	1375.021	1387.612	1381.3165	21.53	100.19
10.0	507.914	520.573	514.2435	10.04	100.4
10.0	505.234	522.175	513.7045	10.03	100.3
10.0	517.848	503.673	510.7605	9.97	99.7

Table 7.8: Outline of accuracy results obtained for AZI during the method validation process

Concentration (µg/ml)	Peak area (mAU) AZI			Recovery	
	Area 1	Area 2	Average	µg/ml	%
1000.15	638.148	622436	630.292	1007.84	100.77
1000.15	609.906	628.517	619.212	990.12	99.00
1000.15	626.437	620.142	623.290	996.64	99.65
499.69	242.206	241.924	242.065	498.63	99.79
499.69	243.156	241.521	242.339	499.19	99.90
499.69	241.563	243.201	242.382	499.28	99.92
100.01	65.749	51.689	58.719	99.74	99.73
100.01	59.143	58.750	58.9465	100.12	100.11
100.01	60.768	57.710	59.239	100.62	100.61

7.3.4 Precision

Precision of an analytical method refers to an expression of how closely the series of events are in relationship to one other in the sample exhibiting the same constituents, preparation method, performed under similar chromatographic conditions. This may be performed in two sections, repeatability (intra-day precision) and reproducibility (inter-day precision) (Paithankar, 2013).

(a) Intra-day precision (repeatability)

Repeatability is the precision of a method under specific conditions during a short period of time (intra-day). A minimum of nine samples (consisting of three different concentrations) are prepared to perform this analysis. These solutions are then analysed in duplicate on the same day. The percentage recovery of the samples should have a %RSD of <5% to be considered acceptable.

The system repeatability of the analytical method was determined to ensure the repeatability of peak areas and retention time under similar sample conditions. The acceptable criteria for the peak areas and retention times is a %RSD of less than 2% to prove adequate repeatability (Paithankar, 2013:235). **Table 7.9**, indicates the data obtained from nine injections of 100 µg/ml for all APIs, this was optimal because the concentration was within the LOD and LOQ range, the %RSD for both peak areas and retention times were below 2%, confirming that this method can be replicated for simultaneous detection and quantification of SUL, PYR and AZI as individual compounds and combinations.
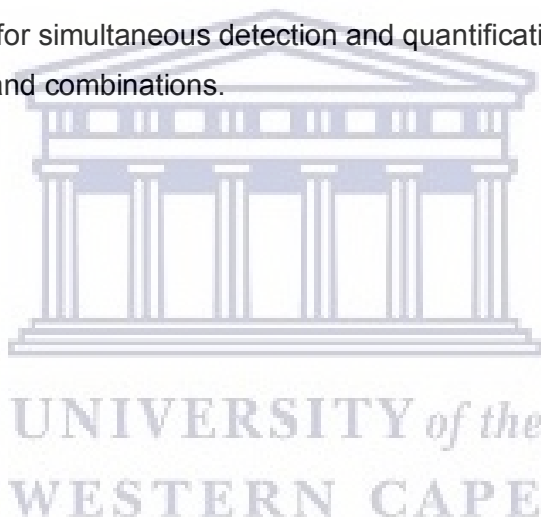
Table 7.9: Repeatability results obtained for SUL, PYR and AZI during the method validation process

Injection	SUL (100 µg/ml)		PYR (100 µg/ml)		AZI (100 µg/ml)	
	Peak area (mAU)	Retention time (min)	Peak area (mAU)	Retention time (min)	Peak area (mAU)	Retention time (min)
1	4930.615	2.20	6017.494	3.92	630.452	9.85
2	5000.838	2.18	6004.566	3.92	629.375	9.84
3	4990.008	2.20	5935.105	3.93	626.437	9.82
4	5004.945	2.17	6002.149	3.92	628.517	9.82
5	4976.633	2.20	6088.986	3.92	609.906	9.85
6	4974.722	2.18	6069.483	3.92	622.436	9.84
7	4980.924	2.18	6003.872	3.92	638.148	9.83
Mean	4979.812	2.19	6017.38	3.92	626.467	9.84
SD	22.79	0.012	46.58	0.003	8.067	0.0118
%RSD	0.46	0.55	0.77	0.09	1.29	0.13

(a) Inter-day precision (reproducibility)

Precision analysed over a longer period of time (three consecutive days) under specific conditions in the same laboratory is also referred to as the reproducibility of an analytical method. Figure 7.10, 7.11 and 7.12 are data obtained for inter-day precision for SUL, PYR and AZI respectively. It can be seen that SUL and PYR were relatively stable with acceptable variation of % RSD under 2%, however, AZI's 3rd day data led to %RSD of over acceptable limit of RSD. It can not be emphasized that AZI's chromatographic results require closely monitored factors among other the general HPLC conditions and external factors such as room temperature and storage conditions.

Table 7.10: Inter-day precision obtained for SUL

Day 1	Day 2	Day 3	
23922.030	23827.464	24140.767	
23831.065	24052.284	23523.931	
23966.118	23870.111	23269.285	
			Between days
Mean 23906.404	23916.620	23644.661	23822.561
SD 56.231	97.496	365.880	125.863
%RSD 0.24	0.41	1.55	0.53

Table 7.11: Inter-day precision obtained for PYR

	Day 1	Day 2	Day 3	Between days
	23431.616	24837.255	23851.356	
	23969.046	24782.515	23319.446	
	23722.503	23065.726	23243.771	
Mean	23707.72	24228.499	23471.524	23802.581
SD	219.653	822.508	270.352	316.229
%RSD	0.93	3.39	1.15	1.33

Table 7.12: Inter-day precision obtained for AZI

	Day 1	Day 2	Day 3	
	935.078	923.837	860.441	
	934.840	929.474	887.204	
	924.311	962.622	874.242	
				Between days
Mean	931.410	938.644	873.962	914.672
SD	5.020	17.11	10.93	28.937
%RSD	0.54	1.82	1.25	3.16

7.3.5 Robustness and specificity

The robustness of an analytical procedure is defined as a critical step that determines the capacity of an analytical method to remain intact irrespective of minor alterations made whether planned or erroneously in the operation parameters, as a measure of its reliability during normal operation. The parameters that may vary to some extent include: pH, mobile phase composition, flow rate, wavelength and column temperature and an endorsement must be clearly noted for future reference. The evaluation of robustness may commence during the method developmental stage already as part of the process to establish operational parameters that may affect the analytical method. Aspects such as the stability of the analytes in the sample preparation solution, the sample preparation procedures, the pH of the sample

diluent used, filtering material and duration of processing of the analyte and method should be assessed to determine the influence of any variations on the accuracy, reproducibility and repeatability of the analytical method (ICH, 2005; Paithankar, 2013).

Specificity is a term used in analytical method validation to assess the degree to which the analytical response will be affected when the analyte is incorporated into different types of solvents or when mixed with other components such as degradants, impurities and matrices (ICH, 2005). In a nutshell, the method should detect and quantify the intended analyte without interference whatsoever. Where no degradants or impurities are available to form part of the validation process, forced degradation may be employed During such a degradation process the analyte(s) may be subjected to physico-chemical stress factors such as strong acid, strong base, oxidative agents, direct light to trigger potential photolysis, and heat in an attempt to degrade the compound(s) into its metabolites (Paithankar, 2013).

The first robustness parameter investigated was that of altering the mobile phase composition ratio. Table 7.13 outlines the differences observed in the retention times of the three analytes when the mobile phase composition was adjusted from an ACN : 0.038M K_2HPO_4 (60:40 v/v) ratio to an ACN : 0.038M K_2HPO_4 (80:20 v/v) ratio. This composition weakens the buffer concentration that may lead to pH fluctuation, AZI is pH sensitive and a slight alteration may affect its elution and hence retention time fluctuation during an analytical operation.

Table 7.13: The effect of mobile phase ratios difference in retention time

Mobile phase composition ratio	Retention time (min) for SUL	Retention time (min) for PYR	Retention time (min) for AZI
80:20	2.38	3.82	6.68
60:40	2.32	4.00	9.43

As part of specificity testing it was important to investigate an injection of a blank sample. In other words just the mobile phase which was used as diluent during standard solution preparation. **Figure 7.5** depicts the chromatogram obtained with only the mobile phase and no APIs added. From this chromatogram it was concluded that the diluent won't cause any interference with either SUL, PYR or AZI peaks during drug assay determination. Since this

method was also intended to be utilised during drug equilibrium solubility testing as well as the determination of dissolution rate of each drug when in combination with one another, either as a mere physical mixture or as a solid-state form modification, it was necessary to determine how different aqueous buffered solvents will influence the retention time of each of the three compounds. In order to investigate this the various aqueous buffered solutions were added to solutions containing SUL, PYR, AZI or SPA-C. The buffered solvents used were 0.1 N hydrochloric acid (pH 1.2), pH 4.5 (acetate buffer), pH 6.8 (phosphate buffer) and pH 8.2 (phosphate buffer). **Figure 7.6 (a) - (d)** depicts the chromatographic responses obtained with a solution of SUL in pH 1.2, pH 4.5, pH 6.8 and pH 8.2 buffered solvents and (**Table 7.14**) shows the actual peak areas obtained for SUL, PYR and AZI. From this it was observed that the retention time of SUL was not affected by the use of any of the buffered aqueous media as solvents. **Figure 7.7 (a) - (d)** shows the PYR peaks obtained when aqueous buffered medium was used as solvent and similar to that observed for SUL it became apparent that these solvents do not influence the retention time of PYR, retention time remained unaltered. When the same was investigated with AZI it was observed that in pH 1.2 the detectable peak was very small. A notable increase in the AZI peak area was observed from pH 4.5 with the best achieved at pH 8.2 (**Figure 7.8**) and a similar trend was obtained for AZI in SPA-C (**Figure 7.9**). It is a known fact that basic drug compounds ionise in an acidic media, this can negatively affect its chromatographic behavior. Furthermore, this method can run samples prepared in solvents with pH range of 6.8 to 8.8, however to establish the best quantification, pH 8.2 was determined best suited (**Figure 7.14**), the solvent and mobile phase pH should be as closely as possible to one another. It became therefore apparent that the poor chromatographic sensitivity of AZI dictates suitability and reproducibility of this novel analytical method. And again it was necessary to ascertain the effect of the buffer diluents in SPA-C, as observed in Figure 6.8, there was no significant alteration in retention time of any of the drugs.

Table 7.14: Effect of preparation solvent pH on SUL, PYR and AZI

pH	1.2	4.5	6.8	8.2
SUL (1000 µg/ml)	13874.481	18824.914	20840.321	16452.231
PYR (1100 µg/ml)	33085.52	19045.451	11662.812	12345.506
AZI (100 µg/ml)	No Peak	487.317	948.832	1050.963
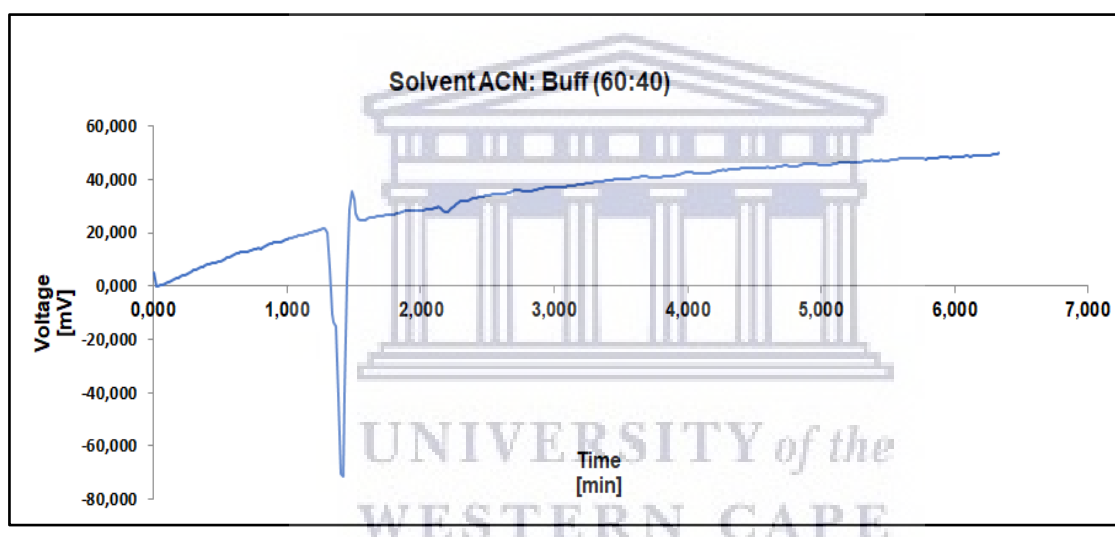
Figure 7.5: Depicting the chromatogram obtained for solvent, acetonitrile (ACN): buffer (dipotassium hydrogen phosphate) 60:40 v/v.
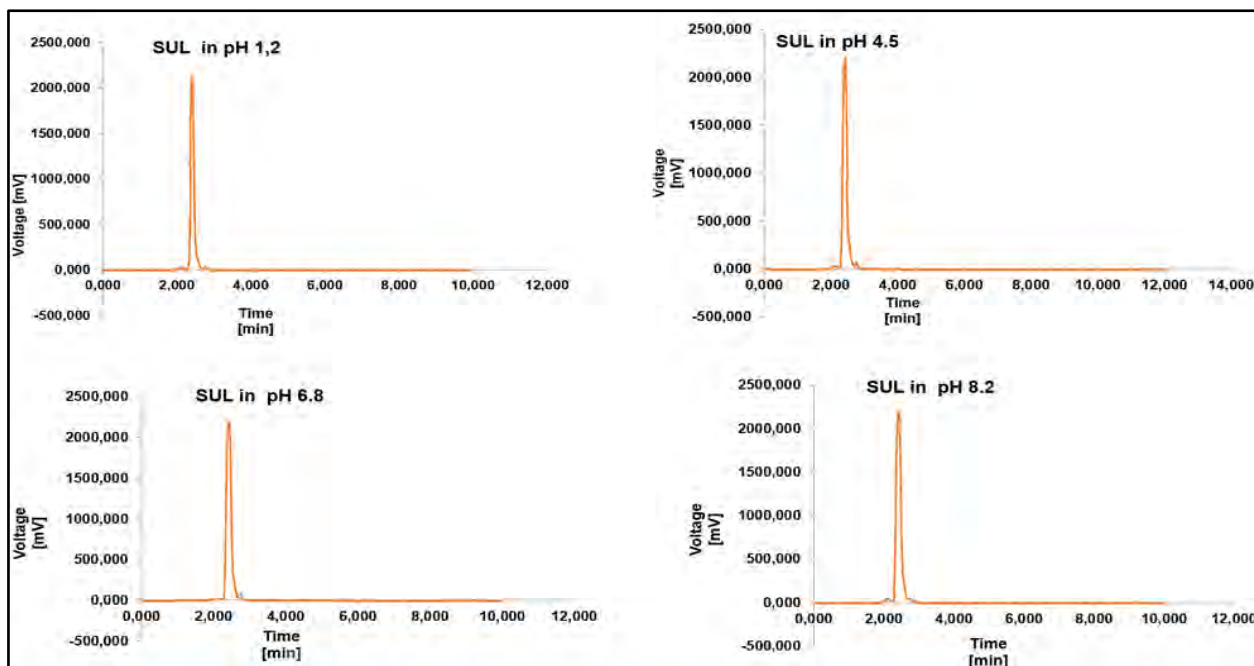
Figure 7.6: Chromatograms obtained for SUL diluted using aqueous buffered solvents (a) pH 1.2, (b) pH 4.5, (c) pH 6.8 and (d) pH 8.2.
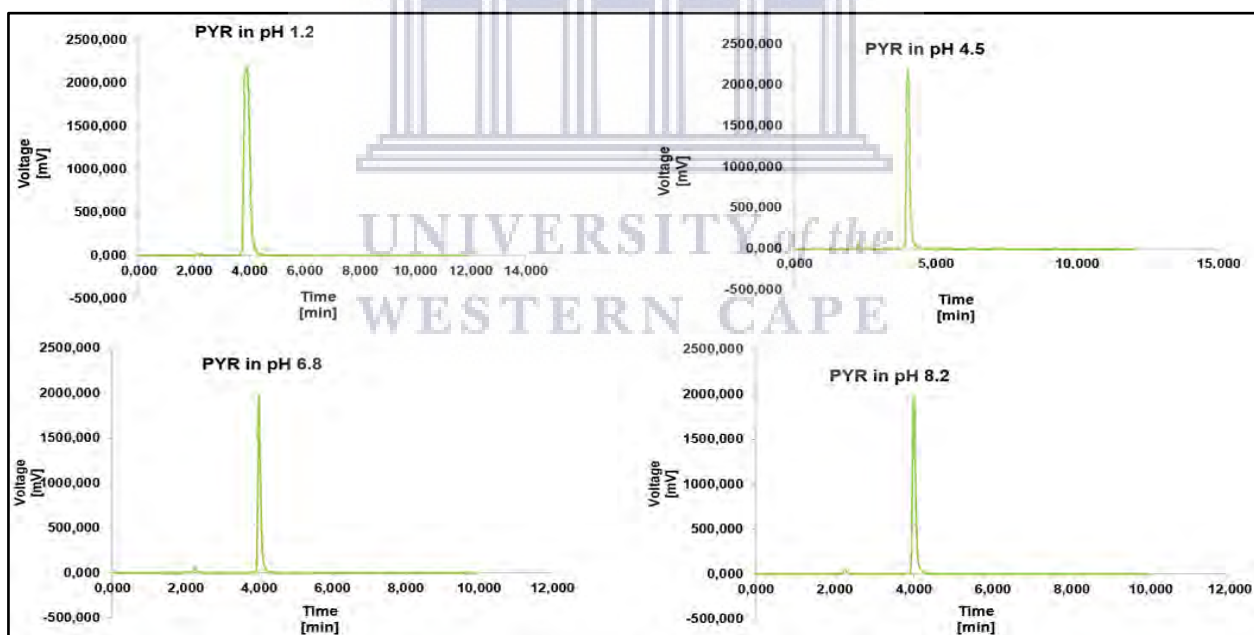
Figure 7.7: Chromatograms obtained for PYR diluted using aqueous buffered solvents (a) pH 1.2, (b) pH 4.5, (c) pH 6.8 and (d) pH 8.2.
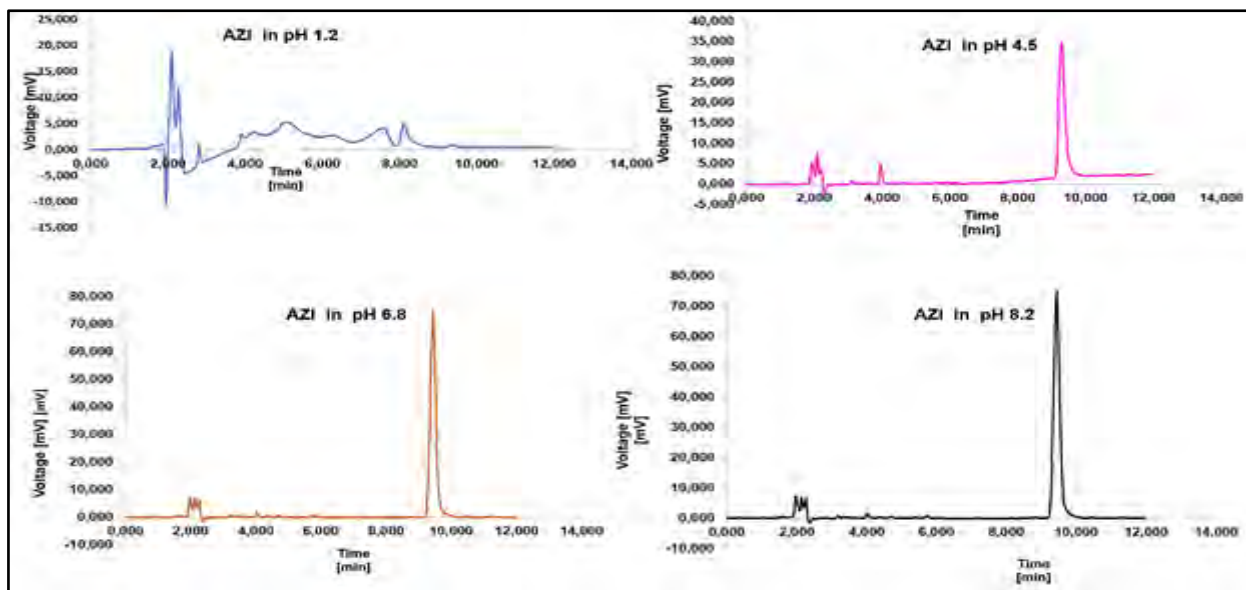
Figure 7.8: Chromatograms obtained for AZI diluted using aqueous buffered solvents (a) pH 1.2, (b) pH 4.5, (c) pH 6.8 and (d) pH 8.2.
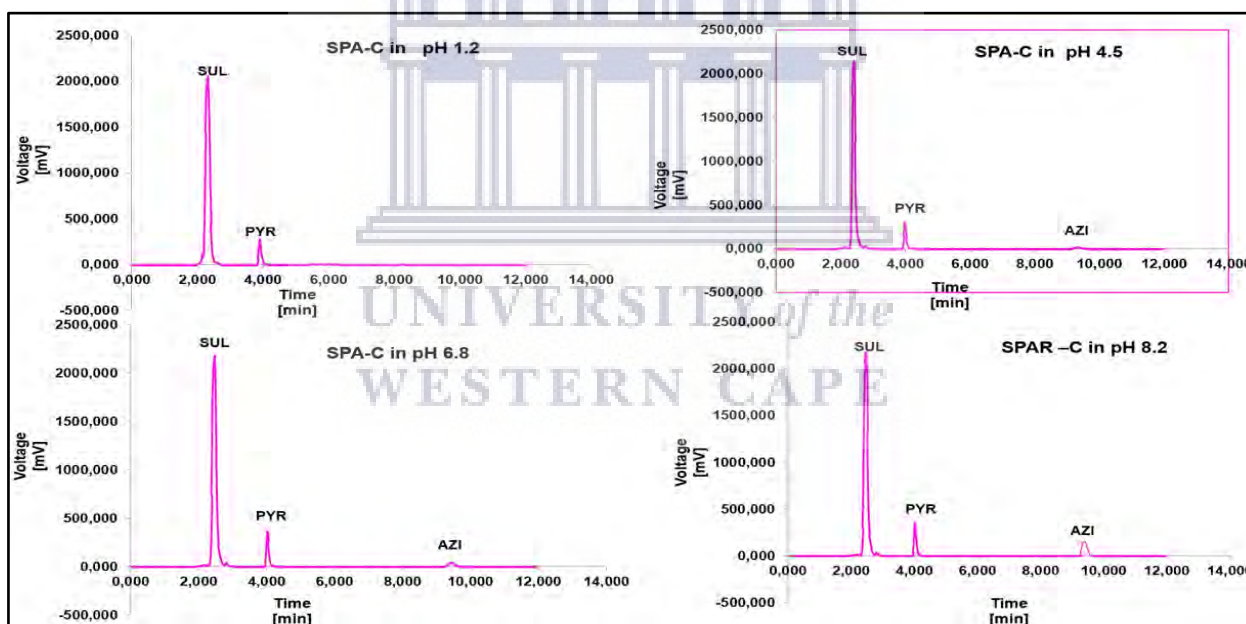
Figure 7.9: Chromatograms obtained for SPA-C diluted using aqueous buffered solvents (a) pH 1.2, (b) pH 4.5, (c) pH 6.8 and (d) pH 8.2.

7.3.6 Stability

Sample solution stability was investigated utilising various storage conditions and forced degradation to ascertain whether this method can be applied to identify possible degradation products which might form in solution, either during storage of the sample solutions or when degradation products are introduced into the sample solutions due to the degradation of SUL, PYR or AZI during sample preparation or manipulation or when these three compounds are subjected to typical shelf-life studies. The samples were relatively stable at most common storage conditions such as when protected from light, 5 °C ± 2 °C, direct room light and at ambient temperature, however as a general observation, samples intended for analysis using this method should not be kept out of the fridge for longer than 3 days **(Table 7.15)**.

Table 7.15: Stability data obtained for standard solutions containing SUL, PYR and AZI upon exposure to typical storage conditions as well as harsh conditions to force compound degradation.

	Conditions	Fridge (mAU)	Direct light (mAU)	Dark (mAU)	HCl (mAU)	NaOH (mAU)	H2O2 (mAU)
SUL	Day 1 (2000 µg/ml)	100.00%	100.00%	100.00%	0.00%	37.96%	0.00%
	Day 2 (2000 µg/ml)	99.12%	99.61%	99.56%	0.00%	37.76%	0.00%
	Day 3 (2000 µg/ml)	94.94%	98.34%	97.09%	0.00%	37.71%	0.00%
PYR	Day 1 (2000 µg/ml)	100.00%	100.00%	100.00%	17.78%	25.21%	0.00%
	Day 3 (2000 µg/ml)	97.98%	96.71%	95.22%	14.86%	19.69%	0.00%
	Day 3 (2000 µg/ml)	97.23%	94.10%	94.39%	9.24%	13.69%	0.00%
AZI	Day 1 (2000 µg/ml)	100.00%	100.00%	100.00%	0.00%	0.00%	0.00%
	Day 2 (2000 µg/ml)	99.94%	99.43%	97.14%	0.00%	0.00%	0.00%
	Day 3 (2000 µg/ml)	94.58%	94.90%	89.39%	0.00%	0.00%	0.00%

Table 7.16: Effect of storage conditions on the retention time of the three analytes

Storage	Retention time (min) for SUL	Retention time (min) for PYR	Retention time (min) for AZI
Dark	2.38	3.82	5.53
Fridge (5 °C ± 2 °C)	2.32	4.00	8.01
Light	2.32	4.00	9.94

AZI remained stable when protected from light, stored at 5 °C ± 2 °C and direct light to some degree, however its retention time was significantly affected (**Table 7.16** and **Figure 7.12).** This would affect elution of other components as overlap and superimposition of peaks may confuse detection and quantification when in combination. SUL and PYR peak intensities and retention were observed unaltered under similar storage of samples (**Table 7.16** and **Figure 7.10** and **Figure 7.11**). Same trend of retention shift was observed between two samples prepared using the mobile phase as diluent (**Table 7.16).**
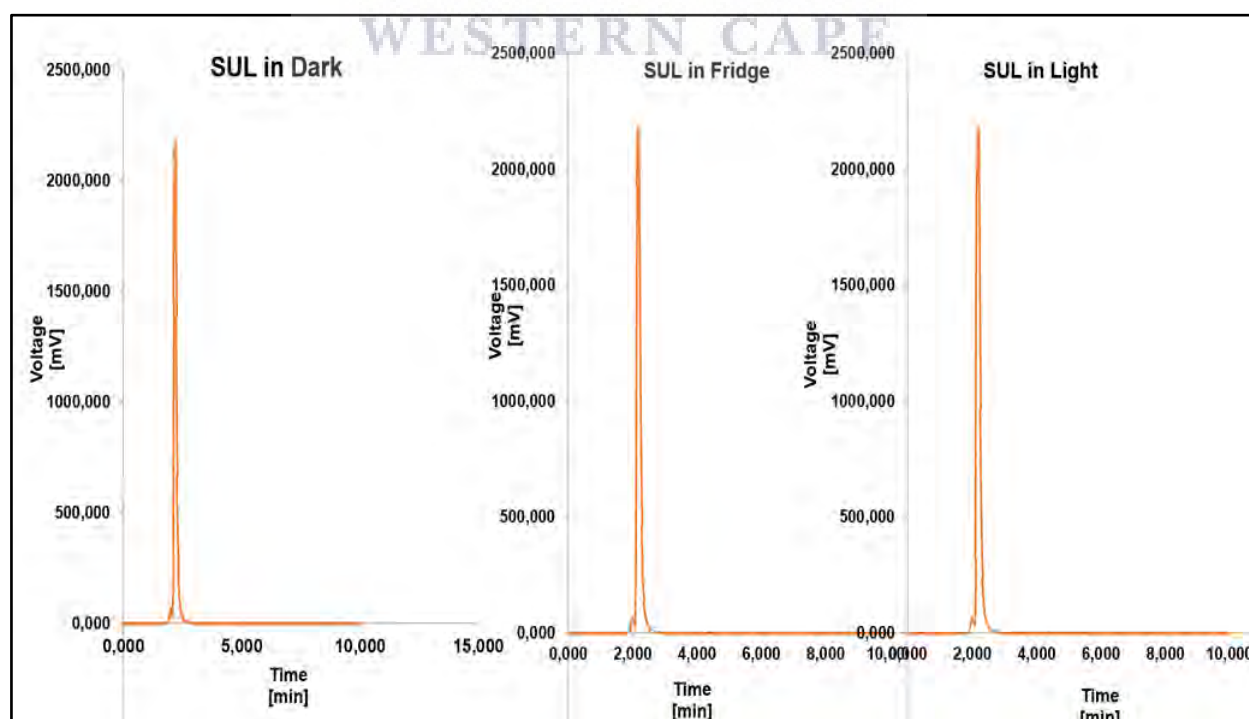
Figure 7.10: Chromatography obtained for SUL upon exposure to varying storage conditions.
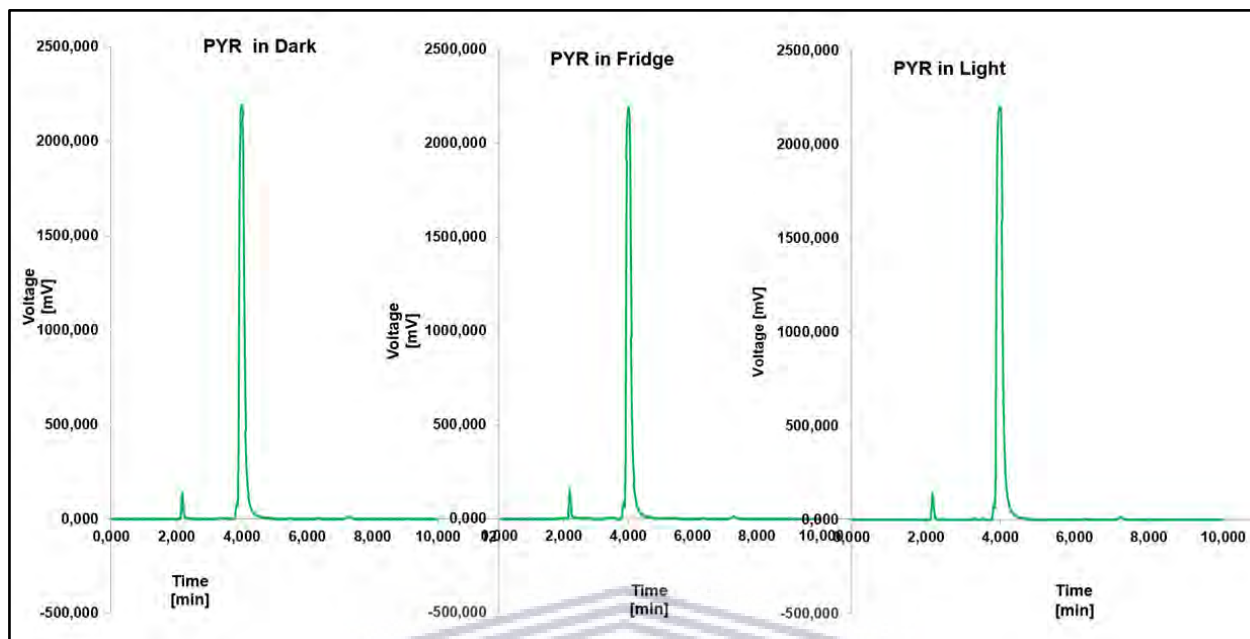
Figure 7.11: Chromatography obtained for PYR upon exposure to varying storage conditions.
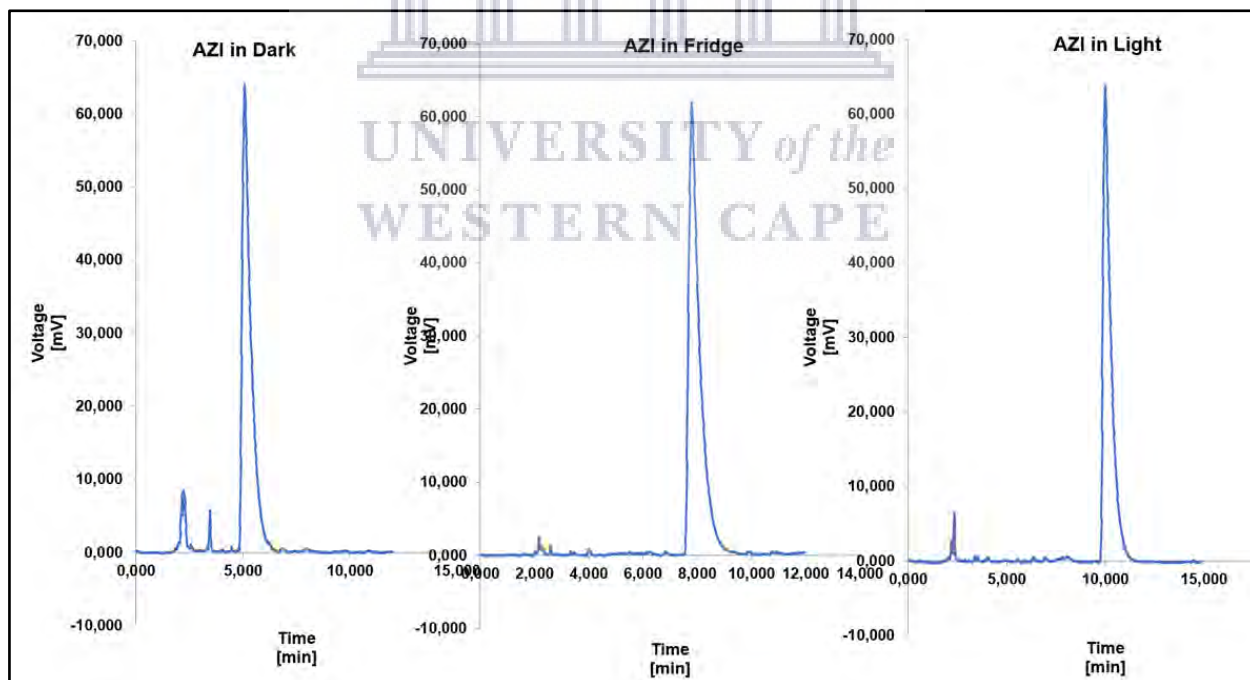
Figure 7.12: Chromatography obtained for AZI upon exposure to varying storage conditions.

To determine the extent of degradation, a forced degradation investigation was employed by addition of 2 N NaOH, 2 N HCl and 3% v/v H_2O_2 to the samples and chromatography data was

obtained. It was apparent that the peak shape for SUL was not affected in the basic environment, however, there was a dramatic decrease in peak area, no additional peaks eluted during the run time **(Figure 7.13** and **Table 7.15).** Hydrolysis due to exposure to a highly acidic environment as well as hydrolytic oxidation of SUL was observed as resultant split peaks. These peaks were subsequently unquantifiable. PYR was completely degraded under oxidative conditions and in acidic and basic conditions a small fraction of 17% and 25% were quantified on day one respectively, and by day 3, 9% and 13% PYR remained, respectively (**Table 7.15**). The obtained peaks are of degradants as no normal elution was possible in the above conditions (**Figure 7.14**). AZI on the other hand depicted peaks of reasonable intensities at 2 min for all hydrolytic and oxidative conditions, this illustrates that AZI degradants are more polar (ionised) leading to shorter retention time as opposed to the neutral counterpart. Furthermore, the spiked areas could not be classified for a normal peak and hence, was considered as unknown degradants (**Figure 7.15** and **Table 7.15**).
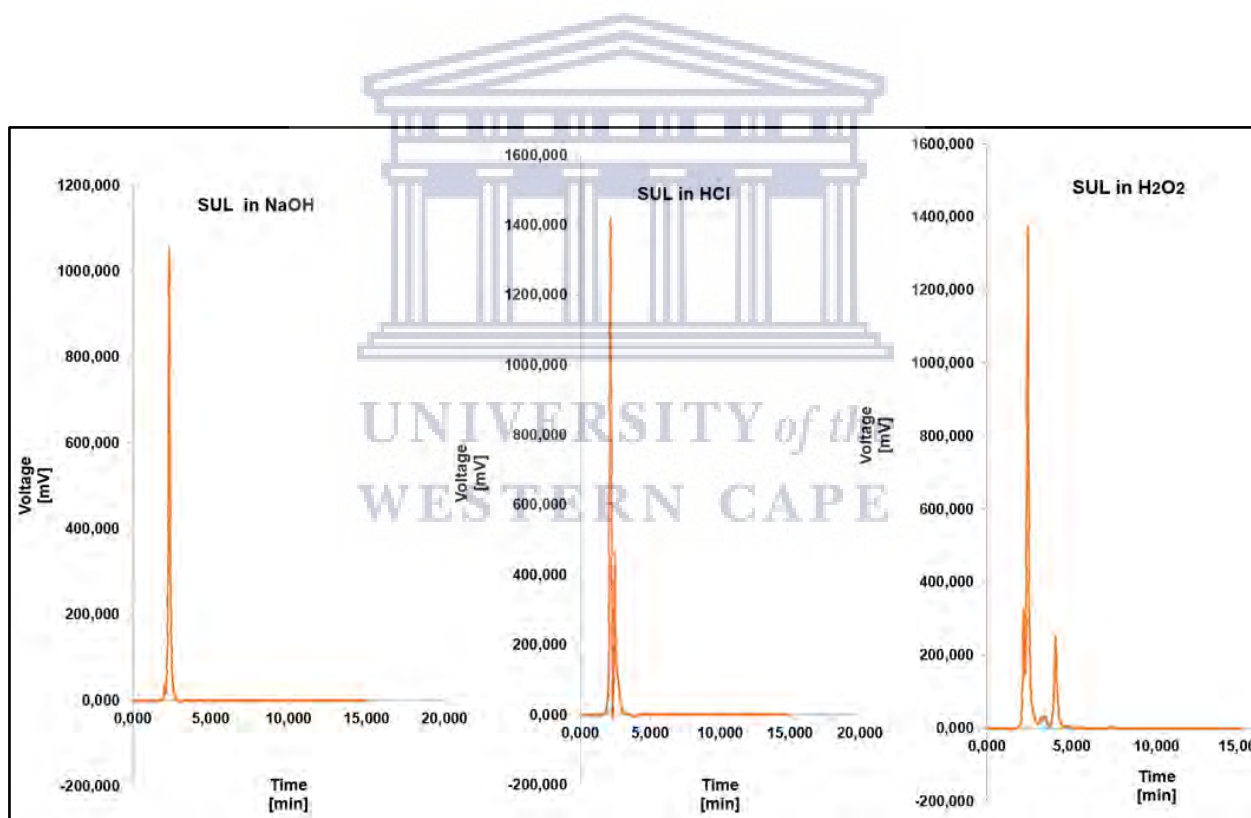
Figure 7.13: Chromatography obtained for SUL after exposure to (a) 2 N NaOH, (b) 2 N HCl and (c) 3% v/v H_2O_2.
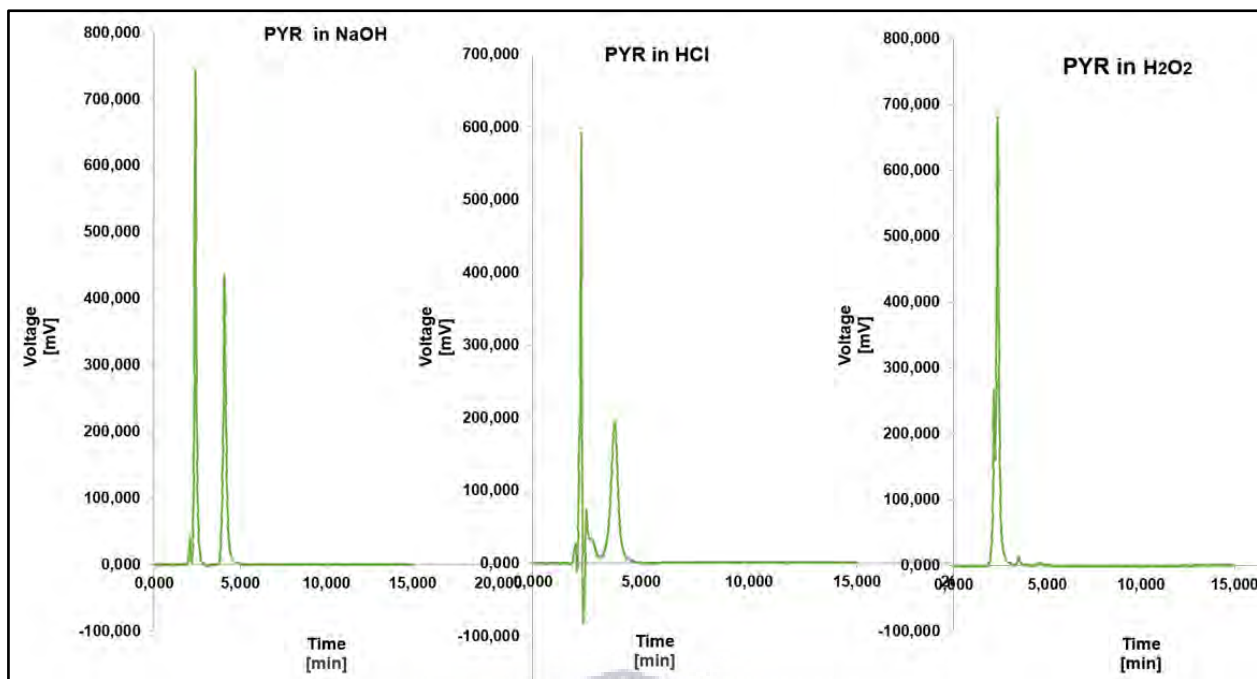
Figure 7.14: Chromatography obtained for PYR after exposure to 2 N NaOH, 2 N HCl and 3% v/v H_2O_2 .
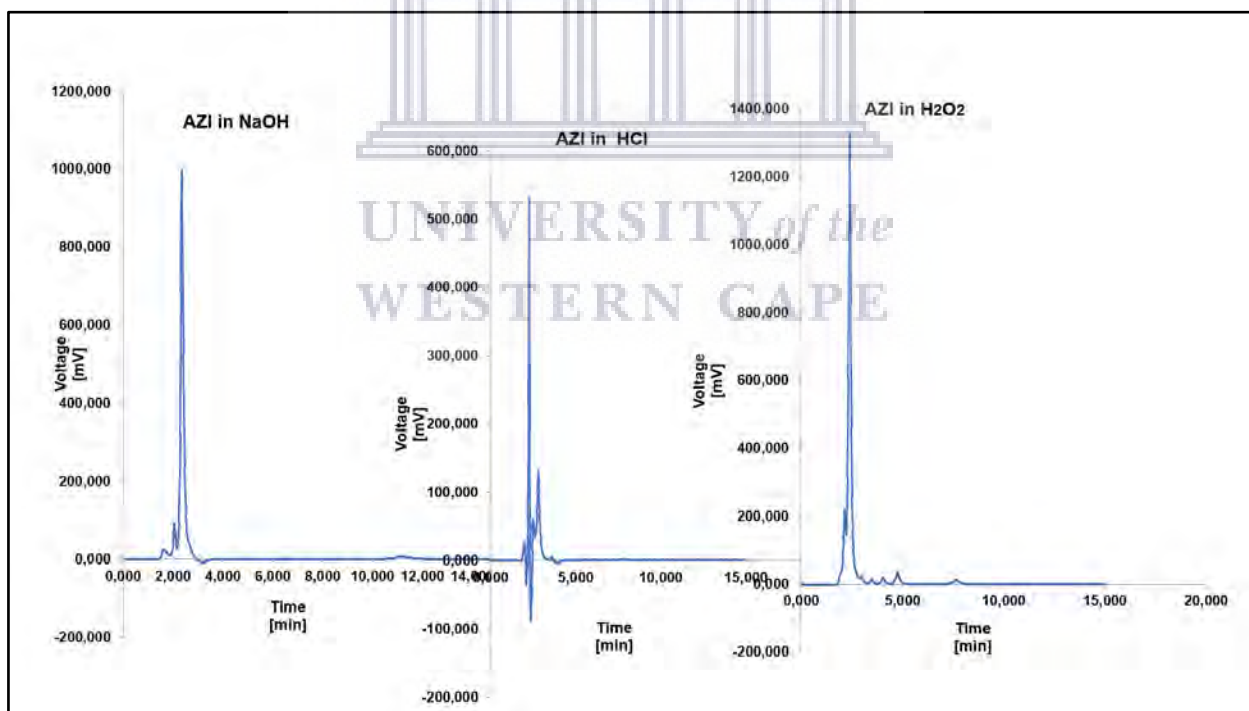
Figure 7.15: Chromatography obtained for AZI after exposure to 2 N NaOH, 2 N HCl and 3% v/v H_2O_2 .

7.4 Conclusion

The new solid-state form preparation that combined SUL, PYR and AZI, three APIs with different physico-chemical properties, required an HPLC method for the simultaneous detection and quantification of all three compounds. This method was developed and validated according to ICH standard guidelines for the method development for identification and quantification of pharmaceutical products (ICH, 2005). Parameters such as accuracy, precision, linearity, robustness, LOD and LOQ were carefully investigated and established. This did not proceed smoothly without challenges; determination of chromatographic conditions to allow the successful detection and quantification of all three compounds simultaneously were challenging. Especially given the fact that AZI exhibits low UV sensitivity and a narrow wavelength zone in which adequate adsorption may be achieved. In comparison SUL and PYR exhibited high levels of UV sensitivity with good UV absorption across a wide wavelength range. However, despite these mentioned challenges a novel RP-HPLC method was successfully developed to be operated with an ACE C_{18} column, 3 μm, 250 mm × 4.6 mm, using acetonitrile/buffer (60:40 v/v) as mobile phase at a flow rate of 1 ml/min, wavelength 210 nm, column temperature set 30, run time of 15 minutes, retention times at 2.19, 3.92, 9.44 minutes for SUL, PYR, and AZI, respectively. This method also proved to be stable since the chromatographic conditions were found to be sensitive towards the identification of drug degradation for all three drugs.

References

Acheampong, A., Gyebi, A., Darko, G., Apau, J., Owusu Gyasi, W., & Addai-Arhin, S. (2018). Development and validation of RP-HPLC method for simultaneous estimation of sulfadoxine and pyrimethamine in tablet dosage form using diclofenac as internal standard. *Cogent Chemistry, 4*(1), 1472198. https://doi.org/10.1080/23312009.2018.1472198.

Ahuja, S. (2007). Overview of HPLC method development for pharmaceuticals. In: Ahuja, S and Rasmussen, H. Ed(s). HPLC method development for pharmaceuticals. Elsevier, pp.1-11.

Belanger, J.M., Paré, J.J. and Sigouin, M. 1997. High performance liquid chromatography (HPLC): principles and applications. In: Paré, J.J. and Belanger. J. Ed(s). *Instrumental methods in food analysis.* Vol. 1. Elsevier, pp37-59

Böttcher, J., Margraf, M., Monks, K. HPLC Basics – principles and parameters. Available at<https://www.knauer.net/Application/application_notes/VSP0019_HPLC%20Basics%20-%20principles%20and%20parameters_final%20-web-.pdf> Date accessed: 28 October 2021.

Dolan, J. W. (2017). *Back to Basics: The Role of pH in Retention and Selectivity*. [online] Chromatography Online. Available at: https://www.chromatographyonline.com/view/back-basics-role-ph-retention-and-selectivity [Accessed 27 Oct 2021].

Driver, J.L. and Raynie, D.E. 2007. Method development for biomolecules. In: Ahuja, S. and Rasmussen, H. Ed(s). HPLC Method Development for Pharmaceuticals. Academic Press, pp. 425-439.

Food and drug administration. (2001). Guidance for Industry: Bioanalytical method validation. https://www.fda.gov/files/drugs/published/Bioanalytical-Method-Validation-Guidance-for-Industry.pdf Date of access: 18 Aug 2021.

Ghari, T., Kobarfard, F., & Mortazavi, S. A. (2013). Development of a simple RP-HPLC-UV method for determination of azithromycin in bulk and pharmaceutical dosage forms as an alternative to the USP method. *Iranian Journal of Pharmaceutical Research*, *12*(SUPPL.), 55–61. https://doi.org/10.22037/ijpr.2013.1272.

Halberstadt (2017) '乳鼠心肌提取 HHS Public Access', *Physiology & behavior*, 176(5), pp. 139–148. doi: 10.1016/j.addr.2016.05.007.BDDCS.

Huber, L. (2007). Validation of analytical methods. Agilent technologies: USA. pp. 1-76.

International Conference of Harmonisation. (2005). Validation of analytical procedures: text and methodology. https://www.gmp-compliance.org/guidemgr/files/Q2(R1).pdf Date of access: 20 Aug 2021.

Jerkovich, A.D. and Vivilecchia, R.V. (2007). Development of fast HPLC methods. In: Kazakevich, Y. and LoBrutto, R. Ed(s). HPLC for pharmaceutical scientists. New Jersey: John Wiley & Son, pp.763-810.

LoBrutto, R. and Patel, T. 2007. Method validation. In: Kazakevich, Y and LoBrutto, R. Ed(s). *HPLC for pharmaceutical scientists.* New Jersey: John Wiley & Sons, pp. 455-502.

Kazakevich, Y. and LoBrutto, R.(2007). Introduction. In: Kazakevich, Y. and LoBrutto, R. Ed(s). HPLC for pharmaceutical scientists. New Jersey: John Wiley & Sons, pp.3-24.

Mahapatra, A. and Sreedhar, C. (2018). HPLC AND ANALYTICAL METHOD VALIDATION : A REVIEW. *Indian Research Journal of Pharmacy and Science*, 5(1), pp.1399–1414.

Meyer, V.R. (2004). Detectors. In: Practical high-performance liquid chromatography. 4th edn. John Wiley & Sons, pp 82-99.

Mwalwisi, Y. H., Hoellein, L., Kaale, E., & Holzgrabe, U. (2016). Development of a simple, rapid, and robust liquid chromatographic method for the simultaneous determination of sulfalene, sulfadoxine, and pyrimethamine in tablets. *Journal of Pharmaceutical and Biomedical Analysis*, *129*, 558–570. https://doi.org/10.1016/j.jpba.2016.07.044.

National Center for Biotechnology Information (2021a). PubChem Compound Summary for CID 17134, Sulfadoxine. Available at:
https://pubchem.ncbi.nlm.nih.gov/compound/Sulfadoxine [Accessed 20, Oct, 2021].

National Center for Biotechnology Information (2021b). PubChem Compound Summary for CID 4993, Pyrimethamine. Available at:
https://pubchem.ncbi.nlm.nih.gov/compound/Pyrimethamine [Accessed 20, Oct, 2021].

National Center for Biotechnology Information (2021c). PubChem Compound Summary for CID 447043, Azithromycin. Available at:
https://pubchem.ncbi.nlm.nih.gov/compound/Azithromycin [Accessed 20, Oct, 2021].

Okaru, A. O., Abuga, K. O., Kamau, F. N., Ndwigah, S. N., & Lachenmeier, D. W. (2017). A robust liquid chromatographic method for confirmation of drug stability of azithromycin in

http://etd.uwc.ac.za/

bulk samples, tablets and suspensions. *Pharmaceutics*, *9*(1).
https://doi.org/10.3390/pharmaceutics9010011.

Paithankar, H.V. 2013. HPLC method validation for pharmaceuticals. *International Journal of Universal Pharmacy and Biosciences,* 2(4):229-240. http://www.ijupbs.com/Uploads/

21.%20RPA1300143.pdf

Pai, S.P. N., Dias, C., & Sawant, N. (2016). Development and validation of a RP-HPLC method for the simultaneous estimation of sulfadoxine and pyrimethamine in combined dosage tablets. *Indian Journal of Pharmaceutical Education and Research*, *50*(3), 489–494. https://doi.org/10.5530/ijper.50.3.24.

Rodriguez, I.R. (2004). Rapid analysis of oxysterols by HPLC and UV spectroscopy. *BioTechniques*, 36(6), pp.952–958.

Saita, M.G., Aleo, D., Melilli, B., Mangiafico, S., Cro, M., Sanfilippo, C. and Patti, A. (2018). pH-Dependent stability of azithromycin in aqueous solution and structure identification of two new degradation products. *Journal of Pharmaceutical and Biomedical Analysis*, 158(171-95127), pp.47–53.

Shabir, G.A. 2003. Validation of high-performance liquid chromatography methods for pharmaceutical analysis. Understanding the differences and similarities between validation requirements of the US Food and Drug Administration, the US Pharmacopeia and the International Conference on Harmonization. *Journal of Chromatography A*, 987:57-66. https://doi.org/10.1016/s0021-9673(02)01536-4.

Singh, A. P., Chauhan, I., Bhardwaj, S., Gaur, P., Kumar, S. S., & J, J. (2019). Hplc Method Development and Validation for Azithro-Mycin in Oral Suspension. *Journal of Applied Pharmaceutical Sciences and Research*, *April*, 7–12. https://doi.org/10.31069/japsr.v2i1.2.

Skinner, M., Taylor, R.B. and Kanfer, I. (1993). The pH-stability and acid degradation of the macrolide antibiotic, josamycin. *European Journal of Pharmaceutical Sciences*, 1(2), pp.61–72.

Suresh, R., Anarthanan, S.V.J., Manavalan, R. & Valliappan, K. 2010. Aspects of validation in HPLC method development for pharmaceutical analysis – comparison of validation requirements by FDA, USP AND ICH. *International Journal of Pharmaceutical Sciences and Research,* 1(12):123-132.

United States Pharmacopeia. 2013. Validation of compendial procedures. http://www.ofnisystems.com/wp-content/uploads/2013/12/USP36_1225.pdf Date of access: 20 Aug 2021.

United Nations Office on Drugs and Crime. 2009. Guidance for the validation of analytical methodology and calibration of equipment used for testing of illicit drugs in seized materials and biological specimens. New York: United Nations. https://www.unodc.org/documents/scientific/validation_E.pdf Date of access: 18 Aug 2021.

Waghule, S. N., Jain, N. P., Patani, C. J., & Patani, A. C. (2013). Method development and validation of HPLC method for determination of azithromycin. *Der Pharma Chemica*, *5*(4), 166–172.

Zacharis, C.K. 2009. Accelerating the quality control of pharmaceuticals using monolithic stationary phases: a review of recent HPLC applications. *Journal of chromatographic science*, *47*(6), pp.443-451.

Zubata, P., Ceresole, R., Rosasco, M. A., & Pizzorno, M. T. (2002). A new HPLC method for azithromycin quantitation. *Journal of Pharmaceutical and Biomedical Analysis*, *27*(5), 833–836. https://doi.org/10.1016/S0731-7085(01)00554-4
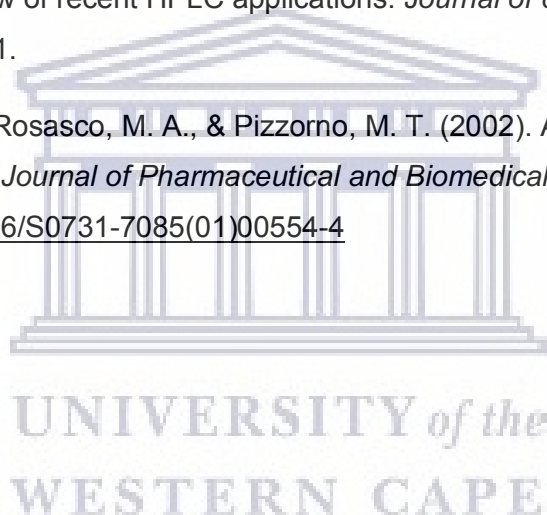
CHAPTER 8

Concluding remarks

Malaria continues to torment the global health system with millions of lives lost on a yearly basis and its socio-economic impact to individuals and affected governments cannot be emphasised enough. According to the WHO, pregnant women, and children under five are the most vulnerable when it comes to malaria infection, with (WHO, 2018; WHO, 2019) sub-Saharan Africa affected the worst. This can be directly linked to socio-economic status, healthcare infrastructure and environmental conditions that promote continued breeding habitats for the female anopheles' mosquito, responsible for the transmission of this life-threatening disease. The nature of the disease requires a multi-sectoral approach if we ever want to achieve a malaria free world. This includes vector control, eradication of vector species by using genetically modified vectors as well as preventative measures such as mosquito repellents, the use of treated mosquito nets, chemoprophylaxis, and chemotherapy. The effect of malaria infection on pregnant women holds serious implications not only to the mother but also to the baby and may include: preterm birth, still birth, low birth weight babies, anaemia of either the mother or baby or both and the worst being death (Chico & Chandramohan, 2011). These are some of the impacts that can be minimised to improve human health and general livelihood at large for the patients suffering from malaria.

The attempt to address the above effects in expectant mothers has included application of sulfadoxine and pyrimethamine as a prophylactic approach brought forth with the intermittent preventive treatment (IPTp-SP) which consist of at least three doses of 1500 mg sulfadoxine and 25 mg pyrimethamine administered in a monthly interval from the second trimester to term. This has yielded positive results for over a decade especially in regions where drug resistance has not been an issue (WHO, 2018). Recently, the WHO communicated its plans to include azithromycin, a macrolide antibiotic to this old regimen to address other conditions pregnant mothers are prone to, such as STIs and UTIs, which worsen the childbearing experiences (Unger *et al*., 2015). This being motivated with ongoing clinical trials on azithromycin inclusion as part of the current IPTp-SP prophylactic strategy.

This proposed treatment involves three compounds that have poor aqueous solubility, this dictates on the amount of an oral dosage form and directly determines the bioavailability of the drugs thereafter and ultimately the therapeutic outcomes. As described above, SUL is

available as an FDC with PYR whilst AZI is recommended as a 500 mg daily dose for 3 days. All three these drugs have long clearance half-life, which positively improve patient compliance, however may increase the risk of toxicity. This challenges both pharmaceutical production and the health sector in general and there is need to improve upon it to have a balance between risk-benefit judgement in medicine application.

The poor solubility of SUL, PYR and AZI are ascribed to their physico-chemical properties. It is a well-known fact that the physico-chemical properties of drugs affect every part of the solid dosage form development process and an understanding of the solid-state chemistry of drugs are imperative to allow the formulation of effective and safe medication. Many strategies may be employed to address the poor solubility of drug compounds which include solid-state form modification to render a drug into a solid-state form which exists at a higher energy level. This type of modification is well-known as amorphisation and may be achieved utilising several types of preparation techniques. In order to address the poor solubility of SUL, PYR and AZI, with the idea in mind that these three drugs might be formulated as an FDC in the near future this study aimed at investigating the potential to combine these three drugs into an amorphous solid-state form. A literature study revealed that crystalline SUL has only recently been prepared into an amorphous solid-state form which exhibited very unstable behaviour that reverts to its stable crystalline form (Aucamp, et al., 2016). Another study discussed the successful preparation of an amorphous solid-state form of AZI (Aucamp et al., 2015) which suggested the possibility to develop SUL and AZI in combination as a co-amorphous form. Putting in consideration the fact that PYR has never been reported to have any other form besides crystalline the research question was asked: "Would it be possible to prepare a ternary amorphous system containing all three compounds in the amorphous state?"

In a typical solid-state chemistry study, multiple solid-state preparation techniques and analytical techniques are used. This study utilised quench cooling and solvent evaporation formulation methods to investigate the potential of preparing a ternary amorphous solid form of these drugs. Quench cooling can also be termed hot melt extrusion, the difference lies in the settings, the latter is commonly applied in the large scale at the industrial level and whereas the first one is easily applicable for small scale laboratory-based production. Solvent evaporation may be applicable depending on the setting and can include either rapid or slow evaporation processes. In order to accurately characterise new solid-state forms of drugs, scientists have to rely on various complementary analytical techniques. In this study thermal techniques coupled with spectroscopy and powder X-ray diffraction were employed to identify newly formed solid-state forms. This was supplemented with studies of stability indicating techniques such as vapor sorption analysis. Ultimately, the true advantage of the ternary

amorphous system was evaluated through equilibrium solubility and dissolution rate studies. It is worth mentioning that no suitable HPLC method that could simultaneously detect and quantify the three drugs incorporated into the novel solid-state form existed. Hence, the development and validation of a novel RP-HPLC method was identified as an important tool to ensure the successful completion of this study.

As aforementioned on the two formulation methods applied in the study, firstly, the choice was made based on yield, scalability, and safety. Quench cooling of the melt technique was the favourable method where product was available almost immediately, however it requires proper skills to attain the final product of quality, good yield and little loss. On the other hand, solvent evaporation produced a good yield too, solvent screening took time, getting a suitable solvent for the combination was challenging. Slow evaporation requires waiting time depending on the level of volatility of the solvent, rapid solvent evaporation utilising rotary evaporator solves the waiting. The main challenging in applying solvent evaporation is getting rid of solvent to an acceptable reservoir limit, TGA data showed significant weight loss in sample obtained via solvent evaporation, this may have risk of forming different solid form (solvates) instead of intended ternary amorphous and adds on the health implication of the final product. And generally, hot melt sample showed a more stable form of ternary amorphous as opposed to solvent evaporation samples.

The aqueous solubility profile of SUL, PYR and AZI was enhanced by formulating a ternary amorphous system. Solubility data obtained showed an increase of 1681.9, 37.4 and 711.8%, for SUL, PYR and AZI, respectively in distilled water. A similar trend of enhancement was achieved in terms of dissolution rate determined in distilled water where over 100% increase was obtained for all the APIs in SPA-A in comparison to their crystalline counterpart. Improved solubility and dissolution rate has a direct positive impact on drug bioavailability, that may potentially alter required dose strength in an oral dosage with the same desired treatment outcome.

This study, like any other research project, presented a few challenges worth highlighting, ranging from personal responsibilities, intricate HPLC and solid-state form preparation method design, the current Covid-19 pandemic, extended lead times on the delivery of raw materials and laboratory supplies, specifically due to the global pandemic and equipment down time. Notwithstanding, these drawbacks were overcome.

It is exciting to imagine advancement that may emanate from this study. The results reported here have opened the doors to further development of a SPA-A containing oral dosage (table, capsule) form. Off course, this will require an *in vitro* investigation especially with regards to intestinal cell permeation together with aqueous solubility being the key indicators of bioavailability and drug toxicity, and in turn to inform on dose strength alteration to reduce the risk of toxicity, pill burden and increase compliance and possibility minimise or delay drug resistance in high malaria endemic zones. It is further recommended that this study should be expanded on by investigating this ternary amorphous solid-state form to ascertain whether this amorphous form could be characterised as a solid solution or a solid suspension. Furthermore, in-depth dosage form formulation studies could be pursued to establish the effect that typical oral solid dosage form formulation processes will have on the processability and stability of this novel amorphous form.

Conclusively, the study that investigated the potential ternary amorphous formulation and the physical stability thereof has deduced that, it's possible to have drug-drug-drug amorphous solid-state form exhibiting increased stability, yielding improved solubility and dissolution rate of all three APIs incorporated into such an amorphous system. This is truly a novel solid-state form since during a very recent and thorough literature search no evidence could be obtained of other similar amorphous systems which consists of three drugs.

Reference

Aucamp, M., Milne, M., & Liebenberg, W. (2016). Amorphous Sulfadoxine: A Physical Stability and Crystallization Kinetics Study. *AAPS PharmSciTech*, *17*(5), 1100–1109. https://doi.org/10.1208/s12249-015-0436-4.

Aucamp, M., Odendaal, R., Liebenberg, W., & Hamman, J. (2015). Amorphous azithromycin with improved aqueous solubility and intestinal membrane permeability. *Drug Development and Industrial Pharmacy*, *41*(7), 1100–1108. https://doi.org/10.3109/03639045.2014.931967.

Chico, R. M., & Chandramohan, D. (2011). Azithromycin plus chloroquine: Combination therapy for protection against malaria and sexually transmitted infections in pregnancy. *Expert Opinion on Drug Metabolism and Toxicology*, *7*(9), 1153–1167. https://doi.org/10.1517/17425255.2011.598506.

Global Malaria Programme: WHO Global. (2019). World malaria report 2019. In *WHO Regional Office for Africa* (Issue December). https://www.who.int/news-room/fact-sheets/detail/malaria

Unger, H. W., Ome-Kaius, M., Wangnapi, R. A., Umbers, A. J., Hanieh, S., Suen, C. S. N. L. W., Robinson, L. J., Rosanas-Urgell, A., Wapling, J., Lufele, E., Kongs, C., Samol, P., Sui, D., Singirok, D., Bardaji, A., Schofield, L., Menendez, C., Betuela, I., Siba, P., … Rogerson, S. J. (2015). Sulphadoxine-pyrimethamine plus azithromycin for the prevention of low birthweight in Papua New Guinea: A randomised controlled trial. *BMC Medicine*, *13*(1), 1–16. https://doi.org/10.1186/s12916-014-0258-3.

World Health Organization (WHO). (2018). Implementing malaria in pregnancy programs in the context of World Health Organization recommendations on antenatal care for a positive pregnancy experience. *Who*, *64*(January), 1–7. https://doi.org/10.1093/cid/civ881.9.

WHO, (2018). WHO | This year's World malaria report at a glance. *Who*, *2030*(December 2019), 1–10. https://www.who.int/malaria/media/world-malaria-report-2018/en/?fbclid=IwAR0qCCptX6pQBJvBSqWkYYnhaHj6O1aInuOl56Y9ycMGIJCM5oTcq4O_jsM.